

UNIVERSITE DE LILLE- SCIENCES ET TECHNOLOGIES
Ecole doctorale Science de la Matière, du Rayonnement et de l'environnement
THÈSE DE DOCTORAT
Spécialité : Biotechnologies agroalimentaires, sciences de l'aliment, physiologie

Présentée par
Alexandre–Ahmad AL SAABI

Pour l'obtention du grade de
DOCTEUR DE L'UNIVERSITÉ DE LILLE

**Mousses en écoulement pour le nettoyage d'équipements fermés contaminés
par des spores de *Bacillus cereus* ou des biofilms de *Pseudomonas fluorescens***

**Foam flow for cleaning of closed equipment contaminated by *Bacillus cereus*
spores or *Pseudomonas fluorescens* biofilms**

Préparée au laboratoire :
Unité Matériaux et Transformations CNRS UMR
Equipe : Processus aux Interfaces et Hygiène des Matériaux

Soutenue le 17 Septembre 2020 devant le jury composé de:

Imca Sampers, Professeur, Faculty of Bioscience Engineering/Université de Gand/ **Rapportrice**

Jack Legrand, Professeur, Laboratoire GEPEA, Université de Nantes/ **Rapporteur**

Marie Laure Lameloise, Professeur, AgroParis Tech/ **Examinatrice**

Nour-Eddine Chihib, Professeur, INRAE-PIHM/Université de Lille/ **Examineur**

Christine Faille, Directrice de recherche, INRAE-PIHM/Université de Lille/ **Co-directrice**

Gaetan Rauwel, Directeur de recherche, Laboratoires ANIOS ECOLAB/ **Co-directeur**

Fethi Aloui, Professeur, ENSIAME-LAMIH/Université Polytechnique/ **Co-directeur**

Thierry Bénézech, Directeur de recherche, INRAE-PIHM/Université de Lille/ **Directeur de Thèse**

This work was supported by the ‘Institut national de recherche pour l’agriculture, l’alimentation et l’environnement’ (INRAE), University of LILLE, ANIOS-ECOLAB laboratories and the European Regional Development fund via the Hauts-de-France region.

Remerciements

Je tiens tout d'abord à remercier mon DIEU, le tout puissant et miséricordieux, qui m'a donné la force et la patience d'accomplir ce modeste travail et qui m'a donné le courage et la volonté durant ces années d'études.

En second lieu, je tiens à remercier Dr. Guillaume Delaplace, de m'avoir chaleureusement accueilli dans son laboratoire et de m'avoir aidé à bien m'intégrer dans l'équipe PIHM.

J'adresse mes remerciements les plus chaleureux à mon directeur de thèse, Dr. Thierry Bénézech pour m'avoir aidé pendant ce voyage. Il était toujours prêt à m'aider et à me donner des conseils.

J'adresse mes remerciements aussi à mes co-directeurs Dr. Christine Faille, Prof. Fethi Aloui et Dr. Gaetan Rauwel (ANIOS) pour leur soutien et les heures qu'ils ont consacrées à diriger cette recherche. Je leurs suis extrêmement reconnaissant pour les conseils, les discussions scientifiques, les corrections et de m'avoir accordé toute liberté pour gérer mon travail. Cela m'a permis de développer mon autonomie et mon indépendance scientifique.

Mes sincères remerciements vont également au Monsieur Jack LeGrand, Professeur de l'Université de NANTES et Madame Imca Sampers, Professeur de l'Université de Gand d'avoir accepté d'être rapporteurs de ce travail. Je remercie aussi les deux Professeurs, Mr. Nour-Eddine Chihib et Mme. Marie-Laure Lameloise d'avoir accepté de participer à ce jury comme examinateurs.

Je tiens à remercier Prof. Cosmin Gruescu pour ses efforts qui a ajouter de valeur importante à ce projet. J'aimerais adresser un remerciement particulier à mon collègue Mr. Heni Dallagi, pour son aide, nos discussions scientifiques et pour les inoubliables moments partagés.

Je tiens à remercier l'ensemble de l'équipe PIHM, particulièrement Mr. Christophe Dufourmantelle, Mrs. Christelle lemy, Mr. Thoumas Dubois, Mr. Pascal Blanpain, Mr. Pascal Debreyne, Mr. Laurent Bouvier, Mme. Anne Moreau, Mr. Laurent Wauquier, Mr. Thierry Six, Mr.

Oussama Khelissa, Mr. Mostapha Najib, Mr. Marwan Abdallah, Mr. Piyush Kumar JHA et les autres thésards/stagiaires du laboratoire pour leur gentillesse et leur aide.

Et bien sûr, je remercie de tout mon cœur ma famille, ma mère, mon père, mes frères et mes sœurs qui m'ont soutenu et encouragé tout au long mes études. Tout ce que je peux leur offrir ne pourra exprimer l'amour et la reconnaissance que je leur porte.

Je remercie aussi mes amis, Mr. Husen Hammoud (Fidèle), Mr. Mohamad Hijazi (Maxime), Mr. Rabih Mezher et Mr. Reda Kassir pour leurs soutiens.

Contents

Nomenclature	11
General Introduction	14
References	19
CHAPTER I: Cleaning challenges in food industry/ Foam flow as an alternative for standard cleaning procedures	22
1.0 Abstract	23
1.1 Introduction	23
1.2 Cleaning in agro-food industries	24
1.2.1 Standard Cleaning in Place (CIP)	24
1.2.2 CIP Technical Regulations	25
1.2.3. Drawbacks in standard CIP	26
1.3. Challenges facing the agro-food industry	26
1.3.1. High water consumption for food production	26
1.3.2. Water consumption in cleaning processes of food: the fresh-cut food industry	27
1.3.3. Water consumption in Cleaning Procedures.	29
1.4 Food contamination	29
1.4.1 World Food Contamination According to World Health Organization, WHO	30
1.4.2. Food Contamination in France	30
1.5 Factors affecting cleaning in the industry	30
1.5.1. Sinner's cycle	31
1.5.2. Factors implicated in Sinner's Cycle	32
1.6 Multi-functional compounds: Surface Active Agents	33
1.6.1 Detergents	33
1.6.2 Surfactants: Chemical Structure	33
1.6.3. Micellisation	35
1.6.4. Different Actions of Surfactants	36
1.7 Flowing Foam for Surface Cleaning	38
1.7.1 Mechanical properties of foam, a key parameter for cleaning.	38
1.7.2 Previous studies on flowing foam	39
1.7.3 Flowing Foam in cleaning practices.	39
1.8 References	40
CHAPTER II: Microbial attachment on surfaces in food industries	46

2.0 Abstract	47
2.1. Microbiological interactions with abiotic surfaces	47
2.2 Physiochemical approaches for microbial adhesion on surfaces	48
2.2.1 The Thermodynamic approach (Free energy theory)	49
2.2.2 DLVO Theories	50
2.2.2.1 Classical DLVO theory	50
2.2.2.2 Extended DLVO theory	50
2.3. Properties and adhesion of bacterial spores	52
2.3.1 Structure of bacterial spores	53
2.3.2 Surface of <i>Bacillus cereus</i> spores	54
2.3.3 Surface of <i>Bacillus amyloliquefaciens</i> spores	55
2.3.4 Resistance properties	56
2.3.5 Spores and contamination in food industry	56
2.4 Biofilms: structure, contamination in food industry	58
2.4.1 Biofilm formation	58
2.4.2 Extracellular polymeric substances (EPS)	59
2.4.3 <i>P. fluorescens</i> , a biofilm former	60
2.4.4 Resistance of biofilm bacteria to antimicrobial compounds	60
2.4.5 Biofilms contamination in Food industries	62
2.5 Summary	64
2.6 References	64
CHAPTER III: Structure and rheology of foam	77
3.0 Abstract	78
3.1 Introduction	78
3.2 Foam structure	81
3.2.1 Bubbles	81
3.2.2 Surface Tension	81
3.2.3 Void fraction and Foam quality	82
3.2.4 Foams wet and dry	82
3.2.5 Foam Density	83
3.2.6 Local Equilibrium Rules	83
3.2.7 The laws of Plateau	84
3.3 Bubble –bubble interaction	85

3.4 Making Foams	86
3.5 Foam creation	86
3.5.1 Nucleation	86
3.5.2 Entrainment of gas occlusions	87
3.6 Practical application	87
3.7 Foam Rheology	88
3.7.1 Linear Elasticity	90
3.7.2 Non-linear Elasticity	90
3.7.3 Yielding	91
3.7.4 Plastic flow	92
3.8 Foam evolution	92
3.8.1 Drainage	92
3.8.2 Coarsening	92
3.8.3 Gibbs-Marangoni mechanism	93
3.8.4 Foam collapse	93
3.9 Foam flow	94
3.10 Foam viscosity	94
3.11 Non-Newtonian flow models	95
3.12 Horizontal flow regimes	96
3.13 Wall-Slip liquid layer	97
3.13.1 Wall slip velocity	98
3.13.2 Thickness of slip layer (film) as a function of foam quality and foam flow regime	99
3.14 Summary	100
3.15 References	100
CHAPTER IV: Materials and Methods	104
4.0 Abstract	105
4.1. Materials	105
4.1.1. Standard Cleaning in Place like conditions prototype	105
4.1.2. Foam Cleaning in Place prototype	107
4.1.3. Stainless steel coupons	110
4.1.4. Test pipes	111
4.1.5. Singularities	112
4.2 Surfactants	113

4.2.1 Sodium dodecyl sulfate	114
4.2.2 Lauramine oxide (AMMONYX LO [®])	114
4.2.3 Ethoxylated nonionic fluoro-surfactant (Capstone FS-30)	114
4.2.4 Microorganism used for coupons fouling: Spores/ Biofilms	114
4.3 Foam Flow Regimes	116
4.3.1 Regime identification	116
4.3.2 Average shear stress measurement	117
4.4. Bubble size measurement	117
4.5 Conditioning of coupons (ageing): Treatment with Milk and NaOH (0.5%)	118
4.6 Roughness Ra, Profilometer (Mahr)	118
4.7 Cleaning and disinfection of stainless steel coupons	119
4.8 Sporulation and Fouling Conditions	120
4.8.1 Sporulation Method	120
4.8.2 Fouling Conditions	121
4.9 <i>P. fluorescens pfl</i> Biofilm Preparation and Fouling Conditions	121
4.10 Evaluation of the hydrophilic/hydrophobic character of spores (MATH test)	121
4.11 Post experimental treatment of coupons	123
4.12 Epifluorescence microscopy	123
4.13 Measurement of surface tension of surfactants using the pendant drop method	124
References	125
CHAPTER V Results part 1 (Article): Removal of Bacillus spores by flowing foam from stainless steel pipes: effect of the foam quality and velocity	128
Abstract	129
1. Introduction	130
2. Materials and Methods	132
2.1. Bacterial strains and solid surfaces	132
2.2 Surface soiling and cleaning	132
2.3 Foam flow visualisation	135
2.4 Kinetics modelling	136
2.5 Statistical analysis	136
3. Results	136
3.1 Foam flow organization and mechanical action induced by the foam	136

3.2 Spores' detachment under the different flowing conditions	141
4. Discussion	147
5. Conclusions and perspectives	151
6. Acknowledgments	152
7. References	152
CHAPTER V, Results part 2: Detachment of <i>B. amyloliquefaciens</i> 98/7 after singularities	157
5.0 Abstract	157
5.1 Introduction	157
5.2 Spores' detachment in test ducts placed post singularities	158
5.2 Foam stability tested after singularities	161
5.4 Qualitative and quantitative analysis of bubbles post singularities	163
5.5 Discussion and Conclusion	166
5.6 References	169
CHAPTER V, Results part 3: Detachment of <i>B. amyloliquefaciens</i> 98/7 spores using foam flow generated from different surfactants	171
6.0 Abstract	172
6.1 Introduction	172
6.2 Testing stability of foam	173
6.3 Bubbles structure and size	174
6.4 Surface tension measurement	177
6.5 Calculation of the thickness of the thin liquid film (case of one bubble)	177
6.6 Detachment of <i>B. amyloliquefaciens</i> 98/7 spores	178
6.7 Discussion and Conclusion	182
6.8 References	184
Chapter V, Results part 4: Detachment <i>P. fluorescens pfl</i> Biofilm using Foam Flow	185
7.0 Abstract	186
7.1 Introduction	186
7.2 Bubbles size and capillary numbers for foam flow regimes	187
7.3 <i>P. fluorescens pfl</i> biofilm detachment by the different foam flow regimes	189
7.4 Statistical analysis (Tukey's grouping, SAS analysis)	193

7.5 Fluorescence Microscopy	197
7.6 Discussion and Conclusion	202
7.7 References	205
Conclusion and Perspectives	209
References	216
Scientific Production	220
International Conference: Fouling and Cleaning in food processing, 17 – 20 April 2018, Lund Sweden (Conference article)	221
Thesis Abstract	233
Resumé de Thèse	234

Nomenclature

Symbol	Description	Units
β	Foam quality	
v	Average speed of the fluid in the pipe	cm.s^{-1}
γ	Strain	N.m^{-2}
$\dot{\gamma}$	Yield strain	N.m^{-2}
k	Consistency index	Pa.s
n	Power law index	
g	Gravity	m.s^{-2}
l_o	Capillary length	m
G	Shear Modulus	Pa
Γ or σ	Surface tension	N/m
Π	Osmotic pressure of the foam	Pa
E	Energy needed to increase a liquid surface	J
S	Entropy	$\text{Kg.m}^2.\text{s}^{-2}.\text{K}^{-1}$
μ_f	Foam viscosity	$\text{m}^2.\text{s}^{-1}$
μ_l	Liquid viscosity	$\text{m}^2.\text{s}^{-1}$
ρ_f	Foam density	Kg.m^{-3}
ρ_l	Liquid density	Kg.m^{-3}
ρ_g	Gas density	Kg.m^{-3}
τ	Shear stress	Pa
τ_c	Yield shear stress	Pa
N_0	Quantity of the population at time 0	cfu.cm^{-2}
$N(t)$	Quantity of the residual population at time t	cfu.cm^{-2}
$k_{\text{max}1}$	Detachment rate of the loosely attached population	s^{-1}
$k_{\text{max}2}$	Detachment rate of the highly adherent population	s^{-1}
f	Percentage detachment of the loosely attached population	$\%$
R_a	Average roughness	μm
r_1, r_2	Radii of curvature of a Plateau border for two adjacent bubbles	m
r	Local radius of curvature of the two adjacent bubbles	m

Sh	Sherwood number	
ϕ	Void fraction	
V_t	Total volume of foam	l
V_l	Volume of liquid	l
V_g	Volume of gas	l
A	Surface area	m ²
Ca	Capillary number	
e	Film thickness	μm
Q_t	Total flow rate	l.h ⁻¹
Q_l	Liquid flow rate	l.h ⁻¹
Q_g	Gas Flow rate	l.h ⁻¹
D_h	Hydraulic diameter	m
ΔP	Pressure difference	Pa
ΔG_{adh}	Total free energy of adhesion	kJ mol ⁻¹
γ_{sm}	Free energy of adhesion between surface and microorganism	kJ mol ⁻¹
γ_{sl}	Free energy of adhesion between surface and liquid	kJ mol ⁻¹
γ_{ml}	Free energy of adhesion between surface and microorganism	kJ mol ⁻¹
CIP	Cleaning In Place	
DR	Decimal reduction	
D-value	The time required to lower the population by a factor 10	
ECM	Extracellular matrix	
Re	Reynolds number	
PMMA	Poly(methyl methacrylate)	
CMC	Critical micellar concentration	

GENERAL INTRODUCTION

GENERAL INTRODUCTION

GENERAL INTRODUCTION

General Introduction

Pathogenic microorganisms are the major security worry for the food industry. The enormous majority of epidemics of food-related illness are due to microbial cleanliness control in the food industry pathogens, rather than to chemical or physical contaminants. As they are mostly unnoticeable by the unassisted human senses (i.e. they do not frequently cause color fluctuations or produce 'off'-flavors or taints in the food) and they are capable of rapid growth under favorable storage circumstances, abundant time and effort are spent in controlling and/or eradicating them. Even if the microbes in food were eventually devastated by cooking, they may have already produced toxins, so it would be important to prevent contamination through the use of hygienic practices. Like microbial pathogens, spoilage entities can either be present naturally or gain access to food (Tamime, 2008).

Usually, some microbial development happens when any one of the aspects that controls the growth rate is at a limiting level. If more than one factor becomes limiting, microbial growth is drastically reduced or even totally prohibited. Actual control of pathogenic and spoilage bacteria thus depends on a full understanding of the development conditions favoring specific organisms. This understanding can be used to reduce contamination from raw materials, to inactivate bacteria during processing and stop produced food from becoming contaminated. It is also important to know where and how microorganisms can become recognized, if growth conditions are favorable. They are particularly attracted to surfaces that deliver a steady surroundings for existence and evolution. Surfaces exposed to air are always susceptible unless frequently and efficiently cleaned and sterilized. However, surfaces within closed apparatus may also be susceptible. There are usually places in processing lines, even when fittingly designed, where some products remain longer than what is wanted. Even if 'dead' parts have been 'designed out', some product will attach to equipment surfaces, regardless of the possibility of speedy liquids. Microbes may live on such surfaces long enough to multiply, and contaminate the product (Tamime, 2008).

The bacterial spores (or endospores) have been longly and thoroughly investigated by the community of the microbiologists since their discovery in the late 19th century by Cohn and Koch (Gould, 2006; Keynan and Sandler, 1983). The bacterial spores are among the most resistant forms of living organisms. Their resistance favors their survival to food processing and long-term persistence in foods. The contamination of foods with bacterial spores is consequently well

documented in almost any sort of foods as it may be seen in the far from exhaustive following selection of relevant papers (Baggesen, 2006; Meer et al., 1991; Anonymous, 2005b). The multiplication of the vegetative cells formed after spore germination and outgrowth can occur at a wide range of temperature (spore-forming bacterial species maybe psychrotrophic, mesophilic or thermophilic), pH and water activity and be the cause of foodborne poisonings (mainly by *Bacillus cereus*, *Clostridium perfringens* and *Clostridium botulinum*) or food spoilage (Carlin, 2011).

Also the formation of biofilms on industry surfaces can lead to serious hygiene problems and economic losses due to food spoilage and equipment impairment because pathogenic and spoilage biofilms could provide a reservoir of contamination increasing the risk for post processing contamination and leading to lowered shelf life of the food product and/or transmission of diseases (Bremer et al., 2006, Gram et al., 2007). Several reports revealed that biofilms are easily formed by various microorganisms on the equipment surfaces of the production line and those containing pathogens represent one of the major causes of contamination of food products (Guðbjörnsdóttir et al., 2005, Shia and Zhua, 2009; Simões et al., 2010). The most common sources involved in biofilm accumulation are the floors, waste water pipes, bends in pipes, rubber seals, conveyor belts, stainless steel surfaces, etc. Buna-N and Teflon seals have also been implicated as important sites for biofilm formation (Chmielewski and Frank, 2003, Chmielewski and Frank, 2006).

Hygienic design of food production facilities, processing equipment, etc., is a most important factor in ensuring that food is safe and wholesome. Poorly designed farms, factories and equipment can easily result in contamination of food products and lead to food poisoning incidents. Furthermore, design deficiencies may result in losses of product due to spoilage increased cleaning costs and reduced production time. These aspects are also of possible environmental concern. Therefore, it is essential that both manufacturers and users of food processing equipment are aware of hygienic design principles and requirements such as those described in EU Directives 98/37/EC and 93/43/EEC, and Hygienic Design DIN EN 1672/2 (1997). Hygienic production of food thus depends upon a combination of food processing procedures and hygienic design of buildings and equipment, in full compliance with legislation (Tamime, 2008).

Fouling of processing lines and especially of the pipe surface in closed processing systems are very common in many industries such as processed food, beverage, dairy, beverage, brewing,

pharmaceutical, and cosmetics industries where timely removal of the deposited substance on process equipment is vital to avoid problems such as efficiency reduction, clogging, contamination and so on. For instance, rapid and effective cleaning of closed processing system is especially important in food and beverage industries, where production lines are often cleaned daily to maintain both high heat transfer rates and low pressure drops in heat treatment units and more importantly, to ensure the appropriate level of microbial quality and thus the safety of the products foodstuff typically involves a warm or cold water rinse, washing with alkaline and/or acidic solution, and a clear rinse with warm water to flush out residual cleaning agents (Dev et al., 2014). Efficient CIP processes will result not only in reduced downtime and costs for cleaning but also reduced environmental impact (in the disposal of spent chemicals) (Gillham et al., 1999). On the other hand, researchers have shown that in some areas some bacteria may remain on equipment surfaces after standard CIP procedures (Lelièvre et al., 2002; Elevers et al., 1999). Insufficient cleaning typically results in reduced efficiency, contamination in final products and energy loss (Avila-Sierra et al., 2019). Traditional methods of improving CIP efficiency include increasing the overall cleaning fluid velocity, the concentration and temperature of the cleaning chemicals and longer running time, giving rise to increased costs and downtime, reduce production efficiency, and additional burden to the environment due to the extra chemical consumption. Moreover, research have shown that increasing temperature beyond 45 °C had limited impact on the rinse water effectiveness and the cleaning efficiency decreased rapidly with increasing rinse time (Fan et al., 2018).

Cleaning is one of the most energy and resource consumption operations. For example, a milk plant is likely to use 13% of its energy and 28% of its water usage on CIP (*Australian Dairy Manufacturing Industry State of the Environment Report*, 2006). It is clear that CIP is an energy-intensive and most water demanding operation in dairy manufacturing. It should bear in mind that reducing water consumption not only helps to save a valuable resource, but also to save additional consumption in energy, chemical and treatment costs. A case study on UK drinks sector reported potential savings of 222,000 L of water per annum through more efficient CIP procedures for vessels and pipes in its Leven package plant, and reduction of water usage by 5 million liters through efficient CIP in its Nangor Road Baileys (WRAP, clean-in-place case study: *UK Drinks sector* 2019). Considering this, it is important to better understand the factors controlling CIP efficiency and techniques to investigate them.

Foams, industrial or natural, are an integral part of our everyday life. Their wide interest in industry lies in the fact that they combine the properties of antagonistic materials such as liquids, gases, and solids. In the food industry, the foam is a collection of liquid-air interfaces stabilized by surface-active molecules. These frequent interfaces constitute spaces of exchange which can be very useful when it comes to a tenfold time. Moreover, the gas contained in the foam makes it possible to make a material that is much less dense than the liquid alone. The composition of the foam can also be adjusted since the nature and quantities of gas and liquid can be varied.

Foamed cleaning agents are already applied to a certain extent in industrial cleaning processes such as CIP of pipes and vessels in the food and pharmaceutical industries and cleaning of heat exchangers and turbines. However, scientific literature on such applications is almost absent. Ideal cleaning foams need to contain satisfactory levels of active cleaning component and have to keep the chemical in place on the filter surface long enough for the active ingredients to penetrate the pores and remove the deposits. Fouling dissolution occurs in the liquid phase by a reaction of the cleaning agent with the fouling layer. Foams should be wet enough to allow rapid replenishment of the spent chemical through diffusion.

Foam, which is frequently used for carrying out exposed plant cleaning, may be used in other cleaning procedures that might be beneficial for numerous closed systems such as pipes, tanks and containers. This may comprise; ease, rapidity and refuge of application, extended interaction time between detergent and soil as well as a reduced labor time to carry out the procedure.

Aqueous foams are complex fluids consisting of concentrated dispersions of gas bubbles in a soapy liquid. Depending on the amount of water they contain, they are either dry or wet. They have original mechanical properties which rely on their low density and high surface area combined with their ability to elastic response to low stresses and to flow like a viscous liquid with large deformations.

Very little works have also been carried out on the elimination of surface deposits using gas-liquid two-phase flows (Kondjoyan et al., 2009), but to our knowledge none relates to the elimination of microorganisms. Foam is largely used throughout the food industries for the cleaning of open surfaces (floor, workshops and equipment). Foam characteristics as density, foamability and quality based on void fraction were recently considered to study the cleaning of closed systems as ultrafiltration processes (Gahleitner et al., 2013). Therefore, foam flows would constitute an actual novelty in surface hygiene as low water load and high mechanical actions under moderate temperatures would permit a very good efficient cleaning and can easily be combined with disinfection.

The characterization of the foam and of the liquid film formed on the wall is of paramount interest in the understanding of phenomena at the interfaces. Indeed, foam flows are governed by the properties of a thin near wall region, which induces a sliding effect. The most important parameter in controlling the flow of foam would therefore be the thickness of this sliding layer (a few micrometers to a few tenth of micrometers). Foams mainly composed of gases have complex rheological properties which can be compared to those of a solid, but also to those of a liquid (Aloui & Madani, 2008). In this case, the wall shear stress (tangential constraint) is a key parameter in the flows of these foams. This constraint, which plays an important role in the characterization of the rheological properties of the foam, depends mainly on the size of the bubbles and particularly on the volume fraction of the liquid (Chovet, 2015; Chovet et al., 2014).

To have our contributions as part of the mentioned studies, we set an objective which is experimenting the efficiency of foam in the detachment of spores and biofilms under different flow conditions. Parameters to be regarded concerned either the foam and the foam flow in straight pipes such as foam quality, velocity, bubbles size, organization and shape. Also we studied foam flow impact in detaching spores post singularities that may obviously happened in actual processing lines design as foam could be impacted by the geometry of the systems. To study the effect of foam in detaching spores from a chemical perspective, we used surfactants with different chemical composition such as fluorinated surfactants. Results of microorganism's detachment by foam flow was compared with standard CIP like conditions.

To carry out these experiments, for spores, two bacterial species were chosen, *Bacillus amyloliquefaciens* 98/7 and *Bacillus cereus* 98/4. The two strains differs in their ability on attaching on stainless steel. For biofilms *Pseudomonas fluorescence pfl* strain was chosen, which is a good biofilm former. This is an exploring work on a possible new cleaning technology with high potential in terms of environmental impact mitigation. An attempt to evaluate potential benefits is proposed at the end.

References

- Aloui, F., & Madani, S. (2008). Experimental investigation of a wet foam flow through a horizontal sudden expansion. *Experimental Thermal and Fluid Science*, 32(4), 905–926. <https://doi.org/10.1016/j.expthermflusci.2007.11.013>
- Australian Dairy Manufacturing Industry State of the Environment Report. (2006). 26.
- Avila-Sierra, A., Zhang, Z. J., & Fryer, P. J. (2019). Effect of surface characteristics on cleaning performance for CIP system in food processing. *Energy Procedia*, 161, 115–122. <https://doi.org/10.1016/j.egypro.2019.02.067>
- Baggesen, D. L. (2006). *Opinion of the Scientific Panel on Biological Hazards on the request from the Commission related to “Risk assessment and mitigation options of Salmonella in pig production: Question No EFSA-Q-2005-019*.
- Bremer, P. J., Fillery, S., & McQuillan, A. J. (2006). Laboratory scale Clean-In-Place (CIP) studies on the effectiveness of different caustic and acid wash steps on the removal of dairy biofilms. *International Journal of Food Microbiology*, 106(3), 254–262. <https://doi.org/10.1016/j.ijfoodmicro.2005.07.004>
- Carlin, F. (2011). Origin of bacterial spores contaminating foods. *Food Microbiology*, 28(2), 177–182. <https://doi.org/10.1016/j.fm.2010.07.008>
- Chmielewski, R. a. N., & Frank, J. F. (2003). Biofilm Formation and Control in Food Processing Facilities. *Comprehensive Reviews in Food Science and Food Safety*, 2(1), 22–32. <https://doi.org/10.1111/j.1541-4337.2003.tb00012.x>
- Chmielewski, R. a. N., & Frank, J. F. (2006). A predictive model for heat inactivation of *Listeria monocytogenes* biofilm on buna-N rubber. *LWT - Food Science and Technology*, 39(1), 11–19. <https://doi.org/10.1016/j.lwt.2004.10.006>
- Chovet, R. (2015). *Experimental and numerical characterization of the rheological behavior of a complex fluid: Application to a wet foam flow through a horizontal straight duct with and without*

flow disruption devices (FDD) [Université de Valenciennes et du Hainaut-Cambresis]. <https://tel.archives-ouvertes.fr/tel-01192955/>

Chovet, R., Aloui, F., & Keirsbulck, L. (2014). *Gas-Liquid Foam Through Straight Ducts and Singularities: CFD Simulations and Experiments*. <https://doi.org/10.1115/FEDSM2014-21190>

Dev, S. R. S., Demirci, A., Graves, R. E., & Puri, V. M. (2014). Optimization and modeling of an electrolyzed oxidizing water based Clean-In-Place technique for farm milking systems using a pilot-scale milking system. *Journal of Food Engineering*, 135(Supplement C), 1–10. <https://doi.org/10.1016/j.jfoodeng.2014.02.019>

Elevers, K. T., Peters, A. C., & Griffith, C. J. (1999). Development of biofilms and control of biofilm in the food industry. *Biofilms: the good, the Bad, the Ugly*, Wimpenny, J., Gilbert, P., Walker, J., Brading, M.G. and Bayston, R.(eds)(Bioline, Cardiff, UK), 139-145.

Fan, M., Phinney, D. M., & Heldman, D. R. (2018). The impact of clean-in-place parameters on rinse water effectiveness and efficiency. *Journal of Food Engineering*, 222(Supplement C), 276–283. <https://doi.org/10.1016/j.jfoodeng.2017.11.029>

Gahleitner, B., Loderer, C., & Fuchs, W. (2013). Chemical foam cleaning as an alternative for flux recovery in dynamic filtration processes. *Journal of Membrane Science*, 431, 19–27. <https://doi.org/10.1016/j.memsci.2012.12.047>

Gillham, C. R., Fryer, P. J., Hasting, A. P. M., & Wilson, D. I. (1999). Cleaning-in-Place of Whey Protein Fouling Deposits: Mechanisms Controlling Cleaning. *Food and Bioproducts Processing*, 77(2), 127–136. <https://doi.org/10.1205/096030899532420>

Gould, G. W. (2006). History of science – spores. *Journal of Applied Microbiology*, 101(3), 507–513. <https://doi.org/10.1111/j.1365-2672.2006.02888.x>

Gram, L., Bagge-Ravn, D., Ng, Y. Y., Gymoese, P., & Vogel, B. F. (2007). Influence of food soiling matrix on cleaning and disinfection efficiency on surface attached *Listeria monocytogenes*. *Food Control*, 18(10), 1165–1171. <https://doi.org/10.1016/j.foodcont.2006.06.014>

Guobjoernsdottir, B., Einarsson, H., & Thorkelsson, G. (2005). Microbial adhesion to processing lines for fish fillets and cooked shrimp: influence of stainless steel surface finish and presence of gram-negative bacteria on the attachment of *Listeria monocytogenes*. *Food Technology and Biotechnology*, 43(1), 55-61.

- Jensen, B. B. B., Friis, A., Bénézech, Th., Legentilhomme, P., & Lelièvre, C. (2005). Local Wall Shear Stress Variations Predicted by Computational Fluid Dynamics for Hygienic Design. *Food and Bioprocess Processing*, 83(1), 53–60. <https://doi.org/10.1205/fbp.04021>
- Keynan, A., & Sandler, N. (1983). Spore research in historical perspective.
- Kondjoyan, A., Dessaigne, S., Herry, J.-M., & Bellon-Fontaine, M.-N. (2009). Capillary force required to detach micron-sized particles from solid surfaces—Validation with bubbles circulating in water and 2µm-diameter latex spheres. *Colloids and Surfaces B: Biointerfaces*, 73(2), 276–283. <https://doi.org/10.1016/j.colsurfb.2009.05.022>
- Lelièvre, C., Legentilhomme, P., Gaucher, C., Legrand, J., Faille, C., & Bénézech, T. (2002). Cleaning in place: Effect of local wall shear stress variation on bacterial removal from stainless steel equipment. *Chemical Engineering Science*, 57(8), 1287–1297. [https://doi.org/10.1016/S0009-2509\(02\)00019-2](https://doi.org/10.1016/S0009-2509(02)00019-2)
- Meer, R. R., Baker, J., Bodyfelt, F. W., & Griffiths, M. W. (1991). Psychrotrophic *Bacillus spp.* in Fluid Milk Products: A Review. *Journal of Food Protection*, 54(12), 969–979. <https://doi.org/10.4315/0362-028X-54.12.969>
- Shi, X., & Zhu, X. (2009). Biofilm formation and food safety in food industries. *Trends in Food Science & Technology*, 20(9), 407–413. <https://doi.org/10.1016/j.tifs.2009.01.054>
- Simões, M., Pereira, M. O., & Vieira, M. J. (2005). Effect of mechanical stress on biofilms challenged by different chemicals. *Water Research*, 39(20), 5142–5152. <https://doi.org/10.1016/j.watres.2005.09.028>
- Tamime, A. Y. (Ed.). (2008). *Cleaning-in place: Dairy, food and beverage operations* (3rd ed). Blackwell Pub.

CHAPTER 1**LITERATURE REVIEW****CHAPTER I**

- Cleaning Challenges in Food Industries
- Foam flow, a Possible Alternative for Standard Cleaning Procedures

CHAPTER 1

LITERATURE REVIEW

1.0 Abstract: Many progress in cleaning procedures in agro-food industries has been achieved in the last 30 years, however problems like high water consumption and contamination of cleaning units have been not fully resolved. Benefiting from the mechanical properties of flowing foam such shearing on surfaces may have a good impact on the detachment of spores/biofilms while using less water and energy.

1.1 Introduction:

Food industry relies on water availability as a main source for their functionality where a significant amount of water is needed for a variety of uses such as cleaning. In a context where more pressure is being set on water consumption, possible shortage of water in the future where food industries may face challenges regarding water availability? Food industries sectors are being engaged in water sparing by implementing new good practices or common sense actions such as comprehensive and systematic re-design of water networks to be achieved, including water recycling or reuse or finding an alternative that uses less water. Not only saving water, however a good efficient cleaning practice has to be taken into account to prevent any contamination. Searching good economical practices by governments and agro-food industries necessitates the use of alternative techniques (Avila-Sierra et al., 2020) or a better modelling of the cleaning processes (Deponete et al., 2020) to allow the use of novel tools e.g. artificial intelligence-driven or fuzzy logic as for ultrafiltration (Villicco et al., 2020). Even though Cleaning in Place is widely used and it is a common cleaning practice in food industries, however, it remains a high-level water consumption technique. Lately some studies, presented some bacterial species that still survived even after CIP and maybe a probable source of product contamination. CIP uses single-phase fluids to clean pipe works or closed processing lines, in other words, water and the detergent used constitute one phase and the circulation of this solution at a determined wall shear stress with a flow velocity at least 1.5 m/s creates a turbulent flow. This will have an impact on pipe walls in which soiled materials including adhering microbial species can be detached. On the other hand, a double phase fluid such as foam can impose the same wall shear stress with less water being consumed. Foam quality, bubbles texture, and a thin liquid film that surrounds bubbles can be key parameters to explain the shearing effect of flowing foam while in contact with surfaces. A

mechanical approach for cleaning of closed systems such as pipes by foam, may be a saving practice for water and a reducer of contamination.

1.2 Cleaning in agro-food industries

Risks associated with biofilms can be controlled either by limiting the number of adherent cells or by facilitating the removal of adherent bacteria. To decrease these risks a better understanding of the factors governing adhesion (in terms of the number of adhering bacteria, as well as adhesion strength) would be needed, in addition, cleaning is indispensable, that is if the surface is not well cleaned and disinfected; the microorganisms will be released later into fluid food circulating in the lines. Bio-fouling whether with spores or biofilms must be treated by industries. Standard Cleaning in place has been a tremendous shift in agro-food industries during the last decades where it reduced time for cleaning processes while increasing productivity. On the other hand, CIP was unable to ensure full safety from microorganisms, in addition to its significant water consumption that has left a burden on industries.

1.2.1 Standard Cleaning in Place (CIP)

The idea of Cleaning in Place by flowing cleaning solutions in addition to water rinsing in an automated or partially automated system in place of food liquids has had a significant pace throughout history. Previously to these systems, food plants or dairies were disassembled and completely washed by hands. The latter technique consumed much time and labor to the extent it limited the practical size of plants. What are the elements of typical Cleaning in Place system? The elements of a typical clean-in-place (CIP) system are chemical storage, solution supply and recovery tanks, supply and return pumps (usually centrifugal), spray devices in tanks, air-controlled automatic valves, manual connection stations (flow meters), additional piping to complete circuits, and automatic control devices such as programmable logic controllers. Design rules have increasingly advanced from experience resulting from flow velocities, intensities of sprays and solution strength for an efficient cleaning of typical soils from food plants (Clark 2003) and were recently detailed in new guidelines issues by the EHEDG (www.ehedg.org, document 50, 2019).

In food processing operations, cleaning is a highly critical stage in quality control (Kulkarni, Maxcy, and Arnold 1975). Cleaning in-place (CIP) is now a commonplace activity in almost all dairy, beverage and processed-food production plants. The beverage and the dairy industry

technologies has been broadly in line together. Both technologies has seen increasing demands from customers in terms of CIP verification and validation to provide improvements in plant hygiene, finished product quality, related shelf-life and microbiological considerations (Tamime 2008). The EHEDG guideline 45 (2016) presenting the general principles is available for free on the web-site of the foundation. Hence, the processed food industry has seen a major shift towards CIP since 1993 (von Rybinski 2007).

1.2.2 CIP Technical Regulations

Experience in Cleaning in Place is mostly from dairy and other liquid-product plants like soft drinks, syrup and fruit juice plants. The minimum mean velocity commonly accepted in the practices in pipelines is 1.5 m.s^{-1} to reach the necessary mechanical action to clean. However, being more complex than this concerning the necessary mechanical action a recent review was proposed by Li et al., (2019). In terms of good design of the processing lines, the diameter of tees and dead legs should not exceed three times the pipe diameter to ensure cleaning. Tanks are sprayed almost at 37 Liters/minute/meter of circumference; a recent paper detailed the process variables acting on the efficiency of surface cleaning using an impinging jet (Li et al., 2020). Frequently, such flow rates overcome the normal process flow rates, hence special pumps may be needed just for CIP. Sometimes, it may be possible to use dual-speed process pumps, a low speed for process flow and for CIP a higher speed. The latter technique can save investment cost and space.

Commonly CIP systems are designed in a way that cleaning solutions and final water rinse are recovered for reuse to save costs and discharge reduction. Caustic soda solutions (1.5%) and nitric, phosphoric, and citric acids are common cleaning agents. Detergents are used sometimes alone or with acids and bases. Moreover, sanitizing agents such as iodophores, quaternary ammonium compounds, and chlorine-releasing agents, may be used, usually as a final rinse that is allowed to take place during the night. In the morning, fresh water displaces the sanitizing agent then the product flows inside. In a proper designed CIP system, most of the plant waste water should be discharged from the CIP unit. This will allow monitoring and pretreatment, if necessary. Sometimes manual labor is involved in cleaning highly automated systems. For example, positive displacement pumps must be disassembled, bypassed, and cleaned by hand because their construction prevents full cleaning by flushing. Commonly manual connections are involved at

flow meters to prevent accidental contamination of food with cleaning solutions. Connections are commonly verified by electronic signals to the controller (Clark 2003).

1.2.3. Drawbacks in standard CIP

Modern food processing industries have revolutionized their clean-up procedures through cleaning in place (CIP) and automation. Recently, advances have been significant in design and operation of CIP, understanding of various factors influencing cleaning and mechanisms of cleaning action, detergent formulations, and cleaning additives designed for specific cleaning jobs, etc. Unfortunately, progress in procedures and criteria for evaluating effectiveness of cleaning has not kept pace with growing complexities of food processing equipment and cleaning processes (Kulkarni, Maxcy, and Arnold 1975) but it sounds that recently more and more interests are given to CIP (Li et al., 2019). Even though decreasing labor and time for cleaning, CIP systems require significant capacities of water, detergent, and energy. In addition, in-place cleaning generates large quantities of waste water with additional economic burden for the industry and environmental burden for the general public (Lyndgaard et al., 2014). Not only it requires significant amount of water, recent studies have shown that standard Cleaning in Place practices does always ensure a safe cleaning practice and this resulted in a residual microorganisms left in the CIP parts or in the production sector in the industries. The following paragraphs highlights about some challenges that is facing the agro-food industries like water consumption and contamination

1.3. Challenges facing the agro-food industry

1.3.1. High water consumption for food production

IME (UK's Institution of Mechanical Engineers) claims that water requirements to meet food demand in 2050 could reach between 10-13.5tn cubic meters per year - about triple the current amount used annually by humans. For example today, 1kg of potatoes uses 287 litres of water for its production (The Guardian, 2013). Table 1.0 below shows the amount of water needed for the production of common foodstuff taking into account all the steps, starting from farming, culturing till its production in the industry. Chocolate being on the top of the list. It is obvious that from the values related to each item that water consumption is huge which clarify the fact that new measurements has to be taken in different sectors to reduce this consumption.

Table 1.0. Typical values for the volume of water required to produce common foodstuffs (Fox and Fimeche 2013)

Foodstuff	Quantity	Water consumption, litres
Source: IME		
Chocolate	1 kg	17 196
Beef	1 kg	15 415
Sheep Meat	1 kg	10 412
Pork	1 kg	5 988
Butter	1 kg	5 553
Chicken meat	1 kg	4 325
Cheese	1 kg	3 178
Olives	1 kg	3 025
Rice	1 kg	2 497
Cotton	1 x 250g	2 495
Pasta (dry)	1 kg	1 849
Bread	1 kg	1 608
Pizza	1 unit	1 239
Apple	1 kg	822
Banana	1 kg	790
Potatoes	1 kg	287
Milk	1 x 250ml glass	255
Cabbage	1 kg	237
Tomato	1 kg	214
Egg	1	196
Wine	1 x 250ml glass	109
Beer	1 x 250ml glass	74
Tea	1 x 250 ml cup	27

1.3.2. Water consumption in cleaning processes of food: the fresh-cut food industry

Depending on the food production sector, water and energy consumption can reach enormous levels which impose on the governments and owners to follow economical measurements. Food

production and processing are known to account for the majority of water use globally (Foster et al., 2006). The fresh-cut industry is one of the major water-intensive industries. Water consumption and wastewater volumes are generally in the range of 2–11 m³/t and 11–23 m³/t of fresh-cut product (Lehto et al., 2014; H. Ölmez 2014). This represents not only a tremendous waste of water but also an impressive waste of energy since most of this water is cooled at refrigeration temperature to accomplish fresh-cut processing needs. The minimization of water use and wastewater discharges are thus big challenges for the fresh-cut industry that will be increasingly required to implement sustainable strategies for water saving (Gómez-López et al., 2013; Hülya Ölmez and Kretzschmar 2009).

Figure 1.0 shows the flow of the product in a typical fresh-cut industry. Almost 90% of water is used to perform washing operations, including primary washing to remove gross contamination, a number of consecutive immersions of the product in washing tanks and a final rinse step (Lehto et al., 2014)

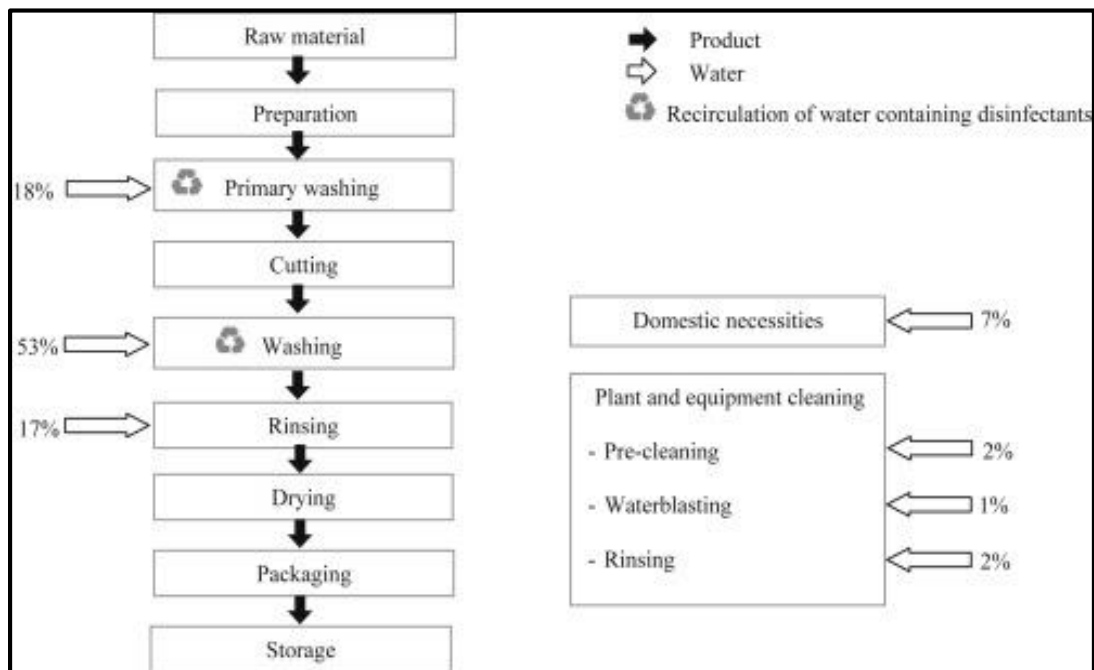


Figure 1.0. Product flow and water needs in a typical fresh-cut salad production process. Water needs of each step are expressed as percentage (v/v) of the overall water required in the process (Manzocco et al., 2015)

1.3.3. Water consumption in Cleaning Procedures.

Indeed water consumption for production of different food items is enormously huge, as it has been shown from the statistical data above. Decreasing water consumption in each step is crucial and it can be achieved through different strategies like water recycling, introducing new technologies as new regeneration processes by absorption-coagulation and flocculation of the cleaning solutions (Blel, Dif, and Sire 2015). In fresh-cut salad cleaning process, water amount can reach about 600L/ton of fresh-cut salad which constitutes 5% of the total water consumption as indicated in Figure 1.0 (plant and equipment cleaning). Furthermore, the dairy industry for instance, consumes large quantities of water for food processing. Depending on the final product (milk, cheese, yogurt or milk powder), water consumption can go from 0.6 L to as high as 6 L per liter of raw milk treated (EDA European Dairy Association, 2002). As for classical cleaning procedures such as Cleaning in Place (CIP), Figure 1.1 shows that in the dairy sector water consumption can reach up to 28% being the highest compared to other processes. Water consumption is imputable to food processing, with significant quantities required for cleaning operations.

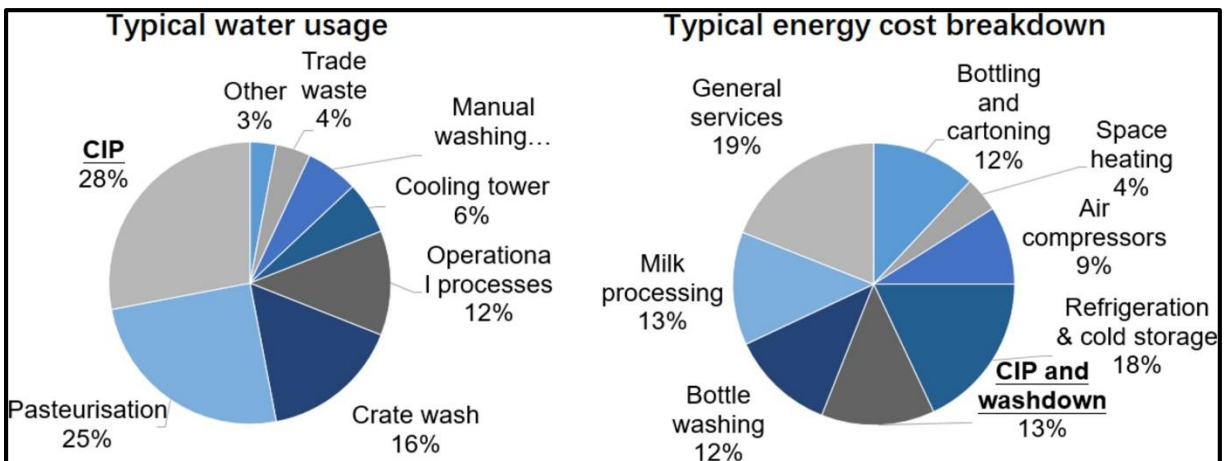


Figure 1.1. Breakdown of water usage and energy cost in dairy manufacturing (Dairy Australia, 2006)

1.4 Food contamination

Each year, various food products can be a source for illness or death in the human population as reported by the World Health Organization. Preventing contamination is a strict measure taken by agro-food industries. Frequent incidences of contaminated food products throughout history have

forced governments to take new preventive practices on produced local food items or imported nutrition goods.

1.4.1 World Food Contamination According to World Health Organization, WHO

Another important issue is that pathogenic microorganisms are the major security worry for the food industry. Food poisoning or foodborne disease (FBD) is one of the main problems in public health worldwide. Food contamination can be due to contamination from raw materials or during the processing stages or lack of good cleaning practices between production cycles. According to the WHO, each year 600 million people around the world, or 1 out of 10, become ill after consuming contaminated food. Among all these people, 420,000 die, including 125,000 children under 5 years of age, due to the vulnerability of this population to develop a diarrheal syndrome, about 43% of FBDs occur in these patients. About 70% of FBDs result from food contaminated with a microorganism (Kirk et al., 2015; WHO, 2015).

1.4.2. Food Contamination in France

Even if the microbes in food are eventually devastated by cooking, they can still produce toxins, so it is highly important to prevent contamination through the use of hygienic practices. Like microbial pathogens, spoilage entities can either be present naturally or gain access to food. (H. L. M. Lelieveld, John Holah, and M A Mostert 2005)

An example on product contamination in France, a total of 35 infants have fell sick with salmonella poisoning resulting from milk powder in France since August 2017. Due to this outbreak, 16 were hospitalized, an unusually high number that sparked fears of an epidemic.

1.5 Factors affecting cleaning in the industry

In order to understand the origin of obstacles that opposes the agro-food industries, it is necessary to understand the cleaning principles that can be summarized by Sinner's cycle. The mechanical action of the detergent which is a part of Sinner's cycle is also associated sometimes with the chemical action at the microscopic level. The following paragraphs protrude in the latter points.

1.5.1. Sinner's cycle

Herbert Sinner, a former chemical engineer for Henkel in 1959, has summarized the basic cleaning principles. Sinner's circle describes the four factors that can be manipulated in any cleaning procedure: chemical action, temperature, time, mechanical action. Based on this circle, the purpose is to show that the reduction of one factor (e.g by using less detergent) can be recompensed by any of the other three factors (time, mechanical energy, temperature). This concept is very useful although more recent research shows that this might not be fully true. An example is that enzymatic activity in enzymatic detergents is ruined when using hot water. This is due to the fact that in general enzymatic activity is retained up to 60°C (Chaplin and Bucke 1990) and these products operate in lukewarm water to achieve effective cleaning results (Mitidieri et al., 2006, Crutzen and Douglass 1999). Nevertheless, it is evident to understand that cleaning can be enhanced by applicable combinations of chemical and mechanical actions, time and temperature.

With the help of Sinner's circle, it is possible to compare the efficiency of different washing processes and how the four factors impact it. Moreover, this circle demonstrates how the four factors are strictly connected between each other to obtain reproducible or equal final washing results (Basso 2017)

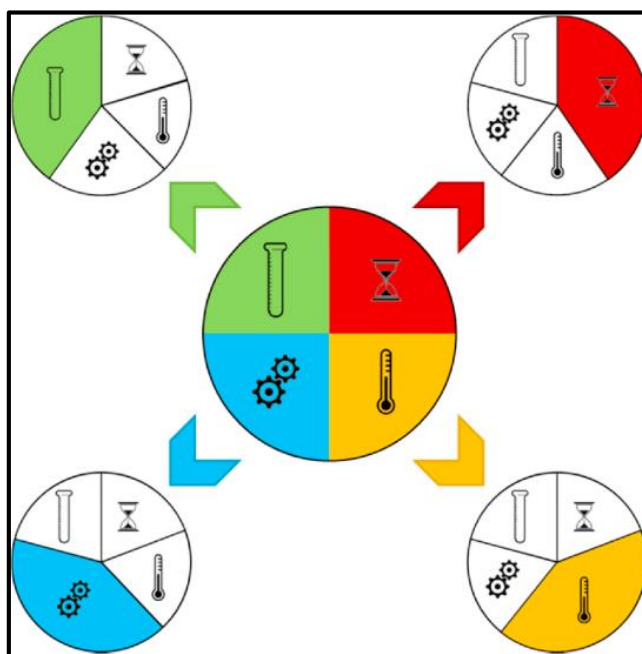


Figure 1.2. General representation of Sinner's circle: the increase in one factor allows decreasing the remaining three obtaining the same washing result (Basso 2017).

1.5.2. Factors implicated in Sinner's Cycle

In Sinner's cycle each factor has a different impact on cleaning performance ((Brown and Wray 2014; Berk 2013) :

- A. Temperature** is directly linked to the thermal energy transferred through water. Heat promotes an increasing reaction rate due to the higher kinetic energy of surfactant ions. As a result, the effective removal of dirt is much easier. Temperature has an impact also on surfactants' performances, in particular on their ability to form micelles or stabilize into liquid crystal phases (Basso 2017).
- B. Mechanical action** is represented by the forces and friction generated during the washing process. In a general case, these phenomena depend on the so-called liquor ratio, corresponding to the quotient of total water volume in the washing cavity to the wash mass. The synergy among mechanical and chemical action is fundamental to reach a good dispersion of detergent in the solution, to reach all the areas (Basso 2017).
- C. Chemical action** is fundamental in the washing process, which is based on the exploitation of chemical reactions and interactions (e.g., between dirt and surfactants) among cleaning products and dirt residuals. The types of chemical reactions involved comprise acid-base, oxidation-reduction and reactions in presence of solvents (among the latter, the most common being water). Moreover, the type of reaction or type of chemical species involved in the washing process can be organized through the correlation with different classes of dirt, as explained in Section "Factors affecting the cleaning processes." In general, the washing efficacy directly increases with the concentration of detergent in the washing solution, due to the higher quantity of active molecules which can react with dirt. Furthermore, it has to be taken into account that some limits to the increase of cleaning products concentration are given by the degradation phenomena which could take place on materials and components, compromising the integrity of the washing systems.
- D. Time** is the only factor reversely linked with mechanical action and concentration, but strictly correlated to temperature: the amount of time in which temperature is maintained is also important for disinfection effects. Moreover, the contact time between substrate, dirt

and washing agent must be balanced to allow the chemical reactions and interactions to take place, avoiding soil redeposit due to prolonged washing time (Basso 2017).

The Sinner's circle is then a useful qualitative tool in predicting the impact on the overall cleaning process of the main 4 inter-dependent factors, suggesting that a change in one of the parameters in Sinner's circle must be compensated for by changes in the other parameters (Friis and Jensen 2005).

1.6 Multi-functional compounds: Surface Active Agents

1.6.1 Detergents

A detergent is a surfactant or a mixture of surfactants with cleansing properties in dilute solutions (IUPAC - detergent (D01643)). Detergents are formed from principle and complementary components. The complementary components may act to enhance the performance and the appearance (López-Mahía et al., 2005). The main components remain as the base of detergents composition. In a detergent, surfactants are not the only active ingredient, however they can be considered as the most important one while the other active ingredients can only have an optimal effect in the presence of surfactants. Detergents are composed of surfactants and chelating agents, the role of the surfactant is implicated in dirt removal from soiled surface. The chelating agent is used to surround unneeded metal ions available in cleaning solutions. The chelating process can be very effective, however it is not always necessary and can increase the cost of the detergent. Builders can be a good alternative (Speight 2017).

Builders are added to a cleaning compound to improve the cleaning efficiency of the surfactants. Different functions are attributed to builders such as emulsifying, softening, buffering. They can soften water by deactivating hardness minerals (metal ions like calcium and magnesium) (Speight 2017).

1.6.2 Surfactants: Chemical Structure

The term surfactant (short for Surface Active Agents) designates a substance which exhibits some superficial or interfacial activity. The surfactant offers a wide range of properties depending on the use in specific industrial areas: capability to disperse, lubricate, softener, dampener. They are amphiphilic organic molecules exhibiting a double affinity also considered as a polar-non-polar duality. A typical amphiphilic molecule consists of two parts: on one hand a polar group which

contents heteroatoms such as O, S, P or N, included in functional groups; on the other hand, an essentially non-polar group which is in general a hydrocarbon chain of the alkyl or alkylbenzene type, sometimes with halogen atoms and even a few non-ionized oxygen atoms (Salager et al., 2002). Figure 1.3 shows Sodium Stearate (makes up about 50% of commercial surfactants) with its polar head and hydrocarbon tail. The relative size and shapes of the hydrophobic and hydrophilic parts of the surfactant molecule determine many of its properties. Surfactants with low branching in their alkyl chains in general show a good cleaning effect but poor wetting action, while more highly branched ones are good wetting agents with unsatisfactory detergency performance. If the number of carbon atoms is the same in the hydrophobic chains, wetting action increases strongly as the hydrophilic groups move to the center of the chain or as branching increases (Smulders et al., 2007).

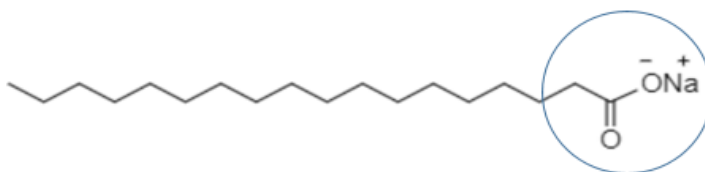


Figure 1.3 Sodium Stearate, the most common component of most soap, makes about 50% of commercial surfactants.

The polar head defines three groups of surfactants (Figure 1.4).

- A. **The ionic surfactant:** the hydrophilic head presents a positive and a negative charge. These types of surfactants ionize themselves in aqueous solution to give negative or positive charged ions. They are used in the cosmetics industry and assisted recovery of oil. For cationic surfactants, the head present positive charged ions where they are applied in the bituminous coal emulsion fabrication
- B. **The amphoteric surfactant:** the head has positive and negative localized charges. They are biodegradable and usually used in cosmetics industry.
- C. **The non-ionic surfactant:** the polar group does not present any type of charge. They are used in pharmaceutical applications.

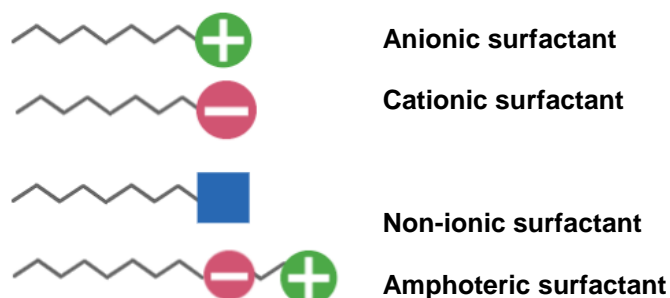


Figure 1.4 Surfactant groups according to their head charge.

The size of a surfactant molecule affects its diffusivity in solution. For example, proteins are large molecules that may have a high active surface, may not diffuse quickly to stabilize a surface that exists for only a short period of time. A surfactant layer must be adsorbed quickly enough to stabilize the bubble before it experiences a collision that risks coalescence (Pichot, Spyropoulos, and Norton 2009).

Industrial applications of these molecules is growing with time because of their physicochemical properties.

1.6.3. Micellisation

Two phenomena result from two opposing forces within the same molecule: adsorption and aggregation. For example, in aqueous media, surfactant molecules will migrate to air/water and solid/water interfaces to orientate in such a fashion as to minimize the contact between their hydrophobic groups and the water. This process is referred to as “absorption” and results in a change in the properties at the interface. Likewise, an alternative way of limiting the contact between their hydrophobic groups and the water is for the surfactants molecules to aggregate in the bulk solution with the hydrophilic head groups orientated towards the aqueous phase. These aggregates of surfactants molecules vary in shape depending on concentration and range in shape from spherical to cylindrical to lamellar (sheets/layers). The aggregation process is called “micellisation” and the aggregates are known as “micelles”. Micelles begin to form at a distinct and frequently very low concentration known as “critical micelle concentration” (CMC). The CMC is actually a narrow range of concentration over which the formation of micelles becomes dominant, ranging from nanomolar to several millimolar (McCaslin 2013). In simple terms, in aqueous media, micelles result in hydrophobic domains within the solution whereby the surfactant may solubilize or emulsify particular solutes (Farn 2008), like food oil, fats and proteins in the

case of detergents for food processing appliances. Temperature is one of the washing factors which heavily impacts on surfactants' performance, and in particular on CMC value: ionic and amphoteric surfactants show a clear change in hydrophobic and head group interaction with temperature, exhibiting a U-shape behavior with a minimum corresponding at about 25 °C (Mohajeri and Noudeh 2011; Kang, Kim, and Lim 2001). Non-ionic surfactants show a decrease in CMC with the increase of temperature: this is due to the demolition of hydrogen bonds between water molecules (Kim and Lim 2004, Tadros 2006), with some exceptions (Mohajeri and Noudeh 2011).

1.6.4. Different Actions of Surfactants

All the properties of surfactants described above can be associated with 4 different types of actions:

- A. **Wetting action:** the characteristic effect of surfactants is their ability to adsorb onto a surface and to modify the surface's properties, both at gas–liquid and at liquid–liquid interfaces, reducing the surface tension and the interfacial tension (Figure 1.5 a). Substrate–liquid and particle–liquid interfaces are influenced by adsorption of surfactants, with the decrease in the work required to remove the soil particle from the substrate due to the lower interfacial tensions in presence of adsorbed surfactants (Rosen and Kunjappu 2012).

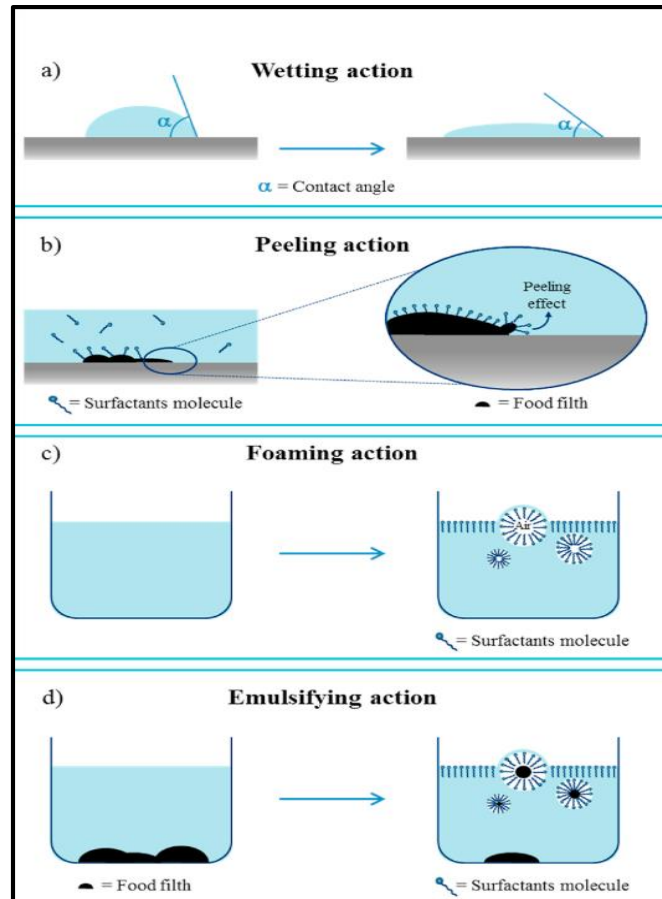


Figure 1.5 Different actions of surfactants in cleaning processes (Basso 2017).

- B. **Peeling action:** in some cases, surfactants are able to insert themselves among soil and substrate to separate them and increase soil suspension and cleaning efficacy of the mixture (Figure. 1.5 b).
- C. **Emulsifying action:** emulsions are defined as thermodynamically unstable two-phase systems consisting of at least two immiscible liquids, one of which is dispersed in the form of small droplets throughout the other, and an emulsifying agent (Figure 1.5 d). Surfactants have a key role in the suspension of dispersed soil, because of their double hydrophilic and hydrophobic nature. As emulsifying agents, surfactants concentrate is adsorbed onto the soil–water interface to provide a protective barrier around the dispersed droplets, reducing the interfacial tension of the system. This action is mechanical and can be used to decrease the amount of mechanical action required to form an emulsion (Tamime 2008).
- D. **Foaming action:** foam consists of a high volume fraction of gas dispersed in a liquid where the liquid forms a continuous phase. Surfactants generate foams through the stabilization of thin liquid films by layers of surfactant molecules (Figure 1.5 c). Foaming and the

control of foam is an important factor in the application of surfactants, particularly for detergents and cleansers (Sawicki 2005). For some applications, high foam is desired because it is understood as an important measure of washing performance by the consumer who expects the product to generate voluminous and dense foam. In other cases, only low foam is acceptable because the use of high foaming detergent would lead to an over foaming and furthermore to a decrease of the washing performance due to a damping of the mechanical action in the washing drum (Farn 2008).

In the following paragraphs we will briefly discuss the mechanical action of flowing foam and highlight on its usage in the agro-food industries.

1.7 Flowing Foam for Surface Cleaning

1.7.1 Mechanical properties of foam, a key parameter for cleaning.

Aqueous foams are complex fluids consisting of concentrated dispersions of gas bubbles in a soapy liquid. Foam can be wet or dry depending on the amount of water they contain. They have various original mechanical properties, which depends on density and high surface area combined with their ability to elastic response to low stresses, and to flow like a viscous liquid with large deformations.

Indeed, foam flows are governed by the properties of a thin liquid near wall region, which induces a sliding effect. The most important parameter in controlling the flow of foam would therefore be the thickness of this sliding layer (a few micrometers to a few tenth of micrometers). Foams mainly composed of gases have complex rheological properties which can be compared to those of a solid, but also to those of a liquid (Aloui and Madani 2008). In this case, the wall shear stress (tangential constraint) is a key parameter in the flows of these foams. This constraint, which plays an important role in the characterization of the rheological properties of the foam, depends mainly on the size of the bubbles and particularly on the volume fraction of the liquid (Chovet 2015; Chovet, Aloui, and Keirsbulck 2014).

Indeed, despite classical cleaning and disinfection procedures, some bacteria are still commonly found on the surfaces of food processing lines, mostly in the form of adherent spores, e.g. *Bacillus* spores in closed equipment (Peng et al., 2002) or in the form of biofilms, e.g. those partially composed of *Pseudomonas spp.* (Dogan and Boor 2003).

The role of hydrodynamics of foam and in particular of the mean wall shear stress and its fluctuations has been demonstrated in the case of the flow of conventional detergent solutions (W. Blé et al., 2010). Thus, the detachment mechanisms are related to shear, local vorticity of turbulence and pressure fluctuations.

1.7.2 Previous studies on flowing foam

Very little works have also been carried out on the elimination of surface deposits using gas-liquid two-phase flows (Kondjoyan et al., 2009), but to our knowledge none relates to the elimination of microorganisms. Foam is largely used throughout the food industries for the cleaning of open surfaces (floor, workshops and equipment). Foam characteristics as density, foam ability and quality based on void fraction were recently considered to study the cleaning of closed systems as ultrafiltration processes (Gahleitner, Loderer, and Fuchs 2013). But even if a better efficiency was demonstrated compared to standard CIP, the foam activity was studied under static conditions: the foam was streamed into the equipment for 2 min and kept in contact to the inner surfaces for 30 min, a limit to the foam stability. Therefore, foam flows would constitute an actual novelty in surface hygiene as low water load and high mechanical actions under moderate temperatures would permit a very good efficient cleaning and can easily be combined with disinfection.

1.7.3 Flowing Foam in cleaning practices.

Foam properties give rise to numerous industrial applications (nuclear engineering, petroleum engineering, agro-food (food), cosmetics, fire extinguishers, etc.). Despite the widespread use of aqueous foams, their use in the cleaning of agro-industrial plants can only be seriously considered on the basis of an appropriate knowledge of the internal structure of the foam (stability, drainage), and also its behavior at contact with surfaces.

The development of the agro-food industrial sector related to the extension of large mega-cities and the increase of the European population, would induce a conflictual demand in potable water and energy consumption becoming more and more expensive in the future.

The use of foam flow cleaning will meet such requirement in reducing the demand in water and energy in the industry while maintaining the high level requirements in food safety and reducing the high cost of the cleaning operations.

Reducing environmental impacts could be largely envisaged depending on the potential use of the foam flow process. Any potential application and/or industrial implementation will need further developments not included in this proposal.

Today, food industries use liquid single-phase turbulent flow (in the majority of cases potable water with cleaning agents) for most of the cleaning processes even for dry products processing. This study shows some research work which is based on a new process enable technology to reduce radically the amount of potable water used in cleaning processes of pipes. The proof of concept was already worked out for the cleaning of heat exchangers in French nuclear power-plants, where bio-fouling representing a significant issue in terms of loss of energy and generating high amount of contaminated waste water load to be treated.

1.8 References

- Aloui, F., and S. Madani. 2008. “Experimental Investigation of a Wet Foam Flow through a Horizontal Sudden Expansion.” *Experimental Thermal and Fluid Science* 32(4): 905–26.
- Avila-Sierra, A., J. M. Vicaria, E. Jurado-Alameda, and J. F. Martínez-Gallegos. 2020. “Removal of Food Soil by Ozone-Based Oxidation Processes: Cleaning and Wastewater Degradation in a Single Step.” *Journal of Food Engineering* 272: 109803.
- Basso. 2017. “Study of Chemical Environments for Washing and Descaling of Food Processing Appliances: An Insight in Commercial Cleaning Products - ScienceDirect.” <https://www.sciencedirect.com/science/article/pii/S1226086X17301582> (October 23, 2019).
- Berk, Zeki. 2013. “Chapter 28 - Cleaning, Disinfection, Sanitation.” In *Food Process Engineering and Technology (Second Edition)*, Food Science and Technology, ed. Zeki Berk. San Diego: Academic Press, 637–50.
- <http://www.sciencedirect.com/science/article/pii/B9780124159235000289> (October 24, 2019).
- Blel, W. et al., 2010. “Cleanability Study of Complex Geometries: Interaction between B. Cereus Spores and the Different Flow Eddies Scales.” *Biochemical Engineering Journal* 49: 40–51.
- Blel, Walid, Mehdi Dif, and Olivier Sire. 2015. “Effect of a New Regeneration Process by Adsorption-Coagulation and Flocculation on the Physicochemical Properties and the Detergent Efficiency of Regenerated Cleaning Solutions.” *Journal of environmental management* 155: 1–10.
- Brown, K. L., and S. Wray. 2014. “7 - Control of Airborne Contamination in Food Processing.” In *Hygiene in Food Processing (Second Edition)*, eds. H. L. M. Lelieveld, J. T. Holah, and D.

Napper. Woodhead Publishing, 174–202.

<http://www.sciencedirect.com/science/article/pii/B9780857094292500073> (February 2, 2020).

Chaplin, Martin F., and C. Bucke. 1990. *Enzyme Technology*. CUP Archive.

Chovet, Rogelio. 2015. “Experimental and Numerical Characterization of the Rheological Behavior of a Complex Fluid: Application to a Wet Foam Flow through a Horizontal Straight Duct with and without Flow Disruption Devices (FDD).” Université de Valenciennes et du Hainaut-Cambresis. <https://tel.archives-ouvertes.fr/tel-01192955/> (June 17, 2017).

Chovet, Rogelio, Fethi Aloui, and Laurent Keirsbulck. 2014. *Gas-Liquid Foam Through Straight Ducts and Singularities: CFD Simulations and Experiments*.

Clark, J.P. 2003. “Encyclopedia of Food Sciences and Nutrition | ScienceDirect.”

<https://www.sciencedirect.com/referencework/9780122270550/encyclopedia-of-food-sciences-and-nutrition> (October 15, 2019).

Crutzen, A., and M.L. Douglass. 1999. “Detergent Enzymes: A Challenge!” *Handbook of Detergents* 82: 639–90.

Deponte, Hannes et al. 2020. “Two Complementary Methods for the Computational Modeling of Cleaning Processes in Food Industry.” *Computers & Chemical Engineering* 135: 106733.

Dogan, Belgin, and Kathryn J. Boor. 2003. “Genetic Diversity and Spoilage Potentials among *Pseudomonas Spp.* Isolated from Fluid Milk Products and Dairy Processing Plants.” *Applied and Environmental Microbiology* 69(1): 130–38.

Farn, Richard J. 2008. *Chemistry and Technology of Surfactants*. John Wiley & Sons.

Foster, C., K. Green, M. Bleda, and P. | Dewik. 2006. “Environmental Impacts of Food Production and Consumption: Final Report to the Department for Environment Food and Rural Affairs.” <http://agris.fao.org/agris-search/search.do?recordID=GB2013202568> (January 24, 2020).

Fox, Dr Tim, and Ceng Fimeche. 2013. “GLOBAL FOOD WASTE NOT, WANT NOT.” : 36.

Friis, A., and B. B. B. Jensen. 2005. “11 - Improving the Hygienic Design of Closed Equipment.” In *Handbook of Hygiene Control in the Food Industry*, Woodhead Publishing Series in Food Science, Technology and Nutrition, eds. H. L. M. Lelieveld, M. A. Mostert, and J. Holah. Woodhead Publishing, 191–211.

<http://www.sciencedirect.com/science/article/pii/B9781855739574500116> (October 24, 2019).

- Gahleitner, B., C. Loderer, and W. Fuchs. 2013. “Chemical Foam Cleaning as an Alternative for Flux Recovery in Dynamic Filtration Processes.” *Journal of Membrane Science* 431: 19–27.
- Gómez-López, Vicente M. et al. 2013. “Operating Conditions for the Electrolytic Disinfection of Process Wash Water from the Fresh-Cut Industry Contaminated with E. Coli O157:H7.” *Food Control* 29(1): 42–48.
- H. L. M. Lelieveld, John Holah, and M A Mostert. 2005. “Handbook of Hygiene Control in the Food Industry - 1st Edition.” <https://www.elsevier.com/books/handbook-of-hygiene-control-in-the-food-industry/lelieveld/978-1-85573-957-4> (January 24, 2020).
- IUPAC. Compendium of Chemical Terminology, 2nd ed. (the "Gold Book"). Compiled by A. D. McNaught and A. Wilkinson. Blackwell Scientific Publications, Oxford (1997). Online version (2019-) created by S. J. Chalk. ISBN 0-9678550-9-8. <https://doi.org/10.1351/goldbook>.
- Kang, Kye-Hong, Hong-Un Kim, and Kyung-Hee Lim. 2001. “Effect of Temperature on Critical Micelle Concentration and Thermodynamic Potentials of Micellization of Anionic Ammonium Dodecyl Sulfate and Cationic Octadecyl Trimethyl Ammonium Chloride.” *Colloids and Surfaces A: Physicochemical and Engineering Aspects* 189(1): 113–21.
- Kim, Hong-Un, and Kyung-Hee Lim. 2004. “A Model on the Temperature Dependence of Critical Micelle Concentration.” *Colloids and Surfaces A: Physicochemical and Engineering Aspects* 235(1): 121–28.
- Kirk, Martyn D. et al. 2015. “World Health Organization Estimates of the Global and Regional Disease Burden of 22 Foodborne Bacterial, Protozoal, and Viral Diseases, 2010: A Data Synthesis.” *PLOS Medicine* 12(12): e1001921.
- Kondjoyan, Alain, Sabine Dessaigne, Jean-Marie Herry, and Marie-Noëlle Bellon-Fontaine. 2009. “Capillary Force Required to Detach Micron-Sized Particles from Solid Surfaces—Validation with Bubbles Circulating in Water and 2µm-Diameter Latex Spheres.” *Colloids and Surfaces B: Biointerfaces* 73(2): 276–83.
- Kulkarni, S. M., R. B. Maxcy, and R. G. Arnold. 1975. “Evaluation of Soil Deposition and Removal Processes: An Interpretive Review¹.” *Journal of Dairy Science* 58(12): 1922–36.
- Lehto, Marja, Ilkka Sipilä, Laura Alakukku, and Hanna-Riitta Kymäläinen. 2014. “Water Consumption and Wastewaters in Fresh-Cut Vegetable Production.” *Agricultural and Food Science* 23(4): 246–56.

- Li, Guozhen, Llewellyn Tang, Xingxing Zhang, and Jie Dong. 2019. “A Review of Factors Affecting the Efficiency of Clean-in-Place Procedures in Closed Processing Systems.” *Energy* 178: 57–71.
- López-Mahía, P., S. Muniategui, D. Prada-Rodríguez, and M. C. Prieto-Blanco. 2005. “SURFACTANTS AND DETERGENTS.” In *Encyclopedia of Analytical Science (Second Edition)*, eds. Paul Worsfold, Alan Townshend, and Colin Poole. Oxford: Elsevier, 554–61. <http://www.sciencedirect.com/science/article/pii/B0123693977006087> (October 24, 2019).
- Lyndgaard, Christian Bøge et al. 2014. “Moving from Recipe-Driven to Measurement-Based Cleaning Procedures: Monitoring the Cleaning-In-Place Process of Whey Filtration Units by Ultraviolet Spectroscopy and Chemometrics.” *Journal of Food Engineering* 126(Supplement C): 82–88.
- Manzocco, Lara et al. 2015. “Efficient Management of the Water Resource in the Fresh-Cut Industry: Current Status and Perspectives.” *Trends in Food Science & Technology* 46(2, Part B): 286–94.
- McCaslin, D. R. 2013. “Detergent Properties.” In *Encyclopedia of Biological Chemistry (Second Edition)*, eds. William J. Lennarz and M. Daniel Lane. Waltham: Academic Press, 644–48. <http://www.sciencedirect.com/science/article/pii/B9780123786302006721> (October 24, 2019).
- Mitidieri, Sydnei, Anne Helene Souza Martinelli, Augusto Schrank, and Marilene Henning Vainstein. 2006. “Enzymatic Detergent Formulation Containing Amylase from *Aspergillus Niger*: A Comparative Study with Commercial Detergent Formulations.” *Bioresource Technology* 97(10): 1217–24.
- Mohajeri, and Noudeh. 2011. “Effect of Temperature on the Critical Micelle Concentration and Micellization Thermodynamic of Nonionic Surfactants: Polyoxyethylene Sorbitan Fatty Acid Esters.” <https://www.hindawi.com/journals/jchem/2012/961739/abs/> (October 24, 2019).
- Ölmez, H. 2014. “Water Consumption, Reuse and Reduction Strategies in Food Processing, 2014 in Sustainable Food Processing.” : 401–34.
- Ölmez, Hülya, and Ursula Kretzschmar. 2009. “Potential Alternative Disinfection Methods for Organic Fresh-Cut Industry for Minimizing Water Consumption and Environmental Impact.” *LWT - Food Science and Technology* 42(3): 686–93.

- Pichot, R., F. Spyropoulos, and I. T. Norton. 2009. "Mixed-Emulsifier Stabilised Emulsions: Investigation of the Effect of Monoolein and Hydrophilic Silica Particle Mixtures on the Stability against Coalescence." *Journal of Colloid and Interface Science* 329(2): 284–91.
- Rosen, Milton J., and Joy T. Kunjappu. 2012. *Surfactants and Interfacial Phenomena*. John Wiley & Sons.
- von Rybinski, Wolfgang. 2007. "A - Physical Aspects of Cleaning Processes." In *Handbook for Cleaning/Decontamination of Surfaces*, eds. Ingegärd Johansson and P. Somasundaran. Amsterdam: Elsevier Science B.V., 1–55.
- <http://www.sciencedirect.com/science/article/pii/B9780444516640500024>.
- Salager, Jean-Louis et al. 2002. "Emulsification Yield Related to Formulation and Composition Variables as Well as Stirring Energy." 25(3): 11.
- Sawicki, George C. 2005. "Impact of Surfactant Composition and Surfactant Structure on Foam Control Performance." *Colloids and Surfaces A: Physicochemical and Engineering Aspects* 263(1): 226–32.
- Smulders, Eduard et al. 2007. "Laundry Detergents." In *Ullmann's Encyclopedia of Industrial Chemistry*, American Cancer Society.
- https://onlinelibrary.wiley.com/doi/abs/10.1002/14356007.a08_315.pub2 (January 24, 2020).
- Speight, James G. 2017. "Chapter Nine - Removal of Inorganic Compounds From the Environment." In *Environmental Inorganic Chemistry for Engineers*, ed. James G. Speight. Butterworth-Heinemann, 427–78.
- <http://www.sciencedirect.com/science/article/pii/B9780128498910000096> (May 14, 2020).
- Tadros, Tharwat F. 2006. *Applied Surfactants: Principles and Applications*. John Wiley & Sons.
- Tamime, A. Y., ed. 2008. *Cleaning-in Place: Dairy, Food and Beverage Operations*. 3rd ed. Oxford, UK ; Ames, Iowa: Blackwell Pub.
- The Guardian. 2013. "How Much Water Is Needed to Produce Food and How Much Do We Waste?" *the Guardian*. <http://www.theguardian.com/news/datablog/2013/jan/10/how-much-water-food-production-waste> (October 20, 2019).
- Villecco, Francesco et al. 2020. "Fuzzy-Assisted Ultrafiltration of Whey by-Products Recovery." *Euro-Mediterranean Journal for Environmental Integration* 5(1): 8.
- WHO. 2015. "WHO's First Ever Global Estimates of Foodborne Diseases Find Children under 5 Account for Almost One Third of Deaths." <https://www.who.int/news-room/detail/03-12-2015->

who-s-first-ever-global-estimates-of-foodborne-diseases-find-children-under-5-account-for-almost-one-third-of-deaths (October 15, 2019).

CHAPTER II**LITERATURE REVIEW****CHAPTER II****Microbial Attachment to Surfaces in Food Industries**

CHAPTER II

LITERATURE REVIEW

2.0 Abstract: Contamination reflects an economic and a health burden on many food industries that remain until today, a challenge to overcome. This chapter demonstrates some mechanisms of microbial attachment to abiotic surfaces from physical and microbiological approaches. Also it demonstrates the structure of spores and biofilms along with their respective impact on contaminating food industries. Indeed understanding the structure of spores and biofilm helps in understanding the capability of these organisms in contaminating different zones of closed processing equipment such as pipes, tanks...

2.1. Microbiological interactions with abiotic surfaces

The first study reported on the adhesion of microorganisms to surfaces (Zobell, 1943) described the adhesion of marine bacteria to submerged surfaces and showed that bacterial adhesion increased over time. Since that time, many efforts have been made to investigate, control or even reduce the contamination of equipment surfaces in various sectors i.e. agro-food industries, biotechnology, cosmetics, pharmacy, in

addition to hospitals (C. Faille et al., 2018; Wilson, 2002). However, despite the current focus on hygiene procedures in the food industries, it remains difficult if not impossible to produce foods free of microorganisms. Thus, the involvement in food contamination such as spores, or biofilms adhering to the surface of food processing equipment is widely recognized. For information, biofilms are communities of microorganisms attached to biotic or abiotic surfaces and embedded in a matrix made of self-produced extracellular polymeric substances (EPS). These biofilms represent a major challenge to the food industry because their formation is regularly observed on all materials, including polymers and stainless steel, thus compromising food safety and quality. Examples of the threat posed by these biofilms concern *Listeria monocytogenes*. Indeed, cross-contamination of food by *L. monocytogenes* can result from biofilms on food-contact surfaces including slicing machines and cutting boards, as well as on non-food contact surfaces such as floors or drain sinks (Rodríguez-López et al., 2018).

Biofilms are problematic in many food production sectors, such as breweries, dairies, poultry or red meat processing factories, as well as fresh-cut industries producing minimal processed vegetables and fruits (MPV) ready-to-eat (Brooks & Flint, 2008). Indeed even after hygiene

procedures these biofilms could be found on every surface that is in direct contact or not with food (Bénézech & Faille, 2018).

Biofilm formation is initiated with surface attachment by planktonic, free-swimming bacteria. that are (i) physicochemical interactions, including van der Waals', Lewis acid–base, hydrophobic, and electrostatic interactions; (ii) adhesion reinforcement through polymer excretion (Flint et al., 1997); and (iii) cell division. Factors known to be involved in adhesion can be grouped into (i) surface characteristics of both the substratum and the microorganism, including surface free energy and topography; (ii) environmental conditions, including transfer conditions and composition of the organic medium; and (iii) bacterial exopolymers (Dufrêne et al., 1996).

2.2 Physiochemical approaches for microbial adhesion on surfaces

Microbial cell surfaces are both chemically and structurally more complex and heterogeneous than most inert substratum surfaces (Handley, 2009), which complicates a physico-chemical approach of microbial adhesive interactions. For instance, the simple concept of distance remains valid for separation distances between inert surfaces up to several nanometers.

The spores belonging to the *B. cereus* group often has more appendages, with a spiral structure (Faille et al., 2010) and a diameter of around 10 nm (Plomp et al., 2005a). In some species, such as *B. cereus*, *B. thuringiensis*, or *B. pumilus* (Hachisuka et al., 1984), spores are surrounded by appendages, which vary in length (up to 2 μm) and in number among strains (Stalheim and Granum, 2001; Tauveron et al., 2006). Other species, like *Bacillus licheniformis* were devoid of exosporia, appendages, or any superficial features (Faille et al 2010). The ability of spores to adhere was also significantly affected by the presence of appendages for spores of the *B. cereus* group, but only to a slight extent when all species are considered. The presence of appendages would promote spore adhesion by facilitating spore penetration of the potential barrier, as hypothesized by the DLVO (Derjaguin, Landau, Verwey, Overbeek) theory (van Loosdrecht et al., 1989).

Two physico-chemical approaches, are available to describe microbial adhesive interactions. In the thermodynamic approach (Absolom, 1988; Busscher et al., 1984), the interacting surfaces are assumed to physically contact each other under conditions of thermodynamic equilibrium, i.e. reversible adhesion.

The thermodynamic approach is based on surface free energies of the interacting system. On the other hand the classical DLVO approach describes the interaction energies between the interacting surfaces on Lifshitz-van der Waals and electrostatic interactions and their decay with separation distance.

2.2.1 The Thermodynamic approach (Free energy theory)

In the thermodynamic approach towards microbial adhesive interactions, the interfacial free energies between the interacting surfaces are compared, as schematically illustrated in Figure 2.0. According to this comparison, this approach is expressed in the so-called free energy of adhesion in which γ_{sm} , γ_{sl} , and γ_{ml} are the solid-microorganism, solid-liquid, and microorganism-liquid interfacial free energies, respectively.

To predict from a physico-chemical perspective whether or not microbial interactions will occur, a free energy balance as expressed by equation 1 is essential:

$$\Delta G_{adh} = \gamma_{sm} - \gamma_{sl} - \gamma_{ml} \quad (1)$$

Obtaining a minimal free energy is a strive for all systems in nature. The system of interacting surfaces will also attempt to obtain a minimal state. Therefore, a microbial adhesion is favorable to occur from a free energy point of view, when ΔG_{adh} is negative ($\Delta G_{adh} < 0$), while adhesion is energetically unfavorable when $\Delta G_{adh} > 0$ (Bos et al., 1999).

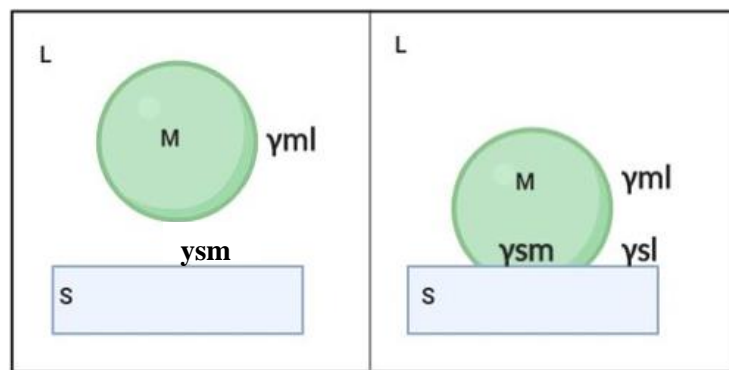


Figure 2.0. Schematic presentation of the interfacial free energies γ_{ij} involved in the adhesion of a microorganism (M) to a solid substratum surface (S) from a liquid suspension (L) (see also Eq. 1). Inspired from: (Rolf Bos et al., 1999)

2.2.2 DLVO Theories

For microbial adhesion, DLVO theories have proven merits up to a certain level when certain collections of strains and species are considered. Nevertheless the two systems have failed so far to yield a generalized description of all aspects of microbial adhesion that can be validated for each and every strain (van Loosdrecht et al., 1989).

Van Oss et al, (C. J. van Oss et al., 1989) introduced a so-called extended DLVO theory by including short-range Lewis acid-base interactions in the above, classical DLVO approach. Presence of acid-base interactions in the classical DLVO approach probably (Van Oss et al., 1988) implies that ‘hydrophobic attractive (J. Wood & Sharma, 1995) and hydrophilic repulsive (Elimelech, 1990; Pashley & Israelachvili, 1984) forces can be accounted for colloid and surface science in a more formal way.

2.2.2.1 Classical DLVO theory

While the Coulomb electrostatic interactions become dominant further away from the surface (Hori & Matsumoto, 2010), the Van der Waals forces are dominant in proximity of the surface, however, on contrary to Coulombs force, it decreases sharply as distance increases. In general, in aqueous solutions bacterial cells and natural surfaces are negatively charged. As the ionic strength of the surrounding aqueous medium decreases, this gives rise to an increasing repulsive electrostatic energy (van Loosdrecht et al., 1989). At low ionic strength, when a bacterial cell adheres a surface, it encounters an energy barrier that cannot be overcome exclusively by motility or Brownian motion; on the other hand ,at high ionic strength, this energy barrier disappears and bacterial cells can simply approach the surface and adhere irreversibly (Bolster et al., 2001). The total interaction force between a surface and a bacterium cell in the classical DLVO theory, is specified by the summation of Lifshitz-van der Waals (LW) attractive forces and electrostatic (EL) interactions (Li & Logan, 2004)

2.2.2.2 Extended DLVO theory

The new XDLVO theory suggests that the total interaction force between the surface and the bacterium, $F_{\text{XDLVOTotal}}$, can be considered as the vector sum of the Lifshitz-Van der Waals attraction (FLW), the electric double layer interactions (FEL), in addition to the new factor which

is the acid-base interaction (FAB) (Li & Logan, 2004). The XDLVO theory accounts for both interactions described in the DLVO, as well as for short range interactions, including hydrogen bonding, an ion pair formation, which are summarized as acid-base (AB) interaction forces (C. J. van Oss, 1993). Short range interactions were later added to the DLVO theory so that later was considered to be modified by van Oss into the extended DLVO (XDLVO) version (C. J. van Oss, 1993) (Figure 2.1). In the short-range, at separation distances of less than 1 nm between bacteria and the surface, The acid-base interaction forces are dominant, but they diminish exponentially in magnitude as the separation distance increases (C. J. van Oss, 1993).

$$F_{XDLVO}(Total) = FLW + FEL + FAB \quad (2)$$

The XDLVO theory was found to be more precise in predicting initial attachment of colloidal particles (Brant & Childress, 2002, 2004) and bacteria (Bayoudh et al., 2009) than the DLVO theory. This can be due to the integration of the acid-base interactions, which can considerably affect the direction of total force taking into account several nm separation distance between the bacteria and a surface. Their magnitude may be up to 100-times greater than that of EL and LW (Bos et al, 2000) . This added value generates a more sensitive model defining a more realistic way of comprehending microbiological interactions.

The AB interactions are an outcome of electron acceptor/electron donor interactions between polar moieties depending on the sign of electrical charges on the surface and bacteria, respectively. On the other hand, the LW interactions are attractive, whereas the EL interactions can be attractive or repulsive, depending on the polarity, or the hydrophobic-hydrophilic properties, the AB interactions can be attractive (hydrophobic attraction) or repulsive (hydrophilic repulsion or hydration effects). Figure 2.1 classifies the mentioned interactions.

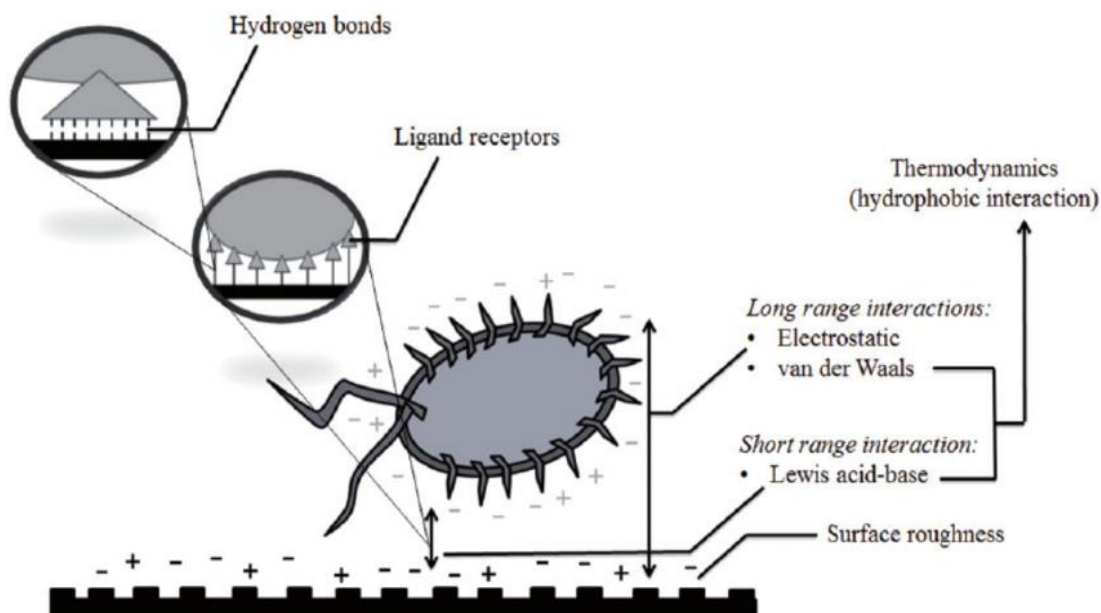


Figure 2.1 Physicochemical interactions/factors in systems of bacterial attachment to abiotic surfaces (DLVO , XDLVO theory) (Wang et al., 2014)

2.3. Properties and adhesion of bacterial spores

Some Gram-positive bacteria such as *Bacillus spp* and *Clostridium spp* have the ability to sporulate when they are subjected to stressful environments such as lack of nutrients in the environment (Leggett et al., 2012). Bacterial spores are a type of differentiated cells, metabolically inactive and highly resistant to heat, pressure, UV and chemicals (Clavel et al., 2004).

The sporulation process begins as soon as the sporangium asymmetrically divides to result in two compartments: the mother cell and the forespore where the two are separated by a septum. Then the forespore is engulfed by the mother cell, which is followed by membrane fission at the opposite pole of the sporangium that result in a double membrane bound forespore. The assembly of the coat begins after the initiation of the engulfment, which will continue throughout sporulation. In late sporulation, the peptidoglycan cortex is assembled between the inner and the outer forespore membrane. Finally, the mother cell will undergo lyses to release a mature spore to the environment. When nutrients are available with adequate environmental factors (temperature, pH..) , spores are capable of quickly germinating and resuming vegetative growth (McKenney et al., 2013). Figure 2.2 clarifies the sporulation phenomenon.

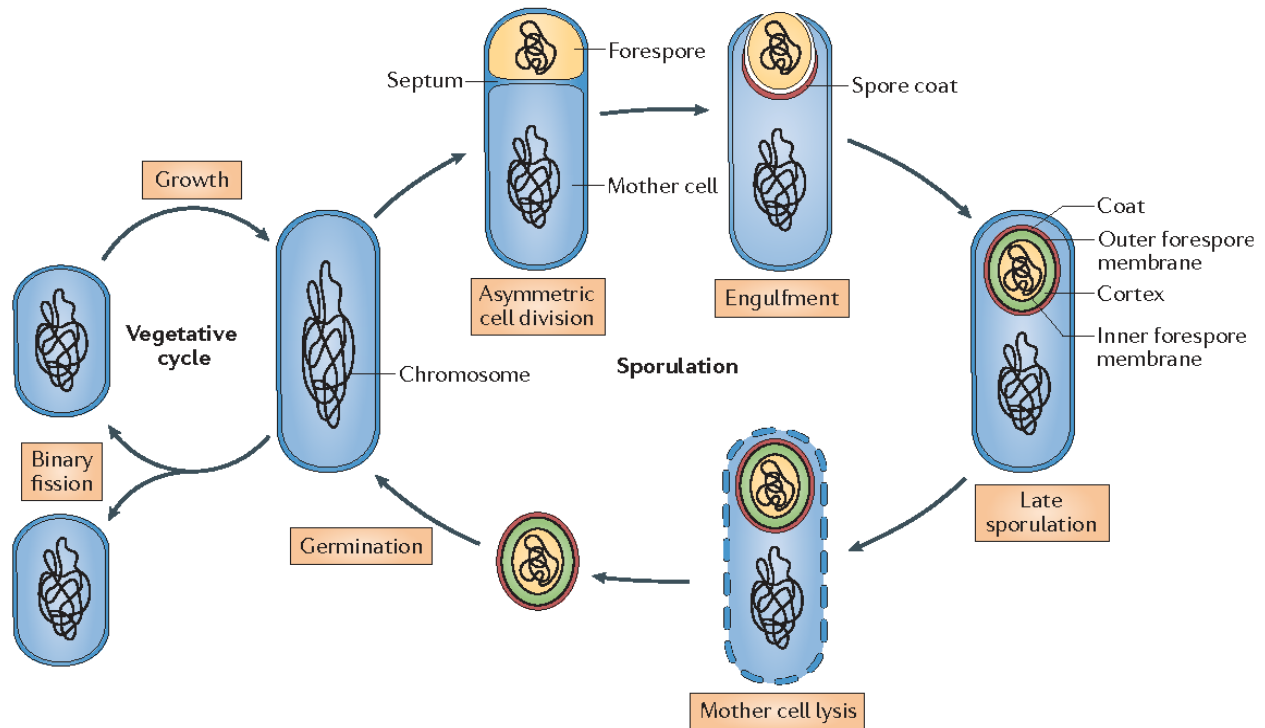


Figure 2.2 The sporulation and germination cycle in *Bacillus subtilis* (McKenney et al., 2013).

2.3.1 Structure of bacterial spores

The structure and chemical composition of bacterial spores differ considerably to those of vegetative cells. These differences are at the origin of the properties of resistance unique to spores. As shown in Figure 2.3, the spore consists of, from the outside towards inside: exosporium (for bacteria belonging to the *B. cereus* group), internal and external crust coat (in some species), an outer membrane, a cortex, an inner membrane and a core. *B. subtilis* spores do not have an outer layer, but they are surrounded by an outermost mucous layer (C. Faillie et al., 2014a), often referred to as the “crust”.

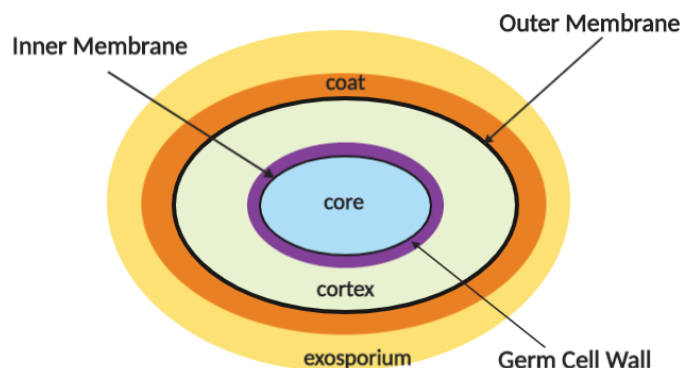


Figure 2.3 Schematic structure of a *B. cereus* spore. Sizes of various layers are not drawn to scale; in many species, several different coat layers can be seen; spores of some species do not have an exosporium. Inspired from: (Peter Setlow, 2014).

Since only the most superficial layers can affect the phenomena at interfaces between spores and materials, in other words adhesion, interaction strength and resistance to detachment, we will focus below on the composition and structure of the outer layers of *B. subtilis* and *B. cereus* strains.

2.3.2 Surface of *Bacillus cereus* spores

The exosporium is a loose balloon-like envelope which consists of a paracrystalline basal layer surrounded by an external hair-like nap (Henriques & Moran, 2007). Previous works performed at PIHM showed the presence of an exosporium around spores from strains belonging to the *B. cereus* group, which includes *B. anthracis* and *B. thuringiensis* (Faille et al., 2010). The exosporium is composed of about proteins and glycoproteins (43-52% of the dry weight) but it also contains 15-18% of lipids, 20-22% of carbohydrates and 4% of ash containing both calcium, magnesium and some undetermined compounds (Leggett et al., 2012). The roles of the exosporium are multiple; it provides resistance to chemical and enzymatic treatments. In addition, it improves the adhesion properties of spores to different surfaces and plays a role in germination (C. Faille et al., 2007)

However, spores of the *B. cereus* group differ in their exosporium characteristics: their length varies from 2.0 to 3.2 μm , and the hair-like nap length from 25 to 60 nm. Although more than 20 proteins have been identified as being associated with exosporium, their abundance, their relationship with other proteins and the processes by which they are assembled to create exosporium are largely unknown (Stewart, 2017). Conversely, the hair-like nap is mainly

composed of the collagen-like glycoprotein BclA which plays an important role in the hydrophobicity and the adhesion properties of spores (Lequette et al., 2011).

In *B. cereus* spores, spores are surrounded by appendages of about 10 nm in width and of unknown function, which vary in length (up to 2 μ m) and in number (between 0 and 20 per spore) among strains (C. Faille et al., 2010).

Lastly, concerning the physicochemical properties, *B. cereus* spore surface is hydrophobic to highly hydrophobic, as indicated by their affinity to an apolar solvent, the hexadecane.

B. cereus represents a significant cause of food poisoning (variable incidence, usually 1–3%). It is widely present in various raw or processed food products such as rice, vegetables, turkey meat and spices (Cohen et al., 2010).

Two types of illnesses arise as a result of consumption of food contaminated with *B. cereus*, emetic and diarrheal. The emetic syndrome is usually associated with starchy foods such as fried rice, pasta, etc. The illness is caused due to the ingestion of a pre-formed toxin in food (i.e., intoxication). The diarrheal syndrome, on the other hand, is associated with other types of foods such as milk, salads, and meat. Unlike the emetic syndrome, the diarrheal illness is caused by ingesting a large number of bacterial cells (i.e., toxico-infection). Healthy individuals usually recover from *B. cereus* illness within a day or two but patients who have other health issues might suffer serious complications. To control this bacterium in food, proper cooking and rapid cooling are required to prevent spores from germinating (El-Arabi & Griffiths, 2013).

2.3.3 Surface of *Bacillus amyloliquefaciens* spores

B. amyloliquefaciens is a spore-forming Gram-positive bacterium, rod-shaped and catalase-positive. The spores are surrounded by an external layer of variable thickness and regularity. The outer layer of *B. amyloliquefaciens* 98/7 spores has been the subject of extensive studies at UMET (Faille et al., 2014). The mechanical removal of this thick layer did not affect their resistance to heat or their ability to germinate but rendered the spore less hydrophilic, more adherent to stainless steel, and resistant to cleaning. This layer was mainly composed of 6-deoxyhexoses, i.e rhamnose, 3-*O*-methyl-rhamnose and quinovose, but also of glucosamine and muramic lactam, known also to be a part of the bacterial peptidoglycan. The specific hydrolysis of the peptidoglycan using lysozyme altered the structure of the required mucous layer and affected the physico-chemical

properties of the spores. Such an outermost mucous layer has also been seen on spores of *B. licheniformis* and *B. clausii* isolated from food environments (Faille et al., 2014).

2.3.4 Resistance properties

The specificity of spores compared to vegetative cells is their remarkable resistance to heat. Spores of some *B. subtilis* strains, for example, can survive wet heat of 100 ° C, with a D value (decimal reduction time, the time required to lower the population by a factor 10) between 20 and 30 min depending on the strains (Nicholson et al., 2000). In addition, spores are approximately 1000 times more resistant to dry heat than moist heat (Nicholson et al., 2000). The damage to spores caused by heat and chemical agents as well as the factors involved in resistance to these agents are summarized in Table 2.0 below.

Table 2.0 Factors involved in the resistance of spores to heat and chemicals.

<i>Bacillus</i> strain	D-value (min)	Reference
<i>B. cereus</i> in phosphate buffer	D ₁₂₁ =2.35	(Bradshaw et al., 1975)
<i>B. cereus</i> in pork luncheon meal	D ₁₀₀ =2.02	(Byrne et al., 2006)
<i>B. cereus</i> in infant formula with 10% total solids	D ₁₀₀ =1.8	(Stoeckel et al., 2013)
<i>B. cereus</i> in infant formula with 50% total solids	D ₁₀₀ =3.5	(Stoeckel et al., 2013)
<i>B. cereus</i> in water	D ₉₀ =2.5	(Stoeckel et al., 2014)
<i>B. cereus</i> in beef slurry	D ₁₀₀ =0.42	(Evelyn & Silva, 2015)
<i>B. licheniformis</i> in UHT milk	D ₁₀₀ =2.37	(Janštová & Lukášová, 2001)
<i>B. subtilis</i> in phosphate buffer	D ₁₀₀ =0.5	(Jagannath et al., 2005)
<i>B. megaterium</i> in tomato juice	D ₁₀₀ =1.6	(Gibbiel et al., 1973)

2.3.5 Spores and contamination in food industry

In the food industries, *Bacillus* spores have been isolated from a wide variety of food items such as pasta, rice, milk and eggs (Desai & Varadaraj, 2010). Many factors affect the presence of *Bacillus* spores in a range of food industries. For example, the presence of spores in dairy products (cheese, milk) has been stated to be due to the initial contamination of the raw milk and subsequent temperature abuse during transportation and distribution (Burgess et al., 2010).

During food processing, a pasteurization step will kill almost all the vegetative cells, while most bacterial spores will resist this heat-treatment. Therefore, such a treatment may provide a suitable environment for the subsequent germination and growth of *Bacillus* spores. The incidence of *B.*

cereus in cooked rice and meat has been reported to be a result of slow cooling and prolonged storage at room temperature. This will lead to spore germination and growth (Ankolekar et al., 2009). The source of contamination can be *B. cereus* spores or *B. cereus* biofilms. During food processing, this can lead to spoilage, food poisoning, and quality issues. *Bacillus* cells are capable to attach on stainless steel surfaces, grow to form microcolonies which produce extracellular polymeric substances (EPS). Over time they will aggregate to form biofilms in areas within the processing parts such as processing lines, storage tanks, and at sites that are hard to clean (Marchand et al., 2012; Shi & Zhu, 2009).

B. cereus biofilms may contain spores and vegetative cells. These biofilms have been reported to be more resistant to antimicrobials, disinfectants, cleaning procedures than the counterpart vegetative cells (Wirtanen et al., 1996). Once the biofilms are detached, spores can be released resulting in contamination of other surfaces or other food products while being processed (C. Faille et al., 2014b; Poulsen, 1999). The control of sources of contamination resulting from spores is an interesting area of research. Bulk processing and storage at room temperatures above 4°C, in addition to lack of ability to eradicate *B. cereus* spores by pasteurization (72°C for 15 seconds), also contribute to the prevalence of these microorganisms in food. *B. cereus* spores may remain in food products without causing harm for long periods. Once the conditions are favorable, spores can germinate, then multiply. Germination of spores, then growth and replication of vegetative cells to a range of 10^5 up to 10^8 cfu.ml⁻¹ in food can result in diarrheal food poisonings (Granum et al., 1993). Emetic when *B. cereus* cells produce a toxin called cerulide in food, emetic food poisoning can occur. This can cause vomiting within 5 to 6 h after consumption if the concentration exceeds 0.01 mg/g (Agata et al., 2002; Granum & Lund, 1997; Messelhäuser et al., 2014).

As vegetative cells are ingested, diarrheal food poisoning occurs. The cells multiply in the human intestine to produce a range of diarrheal enterotoxins, known as Hbl, Nhe, and CytK (Melling et al., 1976; Lindbäck and Granum, 2006). These toxins of *B. cereus* can cause the symptoms of food poisoning such as vomiting, nausea, and diarrhea (Granum & Lund, 1997).

2.4 Biofilms: structure, contamination in food industry

2.4.1 Biofilm formation

A biofilm consists of microbial cell groups with a system of internal channels or voids in the extracellular polysaccharide and glycoprotein matrix (Carpentier & Cerf, 1993). This allows nutrients and oxygen to be transported from the bulk liquid to the cells (Kostyál et al., 1998; Stoodley et al., 1994). Biofilm formation is a relatively slow process and can reach millimeters thickness in a few days depending on the culture conditions (Melo et al., 1992). Microorganisms in a biofilm are not uniformly distributed. They grow in the form of micro-colonies trapped in a matrix interspersed with channels very permeable to water (J. W. Costerton et al., 1994). The composition of a biofilm can be heterogeneous, due to colonization by different microorganisms possessing different nutritional needs. Biofilms do not necessarily exist in the form of uniform layer over the entire surface of the substrate. Increasing the size of a biofilm is favored by the deposition or fixation of other organic and inorganic solutes and particles present in the surrounding liquid phase (Melo et al., 1992). There are a number of mechanisms by which many microbial species can come into close contact with a surface, attached firmly, promote intercellular interactions and grow complex structures. Biofilm formation involves different stages and the mechanism of the formation of biofilms has been widely described by several researchers (Bryers & Ratner, 2004). Identified processes governing the formation of biofilms are presented in Figure 2.4.

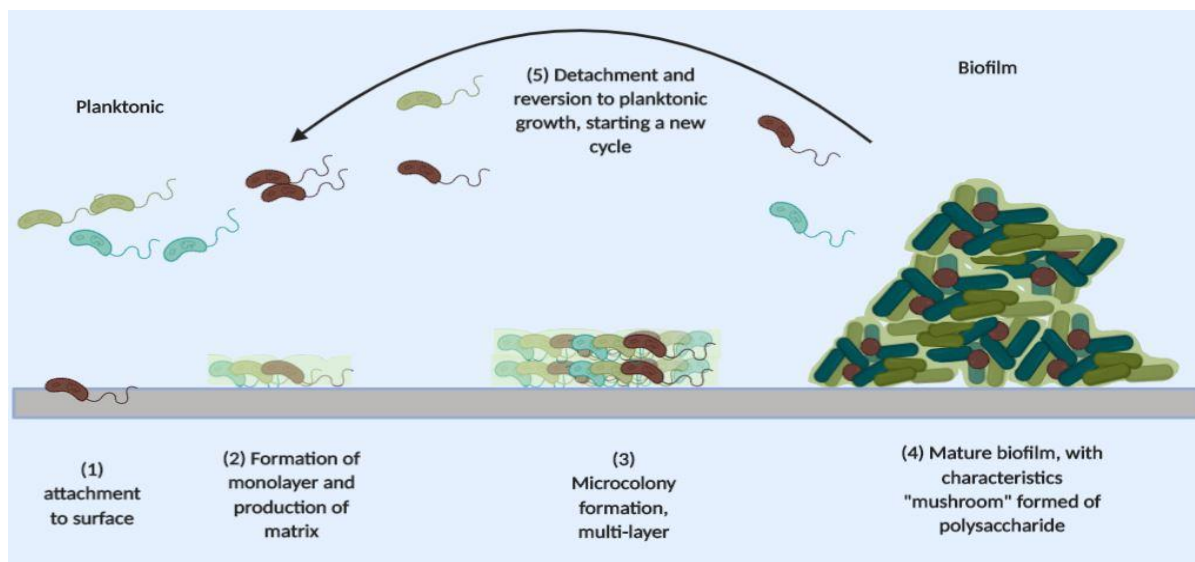


Figure 2.4. Different steps of biofilm formation. Inspired from: (Vasudevan R, 2014).

1. Planktonic cells start a reversible attachment on the surface.
2. A monolayer of bacteria is formed and irreversibly attach while producing an extracellular matrix.
3. Next, a micro-colony is formed where multilayers appear.
4. At the last stages, the biofilm is mature thereby forming a mushroom structure because of the produced polysaccharides.
5. Finally, some cells start to detach and dispersion of the biofilm will occur.

Biofilm can regularly be produced by any microbes under appropriate circumstances, even though some microorganisms naturally have a higher trend to produce a biofilm than others.

2.4.2 Extracellular polymeric substances (EPS)

Most bacteria can produce extracellular polymeric substances (EPS) which form a matrix in which biofilm cells are embedded. This matrix is involved in the strong adhesion of bacteria to surfaces and in the formation of complex biofilms. The EPS are composed for the most part of structural components, polysaccharides, proteins, and DNA, but also of other molecules such as enzymes, lipids, phospholipids, biosurfactants and mostly of water. In most biofilms, the microorganisms account for less than 10% of the dry mass, whereas the matrix can account for over 90% (Wingender and Flemming, 2010). The composition of biofilm matrix formed by different bacterial species markedly differed, but a great heterogeneity is also observed between strains from a single species. It is notably the case for *B. subtilis* strains. Indeed, the matrix produced by the strain NCIB 3610 mainly consists of an exopolysaccharide in combination with the proteins TasA and BslA (Romeroel al., 2017) whereas that of the strain B-1 is reported to consist primarily of γ -polyglutamate (Morikawa et al., 2006). The functions of the EPS matrix are various: stabilization of the structure of the biofilm; formation of a protective barrier against biocides, desiccation or other harmful effects; sorption of exogenous organic and inorganic compounds from the environment; retention of water; accumulation of enzymatic activities, such as those involved in the digestion of exogenous macromolecules, cooperation between cells, and lastly communication between cells.

2.4.3 *P. fluorescens*, a biofilm former

P. fluorescens is a common Gram-negative, rod-shaped bacterium (Holt & Misfeldt, 1984; Nernst, 1904). *P. fluorescens* can cause bacteremia in humans, with most reported cases being attributable either to transfusion of contaminated blood products or to use of contaminated equipment associated with intravenous infusions. Although not suspected of being an etiologic agent of pulmonary disease, there are a number of reports identifying it in respiratory samples. There is also an interesting association between *P. fluorescens* and human disease, in that approximately 50% of Crohn's disease patients develop serum antibodies to *P. fluorescens* (Scales et al., 2014). Many of the numerous species of genus *Pseudomonas* are used in biotechnology. *Pseudomonas* species take advantage of biofilm growth, which generally increases their resistance to various negative environmental influences and enables them to inhabit a broad range of niches and colonize the soil matrix, plant tissue, etc. *Pseudomonas* biofilm formation. As described above, biofilm formation is a targeted process driven by sophisticated regulatory mechanisms, both at the single-cell level and at the level of cell populations (Masák et al. 2014).

2.4.4 Resistance of biofilm bacteria to antimicrobial compounds

According to Jefferson (Jefferson, 2004) the formation of biofilms allows microorganisms to defend against difficult conditions via colonization of favorable niches, ensuring protection and access to nutrients. So, the benefits of life for a microorganism within a biofilm are:

- Protection and defense: reducing the effects of turbulence (Sutherland, 2001); reduction of environmental aggressions related to the presence of molecules intended to destroy the cells such as antibiotics or disinfectants but also against cleaners designed to weaken, cut ... and eliminate biofilms from surfaces (J. William Costerton et al., 1985; Nichols, 1989).
- Colonization: by reduction of the diffusion of exo-enzymes (Sutherland, 2001) and the increase in nutrient concentration (van Loosdrecht et al., 1990).
- Community: the possibility of optimal organizations, thanks to the transfer of signals between cells intended to circulate "genetic information" such as resistance genes (L. Morton & Gaylarde, 2001). The dynamics of training and development of biofilms facilitates the transmission of pathogens by providing a stable protective environment. The

biofilm acts as a source of diffusion of a large number of microorganisms in the environment. Biofilm clusters can be detached either by mechanical action due to a flowing fluid (sloughing) (Hall-Stoodley & Stoodley, 2005) or chemical action (acidic or basic surfactants).

Bacteria in biofilms are inherently more tolerant to antimicrobials when compared to planktonic cells of the same strain. Several factors have been suggested to account for the extraordinary resistance of bacteria within biofilms (Bridier et al., 2011). The matrix has long been considered the major contributor, in particular by limiting the diffusion of biocides, due to the presence of numerous adsorption sites, or by accumulating enzymes able to degrade some biocides. This role of the matrix was highlighted more than 20 years ago, for example on the mixed biofilms of *Klebsiella* and *Pseudomonas*. Indeed, the concentration of chlorine in the depth of these biofilms was less than 20% of that of the fluid in contact (de Beer et al., 1994). However, the supporting evidence for this is conflicting probably due to the great variability of molecules found in matrix produced by different bacterial species or even strains. Conversely, reduced growth rate within biofilms, due to deprivation of nutrients and/or of oxygen, appears to play a far more evident role in biofilm resistance, as does the "biofilm phenotype". Indeed, bacteria in biofilms display unique gene-expression patterns, resulting in phenotypic changes including the increase resistance to antibiotics and disinfectants. Lastly, different studies have generated evidence suggesting that biofilms may constitute an optimum environment for the exchange of genetic material by conjugation or transformation processes. One of the consequences of these exchanges is the dissemination of biocide resistance cassettes within the bacterial population. It's also important to remember that real-environment biofilms are formed of several species. Indeed, numerous studies have demonstrated that multi-species biofilms are generally more resistant to disinfection than mono-species (Bridier et al., 2011).

In some of the studies, it has been shown that disinfectants such as peracetic, have no effect on biofilms located on open surfaces and in particular floor coverings (Carpentier & Cerf, 1993). It has also been reported that *Listeria monocytogenes* adhered to a food surface showed increased resistance to conventional disinfectants such as anionic acid and quaternary ammonium compounds (Frank & Koffi, 1990; Mustapha & Liewen, 1989; Petrocci, 1983). The reasonable explanation for the reduced effectiveness of these agents against biofilms is the incomplete

penetration into the biofilm by these biocides (Huang et al., 1995), and the wide variation of environmental conditions existing on the contact surfaces with food. The presence of abiotic particles, kaolin and calcium carbonate in biofilms of *Pseudomonas aeruginosa* and *Klebsiella pneumoniae* is also involved in reduction of biocide efficiency (Srinivasan et al., 1995). In addition, antimicrobial agents are much more effective against cells during their active growth than is to say that the best disinfectant for the planktonic cells is not necessarily suitable for Biofilm cells (Holah & Thorpe, 1990). The cells in the deep layer of the biofilm receive less oxygen and nutrients than that on the surface of the biofilm (Brown et al., 1988). We talk about dormant cells or simply very weak growth where its modified physiology implies an increase in resistance to antimicrobial agents (Evans et al., 1991). In mixed biofilms, nutrient competition causes nutrient deficiency, which also has a major role in biofilms resistance to antimicrobial agents (Berg, Matin, and Roberts 1982; Jones and Lock 1989). Some studies of bacteria from contaminated foods have shown that resistance against disinfectants is more severe in old biofilms (more than 24 hours) than in young biofilms (Anwar et al., 1990). Several authors have demonstrated the increasing resistance of bacterial biofilms to antibiotics (Anwar et al., 1992; Widmer et al., 1990). The possible mechanism proposed for this resistance to antimicrobial substances by bacteria is the production of enzymes that degrade these substances, i.e. lactamases. These enzymes degrade and inactivate the antibiotics that enter through the envelope of the cell at their target sites. Within biofilms, many enzymes with similar hydrolytics have been found and are suspected of participating in the protection of bacterial biofilm. In addition, the resistance of biofilms may also be due to more trivial way to the bacteria themselves.

2.4.5 Biofilms contamination in Food industries

In food environments, biofilms are often found on products (vegetables, meat...), but also on surfaces of food processing lines such as pipes, vessels, or valves, floors, walls or drains. Indeed, food-processing environments provide a variety of conditions, which might favor the formation of biofilm, e.g. the presence of moisture and nutrients. Among bacteria which can form biofilms in food environments is *Pseudomonas fluorescens* which has been frequently isolated from equipment and utensil surfaces. it can form thick biofilm, difficult to manage and therefore it becomes a source of food spoilage. In real environments, biofilms are often composed of many

bacterial species and often referred to as mixed biofilms which have shown to be more stable than single-species biofilms (Mosteller & Bishop, 1993). This may be important on plant surfaces, where many species are potentially present.

When the environmental conditions are favorable, many microorganisms pathogenic or not would form biofilms both on food and on surfaces potentially in contact with foodstuffs.

We can mention the work on *listeria monocytogenes* (Frank & Koffi, 1990; Herald & Zottola, 1988a), *Yersinia enterocolitica* (Herald & Zottola, 1988b), *Campylobacter jejuni* (Kuusela et al., 1989) and *Escherichia coli* O157: H7 (Dewanti & Wong, 1995). Recent problems were related to the presence of *E. coli* O157: H7 on meat products or enterohemorrhagic *E. coli* (ehc) on plant products.

There are studies on composition of microbial biofilms that form on the surface of treatment equipment. Various industries have been described in several studies (Gunduz & Tuncel, 2006; Sharma & Anand, 2002).

The mentioned investigations have shown the presence of these ‘pathogenic’ biofilms both within machines and on the surfaces adjacent to food.

The health risks in dairy industries according to Kirtley & McGuire (1989) are due to the presence of biofilms on surfaces, microbial colonization of milk storage tanks, fouling of the heat exchange surfaces and the presence of sporulated forms on the packaging and packaging materials. *B. cereus* spores for example, present in raw milk before treatment can remain on some parts of the equipment, in heat exchange zones because of their thermo-resistance which favors their germination and their development in the form of biofilms, thus contaminate the finished product (Te Giffel et al., 1997).

A contamination of milk can be associated with rinsing water that lead to contamination of pasteurized milk packaging by Gram (-) psychotrophic bacteria. This can suggests that these bacteria have formed biofilms in the rinse water distribution system.

Another study by Langeveld (Langeveld et al., 1995) in a pilot plant at the laboratory showed an increase in bacterial concentration by a factor of 10^6 . Thus in their experiment, they heated up milk in a tubular stainless steel exchanger and showed the direct link between the density of bacteria on the walls of the tubes and the concentration of contaminants in the milk after heating.

Langeveld et al., (1995) and Murphy et al., (1999), suggest that the presence and the increase in bacterial contamination of milk is the consequence of a prior contamination of equipment used for

milk processing. Works by Scott (Scott et al., 2007) identify the origin of milk powder contamination by Spore-forming bacteria at the preheating exchangers of milk and the evaporator. The spores were detected between 9 and 18h after the start of production. One of the consequences was the presence of 10^6 cfu.ml⁻¹ in the finished product after 18h.

2.5 Summary

Microorganism contamination is considered to be a basic hurdle for a wide range of food industries. Different studies have been performed for understanding microbial adhesion from different physical approaches such as free energy theory, classical DLVO theory and extended DLVO theory. Also from a biological point of view, microbial membrane integrated structures such as appendages aid the microbe in attachment. As for spores, the exosporium improves the adhesion properties of spores to different surfaces. Exosporium differs in its structure even in the same group of bacteria. Even though many processes have been developed to eradicate spores like pasteurization, however, still spores are able to withstand these treatments. Sometimes under suitable temperature re-germinate, and in a second stage grow to form larger structures such as biofilms. Biofilms can be formed on many surfaces related to pipes, plants, valves.. Many health risks have been reported are associated with biofilm contamination. As vegetative cells are ingested, diarrheal food poisoning occurs. The cells multiply in the human intestine to produce a range of diarrheal enterotoxins thus causing vomiting, nausea, water loss. The control of the source of contamination is an important and interesting field of research.

2.6 References:

- A, A., U, R., & Pe, G. (1995). What problems does the food industry have with the spore-forming pathogens *Bacillus cereus* and *Clostridium perfringens*? *International Journal of Food Microbiology*, 28(2), 145–155. [https://doi.org/10.1016/0168-1605\(95\)00053-4](https://doi.org/10.1016/0168-1605(95)00053-4)
- Absolom, D. R. (1988). The role of bacterial hydrophobicity in infection: Bacterial adhesion and phagocytic ingestion. *Canadian Journal of Microbiology*, 34(3), 287–298. <https://doi.org/10.1139/m88-054>
- Agata, N., Ohta, M., & Yokoyama, K. (2002). Production of *Bacillus cereus* emetic toxin (cereulide) in various foods. *International Journal of Food Microbiology*, 73(1), 23–27. [https://doi.org/10.1016/S0168-1605\(01\)00692-4](https://doi.org/10.1016/S0168-1605(01)00692-4)

- Ankolekar, C., Rahmati, T., & Labbé, R. G. (2009). Detection of toxigenic *Bacillus cereus* and *Bacillus thuringiensis* spores in U.S. rice. *International Journal of Food Microbiology*, 128(3), 460–466. <https://doi.org/10.1016/j.ijfoodmicro.2008.10.006>
- Anwar, H., Dasgupta, M. K., & Costerton, J. W. (1990). Testing the susceptibility of bacteria in biofilms to antibacterial agents. *Antimicrobial Agents and Chemotherapy*, 34(11), 2043–2046.
- Anwar, H., Strap, J. L., & Costerton, J. W. (1992). Eradication of biofilm cells of *Staphylococcus aureus* with tobramycin and cephalexin. *Canadian Journal of Microbiology*, 38(7), 618–625. <https://doi.org/10.1139/m92-102>
- Bayouhdh, S., Othmane, A., Mora, L., & Ben Ouada, H. (2009). Assessing bacterial adhesion using DLVO and XDLVO theories and the jet impingement technique. *Colloids and Surfaces B: Biointerfaces*, 73(1), 1–9. <https://doi.org/10.1016/j.colsurfb.2009.04.030>
- Bénézech, T., & Faille, C. (2018). Two-phase kinetics of biofilm removal during CIP. Respective roles of mechanical and chemical effects on the detachment of single cells vs cell clusters from a *Pseudomonas fluorescens* biofilm. *Journal of Food Engineering*, 219, 121–128. <https://doi.org/10.1016/j.jfoodeng.2017.09.013>
- Beer, D. D., Srinivasan, R., & Stewart, P. S. (1994). Direct measurement of chlorine penetration into biofilms during disinfection. *Applied and Environmental Microbiology*, 60(12), 4339–4344.
- Bolster, C. H., Mills, A. L., Hornberger, G. M., & Herman, J. S. (2001). Effect of surface coatings, grain size, and ionic strength on the maximum attainable coverage of bacteria on sand surfaces. *Journal of Contaminant Hydrology*, 50(3), 287–305. [https://doi.org/10.1016/S0169-7722\(01\)00106-1](https://doi.org/10.1016/S0169-7722(01)00106-1)
- Bos, R., Van der Mei, H. C., & Busscher, H. J. (1999). Physico-chemistry of initial microbial adhesive interactions—its mechanisms and methods for study. *FEMS microbiology reviews*, 23(2), 179–230.
- Bos, R., van der Mei, H. C., Gold, J., & Busscher, H. J. (2000). Retention of bacteria on a substratum surface with micro-patterned hydrophobicity. *FEMS Microbiology Letters*, 189(2), 311–315. <https://doi.org/10.1111/j.1574-6968.2000.tb09249.x>
- Bradshaw, J. G., Peeler, J. T., & Twedt, R. M. (1975). Heat resistance of ileal loop reactive *Bacillus cereus* strains isolated from commercially canned food. *Applied Microbiology*, 30(6), 943–945.

- Brant, J. A., & Childress, A. E. (2002). Assessing short-range membrane–colloid interactions using surface energetics. *Journal of Membrane Science*, 203(1), 257–273.
[https://doi.org/10.1016/S0376-7388\(02\)00014-5](https://doi.org/10.1016/S0376-7388(02)00014-5)
- Brant, J. A., & Childress, A. E. (2004). Colloidal adhesion to hydrophilic membrane surfaces. *Journal of Membrane Science*, 241(2), 235–248. <https://doi.org/10.1016/j.memsci.2004.04.036>
- Bridier, A., Briandet, R., Thomas, V., & Dubois-Brissonnet, F. (2011). Resistance of bacterial biofilms to disinfectants: A review. *Biofouling*, 27(9), 1017–1032.
<https://doi.org/10.1080/08927014.2011.626899>
- Brooks, J. D., & Flint, S. H. (2008). Biofilms in the food industry: Problems and potential solutions. *International Journal of Food Science & Technology*, 43(12), 2163–2176.
<https://doi.org/10.1111/j.1365-2621.2008.01839.x>
- Brown, M. R. W., Allison, D. G., & Gilbert, P. (1988). Resistance of bacterial biofilms to antibiotics a growth-rate related effect? *Journal of Antimicrobial Chemotherapy*, 22(6), 777–780.
<https://doi.org/10.1093/jac/22.6.777>
- Bryers, J. D., & Ratner, B. (2004). *Bioinspired Implant Materials Befuddle Bacteria*.
- Bunt, C. R., Jones, D. S., & Tucker, I. G. (1995). The effects of pH, ionic strength and polyvalent ions on the cell surface hydrophobicity of *Escherichia coli* evaluated by the BATH and HIC methods. *International Journal of Pharmaceutics*, 113(2), 257–261.
[https://doi.org/10.1016/0378-5173\(94\)00205-J](https://doi.org/10.1016/0378-5173(94)00205-J)
- Burgess, S. A., Lindsay, D., & Flint, S. H. (2010). Thermophilic bacilli and their importance in dairy processing. *International Journal of Food Microbiology*, 144(2), 215–225.
<https://doi.org/10.1016/j.ijfoodmicro.2010.09.027>
- Busscher, H. J., Weerkamp, A. H., Mei, H. C. van der, Pelt, A. W. van, Jong, H. P. de, & Arends, J. (1984). Measurement of the surface free energy of bacterial cell surfaces and its relevance for adhesion. *Applied and Environmental Microbiology*, 48(5), 980–983.
- Byrne, B., Dunne, G., & Bolton, D. J. (2006). Thermal inactivation of *Bacillus cereus* and *Clostridium perfringens* vegetative cells and spores in pork luncheon roll. *Food Microbiology*, 23(8), 803–808. <https://doi.org/10.1016/j.fm.2006.02.002>
- Carpentier, B., & Cerf, O. (1993). Biofilms and their consequences, with particular reference to hygiene in the food industry. *The Journal of Applied Bacteriology*, 75(6), 499–511.

- Chmielewski, R. a. N., & Frank, J. F. (2003). Biofilm Formation and Control in Food Processing Facilities. *Comprehensive Reviews in Food Science and Food Safety*, 2(1), 22–32.
<https://doi.org/10.1111/j.1541-4337.2003.tb00012.x>
- Clavel, T., Carlin, F., Lairon, D., Nguyen-The, C., & Schmitt, P. (2004). Survival of *Bacillus cereus* spores and vegetative cells in acid media simulating human stomach. *Journal of Applied Microbiology*, 97(1), 214–219. <https://doi.org/10.1111/j.1365-2672.2004.02292.x>
- Cohen, J., Powderly, W. G., & Steven, M. (2010). Opal. Infectious Diseases, Third Edition. Mosby, 26.
- Costerton, J. W., Lewandowski, Z., DeBeer, D., Caldwell, D., Korber, D., & James, G. (1994). Biofilms, the customized microniche. *Journal of Bacteriology*, 176(8), 2137.
- Costerton, J. William, Marrie, T. J., & Cheng, K.-J. (1985). Phenomena of Bacterial Adhesion. In D. C. Savage & M. Fletcher (Eds.), *Bacterial Adhesion: Mechanisms and Physiological Significance* (pp. 3–43). Springer US. https://doi.org/10.1007/978-1-4615-6514-7_1
- Desai, S. V., & Varadaraj, M. C. (2010). Behavioural pattern of vegetative cells and spores of *Bacillus cereus* as affected by time-temperature combinations used in processing of Indian traditional foods. *Journal of Food Science and Technology*, 47(5), 549–556.
<https://doi.org/10.1007/s13197-010-0099-9>
- Dewanti, R., & Wong, A. C. L. (1995). Influence of culture conditions on biofilm formation by *Escherichia coli* O157:H7. *International Journal of Food Microbiology*, 26(2), 147–164.
[https://doi.org/10.1016/0168-1605\(94\)00103-D](https://doi.org/10.1016/0168-1605(94)00103-D)
- Donlan, R. M., & Costerton, J. W. (2002). Biofilms: Survival Mechanisms of Clinically Relevant Microorganisms. *Clinical Microbiology Reviews*, 15(2), 167–193.
<https://doi.org/10.1128/CMR.15.2.167-193.2002>
- Dufrêne, Y. F., Boonaert, C. J.-P., & Rouxhet, P. G. (1996). Adhesion of *Azospirillum brasilense*: Role of proteins at the cell-support interface. *Colloids and Surfaces B: Biointerfaces*, 7(3), 113–128. [https://doi.org/10.1016/0927-7765\(96\)01288-X](https://doi.org/10.1016/0927-7765(96)01288-X)
- El-Arabi, T. F., & Griffiths, M. W. (2013). Chapter 29—*Bacillus cereus*. In J. G. Morris & M. E. Potter (Eds.), *Foodborne Infections and Intoxications (Fourth Edition)* (pp. 401–407). Academic Press. <https://doi.org/10.1016/B978-0-12-416041-5.00029-9>

- Elimelech, M. (1990). Indirect evidence for hydration forces in the deposition of polystyrene latex colloids on glass surfaces. *Journal of the Chemical Society, Faraday Transactions*, 86(9), 1623–1624. <https://doi.org/10.1039/FT9908601623>
- Evans, D. J., Allison, D. G., Brown, M. R. W., & Gilbert, P. (1991). Susceptibility of *Pseudomonas aeruginosa* and *Escherichia coli* biofilms towards ciprofloxacin: Effect of specific growth rate. *Journal of Antimicrobial Chemotherapy*, 27(2), 177–184. <https://doi.org/10.1093/jac/27.2.177>
- Evelyn, E., & Silva, F. V. M. (2015). Thermosonication versus thermal processing of skim milk and beef slurry: Modeling the inactivation kinetics of psychrotrophic *Bacillus cereus* spores. *Food Research International*, 67, 67–74. <https://doi.org/10.1016/j.foodres.2014.10.028>
- Faille, C., Sylla, Y., Le Gentil, C., Bénézech, T., Slomianny, C., & Lequette, Y. (2010). Viability and surface properties of spores subjected to a cleaning-in-place procedure: consequences on their ability to contaminate surfaces of equipment. *Food microbiology*, 27(6), 769–776.
- Faille, C., Bénézech, T., Midelet-Bourdin, G., Lequette, Y., Clarisse, M., Ronse, G., Ronse, A., & Slomianny, C. (2014a). Sporulation of *Bacillus spp.* within biofilms: A potential source of contamination in food processing environments. *Food Microbiology*, 40, 64–74. <https://doi.org/10.1016/j.fm.2013.12.004>
- Faille, C., Tauveron, G., Le Gentil-Lelièvre, C., & Slomianny, C. (2007). Occurrence of *Bacillus cereus* Spores with a Damaged Exosporium: Consequences on the Spore Adhesion on Surfaces of Food Processing Lines. *Journal of Food Protection*, 70(10), 2346–2353. <https://doi.org/10.4315/0362-028X-70.10.2346>
- Faille, C., Cunault, C., Dubois, T., & Bénézech, T. (2018). Hygienic design of food processing lines to mitigate the risk of bacterial food contamination with respect to environmental concerns. *Innovative Food Science & Emerging Technologies*. <https://doi.org/10.1016/j.ifset.2017.10.002>
- Faille, Christine, Lequette, Y., Ronse, A., Slomianny, C., Garénaux, E., & Guerardel, Y. (2010). Morphology and physico-chemical properties of *Bacillus* spores surrounded or not with an exosporium: Consequences on their ability to adhere to stainless steel. *International Journal of Food Microbiology*, 143(3), 125–135. <https://doi.org/10.1016/j.ijfoodmicro.2010.07.038>
- Feng, G., Cheng, Y., Wang, S.-Y., Hsu, L. C., Feliz, Y., Borca-Tasciuc, D. A., Worobo, R. W., & Moraru, C. I. (2014). Alumina surfaces with nanoscale topography reduce attachment and

- biofilm formation by *Escherichia coli* and *Listeria spp.* *Biofouling*, 30(10), 1253–1268.
<https://doi.org/10.1080/08927014.2014.976561>
- Flint, S. H., Bremer, P. J., & Brooks, J. D. (1997). Biofilms in dairy manufacturing plant-description, current concerns and methods of control. *Biofouling*, 11(1), 81–97.
<https://doi.org/10.1080/08927019709378321>
- Frank, J. F., & Koffi, R. A. (1990). Surface-adherent Growth of *Listeria monocytogenes* is Associated with Increased Resistance to Surfactant Sanitizers and Heat. *Journal of Food Protection*, 53(7), 550–554. <https://doi.org/10.4315/0362-028X-53.7.550>
- Gibbiel, A. Y., & Al, A. T. H. A.-E. (1973). Measurement of Heat Resistance Parameters for Spores Isolated from Canned Products. *Journal of Applied Bacteriology*, 36(2), 321–327.
<https://doi.org/10.1111/j.1365-2672.1973.tb04109.x>
- Granum, E., Brynestad, S., O'sullivan, K., & Nissen, H. (1993). Enterotoxin from *Bacillus cereus*: Production and biochemical characterization. *Enterotoxin from Bacillus Cereus: Production and Biochemical Characterization*, 47(2), 63–70.
- Granum, P. E., & Lund, T. (1997). *Bacillus cereus* and its food poisoning toxins. *FEMS Microbiology Letters*, 157(2), 223–228. <https://doi.org/10.1111/j.1574-6968.1997.tb12776.x>
- Gunduz, G. T., & Tuncel, G. (2006). Biofilm formation in an ice cream plant. *Antonie van Leeuwenhoek*, 89(3), 329–336. <https://doi.org/10.1007/s10482-005-9035-9>
- Hachisuka, Y., & Kozuka, S. (1981). A new test of differentiation of *Bacillus cereus* and *Bacillus anthracis* based on the existence of spore appendages. *Microbiology and immunology*, 25(11), 1201–1207.
- Hall-Stoodley, L., & Stoodley, P. (2002). Developmental regulation of microbial biofilms. *Current Opinion in Biotechnology*, 13(3), 228–233. [https://doi.org/10.1016/S0958-1669\(02\)00318-X](https://doi.org/10.1016/S0958-1669(02)00318-X)
- Hall-Stoodley, L., & Stoodley, P. (2005). Biofilm formation and dispersal and the transmission of human pathogens. *Trends in Microbiology*, 13(1), 7–10.
<https://doi.org/10.1016/j.tim.2004.11.004>
- Handley, P. S. (2009). Structure, composition and functions of surface structures on oral bacteria. *Biofouling*, 2(3), 239–264. <https://doi.org/10.1080/08927019009378148>

- Henriques, A. O., & Moran, C. P., Jr. (2007). Structure, Assembly, and Function of the Spore Surface Layers. *Annual Review of Microbiology*, 61(1), 555–588.
<https://doi.org/10.1146/annurev.micro.61.080706.093224>
- Herald, P. J., & Zottola, E. A. (1988a). Attachment of *Listeria monocytogenes* to Stainless Steel Surfaces at Various Temperatures and pH Values. *Journal of Food Science*, 53(5), 1549–1562.
<https://doi.org/10.1111/j.1365-2621.1988.tb09321.x>
- Herald, P. J., & Zottola, E. A. (1988b). Scanning Electron Microscopic Examination of *Yersinia enterocolitica* Attached to Stainless Steel at Selected Temperatures and pH values. *Journal of Food Protection*, 51(6), 445–448. <https://doi.org/10.4315/0362-028X-51.6.445>
- Holah, J. T., & Thorpe, R. H. (1990). Cleanability in relation to bacterial retention on unused and abraded domestic sink materials. *The Journal of Applied Bacteriology*, 69(4), 599–608.
- Holt, P. S., & Misfeldt, M. L. (1984). Alteration of murine immune response by *Pseudomonas aeruginosa* exotoxin A. *Infection and Immunity*, 45(1), 227–233.
- Hori, K., & Matsumoto, S. (2010). Bacterial adhesion: From mechanism to control. *Biochemical Engineering Journal*, 48(3), 424–434. <https://doi.org/10.1016/j.bej.2009.11.014>
- Huang, C. T., Yu, F. P., McFeters, G. A., & Stewart, P. S. (1995). Nonuniform spatial patterns of respiratory activity within biofilms during disinfection. *Applied and Environmental Microbiology*, 61(6), 2252–2256.
- Jagannath, A., Tsuchido, T., & Membré, J.-M. (2005). Comparison of the thermal inactivation of *Bacillus subtilis* spores in foods using the modified Weibull and Bigelow equations. *Food Microbiology*, 22(2), 233–239. <https://doi.org/10.1016/j.fm.2004.05.004>
- Janštová, B., & Lukášová, J. (2001). Heat Resistance of *Bacillus* spp. Spores Isolated from Cow's Milk and Farm Environment. *Acta Veterinaria Brno*, 70(2), 179–184.
<https://doi.org/10.2754/avb200170020179>
- Jefferson, K. K. (2004). What drives bacteria to produce a biofilm? *FEMS Microbiology Letters*, 236(2), 163–173. <https://doi.org/10.1111/j.1574-6968.2004.tb09643.x>
- Kirtley, S. A., & McGuire, J. (1989). On Differences in Surface Constitution of Dairy Product Contact Materials1. *Journal of Dairy Science*, 72(7), 1748–1753.
[https://doi.org/10.3168/jds.S0022-0302\(89\)79291-2](https://doi.org/10.3168/jds.S0022-0302(89)79291-2)
- Kostyál, E., Borsányi, M., Rigottier-Gois, L., & Salkinoja-Salonen, M. S. (1998). Organic halogen removal from chlorinated humic ground water and lake water by nitrifying fluidized-bed

- biomass characterised by electron microscopy and molecular methods. *Applied Microbiology and Biotechnology*, 50(5), 612–622. <https://doi.org/10.1007/s002530051344>
- Kuusela, P., Moran, A. P., Vartio, T., & Kosunen, T. U. (1989). Interaction of *Campylobacter jejuni* with extracellular matrix components. *Biochimica et Biophysica Acta (BBA) - General Subjects*, 993(2), 297–300. [https://doi.org/10.1016/0304-4165\(89\)90180-3](https://doi.org/10.1016/0304-4165(89)90180-3)
- Langeveld, J. P. M., Kamstrup, S., Uttenthal, A., Strandbygaard, B., Vela, C., Dalsgaard, K., Beekman, N. J. C. M., Meloen, R. H., & Casal, J. I. (1995). Full protection in mink against mink enteritis virus with new generation canine parvovirus vaccines based on synthetic peptide or recombinant protein. *Vaccine*, 13(11), 1033–1037. [https://doi.org/10.1016/0264-410X\(95\)00021-R](https://doi.org/10.1016/0264-410X(95)00021-R)
- Leggett, M. J., McDonnell, G., Denyer, S. P., Setlow, P., & Maillard, J.-Y. (2012). Bacterial spore structures and their protective role in biocide resistance. *Journal of Applied Microbiology*, 113(3), 485–498. <https://doi.org/10.1111/j.1365-2672.2012.05336.x>
- Lequette, Y., Garénaux, E., Tauveron, G., Dumez, S., Perchat, S., Slomianny, C., Lereclus, D., Guérardel, Y., & Faille, C. (2011). Role Played by Exosporium Glycoproteins in the Surface Properties of *Bacillus cereus* Spores and in Their Adhesion to Stainless Steel. *Applied and Environmental Microbiology*, 77(14), 4905–4911. <https://doi.org/10.1128/AEM.02872-10>
- Li, B., & Logan, B. E. (2004). Bacterial adhesion to glass and metal-oxide surfaces. *Colloids and Surfaces B: Biointerfaces*, 36(2), 81–90. <https://doi.org/10.1016/j.colsurfb.2004.05.006>
- Lindbäck, T., & Granum, P. E. (2005). *Methods in Biotechnology vol 21, Food-Borne Pathogens: methods and Protocols*.
- Mah, T.-F. C., & O'Toole, G. A. (2001). Mechanisms of biofilm resistance to antimicrobial agents. *Trends in Microbiology*, 9(1), 34–39. [https://doi.org/10.1016/S0966-842X\(00\)01913-2](https://doi.org/10.1016/S0966-842X(00)01913-2)
- Marchand, S., Block, J. D., Jonghe, V. D., Coorevits, A., Heyndrickx, M., & Herman, L. (2012). Biofilm Formation in Milk Production and Processing Environments; Influence on Milk Quality and Safety. *Comprehensive Reviews in Food Science and Food Safety*, 11(2), 133–147. <https://doi.org/10.1111/j.1541-4337.2011.00183.x>
- Masák, J., Čejková, A., Schreiberová, O., & Řezanka, T. (2014). *Pseudomonas* biofilms: possibilities of their control. *FEMS microbiology ecology*, 89(1), 1-14.

- Melling, J., Capel, B. J., Turnbull, P. C., & Gilbert, R. J. (1976). Identification of a novel enterotoxigenic activity associated with *Bacillus cereus*. *Journal of Clinical Pathology*, 29(10), 938–940. <https://doi.org/10.1136/jcp.29.10.938>
- Melo, L., Bott, T. R., FLETCHER, M., & Capdeville, B. (1992). *Biofilms—Science and Technology*. Springer Science & Business Media.
- Messelhäusser, U., Frenzel, E., Blöching, C., Zucker, R., Kämpf, P., & Ehling-Schulz, M. (2014). *Emetic Bacillus cereus Are More Volatile Than Thought: Recent Foodborne Outbreaks and Prevalence Studies in Bavaria (2007–2013)* [Research Article]. BioMed Research International; Hindawi. <https://doi.org/10.1155/2014/465603>
- Morikawa, M., Kagihiro, S., Haruki, M., Takano, K., Branda, S., Kolter, R., & Kanaya, S. (2006). Biofilm formation by a *Bacillus subtilis* strain that produces γ -polyglutamate. *Microbiology*, 152(9), 2801–2807. <https://doi.org/10.1099/mic.0.29060-0>
- Morton, L., & Gaylarde, C. (n.d.). *The role of microbial slimes in biodeterioration*. 22(2), 8.
- Mosteller, T. M., & Bishop, J. R. (1993). Sanitizer Efficacy Against Attached Bacteria in a Milk Biofilm. *Journal of Food Protection*, 56(1), 34–41. <https://doi.org/10.4315/0362-028X-56.1.34>
- Murphy et al., (1999). *Growth of thermophilic spore forming bacilli in milk during the manufacture of low heat powders—MURPHY - 1999—International Journal of Dairy Technology—Wiley Online Library*. <https://onlinelibrary.wiley.com/doi/abs/10.1111/j.1471-0307.1999.tb02069.x>
- Mustapha, A., & Liewen, M. B. (1989). Destruction of *Listeria monocytogenes* by Sodium Hypochlorite and Quaternary Ammonium Sanitizers. *Journal of Food Protection*, 52(5), 306–311. <https://doi.org/10.4315/0362-028X-52.5.306>
- Nernst, W. (1904). Theorie der Reaktionsgeschwindigkeit in heterogenen Systemen. *Zeitschrift Für Physikalische Chemie*, 47U(1), 52–55. <https://doi.org/10.1515/zpch-1904-4704>
- Nguyen Thi Minh, H., Durand, A., Loison, P., Perrier-Cornet, J.-M., & Gervais, P. (2011). Effect of sporulation conditions on the resistance of *Bacillus subtilis* spores to heat and high pressure. *Applied Microbiology and Biotechnology*, 90(4), 1409–1417. <https://doi.org/10.1007/s00253-011-3183-9>
- Nicholson, W. L., Munakata, N., Horneck, G., Melosh, H. J., & Setlow, P. (2000). Resistance of *Bacillus* Endospores to Extreme Terrestrial and Extraterrestrial Environments. *Microbiology and Molecular Biology Reviews*, 64(3), 548–572. <https://doi.org/10.1128/MMBR.64.3.548-572.2000>

- Nichols, W.W. (1989). Susceptibility of biofilms to toxic compounds. In: Structure and Function of Biofilms (edited by W.G. Characklis & P.A. Wilderer). pp. 321–332. Chichester, UK: John Wiley & Sons Ltd.
- Oss, C. J. V., Chaudhury, M. K., & Good, R. J. (1989). The Mechanism of Phase Separation of Polymers in Organic Media—Apolar and Polar Systems. *Separation Science and Technology*, 24(1–2), 15–30. <https://doi.org/10.1080/01496398908049748>
- Otto, K., Elwing, H., & Hermansson, M. (1999). Effect of Ionic Strength on Initial Interactions of *Escherichia coli* with Surfaces, Studied On-Line by a Novel Quartz Crystal Microbalance Technique. *Journal of Bacteriology*, 181(17), 5210–5218.
- Pashley, R. M., & Israelachvili, J. N. (1984). Molecular layering of water in thin films between mica surfaces and its relation to hydration forces. *Journal of Colloid and Interface Science*, 101(2), 511–523. [https://doi.org/10.1016/0021-9797\(84\)90063-8](https://doi.org/10.1016/0021-9797(84)90063-8)
- Petrocci, M.S., 1983. Surface-active agents: quarternary ammonium compounds. In: Block, S.S.(Ed.), Disinfection, Sterilization and Preservation, 3rd ed. Lea and Febiger, Philadelphia, PA,USA, pp. 309–329
- Plomp, M., Leighton, T. J., Wheeler, K. E., & Malkin, A. J. (2005). Architecture and High-Resolution Structure of *Bacillus thuringiensis* and *Bacillus cereus* Spore Coat Surfaces. *Langmuir*, 21(17), 7892–7898.
- Poulsen, L. V. (1999). Microbial Biofilm in Food Processing. *LWT - Food Science and Technology*, 32(6), 321–326. <https://doi.org/10.1006/fstl.1999.0561>
- Rodríguez-López, P., Rodríguez-Herrera, J. J., Vázquez-Sánchez, D., & López Cabo, M. (2018). Current Knowledge on *Listeria monocytogenes* Biofilms in Food-Related Environments: Incidence, Resistance to Biocides, Ecology and Biocontrol. *Foods*, 7(6), 85. <https://doi.org/10.3390/foods7060085>
- Romero, D., Vlamakis, H., Losick, R., & Kolter, R. (2011). An accessory protein required for anchoring and assembly of amyloid fibres in *B. subtilis* biofilms. *Molecular Microbiology*, 80(5), 1155–1168. <https://doi.org/10.1111/j.1365-2958.2011.07653.x>
- Scales, B. S., Dickson, R. P., LiPuma, J. J., & Huffnagle, G. B. (2014). Microbiology, Genomics, and Clinical Significance of the *Pseudomonas fluorescens* Species Complex, an Unappreciated Colonizer of Humans. *Clinical Microbiology Reviews*, 27(4), 927–948. <https://doi.org/10.1128/CMR.00044-14>

- Scott, S. A., Brooks, J. D., Rakonjac, J., Walker, K. M. R., & Flint, S. H. (2007). The formation of thermophilic spores during the manufacture of whole milk powder. *International Journal of Dairy Technology*, 60(2), 109–117. <https://doi.org/10.1111/j.1471-0307.2007.00309.x>
- Setlow, P. (2006). *Spores of Bacillus subtilis: Their resistance to and killing by radiation, heat and chemicals—Setlow—2006—Journal of Applied Microbiology—Wiley Online Library*. <https://onlinelibrary.wiley.com/doi/full/10.1111/j.1365-2672.2005.02736.x>
- Setlow, Peter. (2014). Spore Resistance Properties. *Microbiology Spectrum*, 2. <https://doi.org/10.1128/microbiolspec.TBS-0003-2012>
- Sharma, M., & Anand, S. K. (2002). Biofilms evaluation as an essential component of HACCP for food/dairy processing industry – a case. *Food Control*, 13(6), 469–477. [https://doi.org/10.1016/S0956-7135\(01\)00068-8](https://doi.org/10.1016/S0956-7135(01)00068-8)
- Shi, X., & Zhu, X. (2009). Biofilm formation and food safety in food industries. *Trends in Food Science & Technology*, 20(9), 407–413. <https://doi.org/10.1016/j.tifs.2009.01.054>
- Srinivasan, R., Stewart, P. S., Griebe, T., Chen, C.-I., & Xu, X. (1995). Biofilm parameters influencing biocide efficacy. *Biotechnology and Bioengineering*, 46(6), 553–560. <https://doi.org/10.1002/bit.260460608>
- Stalheim, T., & Granum, P. E. (2001). Characterization of spore appendages from *Bacillus cereus* strains. *Journal of applied microbiology*, 91(5), 839–845.
- Stewart, G. C. (2017). Assembly of the outermost spore layer: Pieces of the puzzle are coming together. *Molecular Microbiology*, 104(4), 535–538. <https://doi.org/10.1111/mmi.13651>
- Stoeckel, M., Atamer, Z., & Hinrichs, J. (2014). Thermal inactivation of *Bacillus cereus* spores in micellar casein concentrates—effect of protein content and pH development. *Dairy Science & Technology*, 94(6), 539–548. <https://doi.org/10.1007/s13594-014-0178-1>
- Stoeckel, M., Westermann, A. C., Atamer, Z., & Hinrichs, J. (2013). Thermal inactivation of *Bacillus cereus* spores in infant formula under shear conditions. *Dairy Science & Technology*, 93(2), 163–175. <https://doi.org/10.1007/s13594-012-0101-6>
- Stoodley, P., deBeer, D., & Lewandowski, Z. (1994). Liquid Flow in Biofilm Systems. *Applied and Environmental Microbiology*, 60(8), 2711–2716.
- Sutherland, I. W. (2001). Biofilm exopolysaccharides: A strong and sticky framework. *Microbiology*, 147(1), 3–9. <https://doi.org/10.1099/00221287-147-1-3>

- Tam, N. K. M., Uyen, N. Q., Hong, H. A., Duc, L. H., Hoa, T. T., Serra, C. R., Henriques, A. O., & Cutting, S. M. (2006). The Intestinal Life Cycle of *Bacillus subtilis* and Close Relatives. *Journal of Bacteriology*, 188(7), 2692–2700. <https://doi.org/10.1128/JB.188.7.2692-2700.2006>
- Tauveron, G., Slomianny, C., Henry, C., & Faille, C. (2006). Variability among *Bacillus cereus* strains in spore surface properties and influence on their ability to contaminate food surface equipment. *International journal of food microbiology*, 110(3), 254-262.
- Te Giffel, M. C., Beumer, R. R., Granum, P. E., & Rombouts, F. M. (1997). Isolation and characterisation of *Bacillus cereus* from pasteurised milk in household refrigerators in the Netherlands. *International Journal of Food Microbiology*, 34(3), 307–318. [https://doi.org/10.1016/S0168-1605\(96\)01204-4](https://doi.org/10.1016/S0168-1605(96)01204-4)
- van Loosdrecht, M. C. M., Lyklema, J., Norde, W., & Zehnder, A. J. B. (1989). Bacterial adhesion: A physicochemical approach. *Microbial Ecology*, 17(1), 1–15. <https://doi.org/10.1007/BF02025589>
- Van Loosdrecht, M. C. M., Norde, W., & Zehnder, A. J. B. (1990). Physical Chemical Description of Bacterial Adhesion. *Journal of Biomaterials Applications*, 5(2), 91–106. <https://doi.org/10.1177/088532829000500202>
- van Oss, C. J. (1993). Acid—Base interfacial interactions in aqueous media. *Colloids and Surfaces A: Physicochemical and Engineering Aspects*, 78, 1–49. [https://doi.org/10.1016/0927-7757\(93\)80308-2](https://doi.org/10.1016/0927-7757(93)80308-2)
- Van Oss, C. J., Chaudhury, M. K., & Good, R. J. (1988). Interfacial Lifshitz-van der Waals and polar interactions in macroscopic systems. *Chemical Reviews*, 88(6), 927–941. <https://doi.org/10.1021/cr00088a006>
- Vasudevan, R. (2014). Biofilms: microbial cities of scientific significance. *J Microbiol Exp*, 1(3), 00014.
- Verstraeten, N., Braeken, K., Debkumari, B., Fauvart, M., Fransaer, J., Vermant, J., & Michiels, J. (2008). Living on a surface: Swarming and biofilm formation. *Trends in Microbiology*, 16(10), 496–506. <https://doi.org/10.1016/j.tim.2008.07.004>
- Vigeant, M. A., & Ford, R. M. (1997). Interactions between motile *Escherichia coli* and glass in media with various ionic strengths, as observed with a three-dimensional-tracking microscope. *Applied and Environmental Microbiology*, 63(9), 3474–3479.

Wang, Y., Lee, S. M., & Dykes, G. (2014). The physicochemical process of bacterial attachment to abiotic surfaces: Challenges for mechanistic studies, predictability and the development of control strategies. *Critical Reviews in Microbiology*, 41.

<https://doi.org/10.3109/1040841X.2013.866072>

Widmer, A. F., Frei, R., Rajacic, Z., & Zimmerli, W. (1990). Correlation between In Vivo and In Vitro Efficacy of Antimicrobial Agents against Foreign Body Infections. *The Journal of Infectious Diseases*, 162(1), 96–102. <https://doi.org/10.1093/infdis/162.1.96>

Wilson, I. G. (2002). Salmonella and campylobacter contamination of raw retail chickens from different producers: A six year survey. *Epidemiology & Infection*, 129(3), 635–645.

<https://doi.org/10.1017/S0950268802007665>

Wingender, J., Neu, T. R., & Flemming, H.-C. (1999). What are Bacterial Extracellular Polymeric Substances? In J. Wingender, T. R. Neu, & H.-C. Flemming (Eds.), *Microbial Extracellular Polymeric Substances: Characterization, Structure and Function* (pp. 1–19).

https://doi.org/10.1007/978-3-642-60147-7_1

Wirtanen, G., Husmark, U., & Mattila-Sandholm, T. (1996). Microbial Evaluation of the Biotransfer Potential from Surfaces with Bacillus Biofilms after Rinsing and Cleaning Procedures in Closed Food-Processing Systems. *Journal of Food Protection®*, 59, 727–733.

<https://doi.org/10.4315/0362-028X-59.7.727>

Wood, J., & Sharma, R. (1995). How Long Is the Long-Range Hydrophobic Attraction? *Langmuir*, 11(12), 4797–4802. <https://doi.org/10.1021/la00012a035>

Zobell, C. E. (1943). The Effect of Solid Surfaces upon Bacterial Activity¹. *Journal of Bacteriology*, 46(1), 39–56.

CHAPTER III**LITERATURE REVIEW****CHAPTER III****Structure and Rheology of Foam**

CHAPTER III

LITERATURE REVIEW

3.0 Abstract: Aqueous foam is a structured fluid, which can be useful in many applications. This chapter considers the description of foam structure with some points related to its rheology. The aim is to relate dynamic properties of foam through a possible detachment mechanism of microbial structures on surfaces.

3.1 Introduction

Foam is used in our daily life in many applications like shave product, in traditional drinks or cleaners. One may ask, is foam a solid or liquid material? But foam can flow; so it can be considered as a liquid. Yes it can be considered as an aqueous fluid but it is not a simple fluid. Foam is considered to be a complex fluid and its rheology has been studied. It is considered as a non-Newtonian fluid with a complex arrangement of air sacs surrounded by a very thin liquid membrane, which is continually draining when foam is left for a certain time without interference of external forces.

For example, as foam is left in a cylinder for a while, the liquid in the foam will start to drain leaving the bubbles in a beautiful arrangement of elegant polyhedral cells. This appearance in the structure is suddenly broken due to the collapse of bubbles, thus the collapse of foam gradually.

The structure of foam is built on a main key point, which is trapping of gas in pockets or bubbles. The volume of gas is much larger than that of the liquid, where this liquid is embedded between the bubbles. Of course, the amount of liquid can vary between different foams. Wet and dry foam could be considered. Dry foam bubbles have polyhedral shape and the liquid films will meet in lines (Plateau borders; the edges of the polyhedral form), and the lines will meet at vertices (Figure 3.2). As the fraction of liquid increases in foam, water will cause the swelling of the plateau borders, this will lead to the increase in the thickness of the borders between the bubbles. The bubbles will change in their structure from a polyhedral form to a spherical form, thus having wet foam (Figure 3.0)

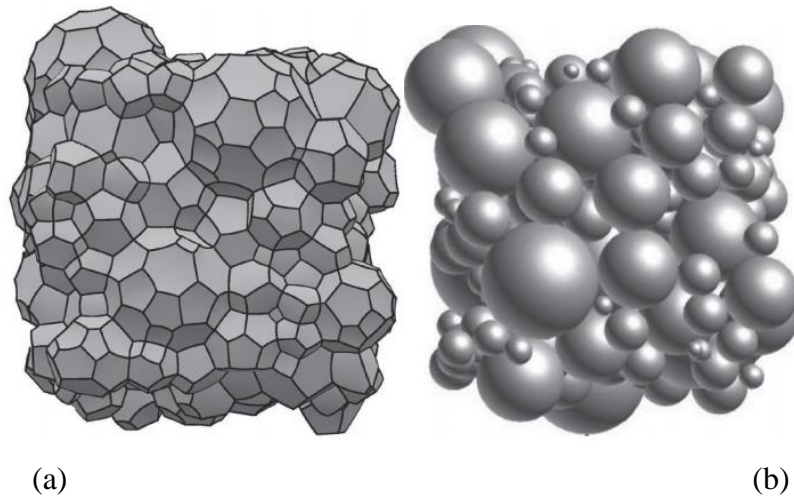


Figure 3.0 (a) Polyhedral cells of dry foam; (b) When foam becomes wet, polyhedral cells become spherical (Stevenson, 2012).

Agitation, nucleation and beating may create foam, the bubbles will be randomly mixed and arranged. The foam structure has no thermal fluctuations and the foam system will explore minimum energy alternative. Foam is considered to be metastable. The foam structure continues to evolve according to the coarsening process (Figure 3.1).

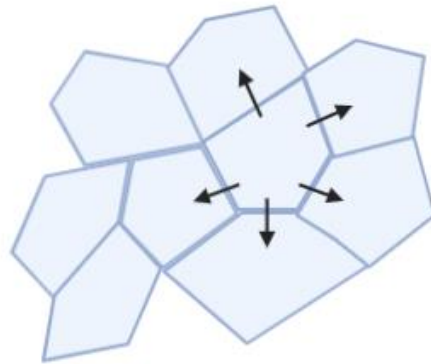


Figure 3.1 Foam coarsening: Air diffusion through the liquid films

Foam's rheological properties are unique. Foam has low densities and an interfacial surface which is important for the structure. Gas is present in high percentage. When the stress is low in the structure of foam then foam behaves as a solid, like the shaving foam, gravitational weak force is incapable of affecting on foam, so flow can occur. This can be due to the elastic shear modulus as it occurs in isotropic solid materials. As the yield shear stress increases over a certain limit then foam flows. The mentioned latter properties are important parameters of foam. Wet foams present the same behavior with a lower yield shear stress.

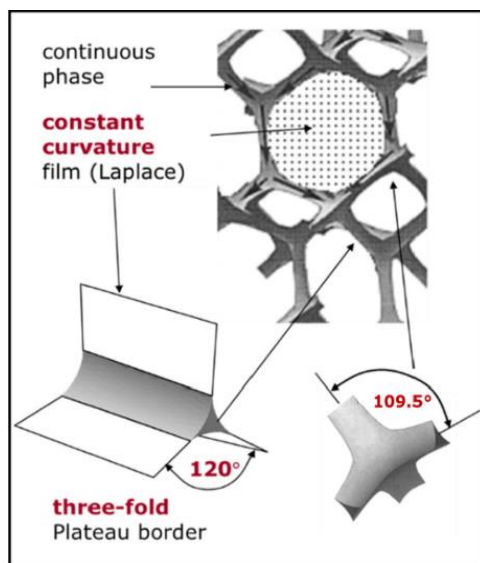


Figure 3.2 Plateau border: Liquid film is embedded between the bubbles (Drenckhan & Hutzler, 2015)

It is relevant to indicate some measurements of foam from macro to micro scale (Figure 3.3). The smallest scale would be in nanometers corresponding to the surfactant molecules. The repulsion force, which can be expressed sometimes as disjoining pressure, will determine the film thickness. The thickness of the film in dry foam varies between 5 and 10 nm. The bubbles diameter is largely variable. It is in the order of few millimeters. The Plateau border width is a small fraction of the bubbles diameter. In engineering approaches, air and liquid are taken as a continuum model which is considered as foam flow (Blondin, 1999).

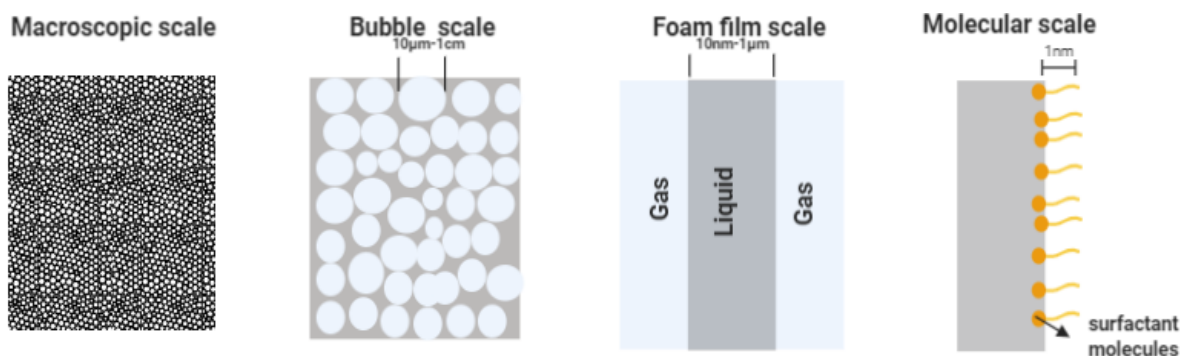


Figure 3.3 Measurement of foam at different scales. Inspired from Chovet (2015)

Studying foam structure and rheology can be indispensable for many industrial sectors. Many studies have been performed on understanding the structure; however, few has been made for comprehending the foam flow (Weaire and Hutzler, 1999). This chapter is a review on foam structure and its rheology in the literature. Due to foam importance as a cleaning detergent of open

surfaces in food industries, understanding foam structure in dynamic conditions such as flowing in pipes and its shearing effect on surfaces can be a cornerstone for future studies on cleaning of microbial structures such as spores and biofilms.

3.2 Foam structure

In order to understand foam structural evolution with time it is very important to understand some critical parameters of foam such as distribution of bubbles, their mean diameter, form, surface tension effect, foam viscosity and void fraction. Foam can have either a closed cells or open cells form. In closed-cell foam, gas form discrete pockets, each surrounded by the continuous phase (liquid). In open-cell foam, the continuous phase can easily flow through the entire structure, displacing the air. These concepts are known as the dry and wet limits.

3.2.1 Bubbles

Real foams have bubbles which are dispersed and disordered. As mentioned above, foam is metastable. The mean size of bubbles tend to increase with time. The most conventional structure of foam is the bcc packing of rectangular octahedral, whose six corners are truncated and create square faces. This structure is named Kelvin cell or bubble, honoring Lord Kelvin.

Lord Kelvin cell shape is a tetrakaidecahedron. Figure 3.4 illustrates the structure. In this structure, there is six square faces and eight hexagonal ones. Kelvin was inspired by Plateau studies and made a conjecture on the ideal structure of monodisperse foam.

In 1994, Weaie and Phelan determined the optimal arrangement for dry foam composed of same bubble size.

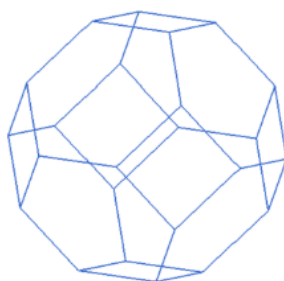


Figure 3.4 Lord kelvin cell or tetrakaidecahedron (Vijay, 2016)

3.2.2 Surface Tension

Surface Tension (γ) is the minimal quantity of energy needed E to increase a liquid surface A , while maintaining a constant entropy S (equation 3.0). This means that liquid has flexibility to increase their surface. This fact has to be related with intermolecular forces inside the liquid.

$$\Gamma = \left(\frac{\partial E}{\partial A} \right)_s \quad (3.0)$$

Surface tension is dependent on some factors such as hydrophobic and hydrophilic part, their nature, and their dispersion.

3.2.3 Void fraction and foam quality

The amount of gas in foam can be referred as V_g ; as for liquid V_l , we can define the void fraction as the measure of the empty spaces in foam:

$$\phi = \frac{V_g}{V_t} \quad (3.1)$$

where V_t corresponds to the total volume of foam, $V_t = V_l + V_g$. For a foam flow the foam quality is referred as:

$$\beta = \frac{Q_g}{Q_t} \quad (3.2)$$

where Q_g represents the gas flow, and $Q_t = Q_g + Q_l$, Q_l being the liquid flow (Boissonnet et al., 1999; Enzendorfer et al., 1995; Thondavadi and Lemlich, 1985)

3.2.4 Foams wet and dry

Depending on the liquid fraction, foam can be wet or dry. The range is between 1 to 30%. At each limit, cells are either packed to form the kelvin cell or the close package of round cells (wet limit). Bubble size is consistent to determine the resulting equilibrium under gravity. If the average bubble diameter is less than the capillary length L_0 , a thin layer of foam bubbles will be wet (i.e. the liquid fraction must be larger than 20%)

$$L_0^2 = \frac{\Gamma}{\Delta p g} \quad (3.3)$$

where Γ is the surface tension of the liquid, g is the acceleration due to gravity and Δp is the density difference between gas and liquid.

A. The Dry Limit

In the dry limit, the films that constitute the interface between the bubbles may be modeled as infinite thin curved surfaces. These surfaces are the faces of the polyhedral cells. In equilibrated foam, many varieties of polyhedral cells exist (Matzke, 1946). In 2D geometry dry foam consists of polygonal cells and the vertices can only be threefold, i.e. the average number of sides of a cell is six (Weaire and Hutzler, 1999).

B. The wet limit

Only spherical bubbles are formed at the wet limit. Each sphere must be in contact with at least three others. For a random compact stacking of the spheres, it has been proven that the sphere bubbles will occupy 63.5% of the volume fraction (Saint-Jalmes and Durian, 1999). As for the 2D structure, the cells are touching disks (Weaire et al., 2007).

C. Between the two limits

The previous idealized cases are the limits where foam has to be. A certain liquid amount has to be added, so that dry can change to wet foam. As liquid increases, it is not obvious what happens at an intermediate system. Some authors say that increasing the liquid content more than 15%, makes you enter in the wet range, others say it is not well defined (Weaire et al., 1997).

3.2.5 Foam density

The density of foam can be defined as its mass per volume unit. It is the measurement of how much matter is compacted. Archimede (Greek scientist) created the first principle of density. Foam is made from two different components: gas and liquid. The density of foam can be calculated as follows (Nakoryakov et al., 1993):

$$\rho_f = (1 - \beta)\rho_l + \beta\rho_g \quad (3.4)$$

where ρ_l and ρ_g are the densities of water and air respectively.

3.2.6 Local equilibrium rules

Each surface of foam cells must normally conform to the law of Laplace-Young. This expresses the balance of forces on a small element of soap film in terms of pressure difference ΔP and the force of surface tension.

$$\Delta P = \frac{2\Gamma}{r} \quad (3.5)$$

r is the local radius of curvature, which is related to the principal curvatures by:

$$\frac{2}{r} = \frac{1}{r_1} + \frac{1}{r_2} \quad (3.6)$$

In the case of dry foam, r_1 differs from r_2 . For the case of sphere (wet foam) $r_1 = r_2$.

The pressure within the films is the mean of the two gas pressures in the adjacent cells. This is inconsistent with the equality of pressure throughout the liquid where a much lower pressure exist inside Plateau borders. To overcome that, one must take into account that the thin film is prevented from shrinking to zero thickness due to the repulsive forces (Figure 3.5) that exist between the two

surfaces. These forces per unit area, may be represented as a pressure to be included in the equilibrium condition. This is called the disjoining pressure (Chovet, 2015).

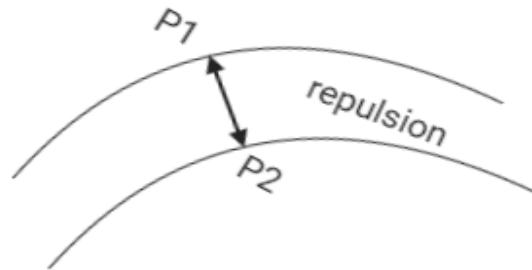


Figure 3.5 Disjoining pressure: presence of a repulsion force inside the liquid films. Inspired from (Weaire and Hutzler, 1999)

3.2.7 The laws of Plateau

Geometrical rules have been developed by Plateau (equilibrium rules). For the foam structure, these rules define an equilibrium configuration to study foams in the dry limit and in a more general case:

- A. Equilibrium rule A1.** The films intersect at 120° at the same time. In two dimensions, this applies to the lines that constitute the boundaries of cells. This union gives a structure named Plateau border, which is the film liquid between the bubbles. This results in an equilibrium of three equal surface tension forces that acts at the intersection.
- B. Equilibrium rule A2.** In dry foams, no more than four intersection lines or six of the surfaces may meet at the vertices of the structure. This tetrahedral vertex is symmetric. All the angles of Maraldi have the value $\phi = \cos^{-1}(-1/3)$. This union is called Plateau junction and the thickness is dependent on the volume fraction and tensioactive quantity (Saint-Jalmes and Durian, 1999).
- C. Equilibrium rule B.** Where a Plateau border meets an adjacent film, the surface is joined smoothly, that is, the surface normal is the same on both sides of the intersection. This means that the Plateau borders terminate in sharp cusps, as shown in Figure 3.6 and in previous figures. No general stability rules for the multiplicity of the intersections at Plateau borders, or their intersection junctions.

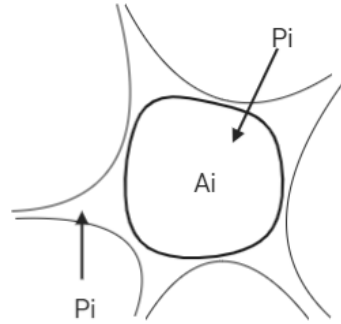


Figure 3.6 Plateau borders are smoothly joined to the adjacent film. Inspired from Weaire and Hutzler (1999).

3.3 Bubble - bubble interaction

When there is high liquid content, bubbles are spherical. As liquid drains due to gravity, bubbles become polyhedral. The osmotic pressure is the average force per unit area needed to balance the increasing bubble-bubble repulsion, as they are pressed together:

$$\Pi = - \left(\frac{\partial E}{\partial V} \right)_{Vg} \quad (3.7)$$

where E is the total surface energy as $E = \gamma S$, and V is the total foam volume (Chovet, 2015). In table 3.0, bubbles' diameter varies according to the daily product used.

Table 3.0 Bubble size and density in different products (Stevenson, 2012)

Products	Bubble diameter (μm)	Estimated number density (cm^{-3})	Notes
Shaving foam	10-20	10^8	Aerosol generated with initial $\Phi=0.926$ (Cohen-Addad et al., 1998)
Ice cream	15-40	10^7	For a 100% overrun ice cream $\Phi=0.926$ (Russell, 2007)

Microcellular starch foam	50-200	10^6	Continuous supercritical CO ₂ fluid extrusion (Alavi et al., 2003)
Bread	2500 area av. 600 number av.	10^3	Many small cells contribute to the foam but the large cohort of the population dominates the visual appearance (Martin et al., 2008)
Hand dish washing up detergent	3000	10^2	Shaking/tumbling/impinged jets, initial $\Phi=0.995$ (Ran et al., 2011)
Bubble bath	5000	10	Bubble size depends on generation method.

3.4 Making Foams

Depending on the consumer product, there exist different foam production techniques. It ranges from micro sized bubbles in shaving products, up to transitory ones, to reach few centimeters in bubble bath. The range of foam creation requirements is in table 3.0.

3.5 Foam creation

Bubbles can develop by different ways: by nucleation of a new small bubble, by introduction of gas into the liquid phase through injection or by break up of smaller bubbles.

3.5.1 Nucleation

Creating a supersaturated solution of a foaming gas in liquid means nucleation where gas spontaneously comes out of the solution to form a gas bubble. To achieve that a pressure drop must occur; for instance, the passage of shaving foam from a pressure canister (Figure 3.7). If the nucleation of the bubbles happens randomly within a continuous liquid phase, it is known as homogenous nucleation. It can be effective at producing large number of small bubbles quickly with a low control over the process. The risk is that when bubbles are formed, they will grow rapidly, thus consuming the supersaturated gas from the solution, instead of propagating the

growth of the new bubbles. This will lead to a decrease in the total number of bubbles with a poly-dispersed bubble size (Shafi et al., 1997).

3.5.2 Entrainment of gas occlusions

It is the process of bringing together of liquid surfaces and trapping gas between them. For example, using hands while massaging shampoo into hair or while using a laundry solution in a rotating drum. The newly formed bubbles undergo changes while formed and incorporated in the fluid like breaking up during the processing stage. Experimental studies entrain gas into a liquid with little amount at the beginning and then increase the amount of gas entrained. The rate of entrainment of a gas depends on the amount of gas along with time. It has been found that in non-soluble gases, volumetric entrainment is largely independent of mixing pressure, and the rate of entrainment per impeller revolution is fairly constant, at typical operation conditions (Niranjan & Silva, 2008).

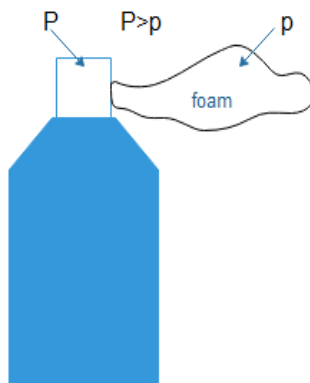


Figure 3.7 Pressure difference in a foam canister (nucleation of the liquid inside) injection.

The direct injection of gas to a liquid is another way of creating foam. The injected bubbles may increase further bubble growth, or remain as the final bubbles in the liquid. This method is used for drinks.

3.6 Practical application

Liquid foam is present in soaps, cleaning agents, shaving products and beverages. In many cases its appeal is for consumer satisfaction. Often it is said that the foam properties of soaps and shampoos have no purpose, however, the rheological properties do have some value, in enabling the clearly visible foam to a vertical surface, being the face of a shaver or the surface of a car or factory before being washed.

In firefighting foam has the ability to coat surfaces without immediately running off. For a fire made out of petrol, foam invades the fire triangle (oxygen, heat and combustion) where it excludes oxygen from the combustion zone, it cools fuel below the ignition point and trapping the fuel vapor of the liquid surface.

In chemical engineering, foam can be used for separation purposes of impurities through foam filtration and flotation. In this method solutes are carried at the surface of bubbles created at the bottom of a fractionation column due to the blow of air in a liquid pool. An application for that is the separation of minerals.

Foam can be used in controlling civil disorders accompanied with violence. It is the fact that foam can stop violent actions during manifestations. It can be a source of entertainment during children parties. Other applications are related to decontamination of material in nuclear reactors.

In the secondary recovery of hydrocarbons, water and surfactants are injected to reservoirs to displace and recover some residual oil and gas in-situ. Foams provide a more efficient mixing of chemicals, optimizing water requirements.

Products in food industry are made out of foam, e.g. ice cream, chocolate.. These products suffer an important change in the structure from the production to packaging (Chovet, 2015).

Regularly, the final foam structure is a combination of a nucleation or entrainment break-up process followed by bubbles growth. This has particular applications in products where foam is created for being used at a certain point by the user.

3.7 Foam rheology

Foam properties such as elasticity, plasticity and viscosity are rheological properties of foam which play a major role in foam production, transportation and application. Examples are foam extrusion through nozzles and slits (used in cosmetics and food applications, and plastic foam production), transportation through pipes (for cleaning of compartments in nuclear plants and foam aided natural gas production), flow through permeable media (in enhanced oil recovery), foam used in personal and home care application (shaving and styling foams, shampoos)(Chovet, 2015).

When foam is subjected to small shear stress, it deforms like a soft solid. This response can be characterized with visco-elastic moduli (Figure 3.9). For applied low yield stress, the response is visco-plastic. In the latter regime foam behaves like shear thinning fluids, being their effective viscosity a decreasing function of shear rate (Chovet, 2015).

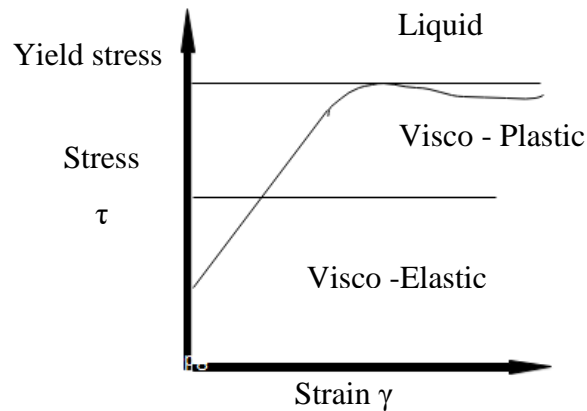


Figure 3.9 Relationship between the shear and the strain for aqueous foam.

There are other phenomena that arise as foam is in contact with confining solid walls: if the surface of the wall is smooth, the foam tends to slip on the wall. In that case, the velocity of the first layer of bubbles, in contact with the wall velocity does not match. This is different from what is observed in simple liquids (Marze et al., 2008).

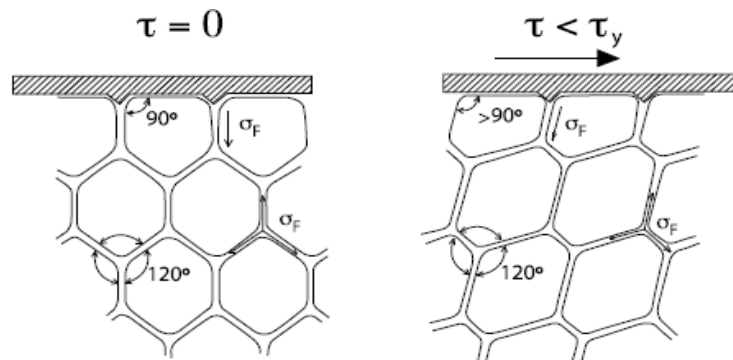


Figure 3.10 Schematic presentation of the origin of elastic response of foam, in that case the shear stress is lower than the foam yield stress close to the channel wall (Stevenson, 2012).

The elastic response is due to surface tension effects: the surface tension in each film is twice that of the surface tension of the liquid from which is the foam generated (Princen H.M, 1983). When external shear stress is applied, the bubbles deform. The result is that the average orientation of the film is inclined in the direction of the applied shear stress.

As long as the applied shear stress is smaller than the yield stress of foam, the consequence is that the films meeting at the Plateau borders are in static mechanical equilibrium and the bubbles are caged in a self-supporting structure (Figure 3.10).

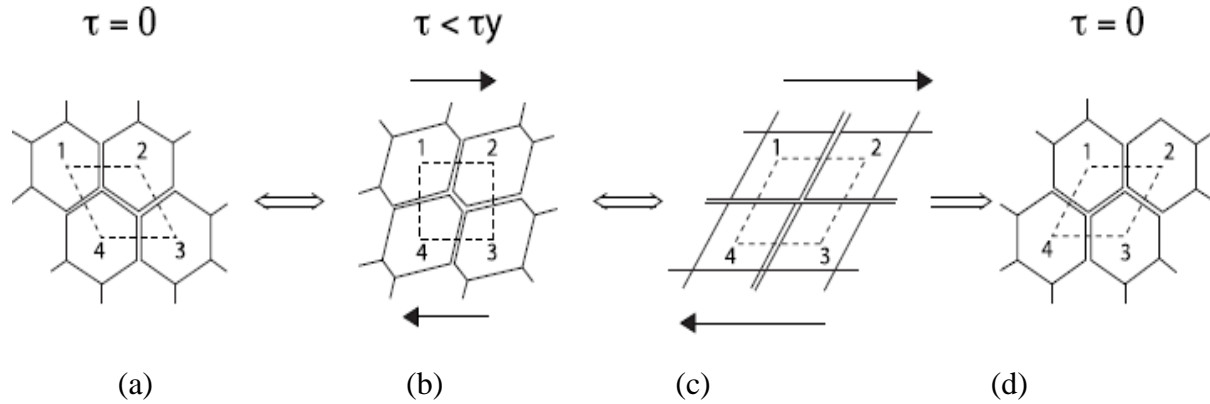


Figure 3.11 Foam yielding and plastic deformation, under applied shear stress, increasing from (a) to (c). This structure can relax either elastically, by going back to structure (a), or by a bubble rearrangement, leading to structure (d). (Princen H.M, 1983; Princen H.M, 2001)

If the magnitude of the stress applied is strong to the extent it can separate neighboring bubbles, then the foam structure yields and a new steady shear flow sets in. The bubbles in that case will slide along each other. The bubbles rearrangement leads to a local shear flow of the liquid inside the foam films. This will result in dissipation of energy and the macroscopic stress will be dependent on a contribution from the shear rate. In the case the applied stress is decreased back to zero, the flow of the liquid will stop and the bubbles will tend toward a new equilibrium (Figure 3.11).

3.7.1 Linear Elasticity

Under small shear strain, foam behaves like an elastic material. In that case the stress τ varies linearly with the strain γ . In this type of regime the bubbles are deformed, but the applied strain is too small to change the topology of their packing. As for the specific area of the foam it increases with the applied strain, thereof the volume density of the bubble surface energy change. Dimensional models have demonstrated that the foam shear modulus $G = \tau/\gamma$ scales as the surface energy density, multiplied by a prefactor, which depends on the foam structure, polydispersity and liquid content. (Princen H.M., 2001).

3.7.2 Non-linear Elasticity

For large strains that still too small to perform bubble rearrangements phenomenon, foam film rotations and stretching, lead to nonlinear mechanical response. For example, shear deformation of foam in the X_1 direction induces shear stress component τ_{12} (proportional to γ) and two normal

stress differences, $N_1=(\tau_{11} - \tau_{22})$ and , $N_2=(\tau_{22} - \tau_{33})$. These differences are the result of increasing strain where the foam films become predominantly oriented perpendicularly to the X_2 direction (Figure 3.12). The result is that the surface tension of the foam films contributes more to the normal stresses τ_{11} and τ_{33} and less to τ_{22} therefore leading to the normal stress difference N_1 and N_2 (Labiausse et al., 2007).

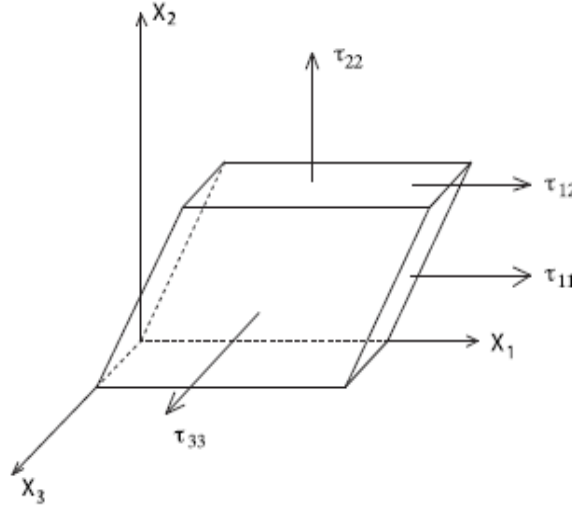


Figure 3.12 A cube of foam is sheared in the X_1 direction. The arrows illustrate the components of the induced stress (Labiausse et al., 2007).

3.7.3 Yielding

When foams are subjected to an increase in shearing or strain, they will exhibit a transition phase from solid-like to fluid-like behavior called yielding (Larson, R.G 1999). As described previously, the stress first increases as in elastic solid. Then the stress reaches a weak maximum and then settles to form a plateau. In the latter regime, the stress was increasing as a function of the applied shear rate, $\dot{\gamma}$. The yield stress denoted by τ_c is the stress threshold beyond which the flow sets in. The corresponding strain threshold in the yield strain is denoted by $\dot{\gamma}$.

3.7.4 Plastic flow

Plastic strain is the irreversible deformation that takes place when the material is sheared beyond its yield strain. One may expect that in a slow plastic shear flow that the sample will relax almost instantaneously towards a static equilibrium when the applied shear rate is released suddenly. This behavior is called quasi-static. Practically, even slow foam flows may only approach quasi-static behavior, due to the viscoelastic relaxations.

3.8 Foam evolution

Aqueous foam never reaches a steady state despite the stabilizing effect of the surfactant. As already mentioned, foam will stay at a metastable state. Foam will exhibit a continuous evolution through time and space; taking into account the thermodynamic point of view, foam will always try to decrease its interfaces to lower its internal energy. Many mechanisms are described to explain the foam evolution (Chovet, 2015).

3.8.1 Drainage

Drainage of foam can be described as the phenomenon by which liquid flows out of foam (Bikerman, 1973). This phenomenon had many applications such as cleaning services, mineral extraction, purification of water, production of porous materials. Two categories of drainage can be identified: the drainage of the film between the bubbles and the flow of liquid to the center of the channel towards the plateau junctions. The flow inside the liquid film is due to phenomena like gravity force, the capillarity force, the pressure between the plateau regions and the film between the bubbles.

3.8.2 Coarsening

It is also known as Ostwald ripening, this phenomenon expresses the gas lost through the bubbles film from a high-pressure bubble to a low-pressure one. This exchange in gas is associated to a decrease in the small bubble size at the expenses of the big ones (Figure 3.13). This shows how liquid foam evolves toward a thermodynamic equilibrium. This process is strongly linked to drainage and other rheological processes.

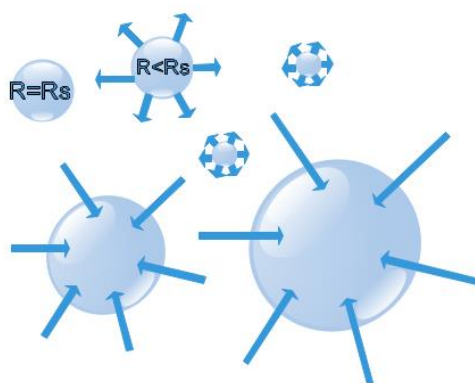


Figure 3.13 Gas goes out from small bubbles to big ones leading to increase in the average size of the bubble system. Inspired from (Chovet, 2015).

3.8.3 Gibbs-Marangoni mechanism

The stability of the dilute aqueous surfactant solution can be explained by Gibbs –Marangoni mechanism. Due to the surface tension difference, this can lead to surfactant shortage, stretching or drainage. When there is a surface tension difference, the surfactant from the neighbor cell will migrate to the weak zone (Figure 3.14). This will result in filling the hole by dragging with them (hydrophilic heads) a liquid part that is present in the film between the bubbles. The entire zone will reform again, and recover its meta-stable property by forming the double surfactant layer (Ivanov, 1988), this phenomenon extends foam life by giving extra elasticity to the system.

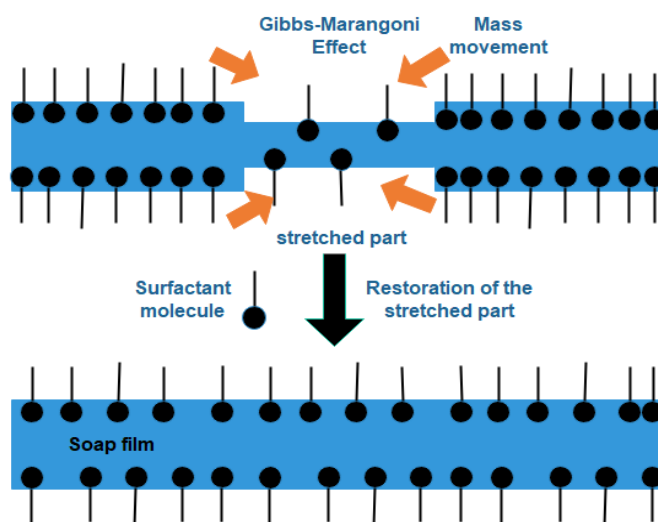


Figure 3.14 Surfactant molecules replace the void places in the stretched film by mass movement. Inspired from (Ueno et al., 2016)

3.8.4 Foam collapse

When a film of soap is formed, it will keep on thinning up till it reaches equilibrium. Usually liquid foams do not last long compared to other types of fluid. They have the tendency to collapse by the rupture of the exposed films. Drainage is one of the most important factors that decrease the film thickness, even evaporation can affect it. Other factors like the surfactant selection or the presence of dust may also impact on the films. The stability of foam is of a great importance as a subject; however, it shows many difficulties regarding its comprehension scientifically. Three reasons may clarify that: the immense variability of chemical composition, even though there might be small levels of impurities they can be highly effective. The dynamic nature of the instability mechanisms (Chovet, 2015).

3.9 Foam flow

Studying foam has been encouraged in order to understand the flow of fire-fighting foams and the transport of cuttings in oil well drilling. Foam is a non-Newtonian fluid that exhibits a slip boundary condition. Due to this flow type, there is an important impact on the wall shear stress, and this can contribute to the entire pressure gradient. The latter characteristic makes foam useful for cleaning of oil pipes and equipment like heat exchanger.

For instance , two types of foam flow can be categorized:

- A. Micro-flow: it is when the confinement space of foam has a size close to the bubbles diameter. (e.g : capillarity tube)
- B. Macro-flow: in that case the confinement space of foam has a size bigger than the bubbles diameter.

For the micro-flow, the bubbles take the space surrounding it or the channel form. As for the macro-flow, the bubbles can move freely and will interact between them. Another important aspect that makes difference between them is the bubble diameter. For the micro-flow, sometimes the bubbles are bigger than the channel, in that case the important size is the porous medium and most frequent interaction is between the bubbles and the walls (Chovet , 2015).

3.10 Foam viscosity (μ_f)

A definition of viscosity can be the resistance exerted by a fluid that is being deformed by either shear stress or tensile stress. The increase in viscosity, decrease the flow capacity of the fluid. Two types of viscosity of fluid which are well referred: the dynamic viscosity and the kinematic viscosity. Most fluids in nature exhibit a Newtonian behavior. Non-Newtonian behavior means that there is lack of proportionality between the stress and the deformation rate. This can have an impact on the viscosity where it will not be constant over an extended shear velocity plateau. These types of fluids can be characterized by visco-elastic behavior laws.

A model which used to calculate foam viscosity is based on volumetric gas fraction Φ_G (Hatschek, 1911):

$$\mu_f = \frac{\mu_l}{1 - \Phi_G^{1/3}} \quad (3.8)$$

where μ_l is the liquid viscosity.

This model is based on a heuristic model for concentrate emulsions, however, this model does not take into account the surface tension.

There are many experiments that have results which allowed adjusting the non-Newtonian model of Herschel-Bulkley. Then the effective viscosity can be expressed as:

$$\mu_{ef} = \frac{\partial \tau}{\partial \dot{\gamma}} = n \cdot k \cdot \dot{\gamma}^{n-1} \quad (3.9)$$

where τ is the stress, $\dot{\gamma}$ the shear rate, k the consistency index and n is the power law index.

3.11 Non-Newtonian flow models

The manner by which foam flows is a non-Newtonian way. Due to this character, a model having at least two parameters will explain more the behavior of such complex flow. As for all continuum models, mechanical properties, such as elastic and viscous moduli, yield stress and effective viscosity are integrated in laws and models that relate the stress, strain and strain's rate. Generally, common models are those that takes into account shearing at the middle of the foam. Continuum non-Newtonian models are:

Table 3.1 Non-Newtonian models present inside the ANSYS CFX software.

Model	Description	Settings
Bingham	A model for viscoplastic fluids. $\mu = \tau_c \dot{\gamma} + k$ Examples of viscoplastic fluids include tomato paste and tooth paste. A few electro-rheological fluids can be modeled as Bingham fluids, with the yield stress as a function of the intensity of the electric field, or the electric current.	Yield Stress: τ_c Viscosity Consistency: k Minimum Shear Strain Rate Maximum Shear Strain Rate
Bird Carreau	A model intended for shear-thinning fluids. $\mu = \mu_\infty + (\mu_0 - \mu_\infty) (1 + (\lambda \dot{\gamma})^2)^{\frac{1-n}{2}}$ The model reverts to a Newtonian behavior of $\mu = \mu_0$ for $n=1$, or $\lambda=0$. Examples of shear-thinning fluids include applesauce, banana puree, and orange juice concentrate.	Low Shear Viscosity: μ_0 High Shear Viscosity: μ_∞ Time Constant: λ Power Law Index: n

Ostwald de Waele	The most popular viscosity model because of its simplicity. However, it does not have bounded either on the low or high shear limits, unlike Carreau's models. $\mu = k(\lambda\dot{\gamma})^{n-1}$	Minimum Shear Strain Rate Maximum Shear Strain Rate Time Constant: λ Power Law Index: n Yield Stress: τ_c
Herschel Bulkley	A model for viscoplastic fluids that, after yield, exhibits a power law behavior in shear stress versus shear strain rate. $\mu = \tau_c \lambda \dot{\gamma} + k(\lambda\dot{\gamma})^{n-1}$	Viscosity Consistency: k Minimum Shear Strain Rate Maximum Shear Strain Rate Time Constant: λ Power Law Index: n

3.12 Horizontal flow regimes

Evaluating foam when it flows horizontally inside a channel can be done through its global velocity. The flow regimes can result from the interpolation of the velocity that is measured at the duct walls, the three foam regimes (M.I. Briceño & D.D. Joseph 2003) are :

- A. One-dimensional flow (1D):** when the stabilized flow behaves as a whole it moves like a block form, or as a piston. In that case velocity vectors have only one uniform axial direction:

$$\vec{u} = u \vec{e}_x = cte \vec{e}_x \quad (3.10)$$

- B. Two-dimensional flow(2D):** it is obtained when the established flow has an axial component velocity, which depends of the y-coordinate (vertical coordinate)

$$\vec{u} = u(y) \vec{e}_x \quad (3.11)$$

- C. Three-dimensional flow(3D):** It is obtained when the established flow velocity has an axial component, which depends of the z (span wise) and y (vertical) coordinates:

$$\vec{u} = u(y, z) \vec{e}_x \quad (3.12)$$

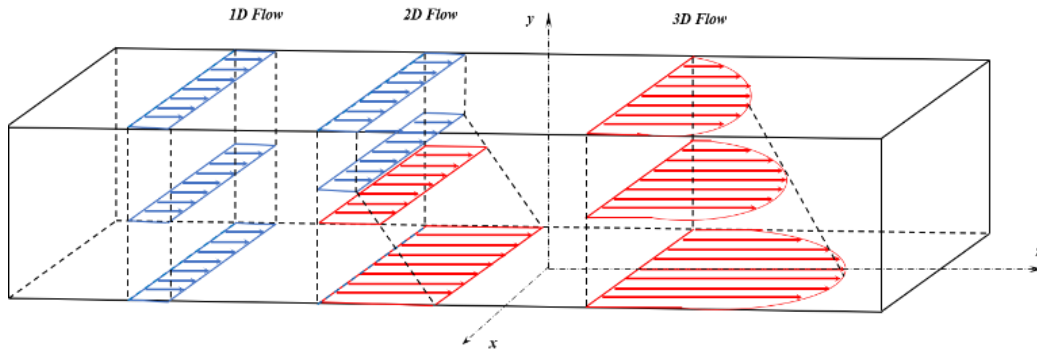


Figure 3.15 Foam flow velocity profiles for the three flow regimes in a square cross section channel (Dallagi , 2019)

The mentioned regimes depend on numerous factors like gas velocity, the liquid velocity, channel geometry, the average velocity in the test section.

3.13 Wall-Slip liquid layer

When foam flows , liquid will be segregated from foam, where it forms a thin liquid layer at the wall. This can provide resistance to shearing and can produce slip at the wall. Particle image velocimetry has been used on horizontal foam flow to determine its velocity profiles (Blondin et al., 1999). The thickness of this liquid film can range from few microns up to the order of millimeters, in addition it presents a laminar regime. This liquid film can be a function of surfactant concentration , channel dimension, wall roughness, gas and liquid flow (Chovet, 2015).

The wall liquid film was described using a rotational rotameter (Wenzel et al., 1967) . As a result of these studies, foam flow can be the cause of two different phenomena, shearing at its middle and the adjacent liquid film. Taking into account the liquid film in any foam flow , its behavior can be described by the Herschel-Bulkley for Non-Newtonian flows (Camp, M. A. 1988).

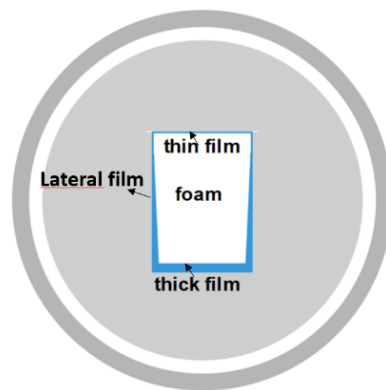


Figure 3.16 A scheme showing cross-section of square channel with the liquid film is surrounding a foam block.

3.13.1 Wall slip velocity

For a flow with a slipping film, the velocity field can be decomposed into two main components: the wall slip velocity u_{slip} , and the shear velocity u_{shear} (Figure 3.17)

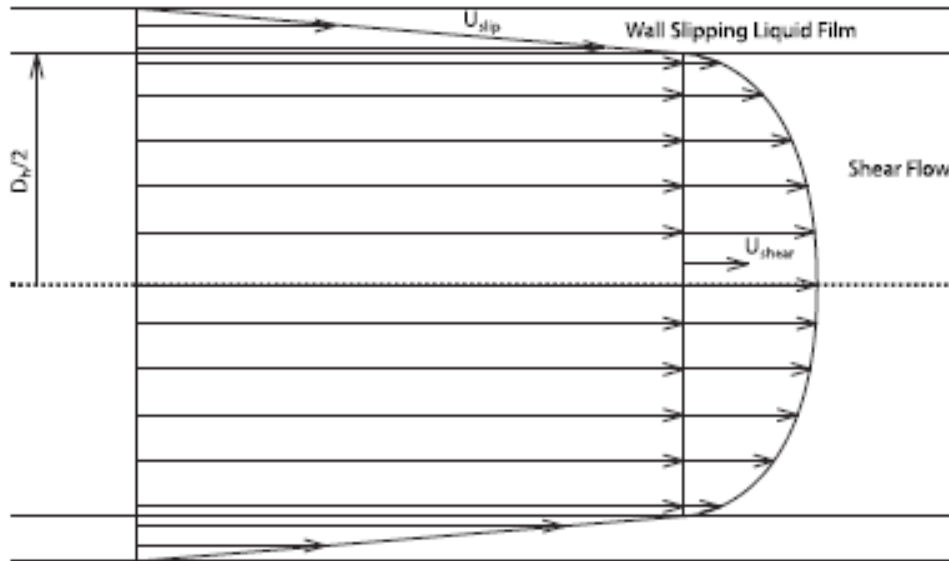


Figure 3.17. Velocity field of a laminar flow with a wall-slip velocity (Chovet, 2015)

Inside the wall liquid film, the higher velocity corresponds to the wall slip velocity. It can be related to the bubbles velocity flowing over the foam flow, inside this film with a shear velocity. Inside this film, composed of liquid, a boundary layer might develop and increase the value of this gradient. The foam flow will always take into consideration both velocity and the contribution from the wall slip velocity (Tisné, 2003).

3.13.2 Thickness of slip layer (top, bottom) as a function of foam quality and foam flow regime

With the actual measurement techniques, the direct measurement of the thin film is not an easy task. Modelling of the foam flow can be an indirect measurement method. Another method can be conductimetry. Using a conductimetry technique the film thickness was measured at the top and the bottom of the square cross section channel (Chovet, 2015).

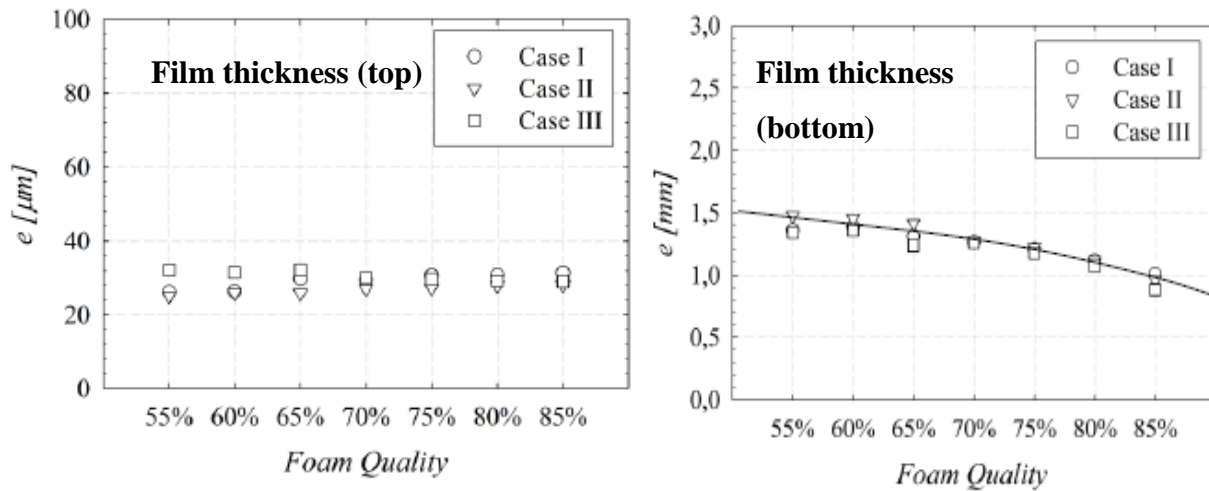


Figure 3.18. Thickness of the top and the bottom liquid film, Case I: 1D flow regime , Case II: 2D flow regime, Case III : 3D flow regime (Chovet, 2015)

The mean of the liquid film (Top) thickness, presents similar values for all qualities and velocities. They tend to 30 μm . For the mean liquid film thickness (bottom wall), the values of the liquid film thickness go from 1.5 to 0.9 millimeters. It can be noted that the change of the foam velocity (case I, case II, case III) does not make an influence over the mean value of the bottom liquid slip layer; there are no major deviations between the thicknesses of the three cases. However, as we alter the foam quality the value of liquid film changes notably. Hence, for wetter foams the bottom slip layer is thicker than that of dryer foams (Chovet, 2015).

3.14 Summary

While flowing over a surface, foam can perform shearing. This shearing behavior can be a key point for cleaning surfaces contaminated by either spores, vegetative cells, or biofilms in food industries. In this study, the shearing efficiency of foam flow for the detachment of different microorganism structures from surfaces of closed systems was tested.

3.15 References

- Alavi, S. H., Rizvi, S. S. H., & Harriott, P. (2003). Process dynamics of starch-based microcellular foams produced by supercritical fluid extrusion. I: Model development. *Food Research International*, 36(4), 309–319. [https://doi.org/10.1016/S0963-9969\(02\)00222-3](https://doi.org/10.1016/S0963-9969(02)00222-3)
- Bikerman, J. J. (1973). Formation and Structure. In J. J. Bikerman (Ed.), *Foams* (pp. 33–64). Springer Berlin Heidelberg. https://doi.org/10.1007/978-3-642-86734-7_2
- BLONDIN, E., Doublier, L., & Université de Nantes (1999). *Etude Experimentale D'une Mousse Humide En Ecoulement En Conduite Horizontale De Section Rectangulaire*. [S.N.].
- Boissonnet, G., Faury, M., & Fournel, B. (1999). Decontamination of Nuclear Components Through the Use of Foams. In J. F. Sadoc & N. Rivier (Eds.), *Foams and Emulsions* (pp. 323–334). Springer Netherlands. https://doi.org/10.1007/978-94-015-9157-7_19
- Camp M.A., The rheology of high gas volume fraction aqueous foam. Southampton, England, 1988.
- Chovet, R. (2015). *Experimental and numerical characterization of the rheological behavior of a complex fluid: Application to a wet foam flow through a horizontal straight duct with and without flow disruption devices (FDD)* [Université de Valenciennes et du Hainaut-Cambresis]. <https://tel.archives-ouvertes.fr/tel-01192955/>
- Cohen-Addad, S., Hoballah, H., & Höhler, R. (1998). Viscoelastic response of a coarsening foam. *Physical Review E*, 57(6), 6897–6901. <https://doi.org/10.1103/PhysRevE.57.6897>
- Drenckhan, W., & Hutzler, S. (2015). Structure and energy of liquid foams. *Advances in Colloid and Interface Science*, 224(Supplement C), 1–16. <https://doi.org/10.1016/j.cis.2015.05.004>
- Enzendorfer, C., Harris, R. A., Valkó, P., Economides, M. J., Fokker, P. A., & Davies, D. D. (1995). Pipe viscometry of foams. *Journal of Rheology*, 39(2), 345–358. <https://doi.org/10.1122/1.550701>

- Hatschek, E. (1911). *Die Viskosität der Dispersoide* / SpringerLink.
<https://link.springer.com/article/10.1007%2FBF01503180?LI=true>
- Ivanov, I. (1988). *Thin Liquid Films*. CRC Press.
- Labiausse, V., Höhler, R., & Cohen-Addad, S. (2007). Shear induced normal stress differences in aqueous foams. *Journal of Rheology*, 51(3), 479–492. <https://doi.org/10.1122/1.2715392>
- Larson R.G., *The Structure and Rheology of Complex Fluids*. New York: Oxford University Press, 1999.
- Martin, P. J., Tassell, A., Wiktorowicz, R., Morratt, C. J., & Campbell, G. M. (2008). Chapter 20 - Mixing Bread Doughs Under Highly Soluble Gas Atmospheres and the Effects on Bread Crumb Texture: Experimental Results and Theoretical Interpretation. In G. M. Campbell, M. G. Scanlon, & D. L. Pyle (Eds.), *Bubbles in Food 2* (pp. 197–206). AACC International Press.
<https://doi.org/10.1016/B978-1-891127-59-5.50024-9>
- Marze, S., Langevin, D., & Saint-Jalmes, A. (2008). Aqueous foam slip and shear regimes determined by rheometry and multiple light scattering. *Journal of Rheology*, 52(5), 1091–1111.
<https://doi.org/10.1122/1.2952510>
- Matzke, E. B. (1946). The Three-Dimensional Shape of Bubbles in Foam—An Analysis of the Rôle of Surface Forces in Three-Dimensional Cell Shape Determination. *American Journal of Botany*, 33(1), 58–80. <https://doi.org/10.1002/j.1537-2197.1946.tb10347.x>
- M.I.Briceño, & D.D.Joseph. (2003). *Self-lubricated transport of aqueous foams in horizontal conduits—ScienceDirect*.
<https://www.sciencedirect.com/science/article/pii/S0301932203001848#FIG6>
- Nakoryakov, V. E., Pokusaev, B. G., & Shreiber, I. R. (1993). *Wave Propagation in Gas-Liquid Media*. CRC Press.
- Niranjan, K., & Silva, S. F. J. (2008). Bubbles in Foods: Creating Structure out of Thin Air! In G. F. Gutiérrez-López, G. V. Barbosa-Cánovas, J. Welte-Chanes, & E. Parada-Arias (Eds.), *Food Engineering: Integrated Approaches* (pp. 183–192). Springer New York.
- Princen, H. M. (1983). Rheology of foams and highly concentrated emulsions: I. Elastic properties and yield stress of a cylindrical model system. *Journal of Colloid and Interface Science*, 91(1), 160–175. [https://doi.org/10.1016/0021-9797\(83\)90323-5](https://doi.org/10.1016/0021-9797(83)90323-5)
- Princen H.M., "The structure, mechanics, and rheology of concentrated emulsions and fluid foams", *Encyclopedia of Emulsion Technology*, 2001.

- Ran, L., Jones, S. A., Embley, B., Tong, M. M., Garrett, P. R., Cox, S. J., Grassia, P., & Neethling, S. J. (2011). Characterisation, modification and mathematical modelling of sudsing. *Colloids and Surfaces A: Physicochemical and Engineering Aspects*, 382(1), 50–57. <https://doi.org/10.1016/j.colsurfa.2010.11.028>
- Russell A., "Process innovation from research and development to production in a large company: development and commercialisation of a low temperature extrusion process.", in *Case Studies in Food Product Development*. Newbury: CPL Press, 2007.
- Saint-Jalmes, A., & Durian, D. J. (1999). Vanishing elasticity for wet foams: Equivalence with emulsions and role of polydispersity. *Journal of Rheology*, 43(6), 1411–1422. <https://doi.org/10.1122/1.551052>
- Shafi, M. A., Joshi, K., & Flumerfelt, R. W. (1997). Bubble size distributions in freely expanded polymer foams. *Chemical Engineering Science*, 52(4), 635–644. [https://doi.org/10.1016/S0009-2509\(96\)00433-2](https://doi.org/10.1016/S0009-2509(96)00433-2)
- Stevenson, P. (2012). *Foam Engineering: Fundamentals and Applications / General & Introductory Chemical Engineering / Subjects / Wiley*. Wiley.Com. <https://www.wiley.com/en-us/Foam+Engineering%3A+Fundamentals+and+Applications-p-9780470660805>
- Thondavadi, N. N., & Lemlich, R. (1985). Flow properties of foam with and without solid particles. *Industrial & Engineering Chemistry Process Design and Development*, 24(3), 748–753. <https://doi.org/10.1021/i200030a038>
- Tisné, P. (2003). *Étude par la méthode polarographique des contraintes pariétales exercées par une mousse en écoulement* [Thesis, Nantes]. <http://www.theses.fr/2003NANT2034>
- Ueno. (2016). *Figure 7. The Marangoni Effect: Practical Chemistry of Long-Lasting Bubbles: Science and Education Publishing*. <http://pubs.sciepub.com/wjce/4/2/2/figure/7>
- Vijay, D. (2016). *Forced convective heat transfer through open cell foams*.
- Weaie, D., & Phelan, R. (1994). A counter-example to Kelvin's conjecture on minimal surfaces: *Philosophical Magazine Letters: Vol 69, No 2*. <https://www.tandfonline.com/doi/abs/10.1080/09500839408241577>
- Weaire, D., Hutzler, S., Verbist, G., & Peters, E. (1997). A Review of Foam Drainage. In *Advances in Chemical Physics* (pp. 315–374). John Wiley & Sons, Ltd. <https://doi.org/10.1002/9780470141618.ch5>
- Weaire, D. L., & Hutzler, S. (1999). *The Physics of Foams*. Clarendon Press.

Weaire, Denis, Langlois, V., Saadatfar, M., & Hutzler, S. (2007). Foam as granular matter. In *Granular and Complex Materials: Vol. Volume 8* (pp. 1–26). WORLD SCIENTIFIC.

https://doi.org/10.1142/9789812771995_0001

Wenzel, H. G., Stelson, T. E., & Brungraber, R. J. (1967). Flow of High Expansion Foam in Pipes. *Journal of the Engineering Mechanics Division*, 93(6), 153–166.

CHAPTER IV

MATERIALS AND METHODS

CHAPTER IV

Materials and Methods

CHAPTER IV

MATERIALS AND METHODS

4.0 Abstract: This chapter, we will briefly summarize the commonly used materials and methods used in this study. It is divided into 2 parts: first, an emphasis will be placed on the properties of these materials (Spores/Biofilm properties, type of material, prototype design, detergents). In the second part, the emphasis is on methods used in this study.

4.1. Materials

4.1.1. Standard Cleaning in Place like conditions prototype.

The CIP like conditions station used in this study replicates an industrial scale facility 1/10. A tank of 200 L makes it possible to prepare and store the cleaning solution which is recycled as in most industrial installations. A second tank allows storage at room temperature of 400 l of osmosed water (Figure 4.0). A centrifugal pump ensures the feeding of the CIP station. The flow rate of this pump is regulated by a motorized diaphragm valve (GEMÜ® 67120 Duprigheim) and is measured using an electromagnetic flow meter (Accometer SLIEDRECHT, Holland), ranging from 0.4-17 m³.h⁻¹. The prototype also includes a sensor of relative pressure ranging from 0-10⁴ Pa (Bourdon-Sedeme, type 2400l E703), as well as probes of platinum resistance for temperature measurement (PT 100). The responses of the different sensors are acquired in real time thanks to an analog-digital converter (Agilent-34970 A, Analog Device) connected to a PC-type computer via an RS232 serial link.

A software (Datalogger) of acquisition allows, taking into account the equations of calibration of the sensors, the follow-up graph of the evolution of measured data, and their storage in a form compatible with the processing software. Data stored by Datalogger software can be saved in a central PC (Hewlett Packard®) and can be displayed on a graphical PC screen during the progress of the experiment.

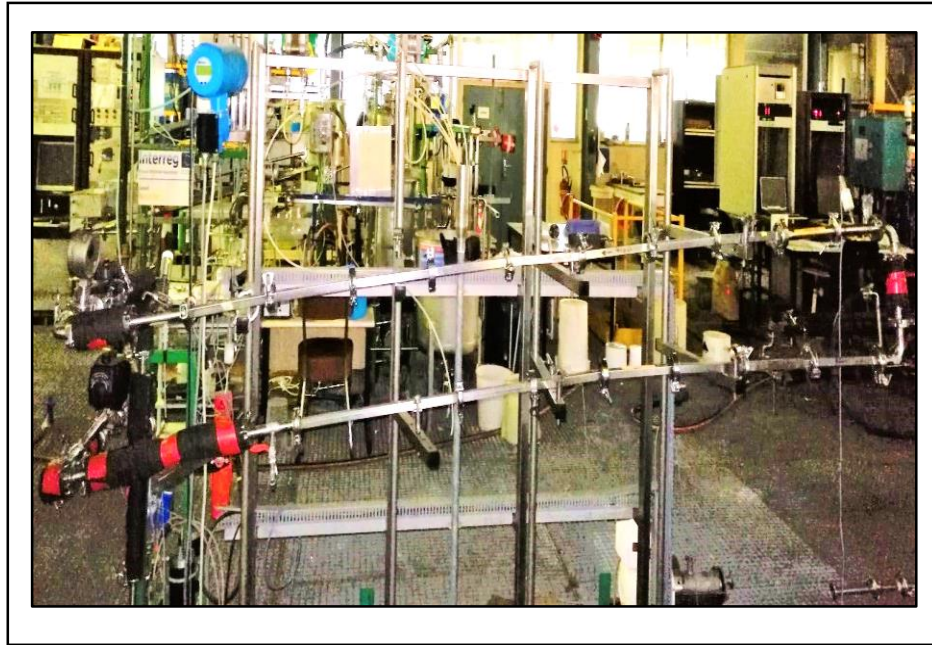


Figure 4.0a. Standard Cleaning in Place like conditions prototype.

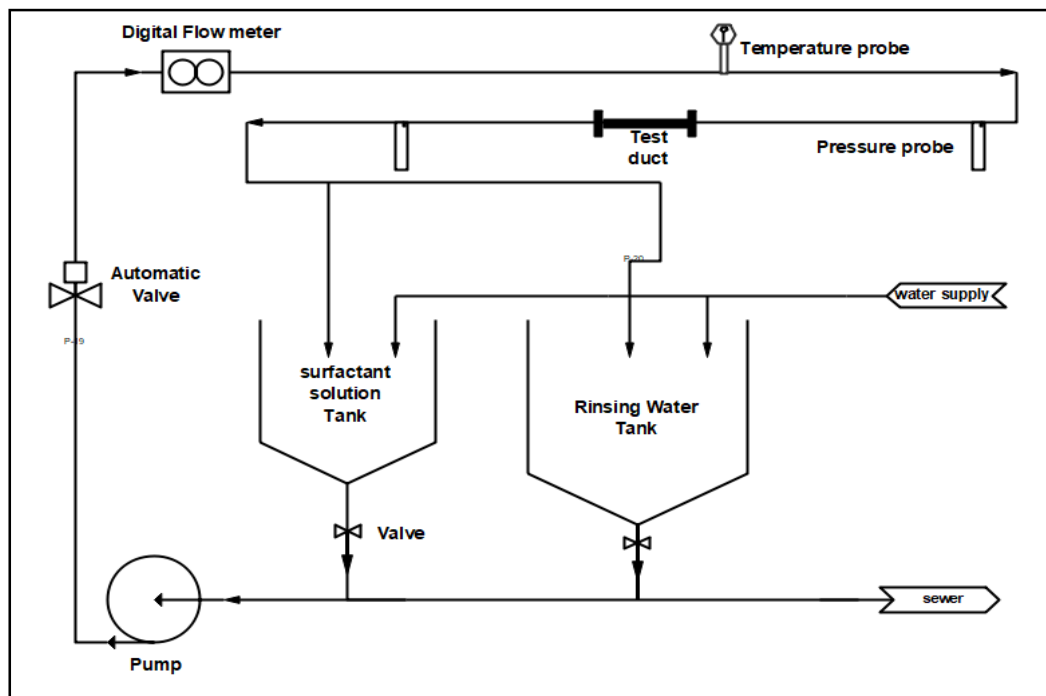


Figure 4.0b : Standard Cleaning in Place like conditions prototype.

4.1.2. Foam Cleaning in Place prototype

The production foam prototype was built according to (Chovet et al., 2015). The experimental set-up was designed to allow the flow of foam within square ducts horizontally placed. The test ducts were placed after a Plexiglas pipe with the same inner size. This pipe allowed us to visualize the foam flow. The measuring section is located at 80 times the hydraulic diameter of the vein inlet. The prototype is sectioned to three parts as described in Figure 4.1.

A. Section 1

Includes the surfactant solution tank (capacity: 100L) filled with the surfactant solution. The solution is pumped from the mother tank to the feeding tank (50L) by a positive displacement pump (VARMECA 21TL055, Leror Somer). The feeding tank is located at a height of 3m from the level of the flow to maintain a constant flow rate to the foam generators.



Figure 4.1a. Foam cleaning in place prototype

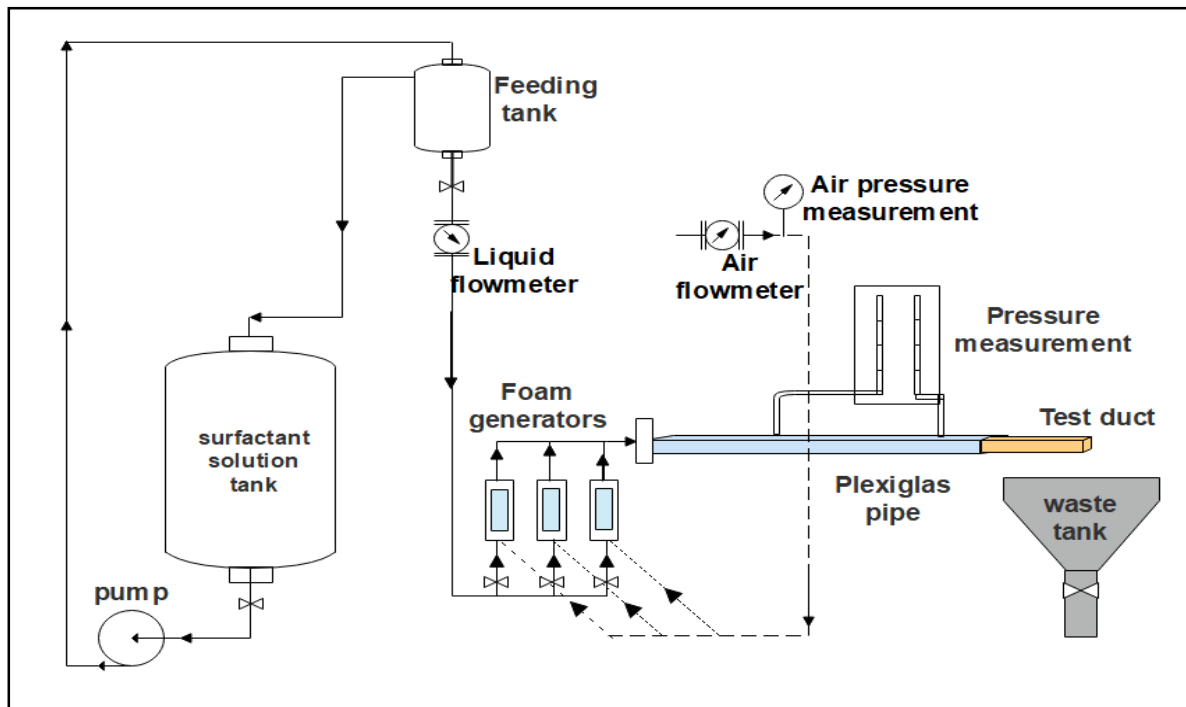


Figure 4.1b. Foam cleaning in place prototype

B. Section 2

This section includes three foam generators that are supplied by the SDS solution (0.15%ww) descending from the feeding tank. The foam is generated by injection of pressure air through a permeable media (DURAN®, pore sizes ranging from 1 to 1.6 μm , Dislab, Lens, France) inside cylindrical containers filled with the SDS solution acting as foam generator. Foams could be considered as dry or wet according to its liquid content, which is represented by the gas volume fraction. According to Chovet and Aloui (2015), the foam quality could be calculated as follows (equation 4.0) where Q_g is the gas flow and Q_l the liquid flow.

$$\beta = \frac{Q_g}{Q_g + Q_l} \quad (4.0)$$

Three independent parallel generators (PIHM, France) allowed us to increase the bulk velocity without affecting the foam structure. The mean velocity was calculated taking into account the global flow rate ($Q_l + Q_g$) divided by the cross section area S of the test duct.

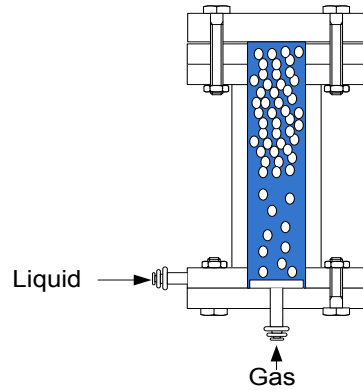


Figure 4.2 Foam generator allows the entry of solution and air simultaneously

The Reynolds number (equation 4.1) was calculated using equation (4.2) and (4.3) taking into account the density of both gas and liquid phases and the calculation of the foam viscosity using the equation proposed by (Hatschek, 1911) based on a heuristic model of concentrated emulsions, where dh is the hydraulic diameter of the pipe and \bar{v} is the average velocity of the flow.

$$Re = \frac{\rho_f \cdot \bar{v} \cdot d_h}{\mu_f} \quad (4.1)$$

$$\rho_f = (1 - \beta) \cdot \rho_l + \beta \cdot \rho_g \quad (4.2)$$

$$\mu_f = \frac{\mu_l}{1 - \mu_l^{1/3}} \quad (4.3)$$

Three liquid and air flow meters enabled the adjustment of the flow rate from 0 to 35 l/h and 0 to 70 l/h respectively.

B. Section 3

Foam passes through a transparent Plexiglas pipe having a length of 1.1 m. The transparent pipe enables the visualization of the foam texture, bubbles size, and measuring foam velocity. Two pressure outlets allows the connection of 2 manifold tubes placed over a scaled plate that measures the pressure drop ΔP .

One test duct that contains fouled coupons to be cleaned is connected to the transparent pipe by clamp connections.

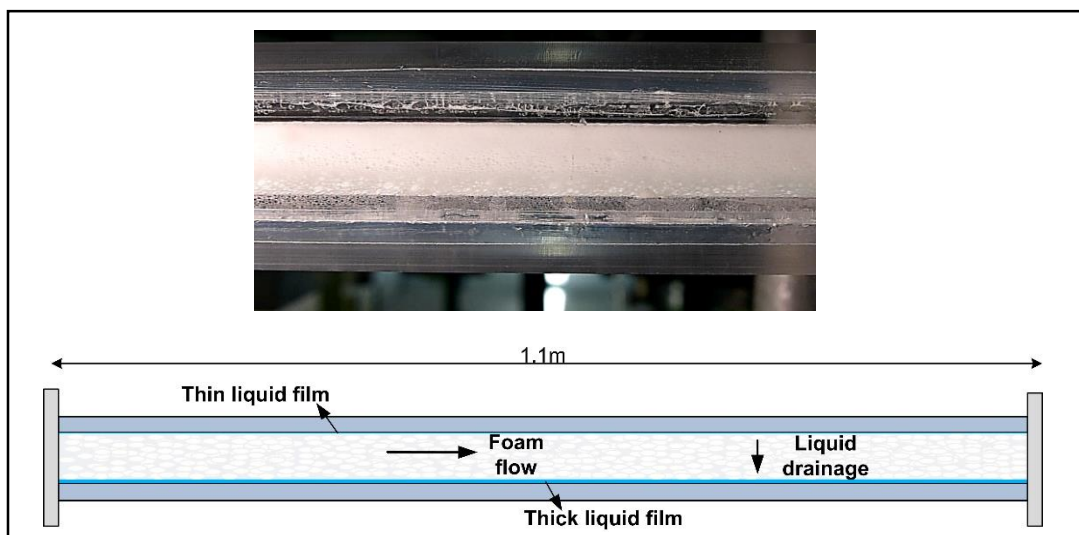


Figure 4.3 Scheme of the transparent PMMA (Poly methyl methacrylate) pipe.

4.1.3. Stainless steel coupons

316L Stainless steel with a 2B finish coupons, kindly provided by APERAM (Isbergues, France) (1.5 *4.5 cm) were used. The coupons have a thickness of 1 mm and have a hole in one end for hanging them from stainless steel wires. The hole allowed the coupons to be held vertically on a stand inside a beaker during the sterilization and fouling process. In order to stabilize their surface properties, the coupons were subjected to an ageing protocol before use, using milk (powder, 150g/l) and sodium hydroxide (0.5% ww) before being used in experiments. The ageing protocol is described in the methods part.

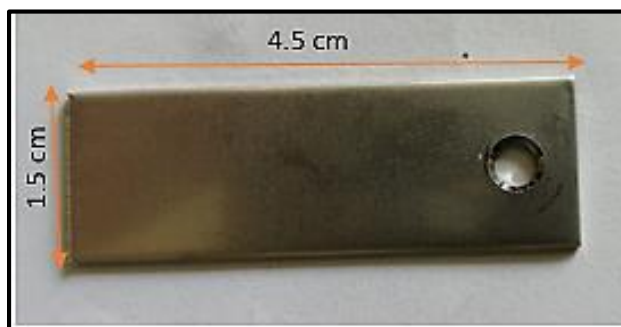


Figure 4.4 316L Stainless Steel coupon with a 2B surface finish.

4.1.4. Test pipes

Test pipes (C. Cunault et al., 2019) were fabricated in a way allowing the insertion of five coupons at a time. The coupons were inserted adjacent to the top wall to study the effect of foam flow effect on that zone. The three coupons in the middle were fouled by the microorganisms (Figure 4.5), while the other coupons at the two extremities were to preserve the foam flow regime from any dynamic perturbations.

The test pipes are clamped in standard Cleaning in Place and foam Cleaning in Place circuits. The hydraulic diameter (D_h) of the test pipe can be calculated according to the following:

$$D_h = \frac{4(ab)}{2(a+b)} \quad (4.4)$$

where a and b are the internal height and width of the pipe. The hydraulic diameter in our case is 0.012 m.

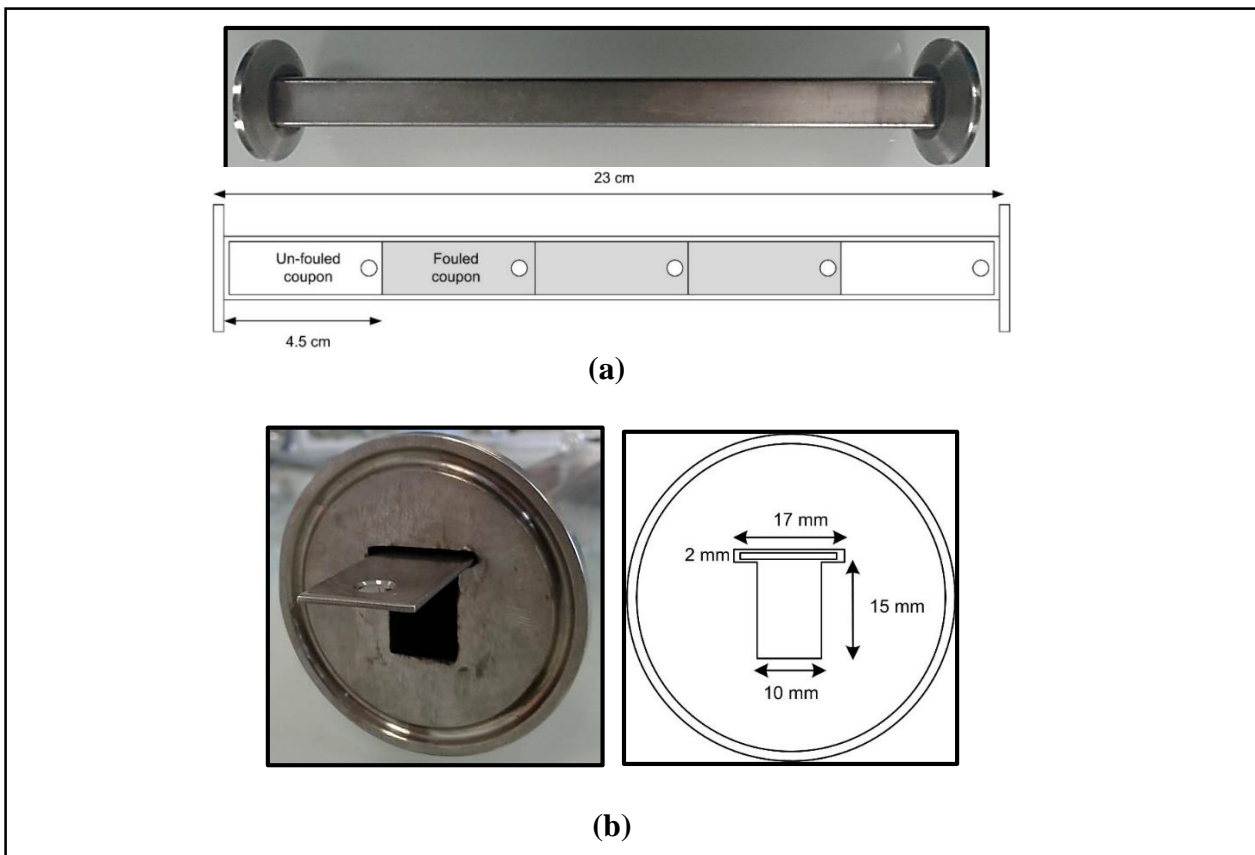


Figure 4.5. Scheme of the test pipe used in cleaning experiments. (a) Top view (b) Entry dimensions of the test pipe.

4.1.5. Singularities

Studying detachment of microorganisms after singularities can provide information on the efficiency of foam flow when subjected to different dynamic changes. In this study, two 316L stainless steel singularities have been used :

- A. A sudden expansion in diameter followed by a gradual reduction.
- B. Two 90° bends that has been used to construct a square circuit to deviate the flow of foam by one/ two times.

A. Sudden expansion/Gradual Reduction singularity

For sudden expansion/gradual reduction, two positions were considered, the first was directly after the foam generation source, and the second position was after 1m of foam flow (Figure 4.6). The test pipe fouled with spores was set directly after the sudden expansion singularity in the two cases. The goal from setting the first position was to study the efficiency of foam in detaching spores when it is subjected to the singularity effect only. The goal of the second position was to study the efficiency of foam in detaching spores after passing through a 1m straight pipe followed by the singularity. In that case the study is on a previously stabilized foam which is then subjected to the singularity disturbance effect. The following illustration clarify the positions of the singularity and the test pipe for the two cases.

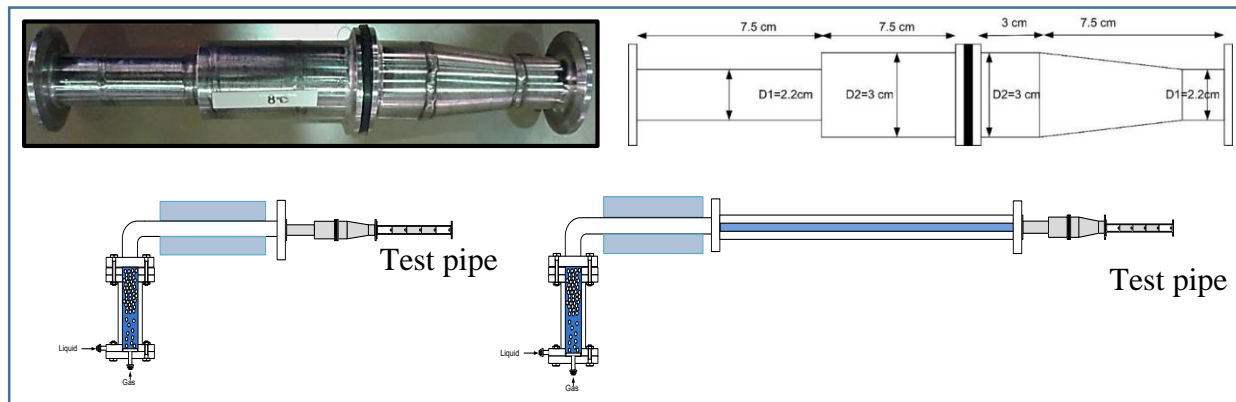


Figure 4.6 The singularity used is an expansion followed by a gradual decrease in diameter up to its initial entry dimension ($D1= 2.2$ cm). The singularity has been clamped after 1meter of straight flow or directly after the foam generation source.

B. Bends

Foam flow efficiency in detaching spores was studied after one/two bends. Two test pipes were installed in a horizontal square shaped circuit: Test pipe 1 was installed after one bend, Test pipe 2 was installed after two bends. Test pipe 1 was set after 2.5 m and Test pipe 2 after 3.75 m from the foam generation source. The goal was to study the efficiency of foam flow on spore detachment when subjected to a directional flow change by 90° .

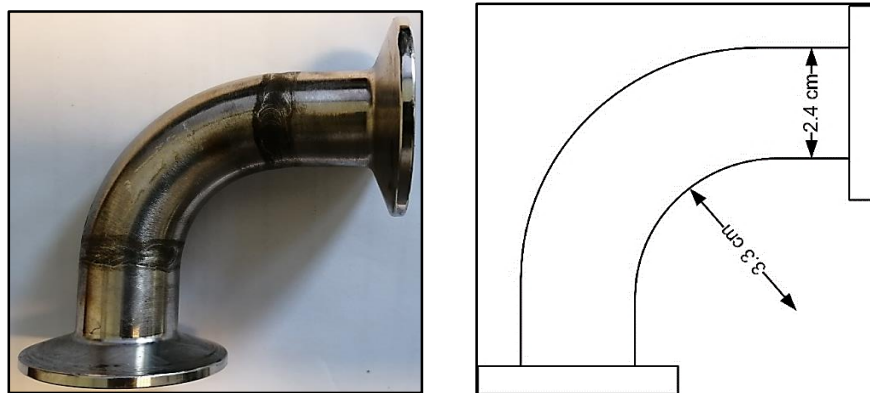


Figure 4.7 Dimensions of 90° bend singularity

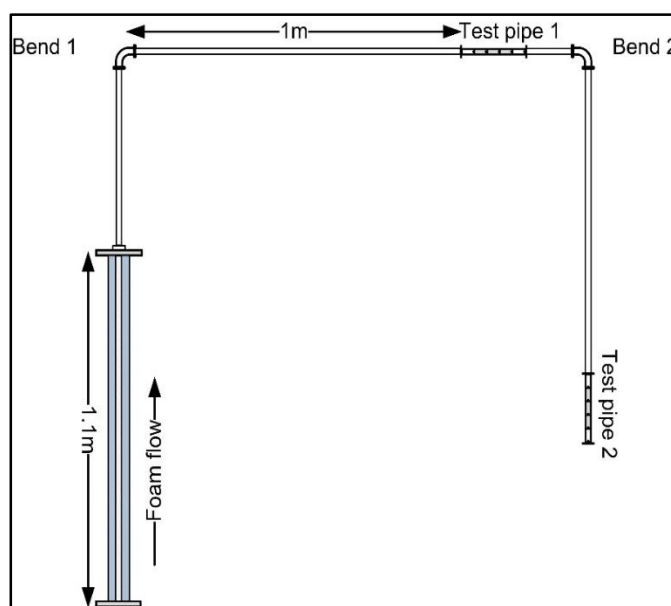


Figure 4.8 Square circuit integrating the two bends (top view)

4.2 Surfactants

Different surfactants, i.e. Sodium dodecyl sulfate (SDS), Lauramine oxides (Ammonyx LO[®] [STEPAN]) and ethoxylated nonionic fluoro-surfactant (Capstone FS-30[®] [CHEMOURS[™]]) have been used in the experiments performed on the cleaning of *B. amyloliquefaciens* 98/7 spores. For

B. cereus 98/4 spores and *P. fluorescens pfl* biofilm only SDS has been used. Surfactant solutions were prepared at the following concentrations: SDS = 1.5 g/L, Ammonyx LO = 0.8 ml/L and Capstone FS-30 = 0.32 ml/L. The chosen concentrations were sufficient to obtain a stable foam. The following is a description of some physical and chemical characteristics of each surfactant.

4.2.1 Sodium dodecyl sulfate

Sodium dodecyl sulfate is the most widely used of the anionic alkyl sulfate surfactants. Its surface-active properties makes it important in hundreds of household and industrial cleaners, personal care products, and cosmetics. It is also used in several types of industrial manufacturing processes, as a delivery aid in pharmaceuticals, and in biochemical research involving electrophoresis. SDS synthesis involves the sulfation of 1-dodecanol followed by neutralization with a cation source (Singer & Tjeerdema, 1993). In this study, powder sodium do-decyl sulfate has been used (SIGMA-ALDRICH) with 98.5% purity.

4.2.2 Lauramine oxide (AMMONYX LO[®])

AMMONYX LO (STEPHAN[®]) is a non-ionic surfactant, which is used as a foam enhancer, detergent, stabilizing and thickening agent. In the textile industry it can be used as lubricant, emulsifier, wetting agent and dye dispersant. It is totally non-ionic at a pH above 7 and is slightly cationic when the pH is slightly acidic. It is totally cationic at pH below 3.

4.2.3 Ethoxylated nonionic fluoro-surfactant (Capstone FS-30)

Capstone FS-30 (CHEMOURS[™]) is a general-purpose, water-soluble, ethoxylated nonionic fluoro-surfactant that modifies surface energies at very low concentrations. It is stable in acidic, basic, brine and hard water environments. According to the provider, it reduces surface tension and provides excellent wetting to achieve cleanability.

4.2.4 Microorganism used for coupons fouling: Spores/ Biofilms

In the food industry, contamination by biological hazards can be encountered by spores or biofilms or with sole bacterial cells. For spores, *B. amyloliquefaciens* and *B. cereus* spores were chosen in this study. *B. cereus* 98/4 spores are hydrophobic while *B. amyloliquefaciens* 98/7 (formerly known as *B. subtilis* 98/7) spores are highly hydrophilic (Figure 4.9). For biofilms, *P. fluorescens* has been chosen known as good biofilm former during a short time and due to its previous

incidences in contamination in food industry. *B. amyloliquefaciens* 98/7 was isolated from a dairy processing line (Faille et al., 2010). *B. cereus* 98/4 wild type was isolated from a dairy processing line (Faille et al., 2007). In this study, *P. fluorescens* Pf1 strain was used, it was isolated by the French Agency for Food, Environmental and Occupational Health & Safety (ANSES) from cleaning in place effluent (C. Cunault et al., 2018). This strain can form biofilms within 24 hrs.



Figure 4.9 *B. amyloliquefaciens* 98/7 wild type spores appear yellow-orange roundly shaped on stainless steel after staining with Orange Acridine (0.01%).

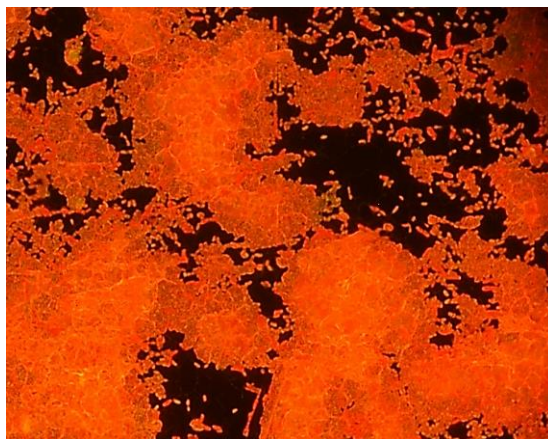


Figure 4.10 24 hrs. *P. fluorescens* pf1 Biofilm. Cells are embedded in the Extra Cellular Matrix (ECM) of the biofilm.

4.3 Foam Flow Regimes

4.3.1 Regime identification

Based on the literature as it is described by Tisné (Tisne et al., 2004), three types of flow regimes were identified at different velocities of foam flow. The flow regimes are also termed as 1D for the plug flow, 2D and 3D flow when foam bubbles acquire different velocities along the lateral and top plane.

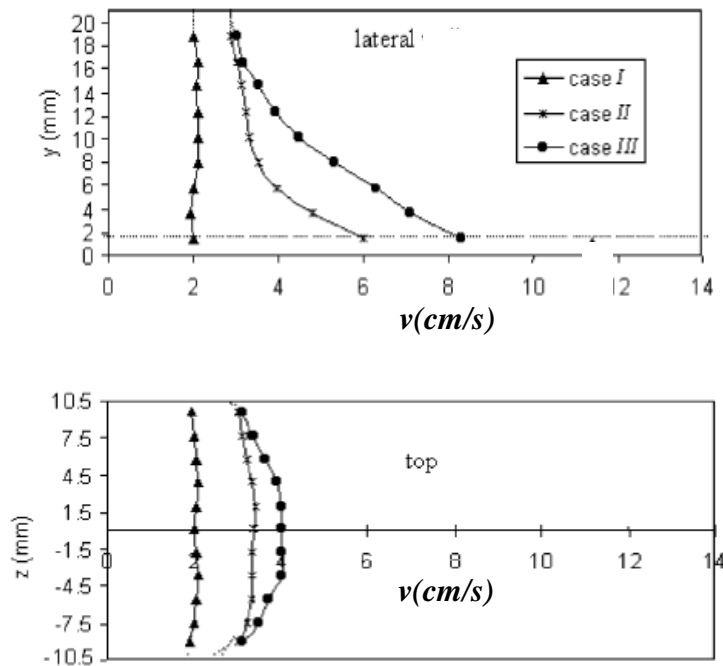


Figure 4.11 Local axial velocity of foam for the flow regimes at the lateral and top face of a square cross sectioned pipe. Average velocity v in Case I is 2cm/s, Case II: 4cm/s, Case III: 6cm/s (Tisne et al., 2004)

The method used in this study is based on the determination of the velocity profile by observation of the moving bubbles at the lateral and top wall of the pipe, during a time interval. In situ measurement of the velocity of bubbles was attained by marking the Plexiglas pipe by two marks with a known distance between them. Both for the lateral and the top plane of the pipe, three locations were chosen to measure the bubble velocity, two at the edges and one at the middle. The time was recorded during which the bubble passes between two marks (Figure 4.12). The distance was divided by the recorded time to obtain the velocity of the bubble. This method gives an approximation of the velocity of the bubbles. Therefore a velocity profile can be concluded to fix

the experimental conditions and work in the three flow regimes presented in the literature (Tisne et al., 2004).

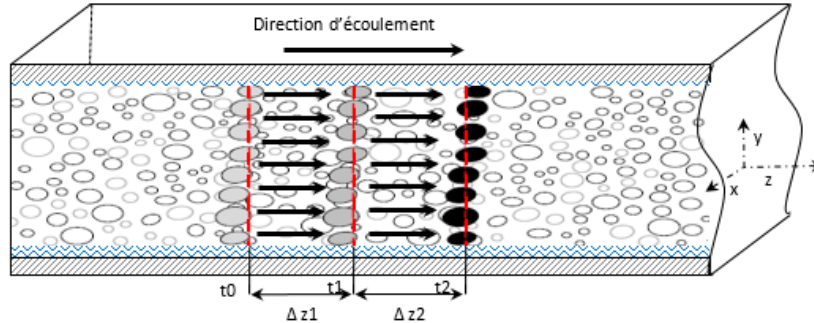


Figure 4.12 Bubbles pass adjacent the marked distance Δz at certain time interval t (H. Dallagi , 2020).

4.3.2 Average shear stress measurement

Two pressure outlets connected to two transparent hoses placed over a scaled plate allowed measurement of the difference in the water level along the Plexiglas pipe, the pressure value at each water column height was calculated according to the Bernoulli equation:

$$P = P_a + \Delta z \cdot \rho \cdot g + v^2 \cdot \rho \quad (4.5)$$

Where P_a is the atmospheric pressure, Δz is the height difference of two water columns, ρ is the density of water, g is the gravity acceleration and v is the velocity of the generated foam.

For average shear stress $\bar{\tau}$ calculation using ΔP ,

$$\bar{\tau} = \frac{\Delta P \cdot d_h}{4L} \quad (4.6)$$

Where L is the pipe length.

4.4. Bubble size measurement

Bubble size has been measured for each flow regime with the foam quality used. After taking images in situ on the transparent Plexiglas pipe, by a camera (Panasonic, DMC-FZ200, ISO-200). The software Pixamètre 5.1 R1540 was used to measure the diameter of bubbles at the top wall.

The measurements were done in a zone having a length of 1.5 mm and a width of 10 mm (transparent pipe width).

4.5 Conditioning of coupons (ageing): Treatment with Milk and NaOH (0.5%)

Before any experiment, coupons were subjected to a conditioning process to obtain surface properties relevant to what could be found in real environments. The process used here mimicked what could happen in the dairy industry (successive steps of food processing and CIP procedures). Milk (INGREDIA, Whole milk powder, 26% fat) and hot NaOH (0.5% w/w) were used.

The ageing process consists of 4 successive steps

- A. The coupons were immersed in 1L of milk (150 g/l) at an ambient temperature for 30 minutes.
- B. Coupons were rinsed under osmosed water overflow for 5 minutes.
- C. The coupons were then immersed in a NaOH (0.5% w/w) solution at 60°C for 30 minutes.
- D. A final rinsing again under osmosed water overflow for 5 minutes.

This cycle is repeated 15 times in order to obtain coupons ready to be used in experiments. Ageing was an indispensable step and resulted in changes in the surface energy.

4.6 Roughness Ra, Profilometer (Mahr)

After the aging process, the surface roughness Ra for the coupons was measured. Ra is the arithmetical mean deviation of the absolute ordinate values within a sampling length (ISO 4287:1997). Average roughness Ra was calculated from the topography profiles obtained with a Perthometer S2 profilometer (Mahr, France). The profilometer is equipped with cantilever (Figure 4.13) that allowed tracing the surface peaks and valleys resulting in x-y profile.

Measurements were taken at 3 different positions on sample surface in the direction of the flow. On each position 5 measurements were performed to have an average value.

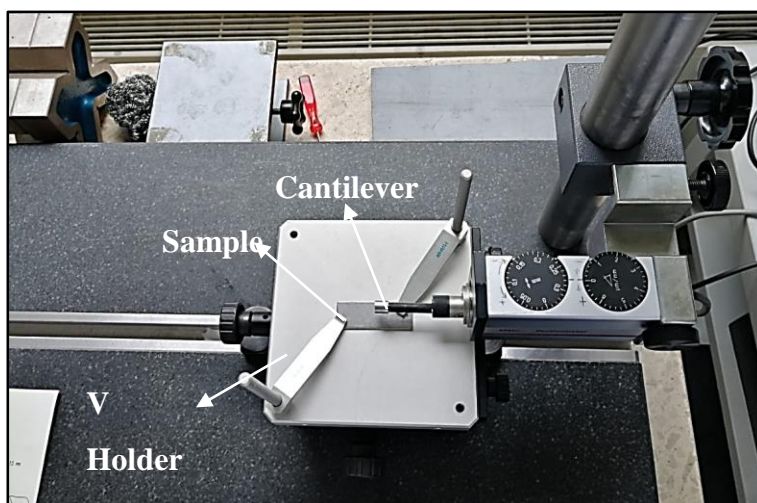


Figure 4.13 Stainless steel coupon was fixed by holders on the sample positioning table of the profilometer.

4.7 Cleaning and disinfection of stainless steel coupons

Before any experiment, coupons were subjected to a cleaning protocol that removes any micro particles –debris on the surface. The cleaning detergent was RBS T 105, pH = 11.8. The detergent was heated at 60°C, then coupons were totally immersed in the detergent. The protocol for cleaning and disinfection of coupons is described below:

- A. Coupons were first rubbed with the pure cleaning detergent.
- B. The coupons are then immersed for 10 min in RBS (20ml.l⁻¹) heated at 60°C then rinsed again with hard and osmosed water for 5 min respectively.
- C. Coupons were separated by bolts, suspended vertically on a holder and then sterilized 24 hrs. before fouling at 175 °C in a dry heat oven for a duration of 1 h.

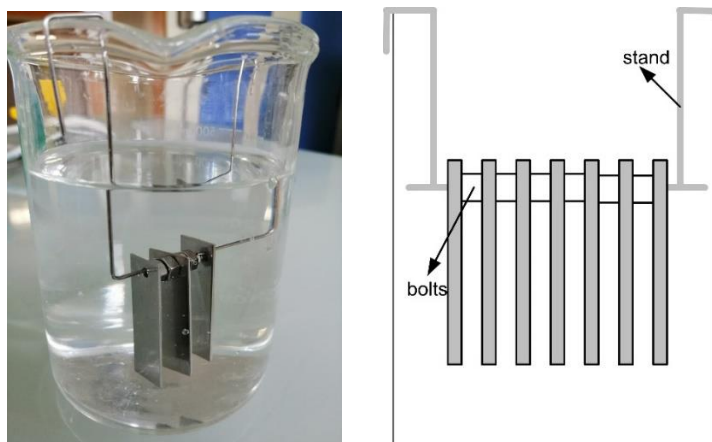


Figure 4.14 Coupons were suspended vertically on a stand and separated by bolts before dry sterilization at 175°C during 1 hr.



(a)



(b)

Figure 4.15 (a) Wet sterilization in autoclave at 120°C, (b) Dry sterilization in oven at 170°C.

4.8 Sporulation and Fouling Conditions

4.8.1 Sporulation Method

Spores were produced at 30 °C on Spo8-agar consisting of 8 g.L⁻¹formate (Biokar Diagnostics, Beauvais, France), 0.51 g L⁻¹ MgSO₄·7H₂O, 0.97 g L⁻¹ KCl, 0.2 g L⁻¹ CaCl₂·2H₂O, 3 × 10⁻³ g L⁻¹ MnCl₂·4H₂O, 0.55 × 10⁻³ g L⁻¹ FeSO₄·7H₂O, and 1.5% agar. When over 95% of spores were obtained, they were harvested by scraping the surface, washed five times in chilled sterile water (by centrifugation at 1500 g [*B. cereus* spores] or 3500 g [*B. amyloliquefaciens* spores] for 15 min), and stored in sterile water at 4°C until use. Before each experiment, a further set of two washes was performed and spores were subjected to a 2-min ultra-sonication step in an ultrasonic

cleaner (Branson 2510E-MT, 42 kHz, 100 W, Branson Ultrasonics Corporation, USA) to limit the presence of clusters (Faille et al., 2013).

4.8.2 Fouling Conditions

Spore suspensions were diluted at a final concentration of 10^6 cfu.ml⁻¹ (*B. amyloliquefaciens* spores) and 10^5 cfu.ml⁻¹ (*B. cereus* spores). After vertical fouling for 4 h (Figure 4.16), the level of coupon contamination is close to 10^5 cfu.cm⁻².

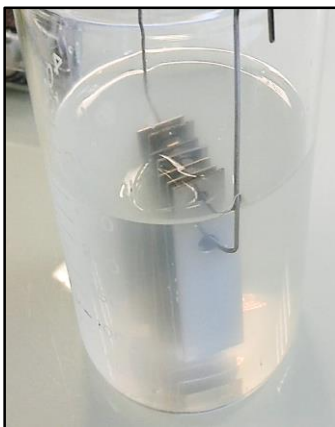


Figure 4.16 Coupons immersed in the fouling suspension of spores

4.9 *P. fluorescens* pfl Biofilm Preparation and Fouling Conditions

The Pf1 biofilms were formed in static conditions on sterilised coupons placed vertically, fully immersed, in beakers containing 450 ml of 1/10 TSB inoculated at around 10^7 cfu.ml⁻¹ with a 24 hrs. preculture of *P. fluorescens*. After 24 hrs incubation, coupons were removed from the fouling suspension and rinsed by gentle immersion in sterilised ultrapure water to remove unattached cells. Some coupons are directly analyzed (measurement of the surface microbial load (cfu), observation of the biofilm structure (observation under microscope). Other coupons are inserted in the test pipes for cleaning experiments.

4.10 Evaluation of the hydrophilic/hydrophobic character of spores (MATH test)

For each spore batch, MATH tests (Measurement of affinity to hydrocarbons) were conducted to estimate the affinity of spores to hydrocarbons (Faille et al., 2019). The partitioning method used in this study is based on the affinity of spores to an apolar solvent, hexadecane (Sigma). Spores were re-suspended in saline, the suspensions being at an absorbance of 0.5 to 0.6 at 600 nm (A₀) in glass tubes (10 mm in diameter × 75 mm). Three milliliter aliquots of the suspensions and 500

μL of hexadecane were vortexed at maximal speed (2400 rpm) for times ranging from 5 s to 240 s and left to settle for 30 min to allow complete separation of the two phases. The absorbance of the aqueous phase at 600 nm was measured before mixing (A_0) and at different vortexing times (A_t). $[(A_t/A_0)*100]$ was plotted against the vortexing time (s). The hydrophilicity/hydrophobicity was evaluated using the Gibbs partitioning energy (ΔG_{par}), calculated from A_{eq} , taking the asymptotic or the lowest absorbance value. Indeed, ΔG_{par} is obtained from the equilibrium constant K ($\Delta G_{\text{par}} = \text{Ln}K$), which expresses the maximal partitioning of bacteria between the aqueous and hexadecane phases. This was calculated from the equation $K=[6(A_0 - A_{\text{eq}}) / A_{\text{eq}}]$. The factor 6 in the equation was used to correct for the different volumes of the aqueous and hexadecane phases (Bos et al., 1999). When hydrophilic particles were analyzed, very little removal from the aqueous phase, if any at all, was observed, resulting in low ΔG_{par} values. Conversely, when slightly hydrophilic, or hydrophobic particles are analyzed, low A_{eq} values are obtained, resulting in high ΔG_{par} values. At UMET, a spore is considered to be hydrophobic for ΔG_{par} values > 4.0 , moderately hydrophilic for ΔG_{par} values ranging from 3.0 to 4.0 and highly hydrophilic for ΔG_{par} values < 3.0 .

The scheme below (Figure 4.17) illustrates the displacement of spores from their own suspension to hexadecane.

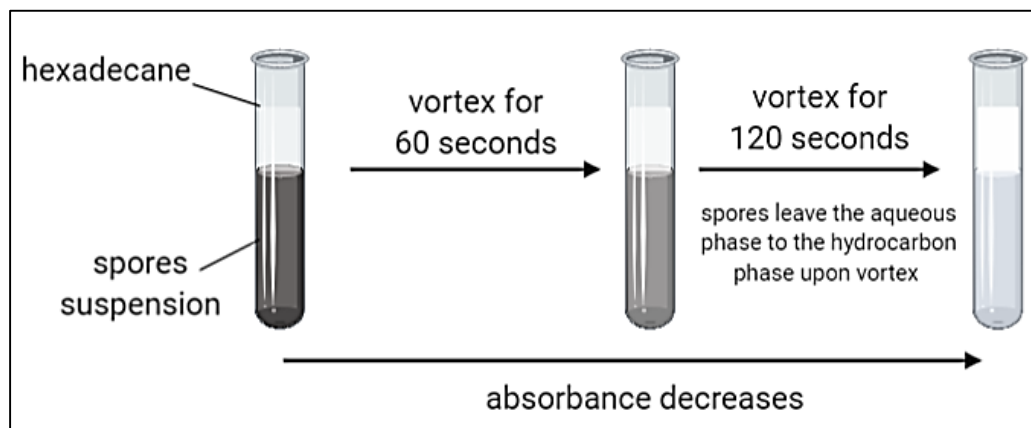


Figure 4.17 As vortex time increases, more spores will leave their aqueous phase where its absorbance to light ($\lambda=600$ nm) decreases.

4.11 Post experimental treatment of coupons

In order to study the kinetics of the detachment, for each cleaning time, one test pipe was used. We chose to work with 6 cleaning times that correspond to: 15sec, 35 sec, 1 min, 3 min, 10 min, 20 min. After each cleaning time with foam CIP or standard CIP, the pipe was unclamped to obtain the coupons. The fouled coupons were taken out and the side of the coupon in contact with the pipe wall was disinfected using a cotton swab dipped for a few seconds in a solution of disinfectant Oxygal (10% w/w, active substances: 2 g of hydrogen peroxide + 0.25 g of peracetic acid) diluted 10 times by water. Adherent spores were then detached from the coupon by ultrasonication in 10 ml TSB 1/10, Tween 80 0.5% v/v (5 min, Ultrasonic bath, 40 kHz, Deltasonic, France). The detached bacteria were enumerated on TSA (Tryptone Soy Agar, Biokar, France) after 48 h.

4.12 Epifluorescence microscopy

Epifluorescence microscopy is a technique that uses an optical microscope taking advantage of the phenomenon of fluorescence and phosphorescence, instead of, or in addition to, classical reflection observation (physics) or absorption of natural or artificial visible light. Before the observation with the microscope, orange acridine (0.01%) staining is performed on the coupons. This dye colors the DNA of viable cells orange and the dead cells green. Previous experiments performed at UMET showed that *B. cereus* spores were stained in green, *B. amyloliquefaciens* ones in red, probably due to the differences in surface composition. The coupons are then left at room temperature for 15 min in the dark. Coupons are then rinsed and observed under an epifluorescence microscope (Zeiss Axioskop 2 plus, Oberkochen, Germany; excitation 495 nm; 519 nm emission).

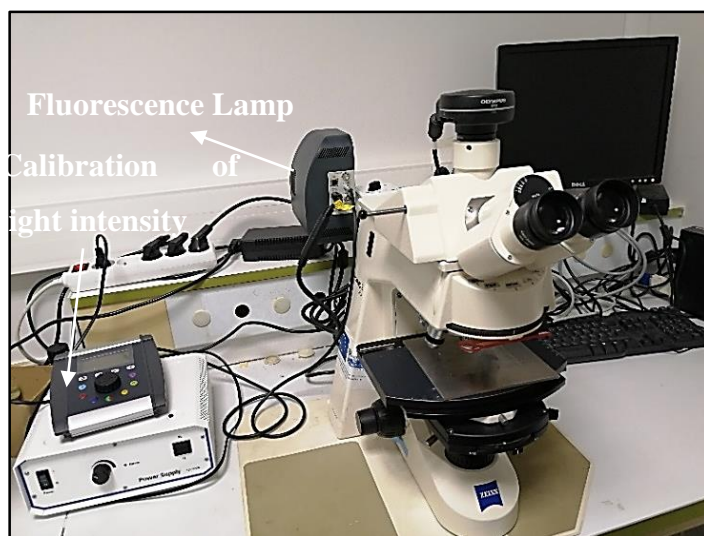


Figure 4.18 Optical microscopy with excitation light frequency used to observe the phenomenon of fluorescence after dyeing of cells

4.13 Measurement of surface tension of surfactants using the pendant drop method

This technique is called the Pendant Drop Method. It is due the shape of the liquid, which assumes a pendant shape under the influence of gravity. The analysis of the drop shape is based on the Young-Laplace equation. The equation describes the pressure difference between the areas inside and outside of a curved liquid surface/interface with the principal radii of curvature R_1 and R_2 and σ being the surface tension:

$$\Delta P = (P_{int} - P_{ext}) = \sigma \left(\frac{1}{R_1} + \frac{1}{R_2} \right) \quad (4.6)$$

Two forces determine the shape of the pendant drop, tension and gravitation. The surface tension tends to minimize the surface area and modifies the shape of the drop to a spherical shape while gravitation stretches the drop from this spherical shape to a pear-like shape (Data-physics-instruments). The equations related to this method is more described by Berry (Berry et al., 2015)

In this study the apparatus DIGIDROP GBX (Figure 4.19) was used along with its software. One of the options is using it as a tension-meter. it is equipped with a light source and a real time recording camera that detects any real time changes in the drop shape.

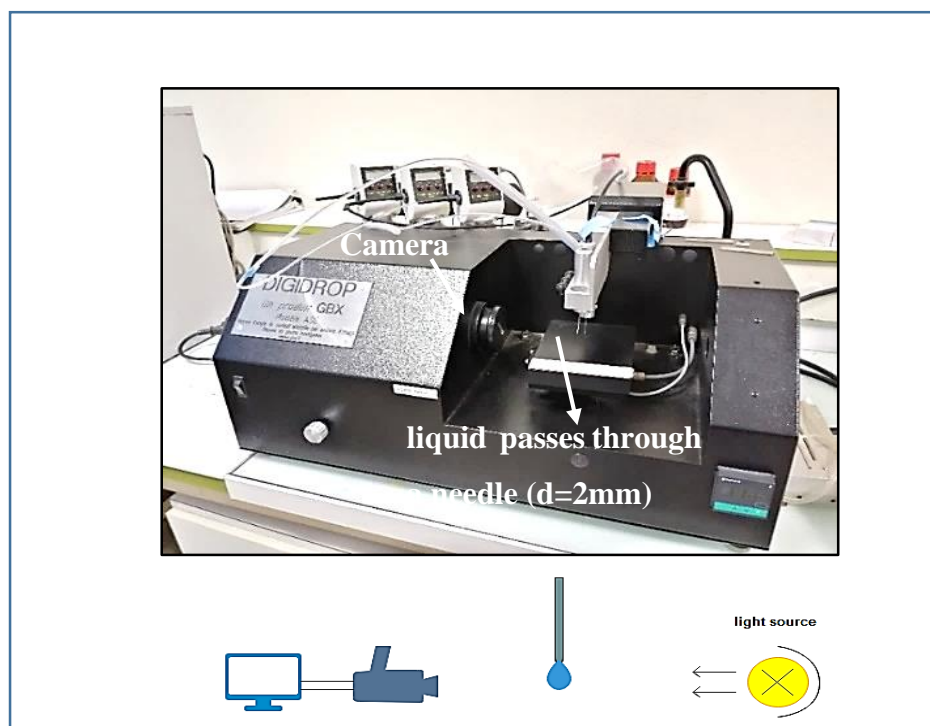


Figure 4.19 The apparatus DIGIDROP GBX was used as a tensiometer.

References 4.19

- Berry, J. D., Neeson, M. J., Dagastine, R. R., Chan, D. Y. C., & Tabor, R. F. (2015). Measurement of surface and interfacial tension using pendant drop tensiometry. *Journal of Colloid and Interface Science*, 454, 226–237. <https://doi.org/10.1016/j.jcis.2015.05.012>
- Bos, R., van der Mei, H. C., & Busscher, H. J. (1999). Physico-chemistry of initial microbial adhesive interactions – its mechanisms and methods for study. *FEMS Microbiology Reviews*, 23(2), 179–230. <https://doi.org/10.1111/j.1574-6976.1999.tb00396.x>
- Chovet, R., Aloui, F., & Keirsbulck, L. (2015). *Wall Shear Stress Generated by Aqueous Flowing Foam*. V001T14A001. <https://doi.org/10.1115/AJKFluids2015-14039>
- Cunault, C., Faille, C., Briandet, R., Postollec, F., Desriac, N., & Benezech, T. (2018). *Pseudomonas* sp. Biofilm development on fresh-cut food equipment surfaces – a growth curve – fitting approach to building a comprehensive tool for studying surface contamination dynamics. *Food and Bioproducts Processing*, 107, 70–87. <https://doi.org/10.1016/j.fbp.2017.11.001>
- Cunault, Charles, Faille, C., Calabozo-Delgado, A., & Benezech, T. (2019). Structure and resistance to mechanical stress and enzymatic cleaning of *Pseudomonas fluorescens* biofilms

formed in fresh-cut ready to eat washing tanks. *Journal of Food Engineering*, 262, 154–161. <https://doi.org/10.1016/j.jfoodeng.2019.06.006>

Faille, C., Lemy, C., Allion-Maurer, A., & Zoueshtiagh, F. (2019). Evaluation of the hydrophobic properties of latex microspheres and *Bacillus* spores. Influence of the particle size on the data obtained by the MATH method (microbial adhesion to hydrocarbons). *Colloids and Surfaces B: Biointerfaces*, 182, 110398. <https://doi.org/10.1016/j.colsurfb.2019.110398>

Faille, C., Lequette, Y., Ronse, A., Slomianny, C., Garénaux, E., & Guerardel, Y. (2010). Morphology and physico-chemical properties of *Bacillus* spores surrounded or not with an exosporium: Consequences on their ability to adhere to stainless steel. *International Journal of Food Microbiology*, 143(3), 125–135. <https://doi.org/10.1016/j.ijfoodmicro.2010.07.038>

Faille, C., Ronse, A., Dewailly, E., Slomianny, C., Maes, E., Krzewinski, F., & Guerardel, Y. (2014). Presence and function of a thick mucous layer rich in polysaccharides around *Bacillus subtilis* spores. *Biofouling*, 30(7), 845–858. <https://doi.org/10.1080/08927014.2014.939073>

Faille, C., Benezech, T., Blel, W., Ronse, A., Ronse, G., Clarisse, M., & Slomianny, C. (2013). Role of mechanical vs. chemical action in the removal of adherent *Bacillus* spores during CIP procedures. *Food microbiology*, 33(2), 149-157.

Faille, C., Tauveron, G., Le Gentil-Lelièvre, C., & Slomianny, C. (2007). Occurrence of *Bacillus cereus* Spores with a Damaged Exosporium: Consequences on the Spore Adhesion on Surfaces of Food Processing Lines. *Journal of Food Protection*, 70(10), 2346–2353. <https://doi.org/10.4315/0362-028X-70.10.2346>

Hatschek, E. (1911). *Die Viskosität der Dispersoide* / SpringerLink. <https://link.springer.com/article/10.1007%2FBF01503180?LI=true>

Nadell, C. D., Drescher, K., Wingreen, N. S., & Bassler, B. L. (2015). Extracellular matrix structure governs invasion resistance in bacterial biofilms. *The ISME Journal*, 9(8), 1700–1709. <https://doi.org/10.1038/ismej.2014.246>

Singer, M. M., & Tjeerdema, R. S. (1993). Fate and effects of the surfactant sodium dodecyl sulfate. *Reviews of Environmental Contamination and Toxicology*, 133, 95–149.

Tisne, P., Doublier, L., & Aloui, F. (2004). Determination of the slip layer thickness for a wet foam flow. *Colloids and Surfaces A: Physicochemical and Engineering Aspects*, 246(1–3), 21–29. <https://doi.org/10.1016/j.colsurfa.2004.07.014>

CHAPTER V, PART 1 (Article)**Journal of Food Engineering**

Removal of *Bacillus* spores by flowing foam from stainless steel pipes: effect of the foam quality and velocity

CHAPTER V, PART 1

RESULTS

Removal of *Bacillus* spores by flowing foam from stainless steel pipes: effect of the foam quality and velocity

Ahmad Al Saabi¹, Heni Dallagi¹, Fethi Aloui², Christine Faille¹, Gaétan Rauwel³, Laurent Wauquier¹, Laurent Bouvier¹ and Thierry Bénézech^{1,*}

¹ Univ. Lille, CNRS, INRAE, ENSCL, UMET, F-59650, Villeneuve d'Ascq, France

² Polytechnic University Hauts-de-France, LAMIH CNRS UMR 8201, Campus Mont-Houy, F-59313 Valenciennes Cedex 9, France ; Fethi.Aloui@uphf.fr

³ Anios-Ecolab, Sainghin-en-Mélantois, France ; gaetan.rauwel@anios.com

*Correspondence: Thierry.benezech@inrae.fr

Abstract

Effective cleaning operations in food industries are considered mandatory to mitigate the risk of remaining unwanted contamination without jeopardizing any further disinfection steps. However, such operations consumed large amount of water, chemicals and energy. In this work an attempt was made to study the cleaning potencies of flowing foams to eliminate *Bacillus* spores from stainless steel surfaces. An original set-up was designed to allow the formation of wet foams to be flown under three flow regime conditions without modifying the foam structure. However, a bubbles' size rearrangement was observed while increasing the velocity affecting the cleaning efficiency visible with the driest foams. The best option was observed with foam at 50% air/water and low velocities to remove 2 log of the initial contamination of *B. amyloliquefaciens* spores being comparable to similar CIP conditions. Removal kinetics were modelled with a simple exponential two-phase kinetics showing in the most favorable cases very high constant rates during the first phase. Hence, comparing with the literature, it was possible to highlight roles on such efficient cleaning to the local high wall shear stress fluctuations and to the presence of capillary forces (low velocities, favorable bubbles size repartition and for the hydrophilicity of bacteria spores).

Keywords: Flowing foam; wall shear stress; Cleaning; *Bacillus* spores; hygiene

1. Introduction

In agro-food industrial environments, surfaces have been reported to be contaminated by a range of microorganisms, including pathogenic and spoilage bacteria (Srey et al., 2013). Once introduced, if environmental conditions are suitable, many bacteria are able to persist on the contaminated surfaces or even to form biofilms. Indeed, despite cleaning and disinfection procedures, some bacteria are still commonly found on the surfaces of food processing lines, mostly in the form of adherent spores, e.g. *Bacillus* spores in closed equipment (Peng et al., 2002) or in the form of biofilms, e.g. *Pseudomonas spp* (Dogan and Boor, 2003).

Cleaning in place (CIP) leading to residue removal from inner surfaces of processing lines without disassembling, has been a crucial factor in guaranteeing the safety and quality of food. If not done properly, consequences can be devastating, especially in the case of pathogen surface contamination (Pietrysiak et al., 2019; Ribeiro et al., 2019). In order to clean rapidly, CIP aims to combine the advantages of the high temperature, detergent and the mechanical action generated by the turbulent flow (or the impact of the spray) (Moerman et al., 2014). The mechanical effect is created by the flow rate and it is generally admitted that high flow rates result in high removal rates because of the high shear forces on the deposit layer. However, some works have detailed the role of hydrodynamics and in particular of the mean wall shear stress and the major role played by its fluctuations (Blel et al., 2013, 2010). This was very recently judged to be mandatory for any CIP improvement (Li et al., 2019).

The addition of foaming surfactants or even gas-stabilized foam means the cleaning solution can be applied as a foam, which can increase the retention time, e.g. on vertical surfaces. Foam is widely used in static conditions throughout the food industry for the cleaning of large open surfaces (floor, conveyors, workshops and equipment). To clean open surfaces, foam requires specific qualities, namely density, foamability, stability and void fraction-based quality. However, foaming cleaning agent could also be used for cleaning some closed equipment such as filtration modules (Gahleitner et al., 2013). Despite its widespread use, very little work has been carried out on the elimination of surface deposits using flowing foam, essentially gas-liquid two-phase flows in capillaries (Kondjoyan et al., 2009) and to our knowledge none have dealt with the elimination of microorganisms.

Almost nothing is known about the potential of foam flow to conduct cleaning operations using much less energy (very low velocity) and much less water. Aqueous foams are non-Newtonian

complex fluids consisting of concentrated dispersions of gas bubbles in a soapy liquid. Depending on the amount of water they contain, they can be either wet or dry. The air fraction defines the so-called foam β quality (Tisné et al., 2004). Foams have original mechanical properties which rely on their low density and high surface area combined with their ability to elastically respond to low stresses and to flow like a viscous liquid with large distortions.

Foams admit an unexpected and nonlinear rheological behavior (shear thinning and yielding), where the properties of the liquid and gas, that compose it, have an influence on it. Their rheological behavior can be compared with some non-Newtonian models such as, power law, Bingham, and Herschel–Bulkley. Recently it was demonstrated that the foam rheological behavior can be better described by Herschel-Bulkley model (Dallagi et al., 2019, 2018).

Among the consequences of foam flow, the mechanical action exerted on the contact-surface depends on the velocity, foam composition (air/liquid) and the ability of the system (foam, geometry and surface properties of the equipment to be cleaned) to maintain a thin liquid film between the solid surface (wall) and the foam flow.

Wall shear stress, especially due to this thin liquid film located between the wall and the foam flow, plays an important role in the characterization of the rheological properties of this foam, depending mainly on the bubble size and particularly on the volume fraction of the liquid (Chovet, 2015; Chovet et al., 2014). These properties can be used to understand the microorganism detachment phenomena, such as spores from solid surfaces. Therefore, foam flows would constitute a true novelty in surface hygiene, as low water load and high mechanical actions under moderate temperatures would permit highly cleaning, which can easily be combined with disinfection.

This study investigates the removal kinetics of *B. amyloliquefaciens* 98/7 and *B. cereus* 98/4 spores using foam flow. The respective roles of the foam quality (importance of air/water balance), and of the flow rate were analyzed through removal kinetics modeling. Results were then compared to spore removal under mild cleaning in place conditions. We then investigated some foam properties (the flow regime and the mean foam flow velocity, bubble-size distribution, bubble-passage frequency, foam quality and mean wall shear stress).

2. Materials and Methods

2.1. Bacterial strains and solid surfaces

In this study, two bacterial strains isolated from dairy processing lines forming spores of very different surface energies one hydrophobic and the second hydrophilic (Faille et al., 2019, 2016, 2010) were used: *B. cereus* CUETM 98/4 (BC-98/4) and *B. amyloliquefaciens* CUETM 98/7 (formerly known as *B. subtilis* 98/7). *Bacillus* spores were produced as previously described (Faille et al., 2019). Before any experiment, two further washes were performed and spores were subjected to a 2.5-min ultra-sonication step in an ultrasonic cleaner (Bransonic 2510E-MT, 42 kHz, 100 W, Branson Ultrasonics Corporation, USA) to limit the presence of aggregates. In order to evaluate the hydrophobic character of spores, Microbial Affinity to Hydrocarbons tests (MATH) were performed as previously described (Faille et al., 2019b).

The material, used in the form of rectangular coupons (45 mm x 15 mm), was AISI 316 stainless steel with pickled (2B) finish (kindly provided by APERAM, Isbergues, France). Prior to each experiment, coupons were cleaned and disinfected using a standard protocol used at UMET. Coupons were first cleaned using pure alkaline detergent (RBS T105, Traitements Chimiques des Surfaces, France). They were then subjected to a 10 min immersion in a 5% RBS T105 at 60 °C, followed by thorough rinsing with tap water, then with softened (reverse osmosis) water for 5 min each. 24 h before the experiments, stainless steel coupons were treated in a dry heat oven at 180°C for 1 h.

2.2 Surface soiling and cleaning

The soiling suspensions were prepared with ultra-purified sterilized water and a spore concentration of around 10^6 cfu.ml⁻¹. The coupons were vertically immersed in a Beaker containing 250 ml of the soiling solution, then kept at room temperature for 4 hrs.

Coupons were then inserted into a 23 10^{-2} m long stainless steel test duct with a 1.5 x 1 10^{-2} m rectangular cross-section. The geometry of the rectangular test ducts used for the experiments was previously described (Cunault et al., 2015). The three central coupons out of the five installed in the ducts were soiled and further analyzed after cleaning.

The production foam prototype was built according to previous work (Chovet and Aloui, 2016; Tisné et al., 2003a). The experimental set-up, with an open foam flow circuit, was designed to allow the foam flow to develop within horizontally-placed square ducts, with the coupons to be

cleaned at the top. The test ducts were situated after a transparent Plexiglas rectangular duct, of identical inner size, to visualize the foam flow. To allow steady state flow conditions, the test ducts were placed at intervals exceeding 80 times the hydraulic diameter of the vein inlet (i.e. 1.5 m). The prototype is presented in Figure 1. The rig includes a mother tank (capacity: 100 L) filled with Sodium Dodecyl Sulfate (Sigma-Aldrich ReagentPlus®, over 98.5% purity) dissolved in osmosed water (0.15% ww). The SDS solution is pumped into the feeding tank (50 L) located at a height of 3 m using a positive displacement pump (VARMECA 21TL055, Leroy-Somer). This set-up creates a constant flow rate in the foam generators due to gravity.

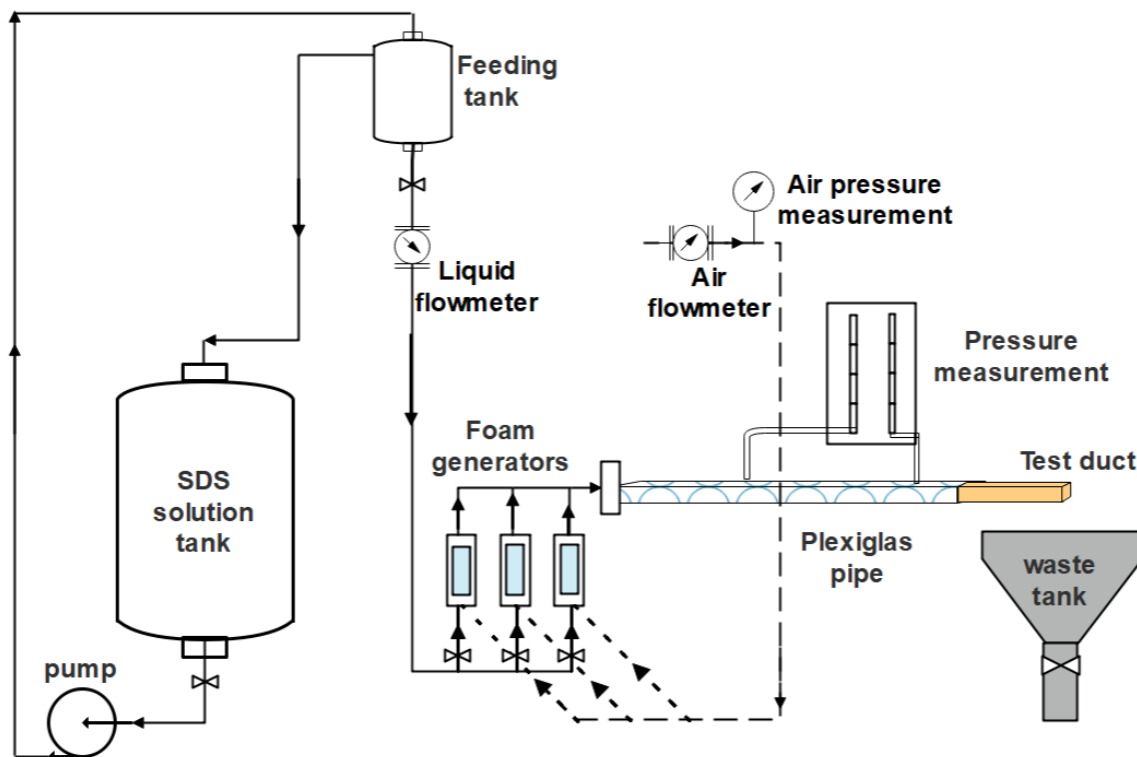


Figure 1. Scheme of foam cleaning in place prototype

Three foam generators were designed as previously described (Tisné et al., 2003a). The foam is generated by injection of pressurized air through a porous medium (DURAN®, pore sizes ranging from 1 to 1.6 μm , Dislab, Lens, France), inside cylindrical containers filled with the SDS solution. The foam quality describing the air/water content of the foam was calculated as follows (Equation 1) according to (Chovet and Aloui, 2016) where Q_g and Q_l are respectively the gas and liquid flow rates:

$$\beta = \frac{Q_g}{Q_g + Q_l} \quad (1)$$

The three independent parallel generators allowed us to increase the bulk velocity without affecting the foam structure. Three foam qualities were chosen for the cleaning experiments 50%, 60% and 70%. The mean velocity was calculated taking into account the global flow rate ($Q_l + Q_g$) divided by the cross-section area S of the test duct. The Reynolds number was calculated according to Equations (2) and (3), taking into account the density of both gas and liquid phases. Foam viscosity was calculated using the relationship based on a heuristic model of concentrated emulsions (Equation 4).

$$Re = \frac{\rho_f \cdot \bar{v} \cdot d_h}{\mu_f} \quad (2)$$

$$\rho_f = (1 - \beta) \cdot \rho_l + \beta \cdot \rho_g \quad (3)$$

$$\mu_f = \frac{\mu_l}{1 - \mu_l^{1/3}} \quad (4)$$

Three liquid/air flowmeters enabled the adjustment of the flow rate from 0 to 35 l h⁻¹ and 0 to 70 l h⁻¹ respectively.

Flowing from the generators, the foam passes through a transparent Plexiglas pipe of 1.1 m length. The transparent pipe enables the visualization of the foam texture, bubble size and foam velocity measurement. Two pressure outlets allow the connection of 2 manifold tubes placed over a scaled plate that measures on a length L of 1m the pressure drop ΔP to calculate the mean wall shear stress $\bar{\tau}$ ($d_h \Delta P / 4 L$). For each cleaning experiment, only one test duct containing the soiled coupons was clamped to the transparent pipe.

The different test ducts were thus cleaned with three foam qualities at 20°C, at foam mean velocities ranging from 2.1 to 6.7 m s⁻¹, for 15 and 35 s, 1, 3, 5, 10 and 20 min and other experiments were carried out to mimic CIP conditions. The test ducts were connected to a CIP

pilot rig (Jullien et al., 2008) and a simple CIP procedure was then carried out under the same conditions as those used for the foam tests, i.e. SDS concentration, temperature, cleaning times. The flow rate was selected to generate a mean wall shear stress of 5 Pa, falling within the range of the mean wall shear stress conditions induced by the flowing foam as described in the Results Section. After the cleaning process, the coupons were removed from the test tubes and rinsed by dipping in a beaker containing one liter of sterile ultrapure water. The residual spore contamination was then analyzed as follows.

To determine the number of adhering spores before (N0) or after the (Nresid) cleaning procedure, coupons were subjected to an ultrasonication step in 10 ml of 2% Tween 80 (v/v) in peptone water without indole 0.015 g/L (Biokar), diluted to 1L with ultra-purified sterilized water (5 min, Ultrasonic bath, Branson 2510, 40 Hz). This treatment has been previously shown, in our laboratory, to remove more than 99% of the adherent spores (Tauveron et al., 2006). The detached spores were enumerated on nutrient agar composed of 1.3% w/v nutrient broth (Biorad, France) and 1.5% w/v bacteriological agar type E (Biokar Diagnostics, France) after 48 h at 30°C. The percentage of residual spores after cleaning was then calculated $[(N_{resid}/N_0) * 100]$.

For microstructure examination, some rinsed coupons were first dried at 20 °C for at least 1 hour to prevent spore detachment during the staining procedure. The coupons were then stained with orange acridine (0.01%) for 15 min at 20°C, gently rinsed with softened water and allowed to dry before observation. Finally, the surface contamination organization was observed using an epifluorescence microscope (Zeiss Axioskop 2 Plus, Oberkochen, Germany) at magnification 1000X.

2.3 Foam flow visualisation

The method is based on the observation of the displacement of moving bubbles at the walls of the pipe, for a given interval. In situ measurements were carried out at the last part of the pipe where the foam flow could be considered as established. The velocity of the bubbles was measured by marking the Plexiglas pipe wall by two thin marks spaced at a known distance. For both the lateral and the top walls of the pipe, three locations were chosen: two at 1 mm from the edges and one in the middle of the observed wall. The time taken for a bubble to pass between the two marks was recorded to calculate its velocity. The smallest easily-visible bubbles (0.3 mm) were considered for tracking and 10 successive measurements were carried out. Mean values were then calculated.

These could be considered as representative of the local velocity at the wall whatever the bubble size (Tisné et al., 2003). This method gives an approximation of the bubbles' speed. A selection of photos of the foam flow (camera Panasonic LUMIX DMC-FZ62, High speed video [HS], at a speed of up to 200 frames / second) were analyzed using Piximètre 5.1 R1540 image analysis software. The clearest two images in terms for each flow condition induced by the generators and for the three foam qualities were filtered to better observe the borders of the bubbles. It was thus possible to evaluate the bubble size distribution in all the cases studied.

An optical probe (© RBI instrumentation, Meylan, France) based on the discrete variation of the refractive indicator optics between the two-phase flow (air/liquid) was used to evaluate the void fraction and the air bubbles' passage frequency at the wall top (at 0.5 mm from the top). Data were analysed using the ISO software provided by RBI.

2.4 Kinetics modelling

A two-phase kinetics model was used to fit the data as previously proposed for the detachment kinetics of biofilms during CIP (Benezech and Faille, 2018). The fitting was performed using GInaFIT (Geeraerd et al., 2005) using a biphasic model composed of two first order kinetics (Dallagi et al., 2018b, 2019).

2.5 Statistical analysis

At least 3 repetitions were carried out for the quantitative analysis of the residual contamination after foam cleaning. Data were analysed by general linear model procedures using SAS V8.0 software (SAS Institute, Gary, NC, USA). Variance analysis was performed to determine how the bacteria removal described by the kinetic parameters (residual contamination at different cleaning times and model parameters were affected by the cleaning conditions tested).

3. Results

3.1 Foam flow organization and mechanical action induced by the foam

Three foam qualities were prepared with a concentration of SDS of 0.15 % w/w in order to exceed the Critical Micelle Concentration (CMC). SDS as an anionic surfactant is a good representative of the “sulphate” surfactants largely used in formulated detergents. The SDS is known to be highly

soluble and easy to rinse and is largely used in academic studies (Mai et al., 2016). Anionic surfactants are recognized for their cleaning, foaming and emulsifying properties. The generated foam was found to be very stable (no changes were observed in terms of foam drainage and bubble size over one hour – data not shown).

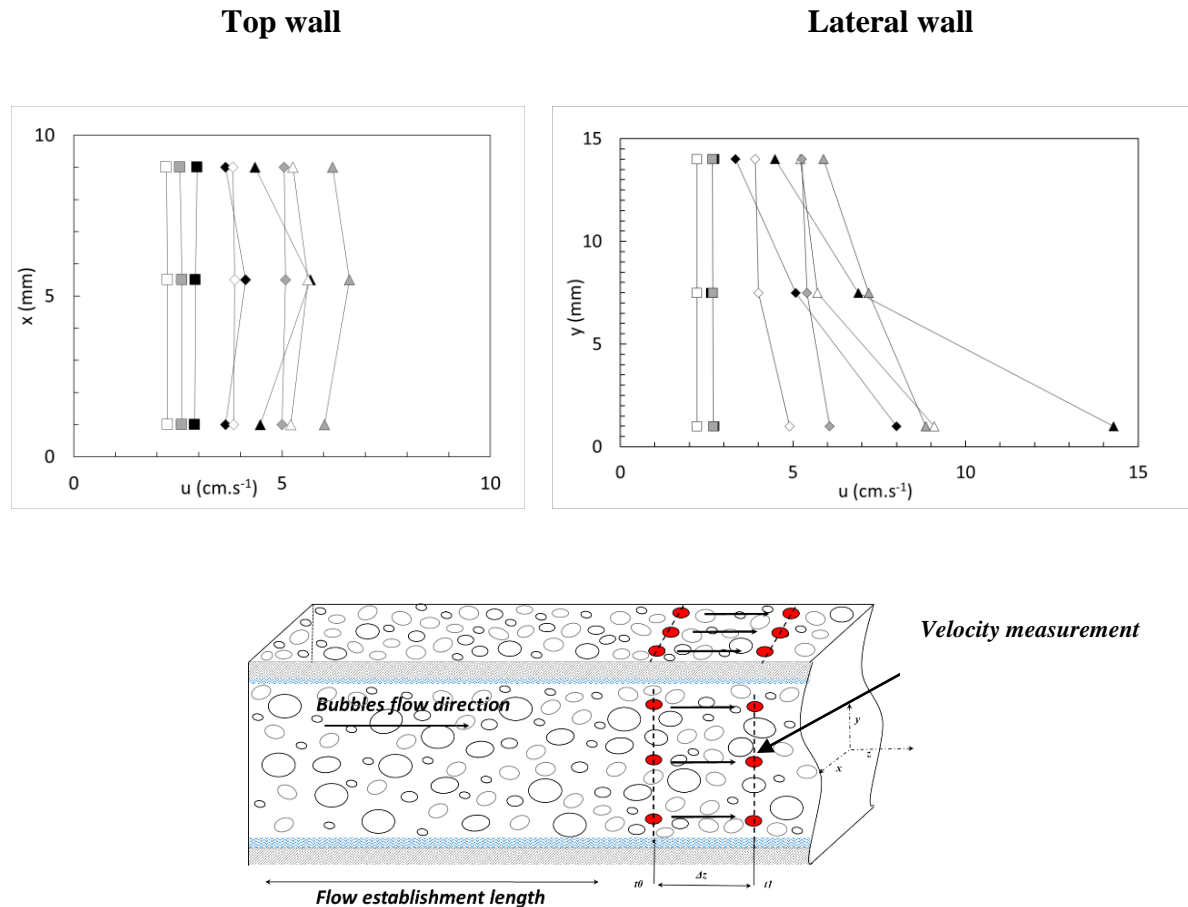


Figure 2: Bubbles velocities measured at the top and lateral walls of the transparent duct measured at three positions (in red) in relation with the number of generators (one: square, two: diamond, three: triangle) and with the foam qualities (white: 50%, grey: 60% and black: 70%)

We also checked that the use of one, two or three generators in parallel failed to modify the foam structure significantly, despite the differences in the foam velocity. Thanks to the transparent Plexiglas tube, placed upstream of the test duct with the soiled coupons subjected to the cleaning

procedure, it was possible to visualise the foam flow through the rig and to take images or videos. Observations were made from one side and from through the top.

The bubble velocity was first measured as shown in Figure 2 in three locations on each selected duct wall (top and lateral). As shown in Figure 2, depending on the experimental conditions (number of generators, foam quality), the velocity profiles were quite different. As the mean velocity increased, a difference in the flow velocity of the bubbles appeared depending on their position in the duct. Indeed, when a single generator was used, bubble velocity was generally constant and the foam flow therefore behaved like a plug flow. The increase induced by two generators showed no change at the top of the duct, except for the foam quality of 70%. Conversely, the bubble velocities increased from the top to the bottom of the duct as shown in Figure 2 B. This is due especially to the underlying liquid film, which pulls the foam in contact because its velocity increases. At the top wall, bubble velocities were highest at the centre of the side, and thus decreased as the flow approached the duct edges. All conditions used are summarized in Table 1.

Table 1. Flowing conditions for the foam flow and the CIP

Liquid flow rate (l.h ⁻¹)	Air flow rate (l.h ⁻¹)	Foam quality β	Mean velocity (cm.s ⁻¹)	$\bar{\tau}w$ (Pa)	Re
6	6	50%	2.0	2.2	43
9	9		4.0	4.2	87
13.5	13.5		6.1	5.9	130
4.2	6.3	60%	2.4	2.2	51
8.4	12.6		4.9	4.4	101
12.6	18.9		7.3	6.0	151
4.2	9.8	70%	2.9	2.4	67
8.4	19.6		5.7	5.1	135
12.6	29.4		8.6	6.4	202
650	-	0 (no foam)	120	5.1	14500

The foams' flow conditions varied from 2.0 to 8.6 cm s⁻¹, whilst for the CIP conditions the velocity was significantly higher at 120 cm s⁻¹ and the flow regime was turbulent ($Re > 14500$). The mean wall shear stress (WSS) condition for the CIP was chosen to fall within those induced by the foam, i.e. ranging from 2.2 to 6.4 Pa, allowing comparison between the CIP mechanical action and the use of foam flow. One can note that the plug flow regime with constant foam velocity profile corresponding to 1 generator flow (all foam qualities) related to a Reynolds number maximum of 67. At over 100, the foam flow velocity profile at the top wall could not be considered as constant (Figure 2A).

In Figure 3, an example of photos of the foam flow arrangement at the top surface of the transparent duct is shown.

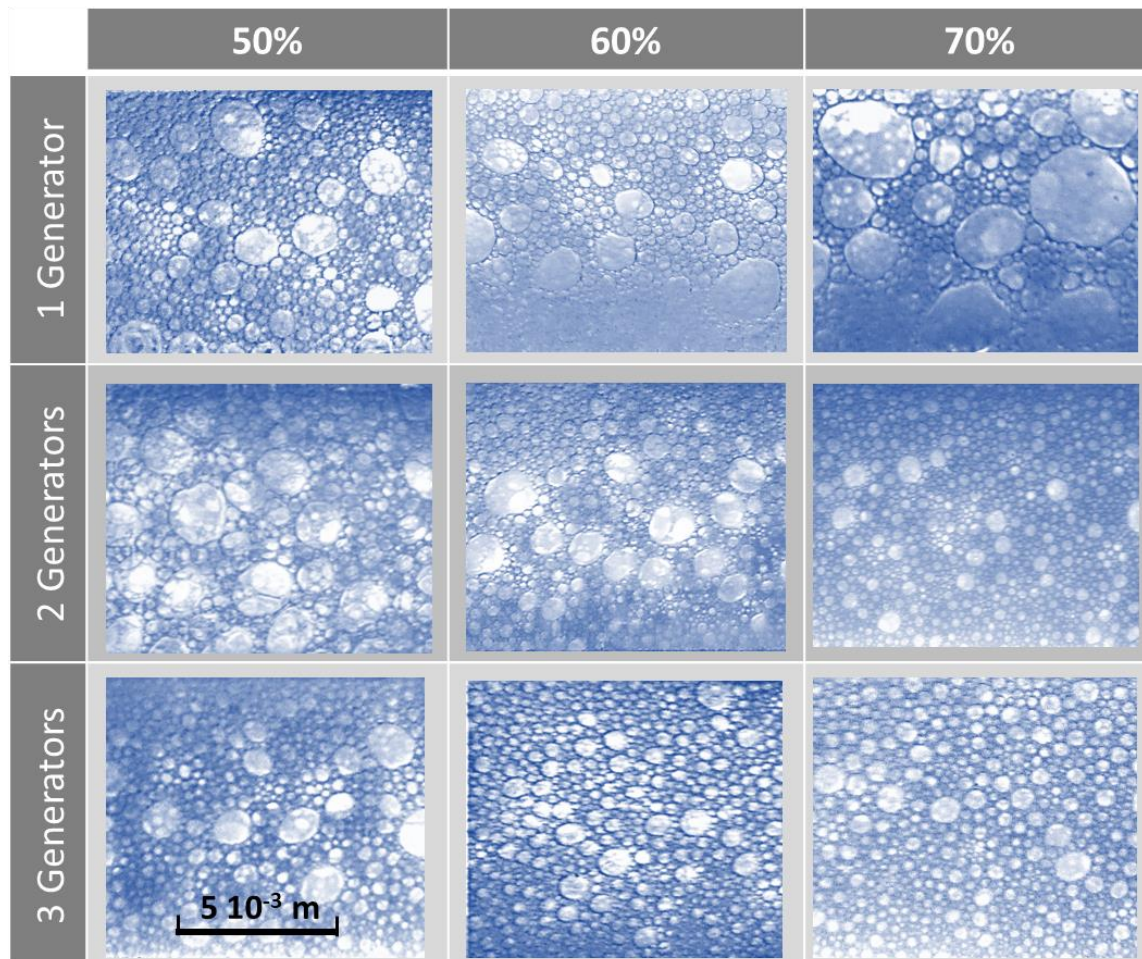


Figure 3. Foam visualization at the top wall of the Plexiglas duct just before the test ducts for the three foam qualities and the foam flow conditions.

In order to identify the distribution of bubble size within the foam under different conditions, photos were taken at the top wall of the Plexiglas duct (Figure 3). The size distribution appeared to be affected by both velocity and foam quality. For example, the greater the velocity at the top wall, the smaller the bubbles.

The bubble sizes were then measured and the data are given in Figure 4. When only one generator was used, the bubble sizes were more heterogeneous than those obtained with two or three generators, whatever the foam quality. Moreover, a significant number of big bubbles (between 1 mm and 10 mm in size) was also observed. The increase in the velocity was thus more conducive to smaller bubbles. In accordance with Figure 3, some larger bubbles (size > 1mm) could still be measured with 2 and 3 generators for the foam flow where $\beta = 50\%$ and with 2 generators for the foam flow where $\beta = 60\%$.

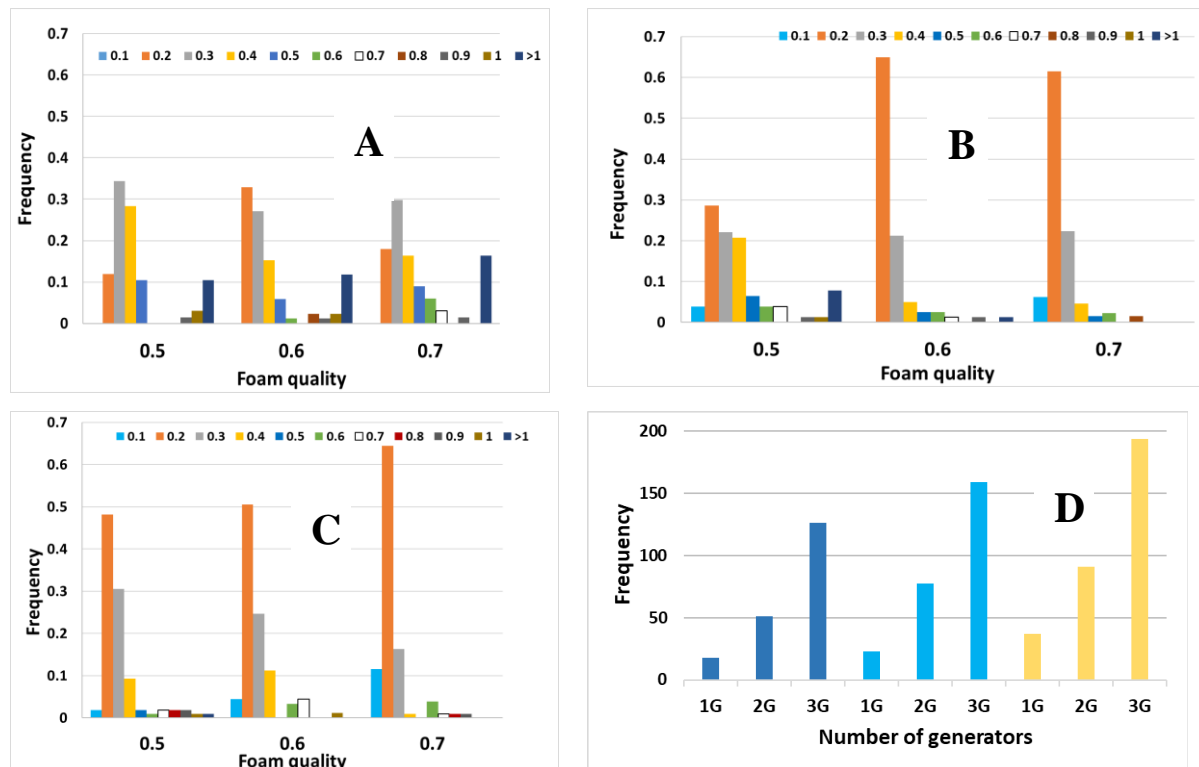


Figure 4. Bubble size (mm) repartition; A: one generator, B: 2 generators & C: 3 generators and frequency of passage of bubbles in front of the optical probe (D) at the top wall for the three foam qualities: 0.5 (dark blue), 0.6 (light blue), 0.7 (yellow)

The mean frequencies of the bubbles' passage observed by the optical probe (Figure 4, D) near the top wall increased with the number of generators. However, this increase could not be explained

solely by the mean velocity, but is apparently also linked to the reduction in the bubble sizes e.g. for the foam 50%, the doubling or the tripling of the mean velocity induced an increase in the frequency by factors of respectively 2.9 and 7.1.

3.2 Spores' detachment under the different flowing conditions

Spore adhesion to the stainless steel coupons (Ra: 0.08 μm) was $5.6 \pm 0.4 \log \text{cfu.cm}^{-2}$ for *B. amyloliquefaciens* and $5.4 \pm 0.3 \log \text{cfu.cm}^{-2}$ for *B. cereus*. Before any detachment experiments, we checked that spore incubation in SDS 0.15% did not result in any significant viability loss (data not shown). The detachment of *B. amyloliquefaciens* spores was investigated under all the flow conditions with each of the three foam qualities. In Figure 5, only the mean values of the remaining contamination at the different kinetic times were presented. In all cases, the detachment curves clearly showed two distinct phases.

Both phases appeared to be exponential and therefore were quite accurately described by the biphasic model, with R^2 ranging from 0.62 to 0.98 and mostly over 0.80.

During the first detachment phase (less than 1 min), the spore detachment was very fast, with a 0.6 to 1.8 log decrease in the population of surface-attached spores. Large differences were observed according to the number of generators used with the 50%, foam quality whereas the number of generators had little effect on the detachment of the other two foams (60% and 70%). Taking into account all the conditions used, it appears that spore detachment during this first phase was much more efficient with the 50% foam quality when 1 or 2 generators were used. After this first step, the detachment continued for at least 20 minutes, i.e. the duration of the cleaning procedure, though more slowly. Here again, the spore detachment rate seemed dependent on the experimental conditions (number of generators, foam quality). The cleaning kinetics with foam were compared to a CIP using the SDS 0.15% and a mean wall shear stress of 5 Pa (Figure 5D). The first detachment step was close to the most efficient one with foam, i.e. allowing the detachment over 1.5 log, close to the one observed when 1 or 2 generators were used with the $\beta = 50\%$ foam. Conversely, no further detachment occurred after this first phase, indicating that a plateau value had been reached.

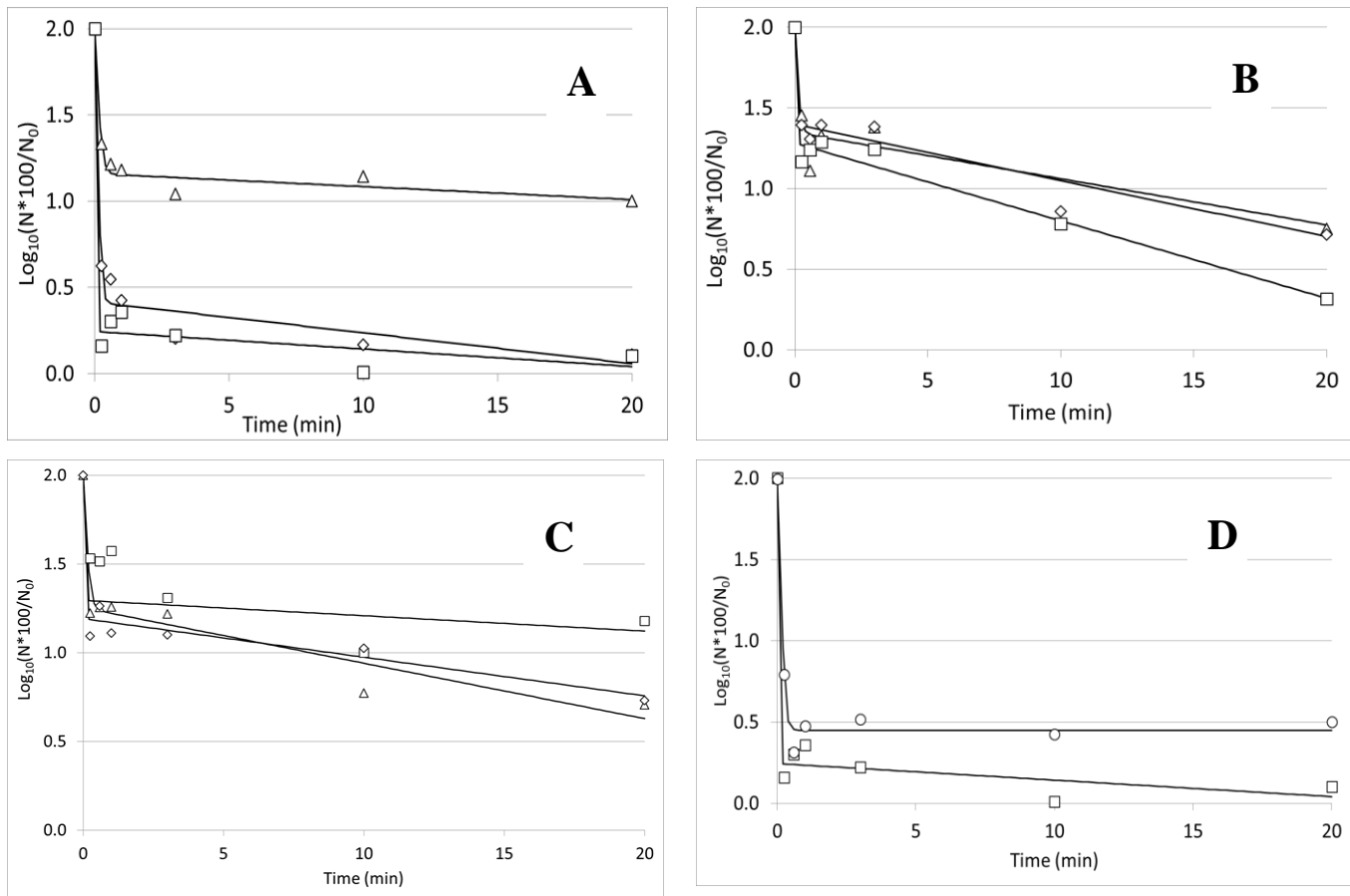


Figure 5. Removal kinetics of *B. amyloliquefaciens* 98/7 spores under different flowing conditions: 1 generator (square), 2 generators (diamond), 3 generators (triangle) for the foam qualities of 50% (A), 60% (B) and 70% (C); Removal kinetics with the foam 50%, one generator compared to CIP (D)

The decimal reduction at 20 min, i.e. the end of the second phase of the cleaning kinetics, was statistically analysed to compare the role of the flow rates conditions induced by the generators, the different foam qualities and by the CIP conditions. At 20 min, cleaning efficiencies observed were comparable between CIP and the flow rates induced by one and two generators (letter A, Tukey's grouping) as shown in Figure 6. In addition, the cleaning efficiency induced by the 50% and 60% foam qualities appeared significantly better than the 70% foam (different letters according to the Tukey's grouping).

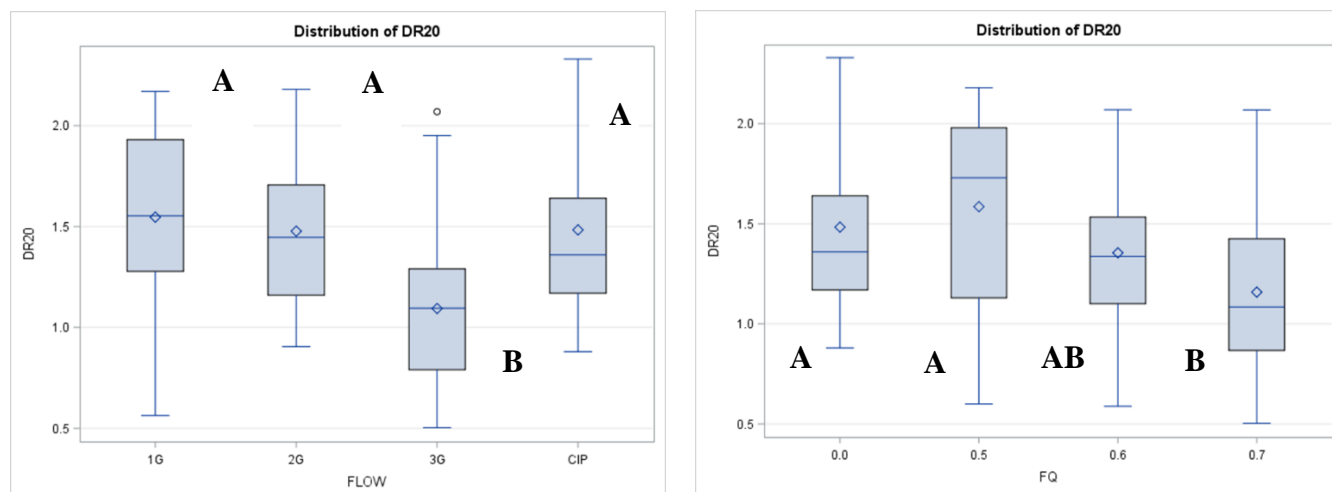
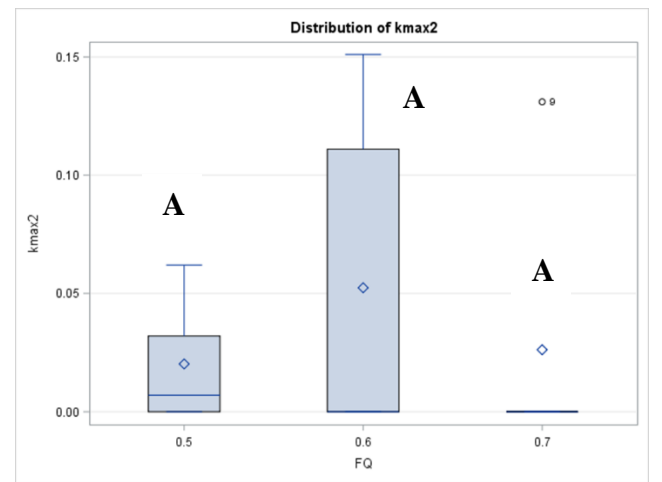
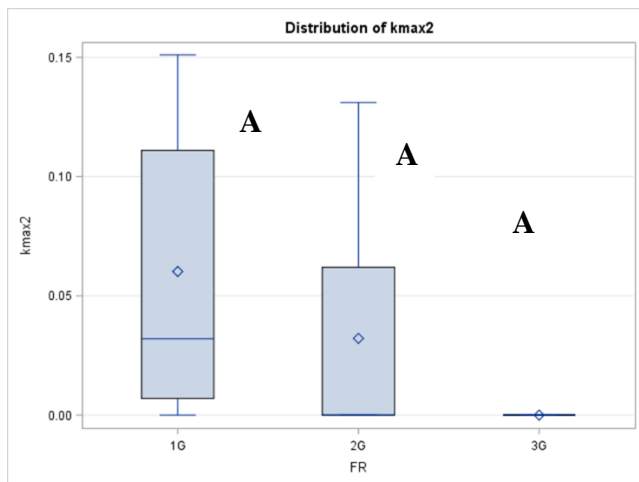
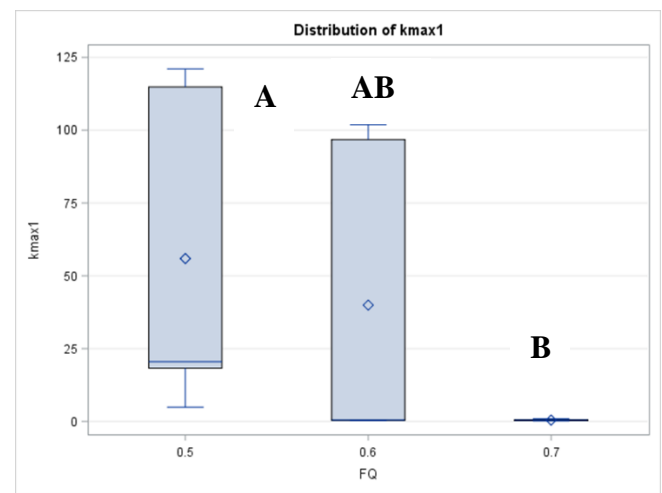
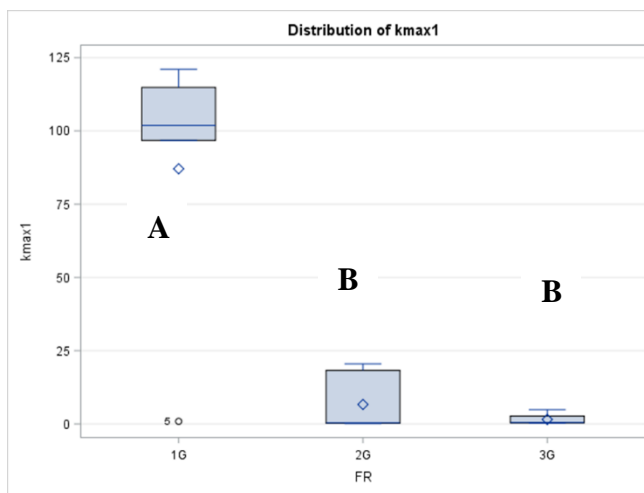
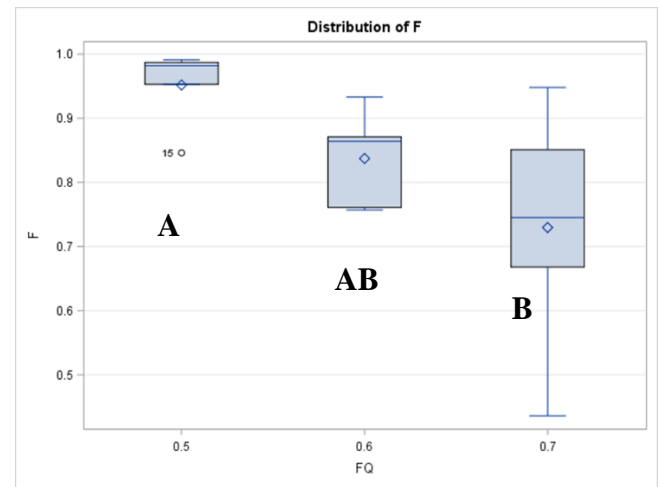
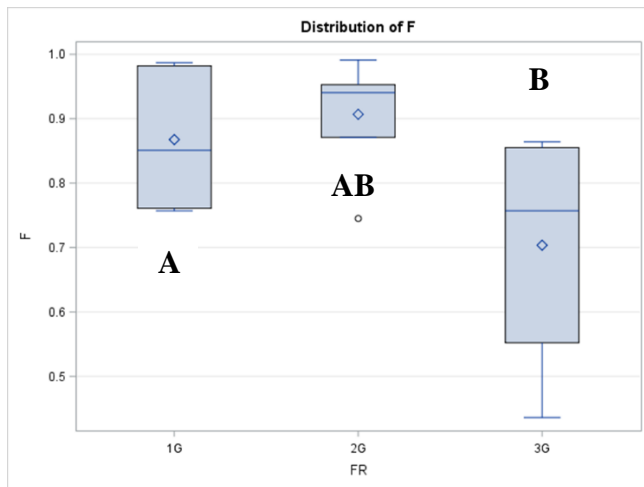


Figure 6. Decimal reduction of the *B. amyloliquefaciens* spores induced by different flowing conditions at 20 min cleaning time: comparison of the combined effects of the flow conditions and the foam quality including CIP conditions (“foam quality” being equal to zero in that case).

Focusing on the cleaning conditions with foam, the variance analysis confirmed that the variability observed on the three kinetics parameters (f , k_{max1} , and k_{max2}), was significantly related to the flow rate induced by the foam generators. However, some discrepancies should be noted (see Figure 7). Considering the potential combined effects of the foam quality and the flow rate (one, two and three generators) on the parameter f (f is the poorly adherent fraction of the population and/or less resistant to detachment), the variance analysis gave a p value of 0.027. The Tukey's grouping as shown in Figure 7, highlighted a slight effect of the flow rate: f being higher under the lowest flow rate conditions and higher with the foam where $\beta=50\%$, compared to the foam with $\beta=70\%$ (no common letters, Tukey's grouping). More visible was the role of the flow rate on the constant rate K_{max1} ($p=0.001$), the lowest flow rate clearly being the most efficient condition for spore removal under this first phase: K_{max1} was multiplied by a factor up to 300. Foam quality appeared to play a role as the Tukey's grouping highlighted that K_{max1} values for the $\beta=70\%$ foam were very low compared to 50% and 60% foams. While taking into account data obtained with the CIP conditions, as also shown in Figure 7, flow conditions were still highly significant ($P=0.0012$) and three classes were defined by Tukey's grouping (A, AB and B). In this case, CIP conditions gave an intermediate mean value of 55 for K_{max1} compared to 87 with one generator and 6.7 or 1.3 respectively for two or three generators



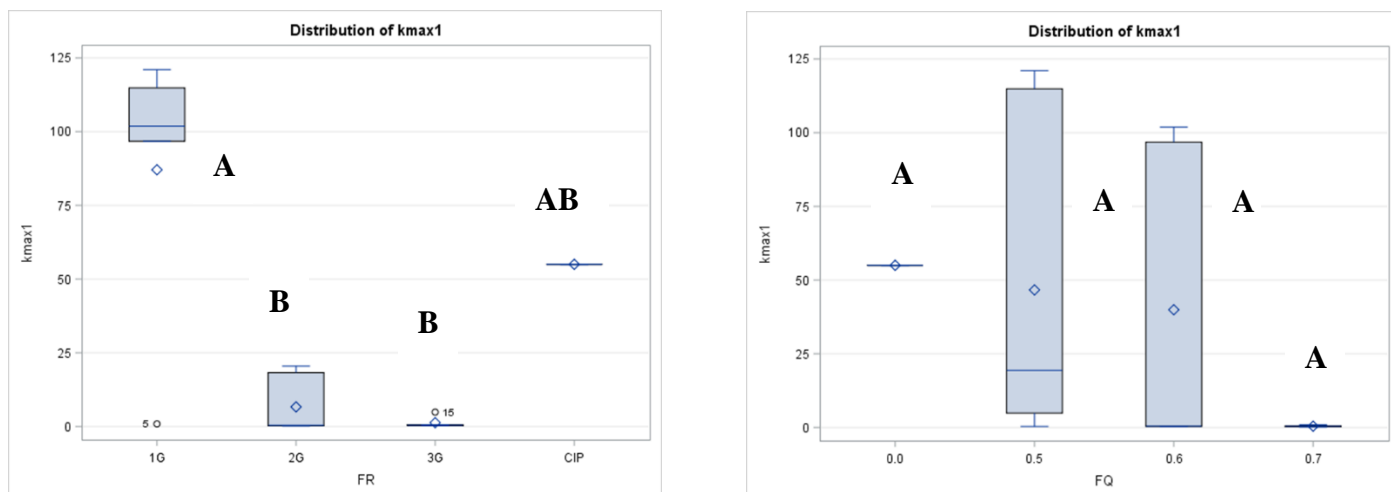


Figure 7. Variations induced by the combination of the foam quality (including CIP conditions for the two last graphs) and the flow rate induced by one, two or three generators on the kinetics parameters f , K_{max1} and K_{max2} . According to the Tukey's grouping letters were indicated with potentially three classes A, AB and B.

The effect of cleaning using foam flow, was tested with another *Bacillus* species. In Figure 8 the two kinetics appeared very similar with a quick detachment in less than one minutes followed by a second phase, with about 0.5 log removal in both cases. Such a cleaning condition was chosen as the most efficient, according to the results described above. The main difference lied in the K_{max1} values, *B. cereus* spores being more difficult to remove than *B. amyloliquefaciens* ones at the initial phase of the kinetics. Conversely, the removal during the second phase of the kinetics appeared very similar and this was confirmed by close values of the detachment rate K_{max2} for the two bacteria.

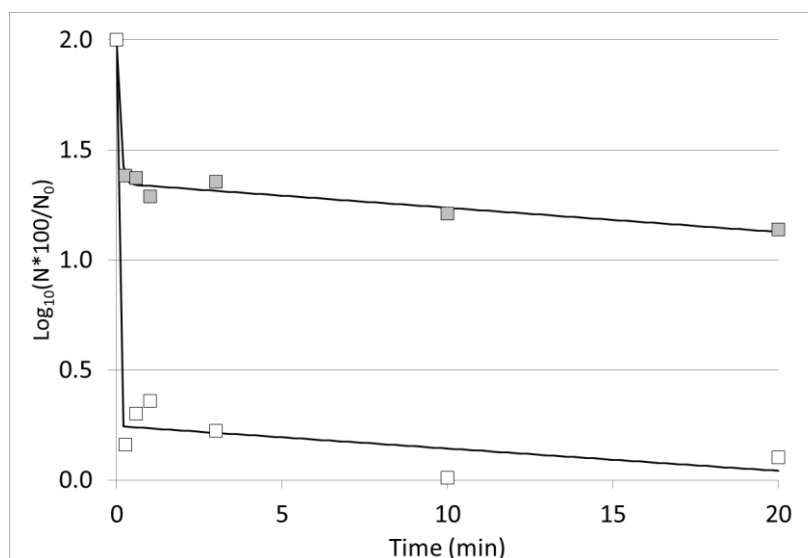


Figure 8. Comparison between the removal of *Bacillus amyloliquefaciens* and *Bacillus cereus* spores: cleaning with foam of $\beta=50\%$ and one generator

The microscopic observations showed the spores distribution on the coupons before and at different cleaning times. Only times 0 (fouling), 15 s, 3 minutes and 20 minutes were considered for comparison between foam cleanings (0.5 and 1 generator), one of the most effective foam cleanings observed and CIP. Microscopic observation showed that *B. amyloliquefaciens* 98/7 spores formed some clusters as shown in Figure 8, but these spores were mainly evenly distributed on the steel surface after the 4 hours soiling. Clusters were limited by the sonication of the spore suspensions prior to the soiling step and these were rapidly removed after only 15 s by both CIP and foam flow. Yet, according to Figure 9, removal was visibly greater with foam flow than CIP. The difference observed here (almost one log) is less than the one given by the removal kinetics (Figure 5B; 0.5 log difference), which considers viable and cultivable bacteria. However, the variability (up to 0.5 log) between trials could easily explain this discrepancy.

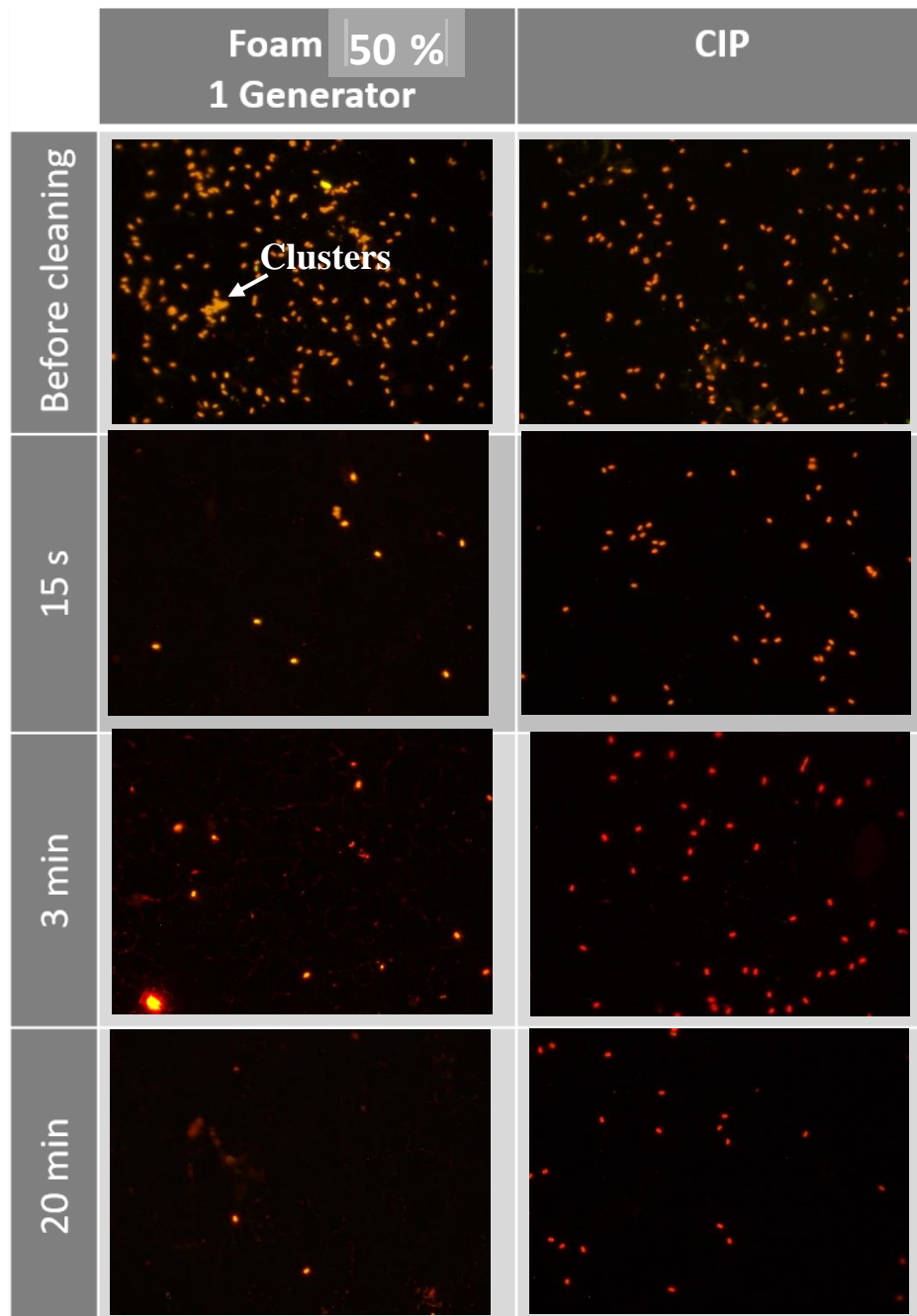


Figure 9. Observations of the stainless steel coupons before cleaning and after 15 s, 3 min and 20 min with a foam flow where $\beta=50\%$ and using one generator and with CIP.

4. Discussion

Foam is a two-phase gas-liquid fluid, in which gas is the dispersed phase and liquid is the continuous phase, where the volume of gas greater than that of liquid. In this work, only wet foam was used, meaning that foam is formed only of spherical bubbles, as observed at the top wall as

previously described (Chovet and Aloui, 2016; Tisné et al., 2004) . Each mean velocity induced by one, two or three generators engendered a different flow regime. Indeed, for the lowest mean velocity, the axial component was uniform over the entire cross-section, thereby corresponding to the mono-dimensional flow regime or plug foam flow regime. For the mean velocity of 4 cm s^{-1} , the flow appeared partially sheared with a sliding at the walls, the axial velocity component no longer being uniform, depending on the ordinate and corresponding to the two-dimensional (2D) foam flow regime. One can notice that the top wall velocity remained constant (foam at $\beta=50\%$ and $\beta=60\%$) or was only slightly modified at the center of the top wall (foam at $\beta=70\%$) under our experimental conditions. For the highest mean velocities, the foam flow was completely sheared with a sliding at the walls and could therefore be considered as three-dimensional (3D), with the underlying liquid film at the bottom of the duct flowing at a higher velocity, pulling the foam flow above and therefore inducing a significant increase in the bubbles' velocity directly in contact with this thick liquid film. This phenomenon is accompanied by a rearrangement of bubble sizes, with the largest bubbles being mostly moved up the pipe. Such a phenomenon was already described by (Tisné et al., 2003). In this work, the cleaning of surfaces by the foam was evaluated at the top wall as a first evaluation of the role of flowing foam in the removal of surface contaminations (bacteria spores). In parallel, even if the experimental conditions were supposed to maintain the foam structure with the increase in the mean velocity, it appeared that the bubble size repartition at the top wall varied with the foam quality tested, meaning that bubble rearrangement had occurred: the increase in the mean velocity induced a reduction in the bubble size at the top wall.

Furthermore, it has been demonstrated that the variation at the top wall of the thin liquid film between the bubbles and the wall is directly affected by the bubbles passage and depends on their size (Tisné et al., 2004), which could have an effect on the effectiveness of adherent bacteria removal. The thickness fluctuations thus induced under their experimental 1D flow conditions varied between $5 \mu\text{m}$ and $35 \mu\text{m}$ with a foam quality of 70%. Under 1D flow conditions for a foam quality of 55%, conditions close to our experimental conditions, Chovet and Aloui (2016), observed fluctuations at the top of the channel liquid film varying from $2 \mu\text{m}$ to $40 \mu\text{m}$. In addition, this amplitude decreased with the increase in the foam quality, probably due to a change in the bubble size arrangement at the wall.

Microscopic scale studies (Tisné et al., 2004), reveal that it is possible to rely on studies of bubble flows inside circular capillaries, which will help in understanding the underlying

phenomena (Bretherton, 1961). Assuming that there was no tangential shear stress at the fluid–fluid interface, he predicted that the film thickness was dependent on four parameters: the tube radius r , the liquid viscosity μ_L , the surface tension γ and the bubbles' velocity V_b . The film thickness is as follows:

$$e = 1.337 r Ca^{2/3} \quad (5)$$

where Ca represents the capillary number defined as:

$$Ca = \mu_L V_b / \gamma \quad (6)$$

In relation to Bretherton's approach, r was assimilated to the radius of the bubble. Tisné et al., 2004 representing the evolution of the measured contact film thickness versus $Ca^{2/3}$ observed a close agreement with the Bretherton law (Bretherton, 1961), the bubble size considered being 0.5 mm. Our experiments are in a capillary number range of $11 \cdot 10^{-4} < Ca < 44 \cdot 10^{-4}$ ($0.011 < Ca^{2/3} < 0.026$) falling within the range proposed by these authors, $3 \cdot 10^{-4} < Ca < 28 \cdot 10^{-4}$ ($0.005 < Ca^{2/3} < 0.02$). Given the agreement observed with the Bretherton law, the contact liquid film thickness in our experimental conditions would have ranged from 7 to 18 μm given a mean bubble radius of 0.5 mm, the thinnest liquid films being observed at the lowest velocities. Such a range of variation is in agreement with previous works (Chovet and Aloui, 2016; Tisné et al., 2004).

In parallel, it was shown (Tisné et al., 2003) that the wall shear stress was lower in the liquid film between each bubble and the wall. The wall friction was especially concentrated at the two ends of the bubbles; the wall shear stress fluctuations' amplitude being linked to the bubble size. When compared with the spore detachment kinetics, the greatest detachment efficiency appeared to be obtained with larger bubble size, notably when their diameter exceeded 0.1 mm, as clearly observed with the foam qualities of 0.5 (1D and 2D foam flow conditions) and 60% (1D foam flow condition) during the first step. Under CIP conditions, the detachment rate appeared to be comparable to the best foam cleaning conditions tested for comparable mean WSS conditions. In both cases the cleaning agent was the SDS under cold conditions (20°C). Previous work (Faille et al., 2018), highlighted the significant role of the fluctuation in the local wall shear stress on the cleaning efficiency under CIP conditions. One can draw a parallel here with these previous observations (Chovet and Aloui, 2016; Tisné et al., 2003), as the presence of the WSS fluctuations induced by the foam at the top wall appeared to play a role in the detachment mechanism and was clearly visibly under the 1D flow regime. However, for the 70%, foam quality, larger sized bubbles were observed at the top wall, which failed to ensure cleaning efficiency. Conversely, the increase

in foam velocity meant a re-arrangement of the bubble sizes at the top wall (smaller bubbles). This phenomenon appeared to be unfavorable for efficient cleaning, as despite an increase in mean WSS, fluctuation amplitude decreased. Local wall shear stress decreases dramatically while bubble passes and increases to a maximum between bubbles (Tisné et al., 2003). Therefore, the frequency of fluctuation of the local wall shear stress with large bubbles is less than the fluctuation with small bubbles but the amplitude is higher and would explain the differences in the spores' removal.

The kinetics of bacteria spore detachment in the different flow and foam quality conditions were investigated and modelled according to previous work (Benezech and Faille, 2018) on biofilm removal under CIP conditions. An identical simple two-phase model was found to be suitable for describing biofilm removal kinetics. The first bacterial removal phase corresponded to a quick removal of biofilm matrix with embedded cells, while the second phase accounted for the removal of cells directly attached to the steel surface. For bacterial spores removed by foam flow, the mechanisms appeared to be totally different, as the bacteria were evenly distributed on the stainless steel surfaces with very few clusters. This is unlikely to explain the quick and strong removal at the very beginning of the cleaning (less than 1 min). The parameter f corresponding to the part of the spore's population easily affected by the foam flow appeared to be significantly higher at the lowest velocities and for the wettest foam ($\beta=50\%$). This also corresponded to the highest values of the K_{max1} constant rate, i.e. the first phase of the removal kinetics. However, the second kinetic phase did not significantly improve the cleaning efficiency as a whole, whatever the conditions. For biofilms, it was observed that the chemical action contrarily to the mechanical action induced by the foam flow, was only involved in the first removal kinetic phase. The addition of chemicals such as NaOH during CIP conditions would largely improve this initial kinetics removal phase (Benezech and Faille, 2018). The difficulty in removing the remaining spores during the second phase of the kinetics was probably due to the stainless steel surface finish 2B used, which was proven to be less hygienic than other finishes, such as bright annealed 2R, as it presents boundary grains where spores can accumulate. The fluctuations in the liquid film thickness and/or of the wall shear stress appeared to impact the detachment phenomenon to a lesser extent.

A comparison with previous work on particles detachment by bubbles moving in a capillary duct, will allow the potential role of the capillary forces in the bacterial detachment to be taken into account. Two types of particles in terms of surface energy (hydrophobic and hydrophilic) of

a size comparable to the *Bacillus* spores were used (Kondjoyan et al., 2009b), the entire air–liquid interface was modelled and the time-variation of the capillary force during transit of the bubble at the surface was determined. The particle detachment curve was thus predicted from near zero velocity to the highest velocity value, at which capillary force was supposed to vanish.

The approach was validated using latex particles 2 μm in diameter. The bell-shaped detachment curves experimentally obtained showed a width dependent on the value of the contact angle of the particles, the curve being narrower for hydrophilic particles than for hydrophobic ones. The effective contact angle values of the particles could thus be deduced directly from the width of the detachment curves. *B. amyloliquefaciens* 98/7 spores according to previous work were highly hydrophilic (Faille et al., 2010) with a contact angle to water of 20.5° (data not shown). For hydrophilic particles (Kondjoyan et al., 2009b), the detachment occurred at bubble velocities of around 3 cm.s^{-1} and dramatically decreased at 5 cm.s^{-1} . As far as a direct comparison is conceivable, such a velocity range corresponded to the variation range ($2.2 - 5 \text{ cm.s}^{-1}$), where the greatest detachment rate was observed, as illustrated by high $K_{\text{max}1}$ constant rate values under 1D flow conditions. For hydrophobic particles, the bell-shaped detachment rate was wider and detachment started at greater bubble velocities, starting at 3 cm.s^{-1} and peaking at around 7 cm.s^{-1} . This could partly explain the very low cleaning efficiency of surfaces soiled by the *Bacillus cereus* 98/4 spores by the best foam cleaning conditions observed for *B. amyloliquefaciens*. *B. cereus* spores presented a high contact angle value (111.1°) as described recently (Faille et al., 2019a), largely over the value of 59° for the hydrophobic particles deduced from the bell-shaped curve (Kondjoyan et al., 2009b). With *B. cereus* spores, greater foam velocities should be tested, while conserving the bubble pattern obtained in this work under 1D flow conditions.

Time-variations relating to the capillary forces as an inlet condition in a modified adhesion and dynamic model were suggested as a way of predict the nano- and micro-movements of particles during their detachment from a surface (Kondjoyan et al., 2009). These movements are probably emphasized by the shear force fluctuations in our experimental conditions, which differ greatly to capillary flow conditions.

5. Conclusions and perspectives

This work constitutes a cornerstone for future work on the implementation of foam flow cleaning. This requires further activities on foam flow characterisation in order to be able to design a new efficient cleaning foam structure (less drainage phenomenon, increase of the wall shear stress at

the bottom of the ducts), which would take into account both the surfactant used (more profitable and usable industrially than the SDS) and the temperature of the foam. The decrease of the temperatures seemed to play a significant role in its cohesion strengths (data not shown) potentially corresponding to food processing sectors working under positive cold conditions e.g. fresh-cut or frozen vegetable and fruit industries. The novelty of this concept is to clean complex equipment while using far less potable water, at a lower energy consumption level.

6. Acknowledgments

This work was supported by the project Veg-I-Tec (programme Interreg V France-Wallonia-Flanders GoToS3), ANIOS laboratories and the European Regional Development fund via the Hauts-de-France region.

7. References

- Benezech, T., Faille, C., 2018. Two-phase kinetics of biofilm removal during CIP. Respective roles of mechanical and chemical effects on the detachment of single cells vs cell clusters from a *Pseudomonas fluorescens* biofilm. *J. Food Eng.* 219, 121–128.
<https://doi.org/10.1016/j.jfoodeng.2017.09.013>
- Blel, W., Legentilhomme, P., Bénézech, T., Fayolle, F., 2013. Cleanability study of a Scraped Surface Heat Exchanger. *Food and Bioproducts Processing* 91, 95–102.
<https://doi.org/10.1016/j.fbp.2012.10.002>
- Blel, W., Legentilhomme, P., Le Gentil-Lelièvre, C., Faille, C., Legrand, J., Bénézech, T., 2010. Cleanability study of complex geometries: Interaction between *B. cereus* spores and the different flow eddies scales. *Biochemical Engineering Journal* 49, 40–51.
<https://doi.org/10.1016/j.bej.2009.11.009>
- Bretherton, F.P., 1961. The motion of long bubbles in tubes. *Journal of Fluid Mechanics* 10, 166.
<https://doi.org/10.1017/S0022112061000160>
- Chovet, R., 2015. Experimental and numerical characterization of the rheological behavior of a complex fluid: application to a wet foam flow through a horizontal straight duct with and without flow disruption devices (FDD). Université de Valenciennes et du Hainaut-Cambresis.
- Chovet, R., Aloui, F., 2016. Liquid Film Thickness: Study and Influence over Aqueous Foam Flow. *J. Appl. Fluid Mech.* 9, 39–48.

- Chovet, R., Aloui, F., Keirsbulck, L., 2014. Gas-Liquid Foam Through Straight Ducts and Singularities: CFD Simulations and Experiments. <https://doi.org/10.1115/FEDSM2014-21190>
- Cunault, C., Faille, C., Briandet, R., Postollec, F., Desriac, N., Benezech, T., 2018. *Pseudomonas* sp. biofilm development on fresh-cut food equipment surfaces – a growth curve – fitting approach to building a comprehensive tool for studying surface contamination dynamics. *Food and Bioproducts Processing* 107, 70–87. <https://doi.org/10.1016/j.fbp.2017.11.001>
- Dallagi, H., Al Saabi, A., Faille, C., Benezech, T., Augustin, W., Aloui, F., 2019. Cfd Simulations of the Rheological Behavior of Aqueous Foam Flow Through a Half-Sudden Expansion, in: *Proceedings of the Asme/Jsm/Ksme Joint Fluids Engineering Conference*, 2019, Vol 1. Amer Soc Mechanical Engineers, New York, p. UNSP V001T01A030.
- Dallagi, H., Gheith, R., Al Saabi, A., Faille, C., Augustin, W., Benezech, T., Aloui, F., 2018a. CFD Characterization of a Wet Foam Flow Rheological Behavior, in: *Volume 3: Fluid Machinery; Erosion, Slurry, Sedimentation; Experimental, Multiscale, and Numerical Methods for Multiphase Flows; Gas-Liquid, Gas-Solid, and Liquid-Solid Flows; Performance of Multiphase Flow Systems; Micro/Nano-Fluidics*. Presented at the ASME 2018 5th Joint US-European Fluids Engineering Division Summer Meeting, ASME, Montreal, Quebec, Canada, p. V003T20A004. <https://doi.org/10.1115/FEDSM2018-83338>
- Dallagi, H., Gheith, R., Al Saabi, A., Faille, C., Augustin, W., Benezech, T., Aloui, F., 2018b. CFD Characterization of a Wet Foam Flow Rheological Behavior, in: *Volume 3: Fluid Machinery; Erosion, Slurry, Sedimentation; Experimental, Multiscale, and Numerical Methods for Multiphase Flows; Gas-Liquid, Gas-Solid, and Liquid-Solid Flows; Performance of Multiphase Flow Systems; Micro/Nano-Fluidics*. Presented at the ASME 2018 5th Joint US-European Fluids Engineering Division Summer Meeting, ASME, Montreal, Quebec, Canada, p. V003T20A004. <https://doi.org/10.1115/FEDSM2018-83338>
- Dogan, B., Boor, K.J., 2003. Genetic diversity and spoilage potentials among *Pseudomonas spp.* isolated from fluid milk products and dairy processing plants. *Appl. Environ. Microbiol.* 69, 130–138.
- Faille, C., Bihi, I., Ronse, A., Ronse, G., Baudoin, M., Zoueshtiagh, F., 2016. Increased resistance to detachment of adherent microspheres and *Bacillus* spores subjected to a drying step. *Colloids and Surfaces B: Biointerfaces* 143, 293–300. <https://doi.org/10.1016/j.colsurfb.2016.03.041>

- Faille, C., Cunault, C., Dubois, T., Benezech, T., 2018. Hygienic design of food processing lines to mitigate the risk of bacterial food contamination with respect to environmental concerns. *Innov. Food Sci. Emerg. Technol.* 46, 65–73. <https://doi.org/10.1016/j.ifset.2017.10.002>
- Faille, C., Lemy, C., Allion-Maurer, A., Zoueshtiagh, F., 2019. Evaluation of the hydrophobic properties of latex microspheres and *Bacillus* spores. Influence of the particle size on the data obtained by the MATH method (microbial adhesion to hydrocarbons). *Colloid Surf. B-Biointerfaces* 182, UNSP 110398. <https://doi.org/10.1016/j.colsurfb.2019.110398>
- Faille, C., Lequette, Y., Ronse, A., Slomianny, C., Garénaux, E., Guerardel, Y., 2010. Morphology and physico-chemical properties of *Bacillus* spores surrounded or not with an exosporium. Consequences on their ability to adhere to stainless steel. *International Journal of Food Microbiology* 143, 125–135. <https://doi.org/10.1016/j.ijfoodmicro.2010.07.038>
- Gahleitner, B., Loderer, C., Fuchs, W., 2013. Chemical foam cleaning as an alternative for flux recovery in dynamic filtration processes. *Journal of Membrane Science* 431, 19–27. <https://doi.org/10.1016/j.memsci.2012.12.047>
- Geeraerd, A.H., Valdramidis, V.P., Van Impe, J.F., 2005. GInaFiT, a freeware tool to assess non-log-linear microbial survivor curves. *International Journal of Food Microbiology* 102, 95–105. <https://doi.org/10.1016/j.ijfoodmicro.2004.11.038>
- Jullien, C., Benezech, T., Gentil, C.L., Boulange-Petermann, L., Dubois, P.E., Tissier, J.P., Traisnel, M., Faille, C., 2008. Physico-chemical and hygienic property modifications of stainless steel surfaces induced by conditioning with food and detergent. *Biofouling* 24, 163–172. <https://doi.org/10.1080/08927010801958960>
- Kondjoyan, A., Dessaigne, S., Herry, J.-M., Bellon-Fontaine, M.-N., 2009a. Capillary force required to detach micron-sized particles from solid surfaces—Validation with bubbles circulating in water and 2µm-diameter latex spheres. *Colloids and Surfaces B: Biointerfaces* 73, 276–283. <https://doi.org/10.1016/j.colsurfb.2009.05.022>
- Li, G., Tang, L., Zhang, X., Dong, J., 2019. A review of factors affecting the efficiency of clean-in-place procedures in closed processing systems. *Energy* 178, 57–71. <https://doi.org/10.1016/j.energy.2019.04.123>
- Mai, Z., Butin, V., Rakib, M., Zhu, H., Rabiller-Baudry, M., Couallier, E., 2016. Influence of bulk concentration on the organisation of molecules at a membrane surface and flux decline

during reverse osmosis of an anionic surfactant. *J. Membr. Sci.* 499, 257–268.

<https://doi.org/10.1016/j.memsci.2015.10.012>

Moerman, F., Rizoulières, P., Majoor, F.A., 2014. 10 - Cleaning in place (CIP) in food processing, in: Lelieveld, H.L.M., Holah, J.T., Napper, D. (Eds.), *Hygiene in Food Processing* (Second Edition). Woodhead Publishing, pp. 305–383.

<https://doi.org/10.1533/9780857098634.3.305>

Peng, J.-S., Tsai, W.-C., Chou, C.-C., 2002. Inactivation and removal of *Bacillus cereus* by sanitizer and detergent. *Int. J. Food Microbiol.* 77, 11–18.

Pietrysiak, E., Kummer, J.M., Hanrahan, I., Ganjyal, G.M., 2019. Efficacy of Surfactant Combined with Peracetic Acid in Removing *Listeria innocua* from Fresh Apples. *J. Food Prot.* 82, 1959–1972. <https://doi.org/10.4315/0362-028X.JFP-19-064>

Ribeiro, M.C.E., Fernandes, M. da S., Kuaye, A.Y., Gigante, M.L., 2019. Influence of different cleaning and sanitisation procedures on the removal of adhered *Bacillus cereus* spores. *Int. Dairy J.* 94, 22–28. <https://doi.org/10.1016/j.idairyj.2019.02.011>

Srey, S., Jahid, I.K., Ha, S.-D., 2013. Biofilm formation in food industries: A food safety concern. *Food Control* 31, 572–585. <https://doi.org/10.1016/j.foodcont.2012.12.001>

Tauveron, G., Slomianny, C., Henry, C., Faille, C., 2006. Variability among *Bacillus cereus* strains in spore surface properties and influence on their ability to contaminate food surface equipment. *Int. J. Food Microbiol.* 110, 254–262.

<https://doi.org/10.1016/j.ijfoodmicro.2006.04.027>

Tisné, P., Aloui, F., Doublié, L., 2003. Analysis of wall shear stress in wet foam flows using the electrochemical method. *International Journal of Multiphase Flow* 29, 841–854.

[https://doi.org/10.1016/S0301-9322\(03\)00038-7](https://doi.org/10.1016/S0301-9322(03)00038-7)

Tisné, P., Doublié, L., Aloui, F., 2004. Determination of the slip layer thickness for a wet foam flow. *Colloids and Surfaces A: Physicochemical and Engineering Aspects* 246, 21–29.

<https://doi.org/10.1016/j.colsurfa.2004.07.014>

CHAPTER V, PART 2

RESULTS

CHAPTER V, PART 2

Detachment of *B. amyloliquefaciens* 98/7 after singularities

CHAPTER V, PART 2

RESULTS

5.0 Abstract: in this part, we studied the effect of singularities on the efficiency of foam flow for the detachment of *B. amyloliquefaciens* 98/7 (*B. subtilis* 98/7) in the test duct. Foam flow was subjected to mechanical perturbations when passing through singularities such as sudden expansion/ gradual reduction and 90° bending once and twice affecting the global efficiency of the cleaning. In this part, 1D 50% flow regime was used for all the tested cases.

5.1 Introduction:

In agro-food industries, singularities are used for different purposes including direction flow changes of fluids in pipes, also when passing from small to larger diameter pipes.

Indeed, most transport systems in industrial facilities have various peculiarities, which cause major changes in flow behaviour (Calvert, 1988; Deshpande & Barigou, 2001b, 2001a), these changes can be very disturbing for the flowing fluid which can change some of its properties. For example, foam which is a non-Newtonian fluid can be subjected to structural changes such as bubbles form as a result of coarsening, bursting.., also liquid drainage level, and film thickness adjacent to the walls of the channel.

The flow of foam through the singularities is not studied frequently. There is not enough information on the reorganization of a foam flow downstream of these singularities to fully understand the accidental degradation of energy (Farahmandfar et al., 2019; Schramm, 2000; Stevenson, 2012). Several experimental works have been performed for studying foam flow in a horizontal square pipe with a built-in cross-section (Blondin & Doublier, 2002; P. Tisné et al., 2003; P. Tisné et al., 2004). They have shown that the flow arrangement, depending on the Reynolds number, can vary from a plug-flow up to a complex regime affecting the liquid films along the surfaces and the foam itself in terms of velocity and structure (bubble arrangement). This identification was confirmed by other studies (Aloui & Madani, 2007, 2008). Reynolds number can be an indicator for the change in foam structure, however to understand the detachment efficiency of foam one should relate different phenomenon occurring at the wall. Bubbles layer thickness, film thickness at the walls of the pipe, bubbles size, distribution and shape can be the key parameters for different phenomena to occur.

Our goal in this study will be concerned in studying the efficiency of foam flow in detaching *B. amyloliquefaciens* 98/7 spores post the singularities in relation with foam structure at the top wall of the duct.

5.2 Spores' detachment in test ducts placed post singularities

For the expansion/ reduction singularity, in both cases, whether the singularity is set after establishment (after 1m) or set directly after the foam generation source, log 10(N) reduction was about 1.2 after 20 minutes of cleaning. The average shear stress in the test duct set after the sudden expansion/ gradual reduction singularity was higher by ~ 1Pa compared to establishment case, however, this did not show an increase in the detachment compared to establishment case (~2 logs).

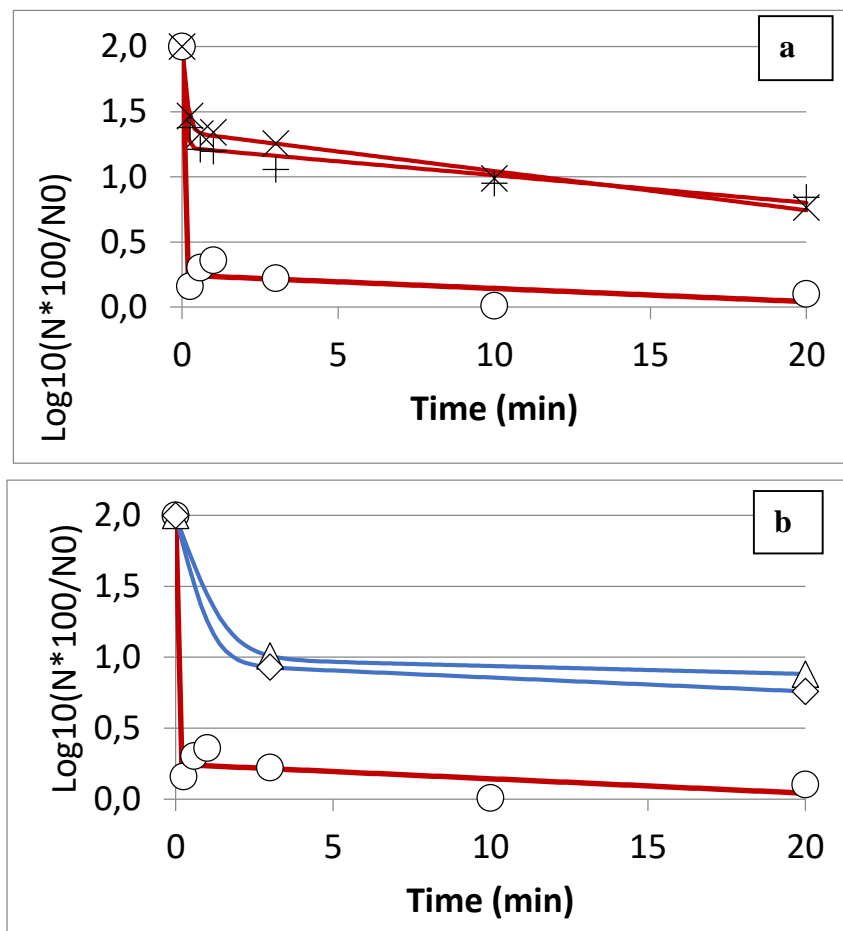


Figure 5.0 (a,b). Cleaning kinetics of *B. amyloliquefaciens* 98/7 in the test duct placed after
 ○: establishment only(1m) , x :expansion only , +: establishment- expansion, △: establishment-one bend , ◇ : two establishments-two bends placed alternatively. Only mean values of the remaining surface contamination were presented.

As for 90° bend, it was technically possible to perform the experiments only for the cleaning times 3 and 20 minutes. For that reason it is relevant to compare with establishment case, only the log reduction (e.g. 20 minutes) and not the cleaning kinetics as the parameters k_{max1} , k_{max2} and f were not identified. When the test duct is placed after 1 bend or 2 bends, the log 10 reduction obtained was almost the same ($\sim 1\log$). Results of log 10 reduction at 20 minutes of cleaning and average shear stress are presented in table 5.0.

Table 5.0 log10 reduction obtained after 20 minutes of cleaning in the test duct after the singularities.

Singularity placed before the test duct	Average shear stress $\bar{\tau}$ (Pa) in test duct	Log10 reduction (20mins)
Estab*+exp/red**	3.3	1.23
Exp/red only	3.6	1.24
Estab	2.2	1.90
1 Bend	2.2	1.12
2 Bends	2.8	1.24

*Estab: Establishment, **Exp/Red: sudden expansion/gradual reduction singularity

To test the significance between the results, student t-test was performed, with paired observations (data from the same experimenter) and unilateral distribution. T-critical = 2.02 was obtained from t-table with α being 0.05 and $n=5$ (degree of freedom).

Table 5.1. Student t-test performed on the log 10 reduction results obtained from each case.

Singularity placed before the test duct	t value	Comments
Estab / Estab+Exp/Red	12.48	Significant
Exp/Red / Estab + Exp/Red	0.63	Not significant
1bend / 2 bends *	4.48	Not significant

* t critical was 6.31 for the bends case due to the considered number of subjects($n=2$).

Results of Student t-test showed that when the singularity is placed after establishment or directly after the foam generation source there was no significant difference between the results. Also for bends, whether the test duct is placed after 1 or 2 bends, no significance difference in the results

was observed. Significant difference in the results was obtained for the comparison of estab with Estab+Exp/Red.

The decimal reduction at 20 min was statistically analysed through a variance analysis (SAS, general linear model and Tukey grouping) to compare the role of the singularities. At 20 min, cleaning efficiencies observed after any singularity tested were found to be lower than the reference (1m for the foam stabilisation and no singularities) as shown in Figure 5.1. In addition, a larger variability was observed after the bends ranging from 2 log reduction down to no cleaning after 2 bends. The Tukey's grouping confirmed these observations, but the role of the singularity (expansion) on the cleaning efficiency just after the generators was not found significantly different from the reference.

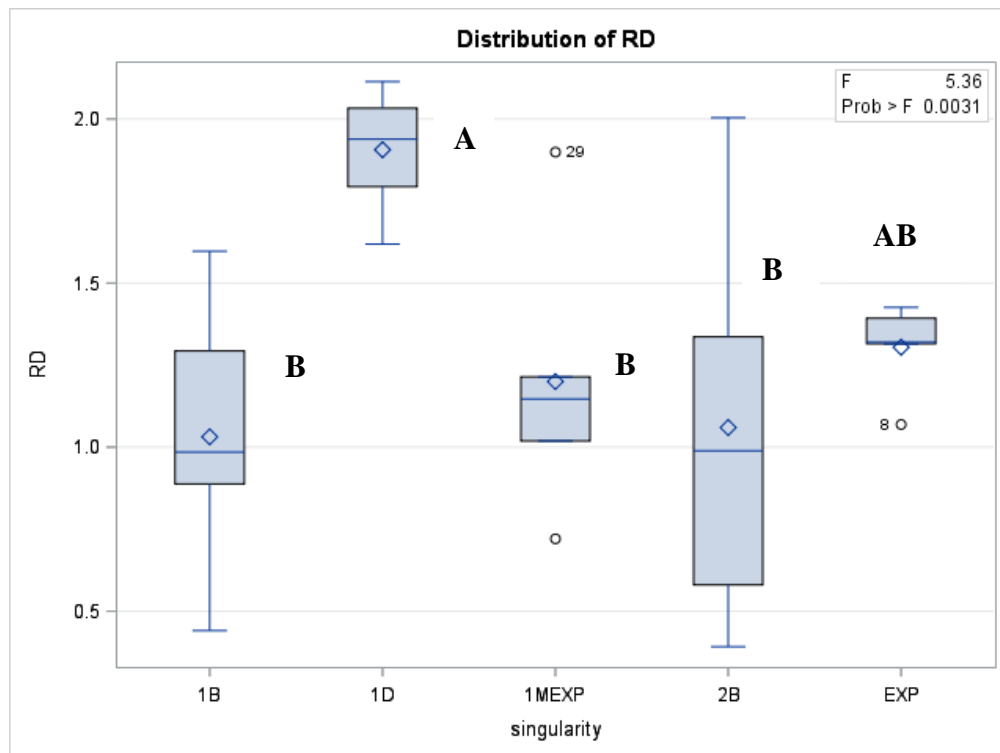


Figure 5.1 Decimal reduction after 20 min cleaning vs the shape of the circuit (after 1 m establishment length: 1D; an expansion/reduction: EXP; an expansion/reduction after 1 m establishment length: 1MEXP; one bend: 1B; 2 bends: 2B)

To study the detachment kinetics of *B. amyloliquefaciens* 98/7 spores for each condition, modeling of the log₁₀ (N) was performed using Ginfat software (biphasic model). The results are presented in table 5.2.

Table 5.2 Kinetic parameters obtained after modeling each condition taking into account all the data whatever the number of repetition.

Cases	Log(10) N_0	$K_{1(s^{-1})}$	$K_{2(s^{-1})}$	F (%)	R^2
Estab only	5.54	114.75	0.023	98.2	0.83
Estab(1m)+ Exp/Red	5.58	16.81	0.05	83.2	0.56
Exp/Red	5.51	9.35	0.07	77.90	0.73

Whether the Exp/Red singularity is placed after establishment or directly after the foam generation source, the rate of detachment of the loosely attached population (K_1) did show close values (16.81, 9.35 s^{-1}) confirmed by the variance analysis, Tukey's grouping (each experiment modelled separately). For the establishment case the rate (K_1) was higher by 7 to 12 times when compared with Exp/Red rates. The rate of detachment of the highly adherent population (K_2) was much slower compared to K_1 being less than 0.1 s^{-1} for the three cases; no significant differences (Tukey's grouping) accounting for the variability within the repetitions.

5.3 Foam stability tested after singularities

After analyzing the results obtained from different singularity conditions, we studied the stability of foam of the 1D 50%. Stability of foam may be linked to behavior of flowing foam concerning detachment of spores. The stability test was performed by pouring the flowing foam which is passing through different singularity in a 1000 ml graduated cylinder. When foam level reaches 1000 ml timing starts and the volume of foam is measured as it decreases with time. The results are presented in the figure 5.2.

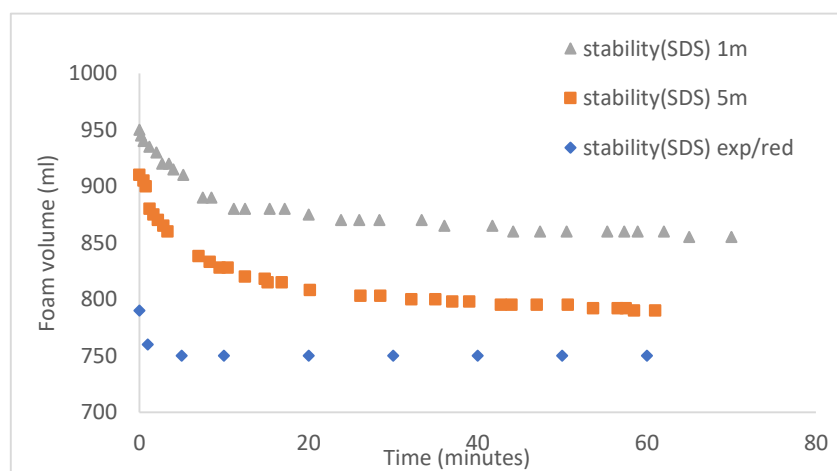


Figure 5.2. Stability of foam measured after passing through different structures.

The stability of foam after establishment case (1m), showed that the first 10 minutes, there was liquid drainage. In turn the drainage with time lead to foam bubbles bursting where the level of foam volume dropped from 945 ml (55 ml liquid drainage) at time 0 minutes till 890 ml during the first 10 minutes. After 10 minutes the volume decrease slowly to reach at 70 minutes a volume of 855 ml. The volume continued to drop to reach 0 ml after more than 24 hrs. (Total collapse of foam). After 5 m, the result showed a different volume at time 0 minutes compared to establishment case (1m) . The volume was about 910 ml of foam at time 0 minutes , indicating about 80 ml of liquid drainage compared to 1 m. After 60 minutes the volume of foam dropped to reach 790 ml and continued to drop to reach a volume of 0 ml after more than 24 hours.

After exp/ red singularity more drainage was observed at time 0 compared to 1 and 5 m cases, where the volume of foam was 790 ml then dropped to reach 750 ml at 5 minutes. After 5 minutes it decreased slowly to reach 0 ml after 18 hours. Upon analyzing the foam and the liquid drained volume, for the exp/red case more drainage of liquid happened inside the singularity while outside the singularity drainage was the lowest when compared to the 1 m and 5 m cases. For the latter cases drainage inside 1m was the lower compared to the 5 m while outside drainage was the highest for the 5 m case. Another important point can be deduced from the ability of foam to withstand during longer times. Foam resulting from the 1 m and 5m showed more tendency to stay structured compared to exp/red case.

Based on the above, we can suggest that stability of foam can have an effect on the efficiency of flowing foam. To investigate the effect of introducing 2 bends in a 4 m circuit we decided to perform cleaning experiment after 5 m straight pipe and compare the detachment results of *B. amyloliquefaciens* 98/7 spores to that of the 4m circuit. Results are presented in the Figure 5.3.

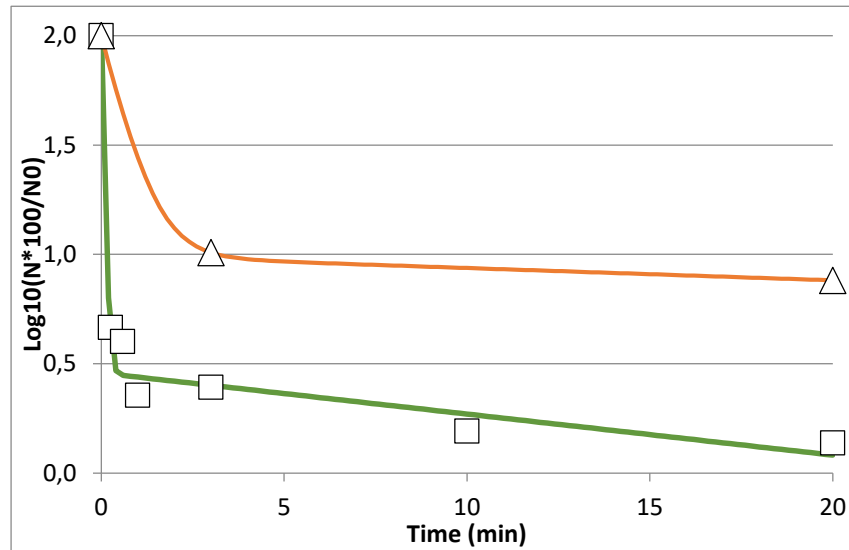
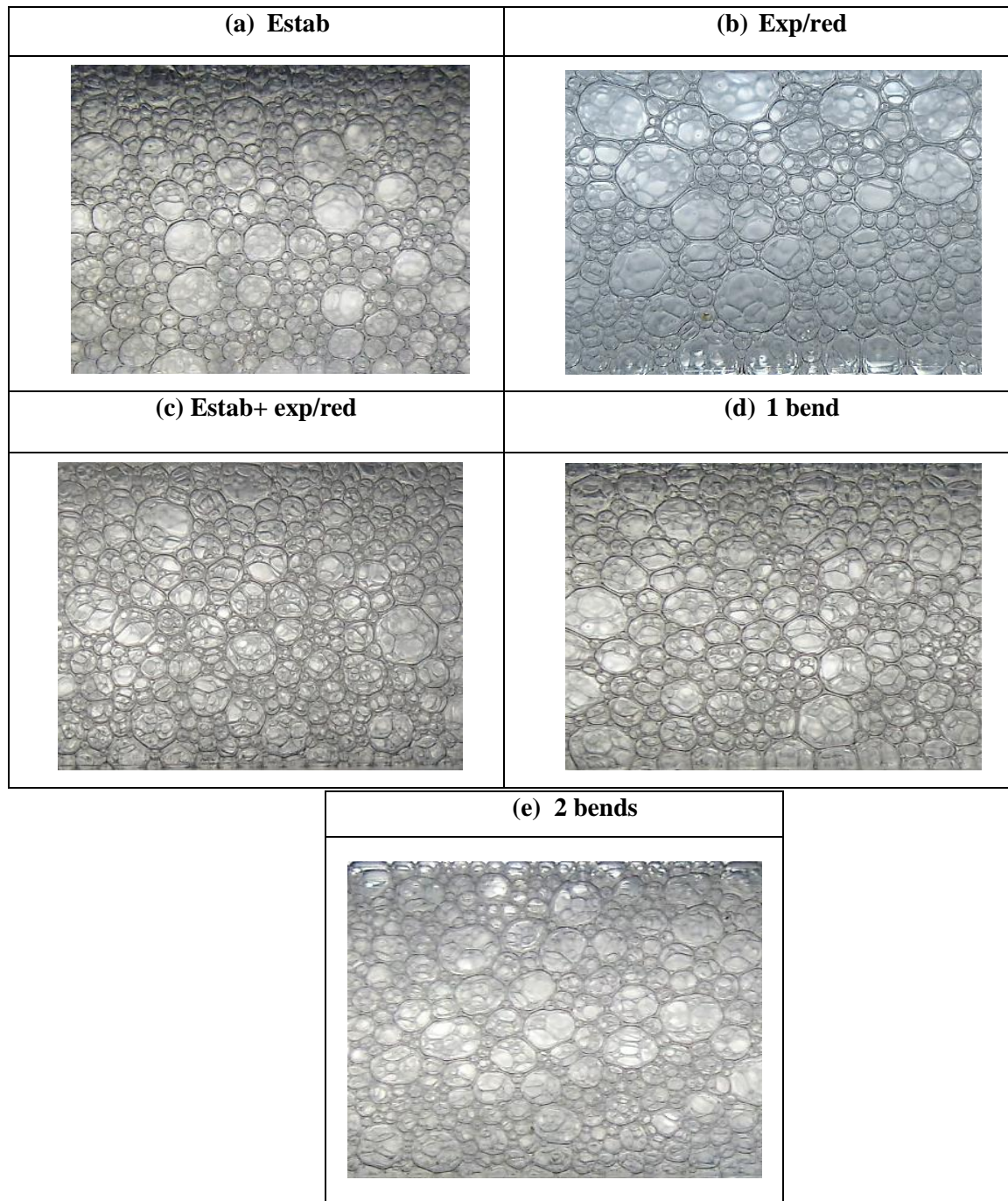


Figure 5.3 Cleaning kinetics of *B. amyloliquefaciens* 98/7 in the test duct placed after □: 5m pipe , Δ: 2 bends.

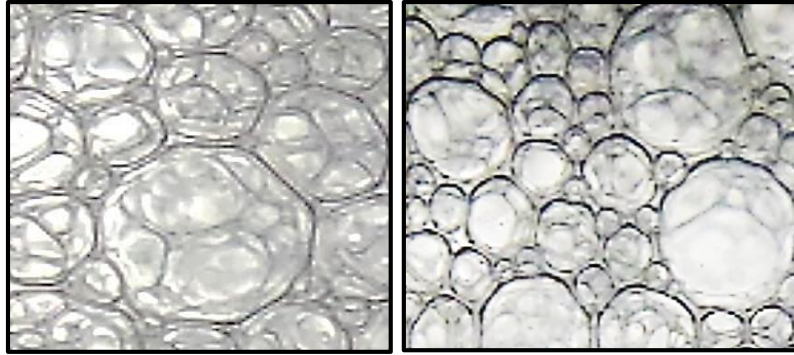
As already discussed, cleaning kinetics for bends cases were not possible to obtain. Results of log10 reduction for the case of 5 m after 20 minutes of cleaning were different from that of the 4 m circuit suggesting a bending effect on the efficiency of detachment. The log 10 reduction was higher in case of 5 m straight channel (2 logs) compared to 4 m circuit including 2 bends, where it almost reached 1.2. After 5 m drainage was higher than that of 4 meter, however, results of detachment were contrary to what was predicted when basing the explanation on drainage as a stability reference. For that reason, we went further to investigate bubbles shape and size to understand the foam structure at the top wall.

5.4 Qualitative and quantitative analysis of bubbles post singularities

After passing through singularities, images for the bubbles at the top wall were compared with bubbles shape and size of the establishment case (1m)



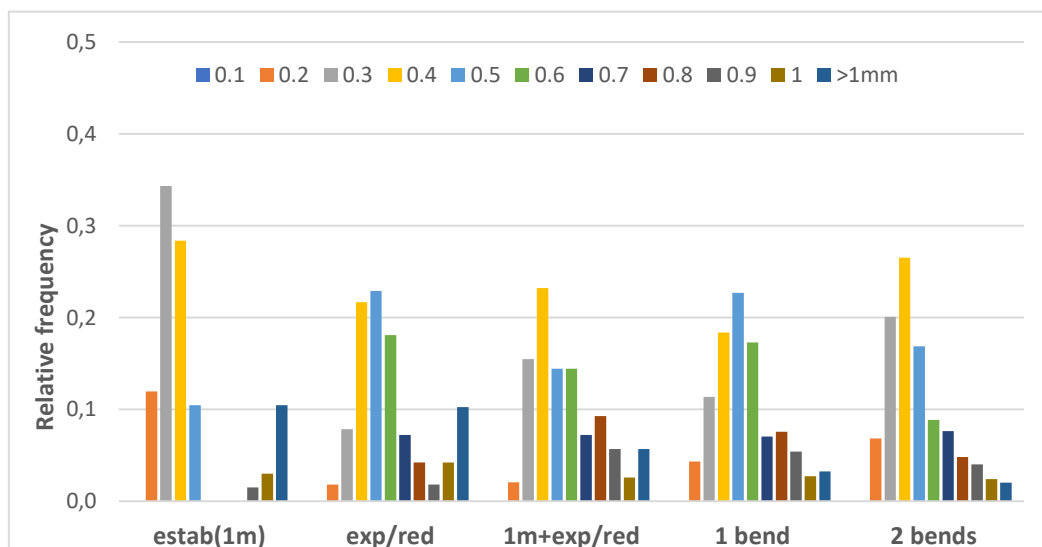
Figures 5.4 Foam bubbles (1D 50%) after passing through the different singularities (b,c,d,e) in comparison with establishment case (a).



Figures 5.5. Bubbles contour after Estab+exp/red case (left; dry foam),; after estab only(right; wet foam). When foam passes the wet limit to the dry limit, foam is structured according to Kelvin or Weaire-Phelan foam organization (Drenckhan & Hutzler, 2015).

In our case, the shape of the bubbles becomes polygonal post singularities compared to establishment case (bubbles a more round) acquiring either Kelvin or Weaire-Phelan organization. When foam passes a singularity, different phenomena can intervene to change foam structure such as coalescence, bursting, drainage and coarsening.

Bubbles size was measured after each singularity and compared with establishment case. The method of size measurement is the same as the one described in part 1 of the results. Results are presented in figure 5.6.



Note: the range of sizes of each legend is bounded by the value of the previous legend, for example <0.5 means that the range of sizes is $0.4 \leq x < 0.5$.

Figure 5.6. Relative frequency for each bubbles size after each singularity compared to the establishment case.

When comparing singularities only, most of the sizes range $0.2 \leq x < 0.7$ mm had a relative frequency higher than 0.1. Their relative frequency was higher compared to other bubble sizes. Other bubble sizes $0.1 < x < 0.2$ mm, $0.7 < x < 0.9$ mm, and > 1 mm showed a relative frequency less or equal to 0.1 in all singularities. Bubbles having the size $0 < x < 0.1$ mm did not exist for all cases. Bubble sizes trends after singularities showed.

When comparing to the establishment case, it was clear that the bubbles having the size $0.5 < x < 0.9$ mm did not exist. The bubbles size $0.2 < x < 0.3$ mm and $0.3 < x < 0.4$ mm showed the highest relative frequency (> 0.2) being the highest when compared to all singularity cases. Also for the smallest bubble size $0.1 < x < 0.2$, it was the highest compared to singularity case being more than 0.1 for the establishment case. Size ranges were different between singularities and the establishment case. Medium bubble sizes in establishment case did not exist, showing either small or large bubbles sizes. It is important to state even if sizes range were different, however, an important point to be taken into account is the stability of foam and bubbles shape which can contribute to the difference in the detachment efficiency.

5.5 Discussion and Conclusion

In our case, regardless of what type of singularity was used, when foam passes through the tested singularities, the \log_{10} reduction of *B. amyloliquefaciens* 98/7 spores decreased by ~ 0.8 when compared to the establishment case ($\sim 2 \log_{10}$ reduction) after 20 minutes of cleaning. As for the kinetics, also the rate of the high detachment phase for expansion / reduction singularity (both cases: exp/red; estab+exp/red) was much lower compared to the establishment case being lower by a factor of 9 and 12. As for bends, whether after 1 or 2 bends K1 and the \log_{10} reduction at 20 minutes was almost the same.

Considering Tukey's grouping, singularities were grouped differently (B) compared to establishment case (A). Only the exp/red case after the foam generation source did show an AB grouping.

Eventhough the flow regime is the same (1D 50%) in all the tested cases, however, the detachment after 20 minutes of cleaning was not the same when comparing the establishment case (1m) with that of the singularity cases. Compared to estab only, when Exp/red was introduced whether after estab or after the foam generation source, the increase in the WSS (wall shear stress) was about 1 Pa. The increase in WSS did not show an increase in the detachment of *B. amyloliquefaciens* 98/7

spores after 20 minutes of cleaning; instead, there was a decrease by 0.8 log indicating an unproportional effect of WSS on detachment of the spores. Because it is the same flow regime (1D 50%) , capillary forces imposed by the bubbles layer on the wall must be the same unless the bubbles shape and size changes.

The stability of foam after different structures (1m , 5m and exp/red) , was compared as a function of the foam volume. Higher drainage out side the pipe (1m; 5m) /singularity (exp/red) showed a faster bursting of bubbles, in turn a faster collapse of foam. As for drainage inside the tested structure , the exp/red singularity showed the highest drainage compared to 1m and 5 m cases. Log 10 reduction for the test duct installed in the 4 m circuit (after 2 bends) was lower by 0.7 log when compared to detachment after 5 m indicating an effect of the bend singularities on foam . For that reason we shifted our studies to investigate bubbles shape and size after the different singularities.

We investigated bubbles morphology after the flow passes through the singularities. In our case, foam structure was reorganized post singularities. Different phenomenon may happen while foam is passing through singularities such as drainage, coalescence, expansion, and coarsening that can result in a new structure of foam. Different parameters can intervene to explain a different behavior of foam in detaching spores:

- As already discussed in part 1 of the results, higher foam quality did not show better detachment of *B. amyloliquefaciens* 98/7. 1D 70% showed lower detachment compared to 1D 50%. In singularities, the results of detachment were lower compared to detachment in the establishment case after 20 minutes of cleaning. In this part related to singularities , the bubbles were not only larger in size compared to the establishment case, however, bubbles had a polygonal contour. According to the literature, in that case foam has passed the wet limit to the dry limit. Dry foam bubbles tend to be ordered and have a packed structure. When decreasing the liquid fraction away from the wet limit, foams are often regarded as frictionless, granular matter since the bubbles are sufficiently large so that Brownian motion can be neglected(Drenckhan & Hutzler, 2015). The surface energy of bubbles decreases with the vertices of the bubbles being fixed (Sadoc & Rivier, 2013).
- According to (Chovet, 2015) the thin film thickness at the top wall decreased slightly where it marked $\sim 27 \mu\text{m}$ at a quality of 70% instead of $24 \mu\text{m}$ at a quality of 50%. In this study, foam was flowing in a 21*21 mm squared cross section channel.

Also the variation at the top wall of the thickness of the thin liquid film between the bubbles and the wall was directly affected by the bubbles passage and depended on their size (Tisné et al., 2004), which could have an effect on the effectiveness of the removal of adherent bacteria. In the detachment mechanisms, the fluctuation of the liquid film thickness due to the wall shear stress weakening the interaction forces between spores and the wall would promote the detachment. Due to new organized structures of dry foam these fluctuations of the thin liquid film decreases due to the limitation of bubbles freedom of movement which is controlled by the packed polyhedral structure of foam.

- Bubble film thickness plays a major role in the determination of both the particle diameter that can be entrapped in the film (Kim et al., 2020). A particle can be entrapped in a thin liquid film when the film thickness is within a specific range depending on the particle diameter [(Hadjiiski et al., 1996; Horozov et al., 2008).
- The capillary forces linked to the bubble size and velocity would play a major role in the detachment rate especially at the lowest velocities. In our case the velocity was the same for all the cases $\sim 2\text{cm}\cdot\text{sec}^{-1}$, however, bubbles after singularities showed a different trend of sizes compared to the establishment case. The sizes 0.6, 0.7, 0.8 mm were not present in the establishment case, which can be considered as moderate sized bubbles compared to the other sizes, on the other hand these sizes were found in all the singularity cases. The distribution of bubbles sizes plays an important role in maintaining a defined capillary force that can have a definite impact on cleaning.

According to the discussed points, the detachment of spores is not affected by one factor, instead different factors may intervene from bubbles film thickness, top wall film thickness, bubbles shape and size. The mechanism can be a coordination of all the mentioned factors resulting in an either efficient cleaning or not. Singularities plays the role of foam reorganizer where its presence at different points in an installation can induce a mechanical change in foam flow on the level of structure and detachment efficiency.

5.6 References

- Aloui, F., & Madani, S. (2007). Wet foam flow under a fence located in the middle of a horizontal duct of square section. *Colloids and Surfaces A: Physicochemical and Engineering Aspects*, 309(1-3), 71-86. <https://doi.org/10.1016/j.colsurfa.2007.01.009>
- Aloui, F., & Madani, S. (2008). Experimental investigation of a wet foam flow through a horizontal sudden expansion. *Experimental Thermal and Fluid Science*, 32(4), 905-926. <https://doi.org/10.1016/j.expthermflusci.2007.11.013>
- Blondin, E., & Doublier, L. (2002). Particle imaging velocimetry of a wet aqueous foam with an underlying liquid film. *Experiments in Fluids*, 32(3), 294-301. <https://doi.org/10.1007/s003480100318>
- Calvert, J. R. (1988). The flow of foam through constrictions. *International Journal of Heat and Fluid Flow*, 9(1), 69-73. [https://doi.org/10.1016/0142-727X\(88\)90032-X](https://doi.org/10.1016/0142-727X(88)90032-X)
- Chovet, R. (2015). *Experimental and numerical characterization of the rheological behavior of a complex fluid : Application to a wet foam flow through a horizontal straight duct with and without flow disruption devices (FDD)* [Université de Valenciennes et du Hainaut-Cambresis]. <https://tel.archives-ouvertes.fr/tel-01192955/>
- Deshpande, N. S., & Barigou, M. (2001a). Foam flow phenomena in sudden expansions and contractions. *International Journal of Multiphase Flow*, 15.
- Deshpande, N. S., & Barigou, M. (2001b). *The flow of gas-liquid foams through pipe fittings*. 8.
- Drenckhan, W., & Hutzler, S. (2015). Structure and energy of liquid foams. *Advances in Colloid and Interface Science*, 224(Supplement C), 1-16. <https://doi.org/10.1016/j.cis.2015.05.004>
- Farahmandfar, R., Asnaashari, M., Taheri, A., & Rad, T. K. (2019). Flow behavior, viscoelastic, textural and foaming characterization of whipped cream : Influence of Lallemandia royleana seed, Salvia macrosiphon seed and carrageenan gums. *International Journal of Biological Macromolecules*, 121, 609-615. <https://doi.org/10.1016/j.ijbiomac.2018.09.163>
- Hadjiiski, A., Dimova, R., Denkov, N. D., Ivanov, I. B., & Borwankar, R. (1996). Film Trapping Technique : Precise Method for Three-Phase Contact Angle Determination of Solid and Fluid Particles of Micrometer Size. *Langmuir*, 12(26), 6665-6675. <https://doi.org/10.1021/la9605551>
- Horozov, T. S., Braz, D. A., Fletcher, P. D. I., Binks, B. P., & Clint, J. H. (2008). Novel Film-Calliper Method of Measuring the Contact Angle of Colloidal Particles at Liquid Interfaces. *Langmuir*, 24(5), 1678-1681. <https://doi.org/10.1021/la703414q>

- Kim, J., Lee, S., & Joung, Y. S. (2020). Schlieren imaging for the visualization of particles entrapped in bubble films. *Journal of Colloid and Interface Science*, 570, 52-60.
<https://doi.org/10.1016/j.jcis.2020.02.085>
- Sadoc, J. F., & Rivier, N. (2013). *Foams and Emulsions*. Springer Science & Business Media.
- Schramm, L. L. (Éd.). (2000). *Surfactants : Fundamentals and applications in the petroleum industry*. Cambridge University Press.
- Stevenson, P. (Éd.). (2012). Front Matter. In *Foam Engineering* (p. i-xv). John Wiley & Sons, Ltd. <https://doi.org/10.1002/9781119954620.fmatter>
- Tisné, P, Aloui, F., & Doubriez, L. (2003). Analysis of wall shear stress in wet foam flows using the electrochemical method. *International Journal of Multiphase Flow*, 29(5), 841-854.
[https://doi.org/10.1016/S0301-9322\(03\)00038-7](https://doi.org/10.1016/S0301-9322(03)00038-7)
- Tisne, P., Doubriez, L., & Aloui, F. (2004). Determination of the slip layer thickness for a wet foam flow. *Colloids and Surfaces A: Physicochemical and Engineering Aspects*, 246(1-3), 21-29. <https://doi.org/10.1016/j.colsurfa.2004.07.014>
- Tisné, Patrice, Doubriez, L., & Aloui, F. (2004). Determination of the slip layer thickness for a wet foam flow. *Colloids and Surfaces A: Physicochemical and Engineering Aspects*, 246(1-3), 21-29. <https://doi.org/10.1016/j.colsurfa.2004.07.014>

CHAPTER V, PART 3

Detachment of *B. amyloliquefaciens* 98/7 spores using foam flow generated from different surfactants

CHAPTER V, PART 3

RESULTS

6.0 Abstract: In this part we studied the detachment of *B. amyloliquefaciens* 98/7 spores by foam flow produced from surfactants that differs by their chemical and physical properties. In addition to SDS which was already previously used, the surfactants used in this part are: Capstone® fluorosurfactant FS-30 which is a general-purpose, water-soluble, ethoxylated non-ionic fluorosurfactant that modifies surface energies at very low concentrations. The second surfactant is Ammonyx® LO which is an amphoteric nonionic surfactant having applications in personal care, as foam enhancers. One foam flow regime was tested which is 1D 50% (plug flow). Surfactant properties were investigated such as surface tension, capillary number, thickness of the top thin film and foam structure adjacent to the top wall (bubble shape, pattern and size). The efficiency foam flow resulting from surfactants was tested in the detachment of *B. amyloliquefaciens* 98/7 spores and was compared to that of SDS.

6.1 Introduction

The interaction of air bubbles with solid particles is an important mechanism in many industrial processes. Significant applications are found in the chemical and process industry (separation of coal, mineral ores, or plastics by flotation) or wastewater treatment (Basařová et Zedníková 2019), however, in our study, the application was settled for detaching *B. amyloliquefaciens* 98/7 spores from pipes. When changing the surfactant, different chemicals will be involved in producing different foams that are different by their physical properties.

Capstone® FS 30 and Ammonyx® LO surfactants are known for their uses in different industrial applications. For instance, Capstone® FS 30 can be used in coatings to reduce surface tension and provides excellent wetting to achieve cleanability. As for Ammonyx® LO it can be used as a foam enhancer, detergent, stabilizing and thickening agent. In the textile industry it can be used as lubricant, emulsifier, wetting agent and dye dispersant. Also Ammonyx® LO is a very good dispersing agent for calcium soaps and has a very good resistance to hard water where it limits flocculation.

Concerning detachment of microorganisms by foam flow produced from surfactants, it is important to understand the action of foam flow (double phase fluid) taking into account properties of foam such as stability, bubbles size, film thickness adjacent to the walls. Bubbles and thin

film plays an important role in imposing a mechanical action on the walls of the pipe which can provoke detachment of microorganisms.

Studying stability of foam resulting from each surfactant can provide information on the foam structure rigidity which is important in our case for preserving a good contact with the top wall of the pipe while foam is flowing. Another point is that different bubble sizes can have a different impact on the thin liquid film. When bubbles pass beneath the top thin liquid film, each bubble will create a local shear stress that reaches maximum at the edges of the bubble while at the middle of the bubble it tends to be zero (Tisné, Aloui, et Doublier 2003). As already discussed in part 1, the fluctuation of the thickness of thin liquid film as a result of bubbles passage will weaken the attachment forces between the microorganisms and the top wall that will later lead to detachment afterwards. The efficiency of this synergetic action of the bubbles on the thin film depends on many factors that lie in the physicochemical properties of the surfactant. In this part we intended to study only the properties that were useful in our case to calculate the top thin liquid film such as surface tension and capillary number, As for bubbles size a qualitative and a quantitative study was performed to investigate the morphology of bubbles.

6.2 Testing stability of foam

We compared the stability of the foam resulting from the three surfactants. Three 1000 ml cylinders were filled by the foam resulting from each surfactant (regime: 1D 50%) after passing through a 1 m establishment (only 1 m establishment was used before the test duct in this part of the results). The time needed for total dispersion of foam resulting from each surfactant was measured. The concentrations considered for the three surfactants in water were, SDS: 1.5 g.L^{-1} , Ammonyx® LO: 0.8 mL.L^{-1} , Capstone® FS 30 : 0.32 mL.L^{-1} (minimum concentrations to obtain stable foam flow in the Plexiglas pipe). Data are presented in figure 6.0.

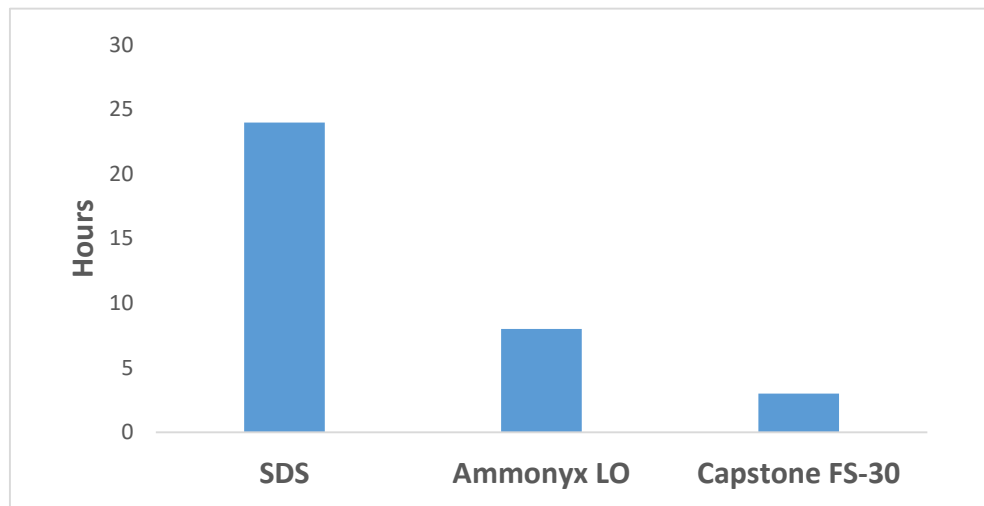


Figure 6.0 Time needed for the total dispersion of foam resulting from SDS, Ammonyx® LO, Capstone® FS 30 .

Foam resulting from SDS showed a total dispersion of foam after 24 hours where foam has totally changed to liquid, on the other hand for Ammonyx® LO and Capstone® FS 30 it was about 8 and 3 hours respectively. Foam resulting from SDS showed a more stable structure and an ability to withstand for longer times before changing completely to liquid, while for Ammonyx® LO and Capstone® FS 30 a total dispersion was observed during a time which is lower by a factor of 8 and 3 respectively. Even though in our case the maximum cleaning time was about 20 minutes, however, the stability test performed in our case can be an indicator for the ability of foam to withstand its structure and stay rigid. Of course from the results, SDS foam would be the most long lasting structured foam. The importance in closed system to have a good structured foam is related to the fact that a good detachment behavior by foam needs a very good contact between foam and the surface.

6.3 Bubbles structure and size

For the three surfactants, the pattern of bubbles adjacent to the top wall was studied. A clear difference in the pattern was observed between the surfactants. As discussed in part 1 and 2, SDS foam (1D 50%, 1 m establishment) at the top wall showed small, moderate and large sizes of bubbles as shown in figure 6.1. Comparing Ammonyx® LO to SDS, it is obvious that in addition to the small, medium and large sized bubbles that were recognized in SDS, there was tiny bubbles which were found in between the other mentioned bubbles. The bubbles are much smaller in size

than the smallest bubbles in SDS. As for Capstone® FS 30, giant bubbles were observed, which are much larger compared to the largest bubbles of SDS and Ammonyx® LO. It is important to mention that giant bubbles in the case for Capstone® FS 30, acquired a polygonal shape rather than the rounded one which was observed in the case of SDS and Ammonyx® LO. Figure 6.1 (a, b, c) and table 6.0 show a qualitative clarification of the latter description.

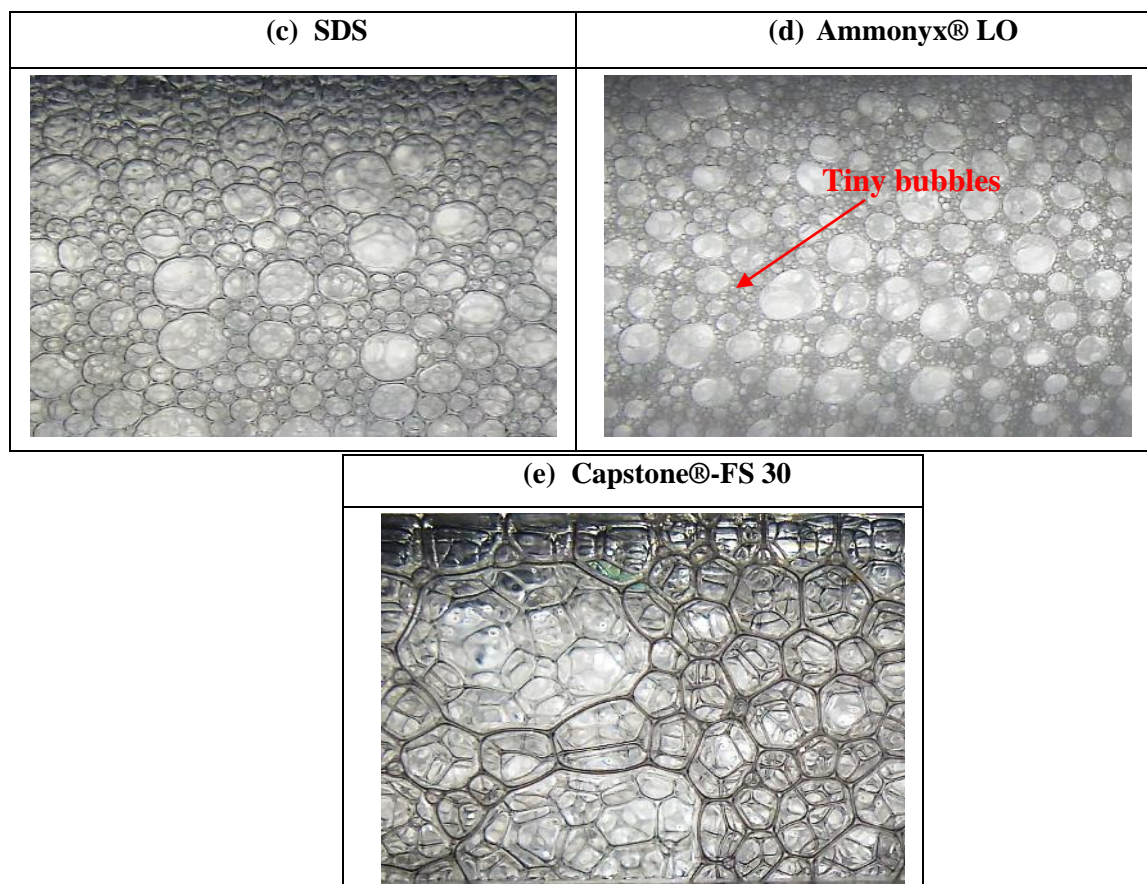


Figure 6.1 (a, b, c) shows bubbles morphology at the top for the three surfactants

Table 6.0 shows bubbles size description found in each surfactant

Surfactant/Bubble size description	tiny	small	moderate	large	Giant
SDS		×	×	×	
Ammonyx® LO	×	×	×	×	
Capstone® FS 30				×	×

To perform a numerical analysis for the size of bubbles we did measurement of bubbles size using the software Piximètre as described in part 1 of the results. Figure 6.2 shows the distribution of bubbles sizes for the three surfactants.

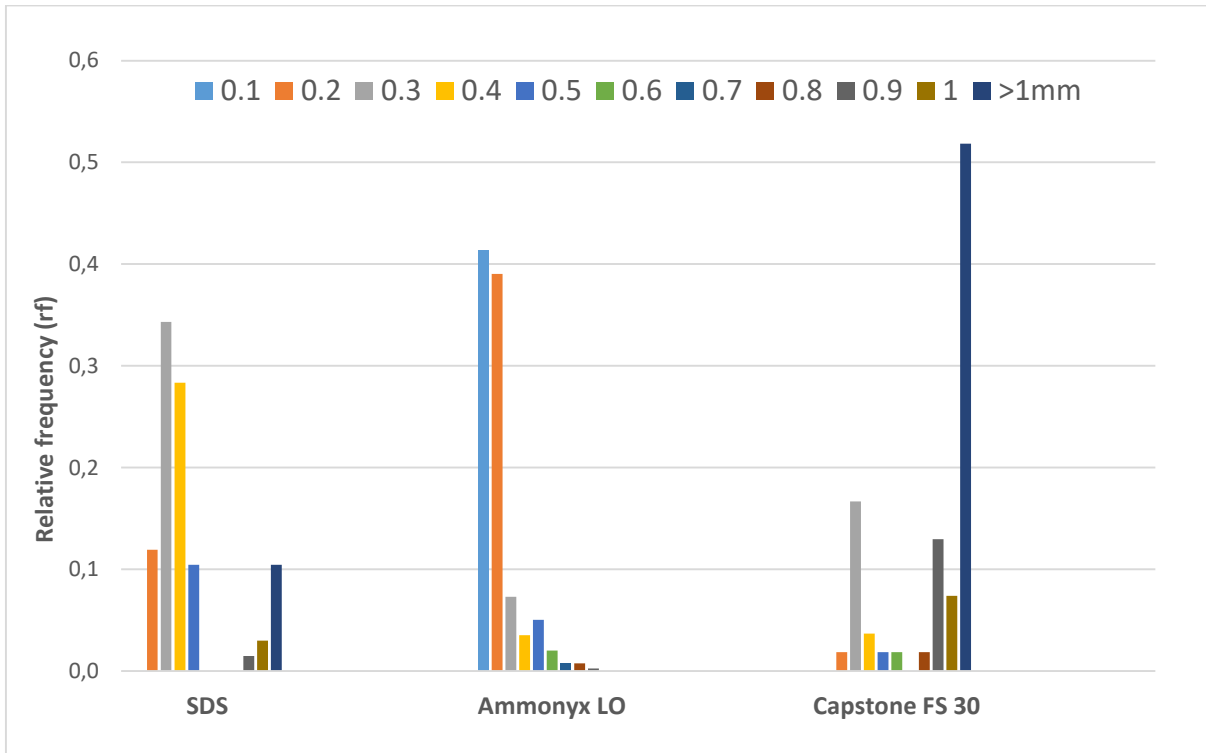


Figure 6.2 Bubble sizes (diameter) distribution for the different surfactants at the top wall of the test duct.

The results of bubble sizes showed that Ammonyx® LO had the highest relative frequency for bubble sizes $s < 0.1$ where the rf (relative frequency) exceeded 0.4. As for bubbles $0.1 < s < 0.2$, the rf was almost 0.4.

On the other hand Capstone® FS 30 showed that the bubble size $s > 1$ had the highest rf where it reached > 0.52 , while the other sizes varied between $0 < s < 0.2$.

As for SDS it was different, where it did not show bubbles with sizes < 0.1 . Also the sizes 0.6, 0.7, 0.8 mm were not observed which can be considered as bubbles having a moderate size. On the other hand, it did show bubbles with size s being between $0.1 < x < 0.4$ mm with an rf ranging $0.1 < rf < 0.4$. As for the sizes $0.9 < s < 1$, rf was lower than 0.1. For large bubbles > 1 mm, the rf was slightly > 0.1 .

6.4 Surface tension measurement

Surface tension is a property of liquids arising from an imbalance in molecular cohesive forces at the surface of the liquid. In our case, the surface tension for SDS and Capstone FS 30 each were measured using the pendant drop method as it was described in materials and methods chapter. As for Ammonyx® LO data was provided by the supplier (Stephan®), different concentrations were prepared for each surfactant. For each concentration of each surfactant, the surface tension was measured.

The concentration after which there is no more decrease in the surface tension (becomes stable) is considered as the critical micellar concentration (CMC). The data is presented in table 6.1.

Table 6.1 Surface tension obtained using the pendant drop method for the three surfactants

Surfactant	Critical Micellar Concentration(CMC)	Surface tension (mN/m)
SDS	500 mg.l ⁻¹	24.9
Ammonyx® LO	11 µl.l ⁻¹	32*
Capstone® FS-30	100 µl.l ⁻¹	18

*Data from the manufacturer

At the corresponding CMCs, Ammonyx® LO showed the highest surface tension (24.9 mN/m) followed by SDS then Capstone® FS 30 (18 mN/m).

6.5 Calculation of the thickness of the thin liquid film (case of one bubble)

The capillary number was calculated according to the equation 6.0 which relates viscosity of the surfactant with its velocity while flowing in the pipe and its surface tension. The velocity V_b is 0.02 m/s which is the foam flow velocity for 1D 50% flow regime.

$$Ca = \mu_L V_b / \gamma \quad (6.0)$$

Table 6.2 Capillary number obtained corresponding to each surfactant.

Surfactant solution	Viscosity , μ_L (10^{-3} . Pa.s)	Capillary Number
SDS	0.98	$7.8 \cdot 10^{-4}$
Ammonyx® LO	1.1	$6.8 \cdot 10^{-4}$
Capstone® FS 30	1	$1.2 \cdot 10^{-3}$

From the capillary number obtained in our case we notice that the numbers fall in the range proposed by Bretherton law ($3.10^{-4} < Ca < 2.8.10^{-3}$). In that case the equation (6.1) for measuring the thin liquid film can be used which takes into account the passage of one bubble in a capillary tube having a radius r (in our case average radius of bubbles at the top wall was considered).

$$e = 1.337 r Ca^{2/3} \quad (6.1)$$

The thickness e of the thin film above one bubble (average radius r) was calculated for the three surfactants

Table 6.3 Top film thickness e calculated for each surfactant solution (concentration used for the experiments)

Surfactant solution	Film thickness e (μm)
SDS	2.4
Ammonyx® LO	0.81
Capstone® FS 30	7.9

Although Capstone® FS 30 foam showed the lowest stability where in almost 3 hours it was totally dispersed; however, it showed the highest film thickness taking into account the case of one bubble.

6.6 Detachment of *B. amyloliquefaciens* 98/7 spores

The properties of the surfactants Ammonyx® LO and Capstone® FS 30 were presented in materials and methods chapter. Their efficiency to remove *B. amyloliquefaciens* 98/7 spores was compared to SDS (part 1) after establishment (1m) with a flow regime of 1D 50%. The concentration used for Ammonyx® LO was 0.8 ml.L^{-1} of distilled water, for Capstone® FS-30 it was 0.32 ml.L^{-1} . Concentrations were sufficient to obtain a visible foam flow. Below those concentrations foam collapsed immediately in the establishment pipe. As for SDS, the same concentration was used as in part 1 of results (1.5 g.100 L^{-1}). The concentrations used in our case was above the CMC.

The log 10 kinetics of residual *B. amyloliquefaciens* 98/7 spores upon using Capstone® FS 30 and Ammonyx® LO is compared with SDS in figure 6.3.

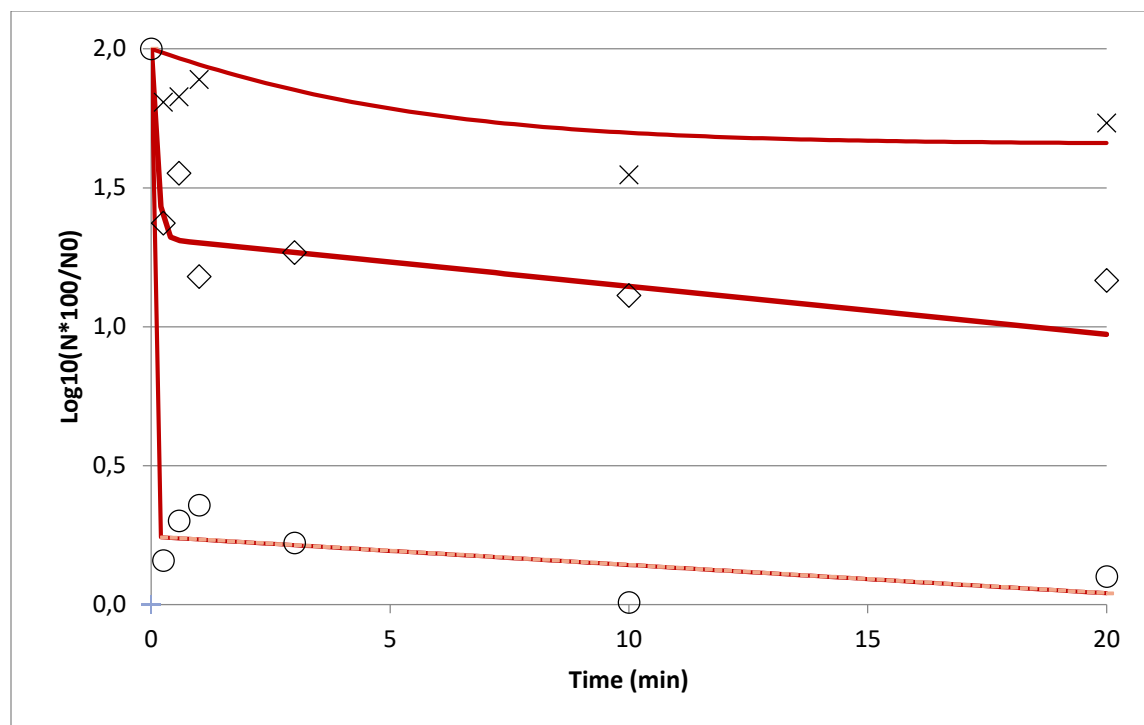


Figure 6.3 Cleaning kinetics of *B. amyloliquefaciens* 98/7 under the effect of different surfactants, ○: SDS, ◇: Ammonyx LO , ×: Capstone® FS 30.

Table 6.4 log 10 reduction of *B. amyloliquefaciens* 98/7 after 20 minutes of cleaning using the different surfactants.

Surfactant	Log10 reduction after 20 minutes of cleaning
Ammonyx® LO	0.83
Capstone® FS-30	0.55
SDS	1.90

It was clear that the detachment after 20 minutes of cleaning was different between the surfactants. SDS showed still the highest detachment compared to the other two surfactants (<1 log10 reduction).

To test if there is a significant difference between the cleaning kinetics (all the log 10 reduction at the different cleaning times) of the three surfactants, student t- test was performed with the conditions: $\alpha=0.05$; unilateral distribution; two tailed test. t critical = 2.02 was obtained from the t-table (percentage points of the t distribution). The results are presented in table 6.5 below,

Comparison	t value obtained	Result
Ammonyx® LO-SDS	15.63	Significant
Capstone® FS 30-SDS	30.83	Significant
Ammonyx® LO-Capstone® FS 30	3.84	Significant

Table 6.5 Student t-test performed on the log 10 reduction results obtained from each surfactant.

For the three comparisons, a significant difference was obtained for the log 10 reductions at all cleaning times between the three surfactants.

Using Ginfat software, the cleaning kinetic parameters for each surfactant were obtained. The results are indicated in table 6.6.

Parameters	Log(10) N_0	$K_1(s^{-1})$	$K_2(s^{-1})$	f (%)	R^2
Ammonyx® LO	5.69	12.61	0.04	79.1	0.41
Capstone® FS-30	5.29	0.25	0	54.5	0.16
SDS	5.54	114.75	0.023	98.2	0.83

Table 6.6 Kinetic parameters obtained for each surfactant

Concerning K_1 , the difference in the values was huge. The ratio of K_1 of SDS to that of Ammonyx® LO and Capstone® FS-30 was 459 and 9 times respectively. Capstone® –FS 30 showed the lowest value for K_1 and the percentage of loosely adherent population F value was also the lowest (54.5%). As for Ammonyx® LO it was 79.1%. Both surfactants had a lower f compared to SDS (98.2%). As for K_2 , it did not show high values, instead all values were < 0.05 indicating a very low detachment of the highly adherent population of *B. amyloliquefaciens* 98/7 spores during the second phase. The decimal reduction at 20 minutes and the kinetic parameters for the three surfactants were statistically analysed by means of a variance analysis (SAS, general linear model and Tukey grouping) to compare between the efficiencies.

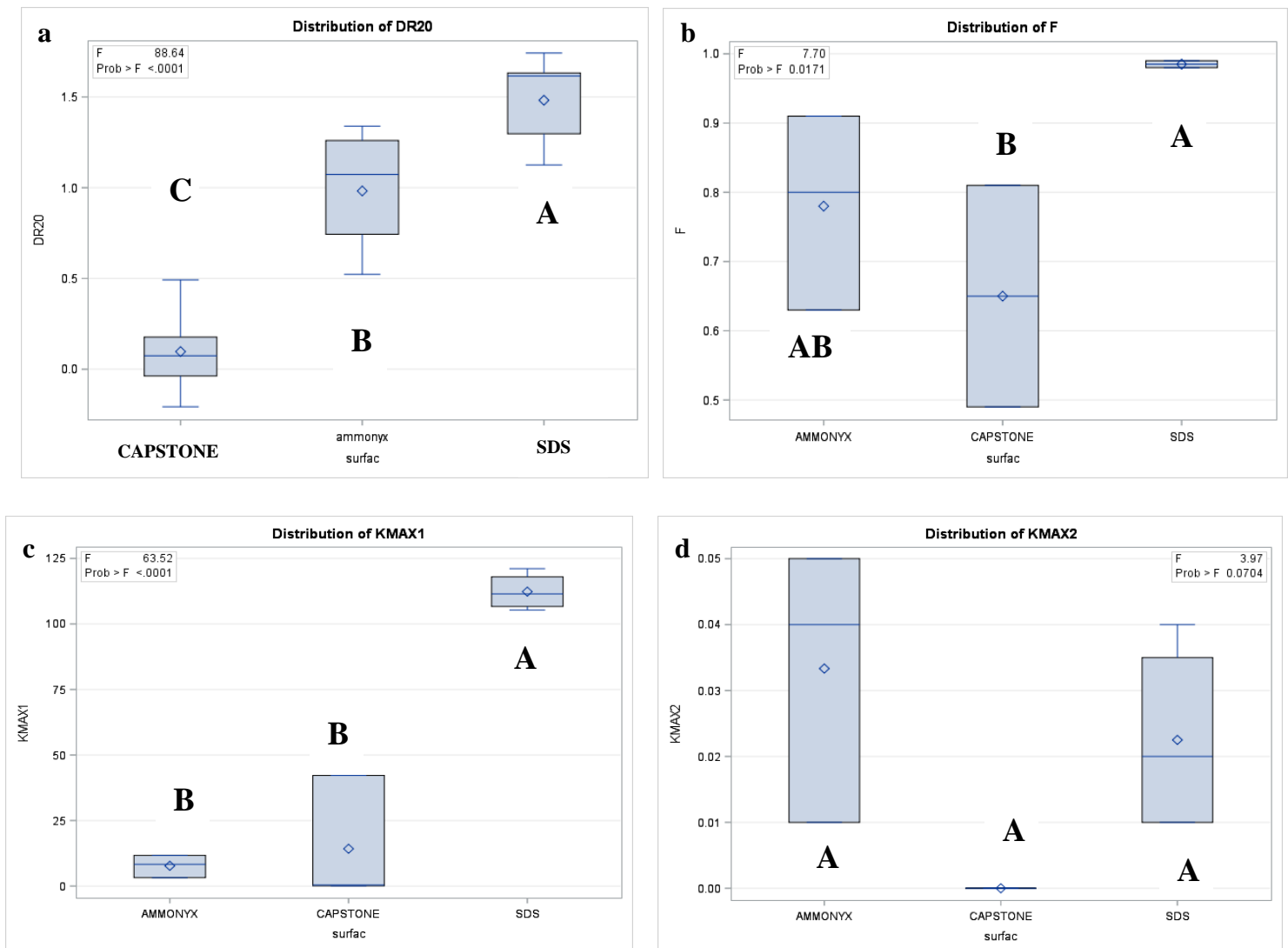


Figure 6.4 (a, b, c, d) : Tukey's test results showing the comparison between the decimal reduction (after 20 minutes of cleaning) and the obtained kinetic parameters between the three surfactants.

For the decimal reduction (log 10 reduction after 20 minutes of cleaning) , Tukey test showed a significant difference (showing 3 cases) between the efficiencies of surfactants in the detachment of *B. amyloliquefaciens* 98/7 spores after 20 minutes of cleaning , where SDS showed the highest decimal reduction . As for the detached fraction F under the rate K1(rate for the detachment of the loosely attached population of spores), Tukey test showed that Capstone® FS 30 and SDS are significantly different, however, Ammonyx® LO was not significantly different from both of them. As for K1 SDS was significantly different from Ammonyx® LO and Capstone® FS 30

which showed no significance between them. K2 showed no significant difference between the three surfactants.

6.7 Discussion and Conclusion

Different foam flow resulting from different surfactants showed that their efficiency differs regarding the detachment of *B. amyloliquefaciens* 98/7 spores. The log 10 reduction of Capstone® FS 30 was $0.5 \log < \text{Ammonyx® LO} (0.8 \log) < \text{SDS} (1.9 \log)$. Not only SDS showed the highest log10 reduction after 20 minutes of cleaning, also concerning the kinetic parameters K1 and F for SDS, they were the highest among the other surfactants.

To understand the reason behind this difference in the detachment efficiency of *B. amyloliquefaciens* 98/7 between the three tested foams from a mechanical point of view, it is important to take into account the synergetic mechanism between the bubbles and the thin liquid film adjacent to the top wall. to understand this relation different points need to be discussed:

It was clear that SDS foam showed the highest stability (more than 24 hrs for total dispersion) compared to the other two surfactants, however, this considers foam structure as a whole entity and its ability to withstand without collapsing for longer times. An advantage for stable foam in our case can be linked to a coherent stable foam flow which have a good contact with the walls. It is important to take into account that one must not relate stability with drainage phenomenon. Foam drainage was described as the phenomena by which liquid flows out of foam (Bikerman 1973). In our case, the phenomenon of drainage can impact the top thin liquid film. For that reason, the capillary number for each surfactant was calculated in order to calculate the thickness e of the top liquid film.

The values of the capillary numbers obtained falls in the range considered by Bretherton law. Based on that, one can assume foam as a one bubble(having an average radius of the bubbles adjacent to the top wall) passing through a capillary tube which has the same diameter as the bubble. The thin liquid film in that case is considered to be over one bubble. The results obtained showed that the largest film thickness adjacent to the top wall was for the Capstone® FS 30 case which was $7.9 \mu\text{m}$ compared to SDS and Ammonyx® LO which were 2.4 and $0.81 \mu\text{m}$ respectively. Considering one bubble in a capillary tube showed that less drainage can be in the case of Capstone FS 30 hence a thicker top film. To investigate this fact , images of bubbles were obtained at the top wall which showed a contrary situation. Bubbles in the case of Capstone FS 30 where large and polygonal in shape which suggests that foam in contact with the top wall is more

dry compared to SDS and Ammonyx LO which showed a circular bubble shape. The images at the top wall ensure that drainage was faster as in the case of Capstone FS 30. Even though we considered in our case the assumption of one bubble passing in a capillary tube, however, one must take into account that foam is a coordination of bubbles that undergoes different phenomenon such as bursting, coalescence, coarsening, dynamic interactions with the neighboring bubbles that can impact the top thin liquid film differently.

To calculate the capillary number for each surfactant, surface tension was calculated first. Capstone® FS 30 which had the lowest detachment of *B. amyloliquefaciens* 98/7 spores after 20 minutes of cleaning showed the highest capillary number (highest adhesion force to the top wall) while SDS showed the inverse case. One can predict that the cases must be inversed, Capstone® FS 30 must show the lowest capillary number when linking it with detachment of spores (efficiency). The reason can be explained by the fact that the phenomenon of drainage was so high in Capstone® FS 30 compared to SDS and Ammonyx® LO. This will lead to the accumulation of the surfactant molecules more quickly at the bottom in case of Capstone® FS 30 thus less liquid adjacent to the top wall resulting in a lower capillary force at the top while remaining high at the bottom. One must not forget that the capillary force calculated in this study takes into account the surfactant as a whole without interference of other phenomena and considering the surfactant as being homogenous.

The next step was to go deeper in the study, where bubbles shape, pattern and size were investigated. It seems to be that not only stability (drainage) of foam adjacent to the top wall of the pipe affects the detachment of *B. amyloliquefaciens* 98/7 spores, however, the shape of bubbles can play an important role. Large polyhedral bubbles as in the case of Capstone® FS 30 can have lower fluctuation rate of the local wall shear stress at the top wall (lower frequency), however, the amplitude (magnitude of the local wall shear stress) can be higher compared to small bubbles which have a higher fluctuation rate of the local wall shear stress (higher frequency). The balance between fluctuation rate of the local wall shear stress and its magnitude can be a result of different pattern of foam bubbles at the top wall having different sizes and shapes. Aside from stability and capillary forces, this pattern can constitute an important impact translated by the efficiency of foam to detach microorganisms. Not only the pattern, as already mentioned, to understand more about bubbles at the top wall, a quantitative study can be performed for the sizes of bubbles as a function

of their relative frequency as in our case. All of the above parameters can establish a unique foam structure as a result of different surfactant properties and physical parameters, leading to a distinctive detachment efficiency for each foam.

6.8 References

- Basařová, Pavlína, et Mária Zedníková. 2019. « Effect of Surfactants on Bubble-Particle Interactions ». *Surfactants and Detergents*, mars. <https://doi.org/10.5772/intechopen.85436>.
- Bikerman, J. J. 1973. « Formation and Structure ». In *Foams*, édité par J. J. Bikerman, 33-64. Foams. Berlin, Heidelberg: Springer Berlin Heidelberg. https://doi.org/10.1007/978-3-642-86734-7_2.
- Tisné, P, F Aloui, et L Doubriez. 2003. « Analysis of Wall Shear Stress in Wet Foam Flows Using the Electrochemical Method ». *International Journal of Multiphase Flow* 29 (5): 841-54. [https://doi.org/10.1016/S0301-9322\(03\)00038-7](https://doi.org/10.1016/S0301-9322(03)00038-7).

Chapter V, Part 4

Detachment *P. fluorescens pfl* Biofilm using Foam Flow

7.0 Abstract

Biofilms formation is considered to be one of the main concerns of agro-food industries. Even after tough cleaning procedures from surfaces of machineries, biofilms may stay resistant to detachment. Many reasons can be involved that prevent the removal of biofilms such as type of the biofilm and its properties, non-hygienic designs either open systems or closed systems as processing lines.

In this part, we studied the detachment of *P. fluorescens pfl* biofilms grown during 24 hrs. under static conditions on stainless steel surfaces and cleaned using foam flow. The foam flow velocity (4 cm.s^{-1}) showed the highest log 10 reduction (~2 logs) after 20 minutes of cleaning, stainless steel coupons being soiled by *pfl* biofilms grown in vertical position (no sedimentation) compared to 2 and 6 cm.s^{-1} . Comparing to the detachment of *Bacillus* spores, it sounds that the capillary forces exerted a significant influence in the detachment phenomenon. Conversely, for horizontally grown *pfl* biofilms, no difference in the log10 detachment after 20 minutes of cleaning with the different foam flow velocities (1 log) probably in line with the thicker biofilm structure observed due to the sedimentation phenomenon.

7.1 Introduction

In agro-food industrial environments, such as breweries, dairies, poultry or meat processing factories, as well as fresh-cut industries, surfaces have been reported to be contaminated by a range of microorganisms, including pathogenic and spoilage bacteria (Srey et al., 2013). Once introduced, many bacteria are able to persist on the contaminated surfaces or even to grow if environmental conditions are suitable. These adherent microorganisms may in turn cross-contaminate food products in contact (Reij et al., 2004). Hence, 80% of all microbial diseases, including foodborne illnesses, would be caused by microorganisms in biofilms (National Institutes of Health, USA, 1997), and foodborne illness would cost up to \$144 billion a year (Scharff, 2012). Some of the threats associated with the presence of bacteria in the food environment include: accumulation of biofilm on food surfaces, microbial colonization in milk storage tanks, fouling of heat exchangers (Kirtley & McGuire, 1989); in addition, biofilms are formed in food processing lines having a negative impact on food quality and food safety and subsequent economic losses (Kusumaningrum et al., 2003).

Biofilm structure is complex. Biofilms are surface-attached, structured microbial communities containing sessile cells (bacteria and/or fungi) embedded in a self-produced extracellular matrix composed of polysaccharides, DNA, and other components (Maloy & Hughes, 2013). Pathogenic bacteria could either adhere to surfaces directly and form biofilms, or attach themselves to an existing biofilm, which facilitates adherence (Gibbs et al., 2004) and potential development (Marouani-Gadri et al., 2010). Bacterial adhesion is governed by physicochemical interactions, e.g. Van der Waals, Lewis acid/base or electrostatic. Therefore, for a cleaning procedure to be effective, the physicochemical interactions must be overcome by the mechanical action of the flowing fluid, in particular due to the mean wall shear stress and its fluctuations (Blel et al., 2013; Faille et al., 2013). When the biofilm forms in pipelines, the traditional methods would not be available to eliminate it completely (O'Toole & Kolter, 1998), for instance in standard Cleaning in Place, cells will remain trapped in the biofilm structure even after cleaning (Liu et al., 2014). Flowing foam as already described in the previous chapters with its shearing properties, showed an efficient detachment when compared to with standard Cleaning in Place conditions. Results obtained by flowing foam on *B. amyloliquefaciens* 98/7 spores can be a start for trying foam flows on biofilms.

In this part, we used *Pseudomonas fluorescens pfl* strain for the formation of biofilms on 316L stainless steel coupons. This *Pseudomonas* strain, isolated by ANSES from waste cleaning water, was selected as a model of spoilage bacteria for fresh food industry due to its ability to grow and form biofilms (Cunault et al., 2015). As for foam flow, velocities used were 2, 4, and 6 cm.s⁻¹ while fixing the foam quality at 50% which gave quite good results on the removal of *B. amyloliquefaciens*. The purpose of this part is to understand the efficiencies of different foam flow conditions (velocity) in the detachment of *pfl* biofilms from the interior walls of pipes.

7.2 Bubbles size and capillary numbers for foam flow regimes

Three foam flow velocities (2, 4, 6 cm.s⁻¹) were tested on *pfl* biofilms that correspond to the three flow regimes 1D, 2D and 3D (as in part 1). Foam quality β was 50%.

The capillary numbers were calculated according to the equation stated in part 1, which relates viscosity μ_L of the surfactant with its velocity V_b while flowing in the pipe and its surface tension γ . The viscosity of the SDS solution (0.15%ww) was 0.98.10⁻³ Pa.s. SDS surface tension was 24.9 mN.m⁻¹ as measured in part 4.

$$Ca = \mu_L V_b / \gamma \quad (7.0)$$

Table 7.0 Capillary number obtained corresponding to each foam flow.

Velocity (cm.s ⁻¹)	Capillary Number
2	$7.8.10^{-4}$
4	$1.5.10^{-3}$
6	$2.3.10^{-3}$

From the capillary numbers obtained in our case, we noticed that the numbers fall in the range proposed by Bretherton law ($3.10^{-4} < Ca < 2.8.10^{-3}$).

In that case, equation (7.1) for measuring the thin liquid film can be used which takes into account the passage of one bubble in a capillary tube having a radius r (average radius of bubbles at the top wall was considered).

$$e = 1.337 r Ca^{2/3} \quad (7.1)$$

The thickness e of the thin film above one bubble (average radius r) was calculated for the three flow regimes. Results are presented in table 7.1.

Table 7.1 Film thickness e obtained for each flow regime

Velocity (cm.s ⁻¹)	Bubbles average radius r (μm)	Film thickness e (μm)
2	212.4	2.40
4	187.2	3.28
6	94.8	2.20

Based on the obtained results, it is clear that different average bubbles radius can be realized upon increasing the velocity of the foam flow while keeping the same foam quality 50%, where the largest bubbles radius was obtained when the velocity was 2 cm.s⁻¹ (Results obtained from part1). As for film thickness e , it was slightly higher when the flow velocity was 4 cm.s⁻¹, compared to the foam flow velocities 2 and 6 cm.s⁻¹, showed almost the same top film thickness (2 μm).

7.3 *P. fluorescens pf1* biofilm detachment by the different foam flow regimes.

In materials and methods chapter, we discussed the method conducted for *P. fluorescens pf1* biofilm formation on 316L stainless steel coupons. Fouling was performed while the coupons are in a vertical or a horizontal position. The reason is that biofilms can grow on various parts of the machineries including vertical and horizontal surfaces. The horizontal fouling can lead to sedimentation. The increase in N_0 on the coupons placed in the horizontal position during fouling can be a result of sedimentation of cells on the coupons surface leading to more attachment of cells and more growth during the incubation period. Coupons in horizontal positions have higher initial number of cells N_0 (by almost 0.6 log) compared to the biofilms formed during vertical fouling. The detachment kinetics results of the 24 hrs. *P. fluorescens pf1* biofilm (vertical and horizontal fouling cases) are presented in figures 7.0 and 7.1 respectively. It is important to mention that the values of the decimal reduction (log 10 reduction) and the kinetic parameters presented in the previous tables present average values of the experimental series.

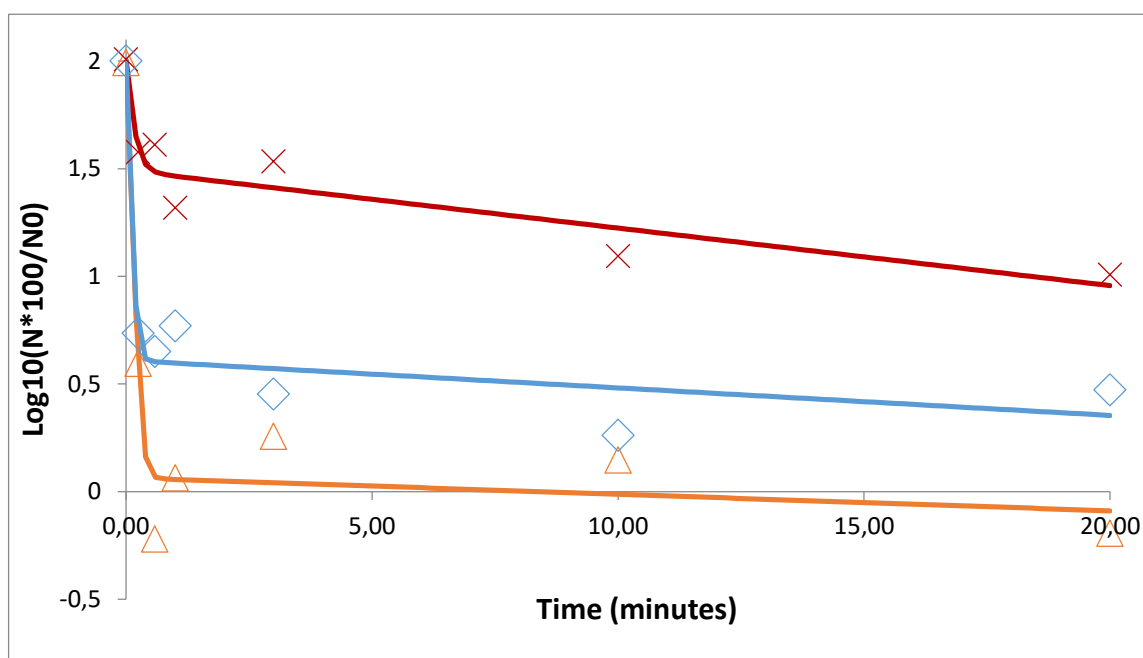


Figure 7.0 Cleaning kinetics of 24 hrs. *P. fluorescens pf1* biofilm (vertical fouling) obtained after cleaning with the foam flow regimes, x: 2cm.s⁻¹ (1D50%) , Δ: 4cm.s⁻¹ (2D50%) , ◇: 6 cm.s⁻¹ (3D50%)

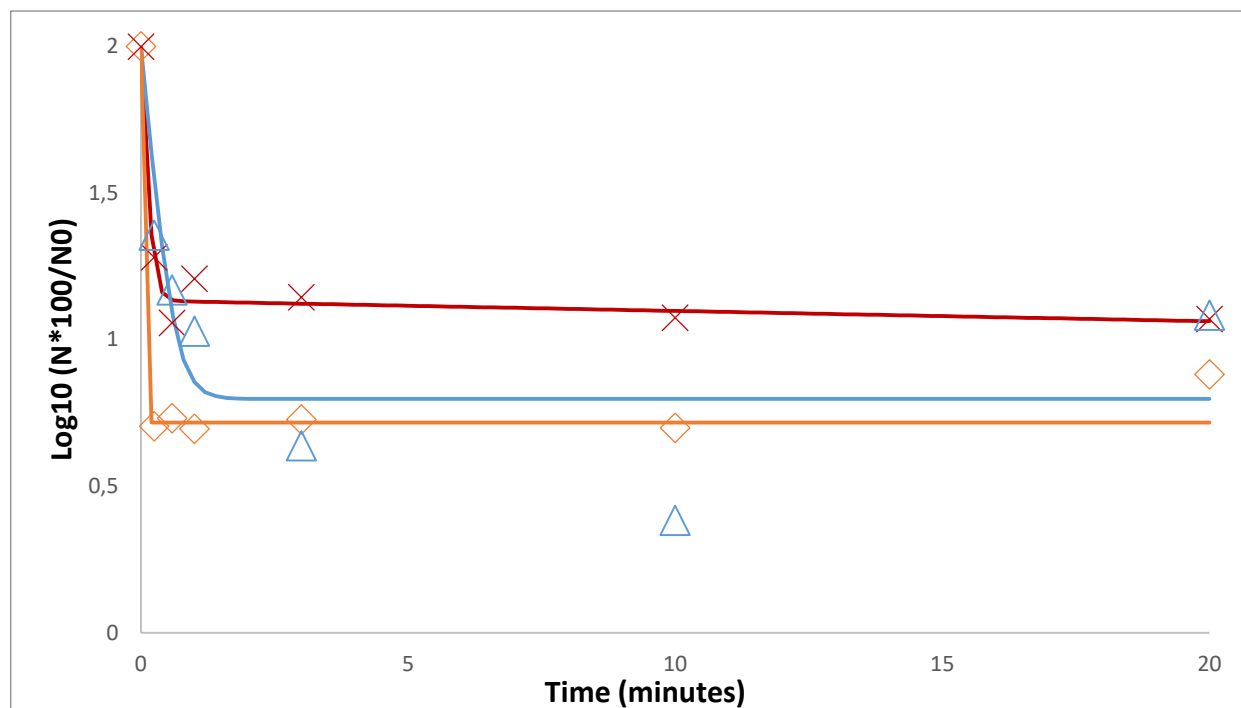


Figure 7.1 Cleaning kinetics of 24hrs. *P. fluorescens pf1* biofilm (horizontal fouling) obtained after cleaning with the foam flow regimes x: 2cm.s⁻¹ (1D 50%), Δ: 4cm.s⁻¹(2D 50%), ◇: 6 cm.s⁻¹(3D 50%).

Results showed that in the case of vertically formed biofilms, the foam flow velocity 2cm.s⁻¹ (1D50%) did not show the highest log10 reduction after 20 minutes of cleaning as in the case of detachment of *B. amyloliquefaciens* 98/7 spores (results part1).

The velocity 2cm.s⁻¹(1D50%) showed about 1 log10 reduction after 20 minutes of cleaning, while for 4 cm.s⁻¹(2D50%) and 6 cm.s⁻¹ (3D50%) flow regimes, the log 10 reduction values after 20 minutes of cleaning was about 2.1 and 1.5 logs respectively.

As for horizontal fouling, the three foam flow velocities showed almost the same log10 reduction (about 1 log) after 20 minutes of cleaning. Detachment results of *P. fluorescens pf1* biofilm after 20 minutes of cleaning for the vertical and horizontal fouling cases is presented in table 7.2.

Foam cleaning was compared with standard Cleaning in Place like conditions. Results have shown that the velocities 2 and 6 cm.s⁻¹ (Vertical fouling) showed lower log 10 reduction (1 and 1.5 respectively) after 20 minutes of cleaning compared to standard CIP like conditions (~2.3 log 10

reduction). The velocity 4 cm.s^{-1} (2D 50%) of the foam flow showed a log 10 reduction around ~ 2 , thus presenting a closer result to cleaning with standard CIP like condition.

We performed standard CIP like conditions (SDS, 0.15% ww, 650l/h, 120 cm.s^{-1}) for cleaning of 24 hrs. *P. fluorescens pf1* biofilm obtained by vertical fouling under same conditions as the one cleaned by foam. The average shear stress in CIP like conditions was about 5.1 Pa, whereas for foam flow (4 cm.s^{-1}) it was 4.1 Pa.

Kinetic curves for both Cleaning in Place like conditions and the foam flow cleaning 4 cm.s^{-1} (2D 50%) are presented in figure 7.2 below.

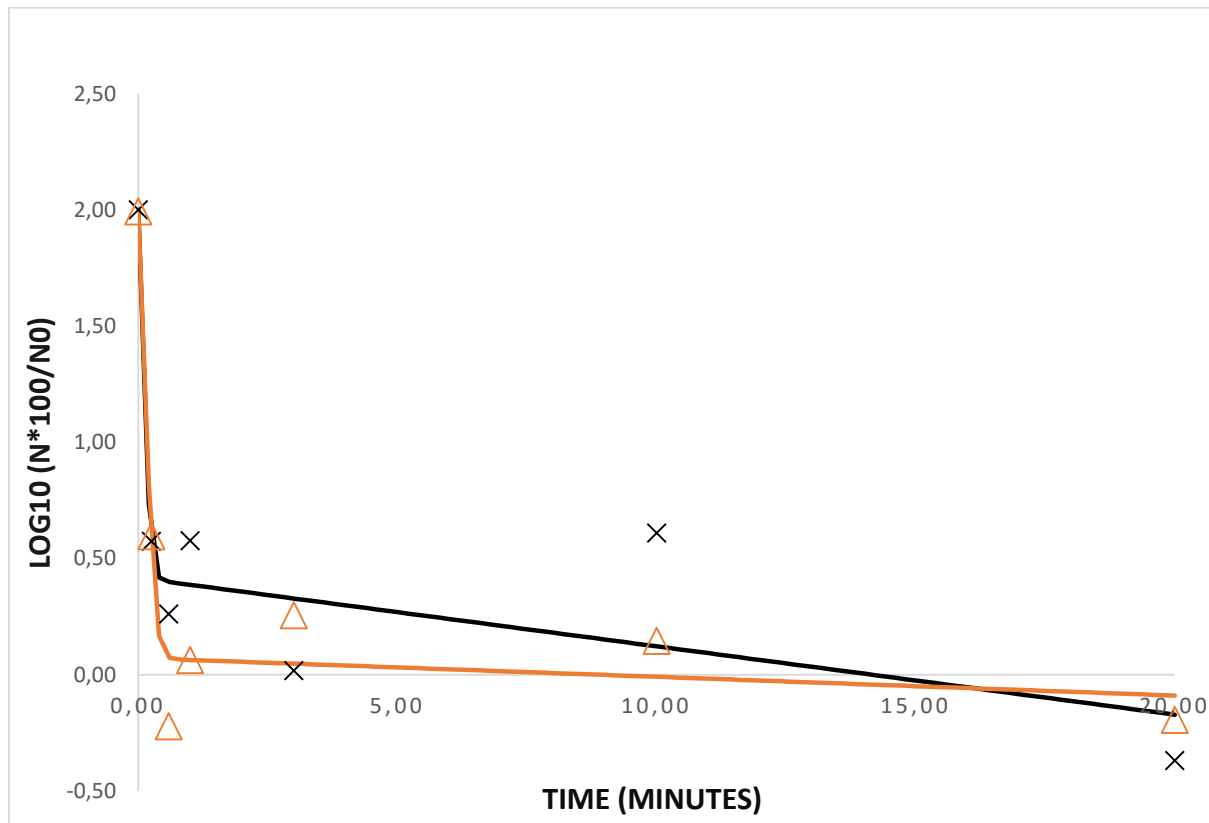


Figure 7.2 Cleaning kinetics of *P. fluorescens pf1* 24 hrs. biofilm (vertical fouling) after : ×: CIP(650l/h, 120 cm.s^{-1}) , Δ: 2D50% (4 cm.s^{-1}).

Table 7.2 log 10 reduction \pm SD of *P. fluorescens* *pf1* after 20 minutes of cleaning for the two cases vertical and horizontal.

Velocity -Flow regimes	Log 10 \pm SD (vertical)	Log 10 \pm SD (horizontal)
2 cm.s ⁻¹ (1D)	1.00 \pm 0.50	0.93 \pm 0.67
4 cm.s ⁻¹ (2D)	2.18 \pm 0.48	1.03 \pm 0.60
6 cm.s ⁻¹ (3D)	1.53 \pm 0.36	1.12 \pm 0.25
120 cm.s ⁻¹ (CIP)	2.37 \pm 0.82	-----

Table 7.3 Cleaning kinetics parameters obtained after cleaning with the different foam flow regimes and Cleaning in Place like conditions.

Fouling type	Cases	Log(10) N ₀	K ₁ (s ⁻¹)	K ₂ (s ⁻¹)	F (%)	R ²
(Foam)Vertical	2 cm.s ⁻¹ (1D)	6.44	7.46	0.06	69.01	0.32
	4 cm.s ⁻¹ (2D)	6.83	14.51	0.02	98.8	0.65
	6 cm.s ⁻¹ (3D)	6.83	17.48	0.03	95.7	0.44
(Foam)Horizontal	2 cm.s ⁻¹ (1D)	7.59	11.22	0.01	86.4	0.17
	4 cm.s ⁻¹ (2D)	7.37	4.66	0	93.7	0.46
	6 cm.s ⁻¹ (3D)	7.05	106.9	0	94.7	0.66
(CIP) Vertical	Monophasic flow	7.03	17.66	0.07	97.3	0.50

Cleaning kinetics parameters values obtained using Ginfat software for the all the tested experimental conditions are presented in table 7.3 above.

As for K₁ (rate of detachment for the loosely attached population) for vertically formed biofilms, it can be realized that there was an increase for the rate while increasing the velocity (when shifting from 2cm.s⁻¹ (1D) to 4cm.s⁻¹ (2D) and 6cm.s⁻¹ (3D)). K₁ for the 4 cm.s⁻¹(2D) flow regime is almost double that of 2 cm.s⁻¹ (1D) foam flow (7.46 s⁻¹), however, when shifting from 4cm.s⁻¹ to 6cm.s⁻¹, the increase was slight, where it was almost by 3 units. On the contrary for K₂ (rate of detachment for the strongly attached population), values for the three regimes were between 0 and 0.1 s⁻¹ showing very low removal compared to K₁. The value of F (percentage removal of the loosely attached population under K₁) for the 2cm.s⁻¹ flow was the lowest(69%) whereas for 4

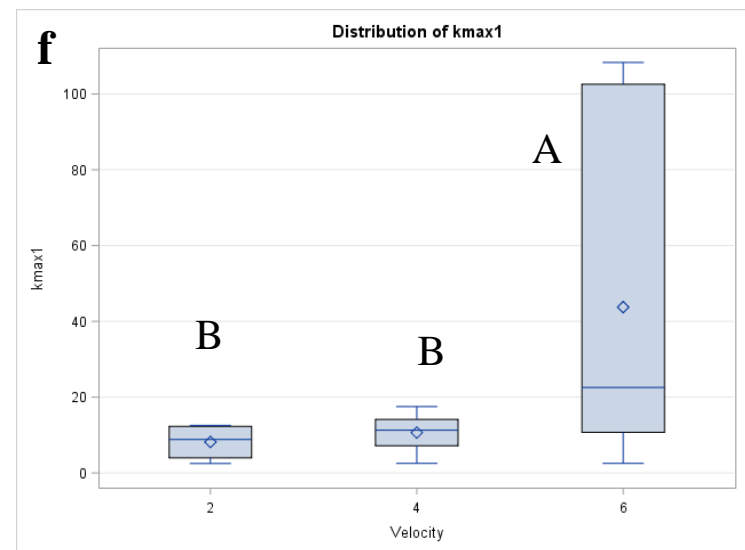
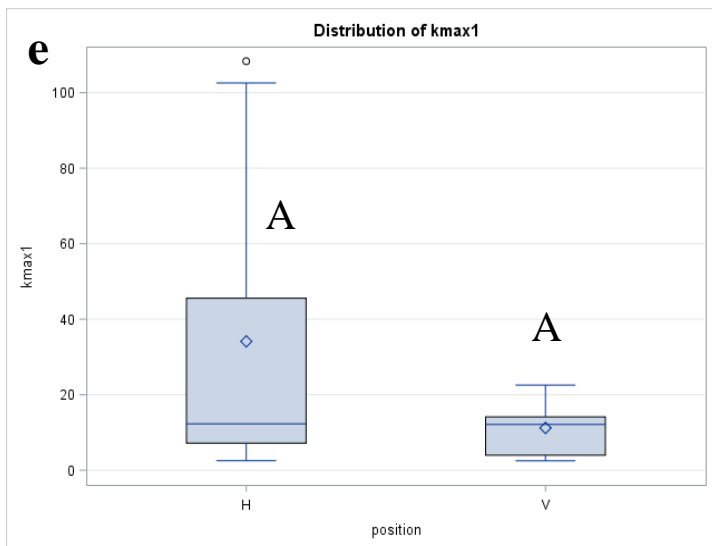
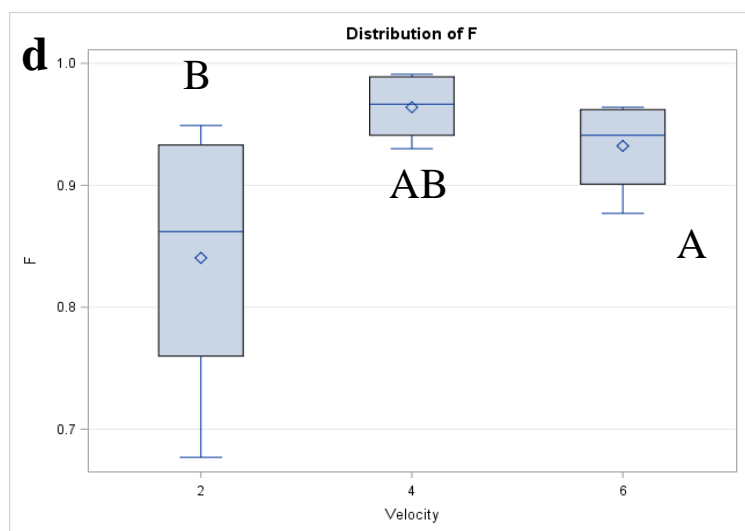
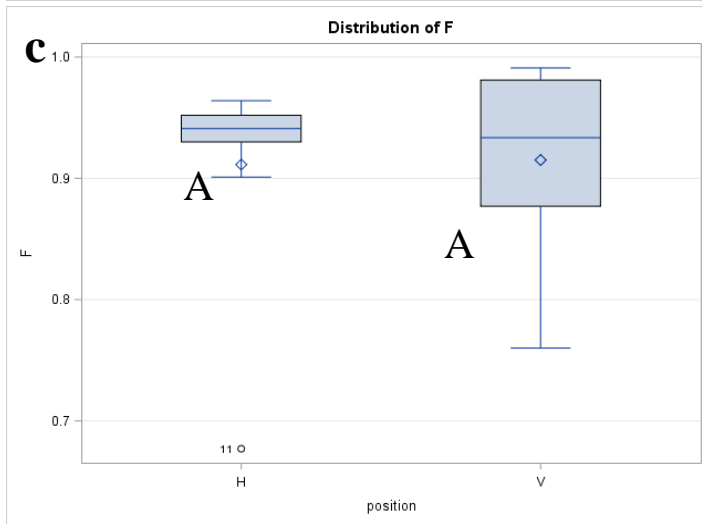
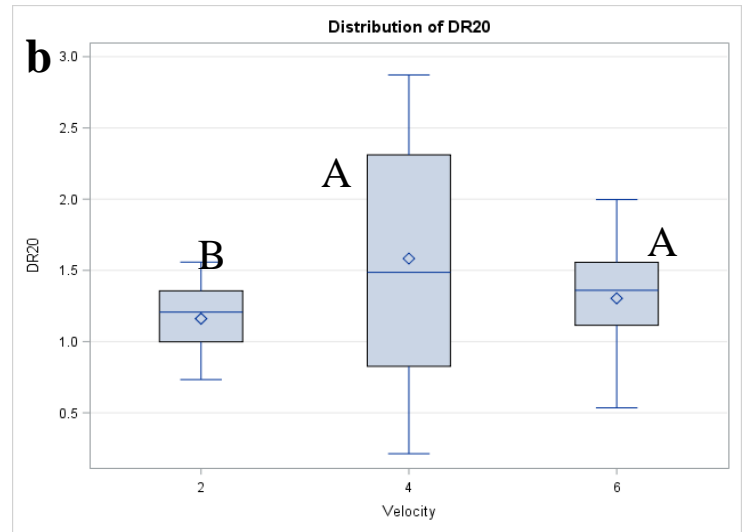
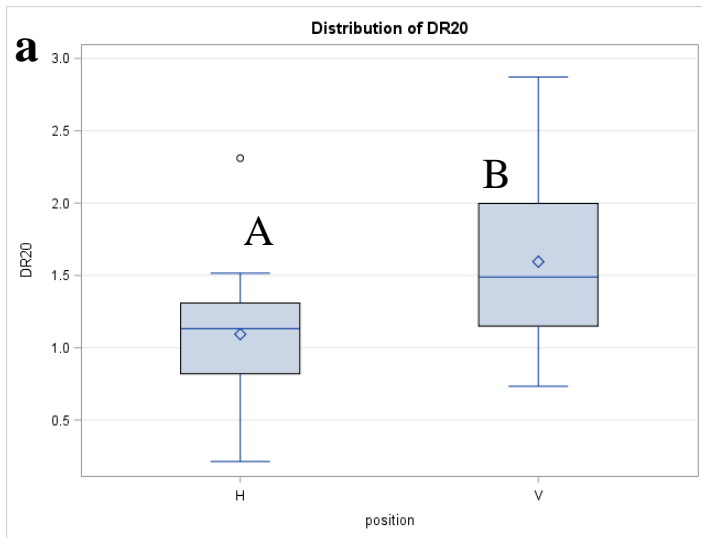
cm.s^{-1} (2D50%) and 6 cm.s^{-1} (3D50%) the values of F were close being higher than 95% indicating almost the same percentage of the detached population of *P. fluorescens pf1* cells.

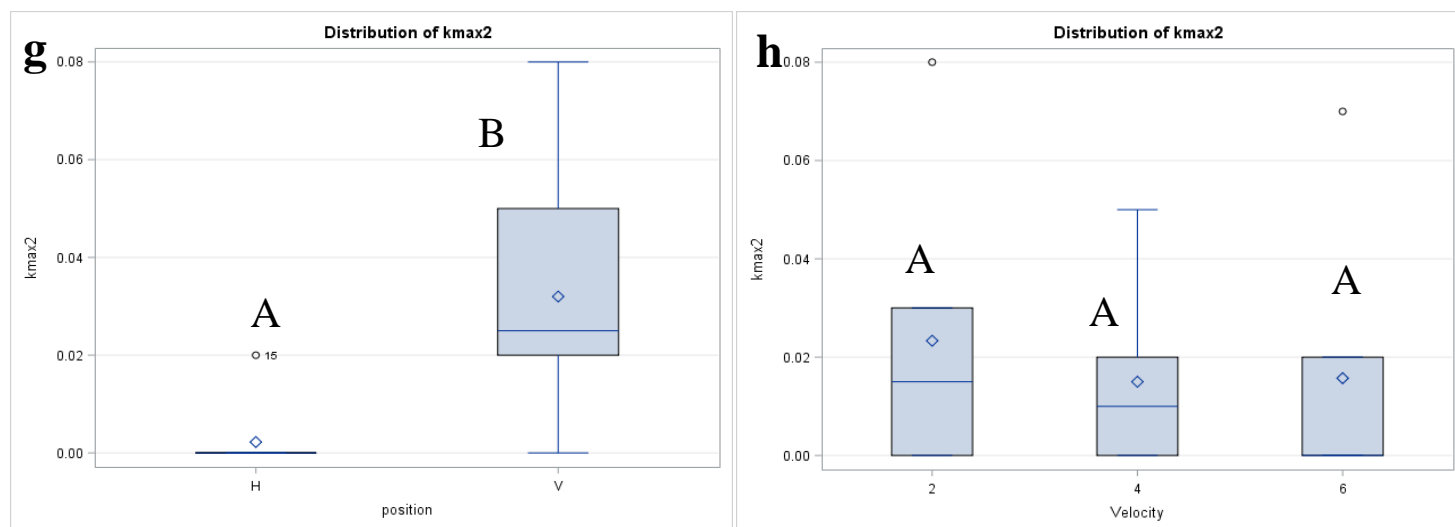
For horizontally formed *pf1* biofilms, K1 for the 2 cm.s^{-1} foam flow (1D50%) was almost double that of 2D (4.6 s^{-1}). As for 3D, K1 was much higher showing an increase of almost 23 times (106 s^{-1}) compared to K1 value for the 2D flow regime (4.6 s^{-1}). This can be explained by shearing forces exerted by the 6 cm.s^{-1} foam flow on the *pf1* biofilm that include higher number of loosely attached *pf1* cells that shows a rapid detachment response probably leading to a quite similar efficiency than 4 cm.s^{-1} .

As for the highly adherent population of cells in cleaning of horizontally formed biofilms, K2 showed a zero value for the 2 cm.s^{-1} (2D50%) and 4 cm.s^{-1} (3D50%) flow regimes, however, for 1D it was slightly higher (0.01 s^{-1}) indicating a very weak impact of foam on the strongly attached population. The value of F for the 2 cm.s^{-1} foam flow (1D50%) was 86.4 % compared to F values for 4 cm.s^{-1} (2D) and 6 cm.s^{-1} (3D) foam flow regimes which fall in a range between 90 and 95% in line with a better efficiency of the foam flow.

7.4 Statistical analysis (Tukey's grouping, SAS analysis)

The comparison between the decimal reductions after 20 minutes of cleaning for horizontally and vertically formed biofilms was studied statistically. Also the decimal reduction (after 20 minutes) was compared between the three velocities ($2, 4, 6 \text{ cm.s}^{-1}$) regardless of the fouling position. The kinetic parameters K1, K2 and F were also compared taking into account the fouling position and foam flow velocity. The influence of the foam velocity on the different kinetics parameters and on the cleaning efficiency at 20 min were analysed statistically through a variance analysis (SAS, general linear model and Tukey grouping). In the SAS analysis, kinetic parameters values for each experiment performed were taken into account in the comparison between the considered conditions.





Figures 7.3 (a, b, c, d, e, f, g, h) Tukey's grouping for the decimal reduction and kinetic parameters taking into account the fouling the position and the velocity (regardless of the fouling position)

The decimal reduction at 20 min (DR20) was significantly different when comparing detachment of *pf1* biofilm between horizontal with vertical fouling positions, however, the influence of the foam flow velocities, showed a significant differences between the velocities 2 and 4 cm.s⁻¹, but the latter one was not significantly different from 6 cm.s⁻¹ (7.3a, 7.3b). It is clear from the obtained results that the fouling position matters when detachment of cells is concerned; On the other hand, regardless of the fouling position, 2 and 4 cm.s⁻¹ were not significantly different, however, they were significantly different from the foam flow velocity 2 cm.s⁻¹.

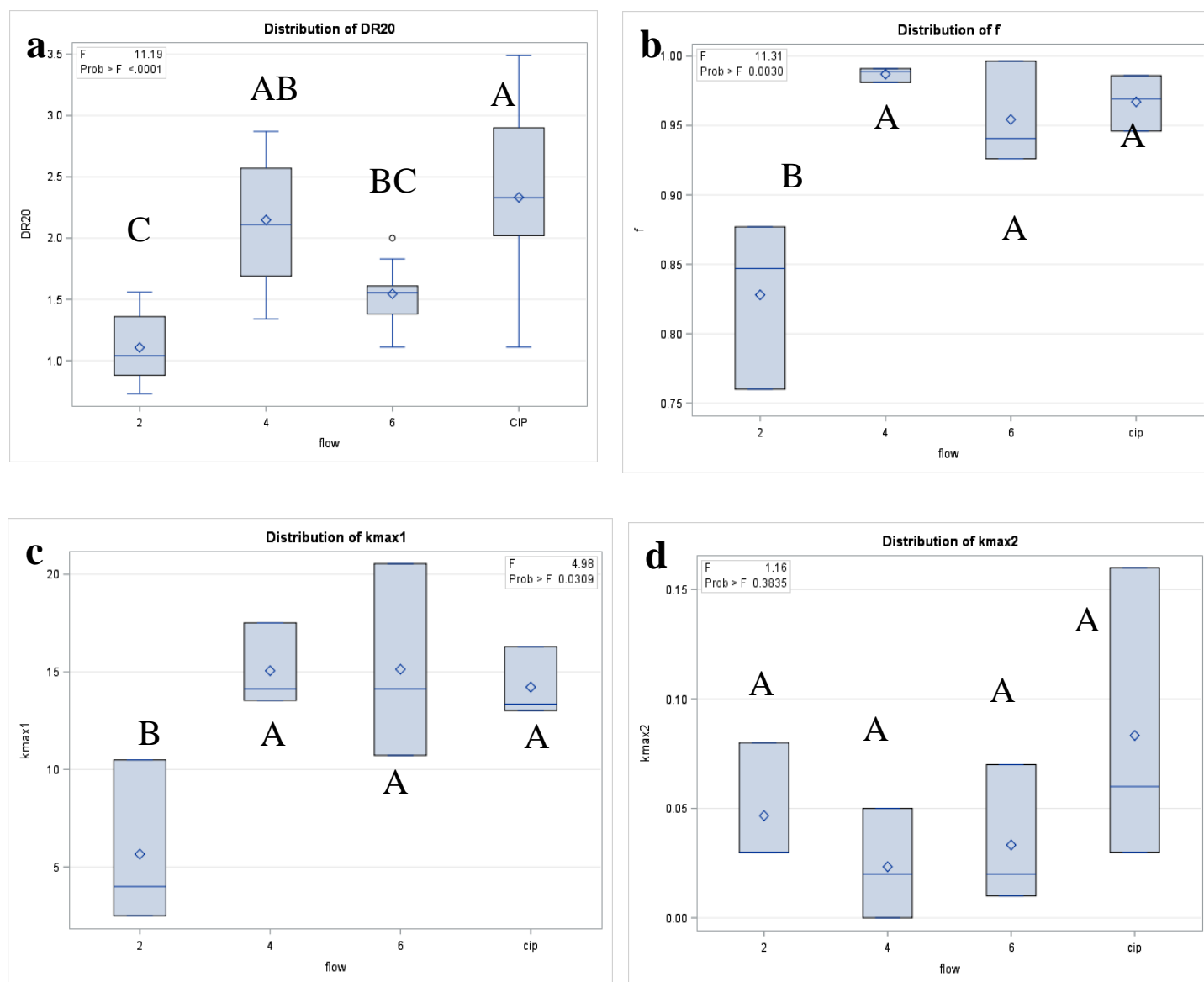
For K1, no significant difference was obtained, between the fouling position, however, when comparing K1 as a function of velocities, 6 cm.s⁻¹ was significantly different from 2 and 4 cm.s⁻¹ which showed no significant difference between them. F did not show a significant difference when comparing positions, however, when comparing velocities, 2 cm.s⁻¹ was significantly different from 6 cm.s⁻¹, while the latter two cases were not significantly different from 4 cm.s⁻¹. Contrary to K1, tukey grouping between the horizontally and vertically fouled biofilms showed significant difference concerning K2, however, for the impact of velocity on K2 values, no significant difference was observed between the cases.

The previous statistical analysis was dedicated to the decimal reduction and the cleaning kinetic parameters only for foam cleaning. The following statistical analysis was performed (SAS, general

linear model and Tukey grouping) to compare between Cleaning in Place like conditions (CIP) and foam flow cleaning, biofilms being grown on vertical surfaces.

As for the Decimal reduction after 20 minutes of cleaning, it can be realized that the detachment under CIP like conditions (120 cm.s^{-1} , 650 l/h) and the 4 cm.s^{-1} foam flow was not significantly different, however, they were significantly different from the velocities 2 and 6 cm.s^{-1} which showed an insignificant difference between them. This result categorizes our flows into two groups, flows with high decimal reduction (CIP and 4 cm.s^{-1} ; more than 2.0 logs) compared to low decimal reduction flows (2 and 6 cm.s^{-1} ; less than 2 logs).

As for F (percentage detached population under rate K1), 4 and 6 cm.s^{-1} foam flows and CIP like condition (120 cm.s^{-1} , 650 l.h^{-1}) did not show a significant difference between them, however, the latter three cases were significantly different from 2 cm.s^{-1} foam flow. Concerning K1, 4 and 6 cm.s^{-1} flow velocities (2D and 3D flow regimes) were significantly different from 2 cm.s^{-1} , however, the three foam velocities were not significantly different when compared with CIP like conditions. As for K2, no significant difference between the four compared cases. When compared to CIP like conditions, 4 cm.s^{-1} flow velocity did not show a significant difference between the four indicated parameters (DR20, F, K1, K2), indicating a high resemblance between the flows concerning their impact on the detachment of pf1 biofilm.

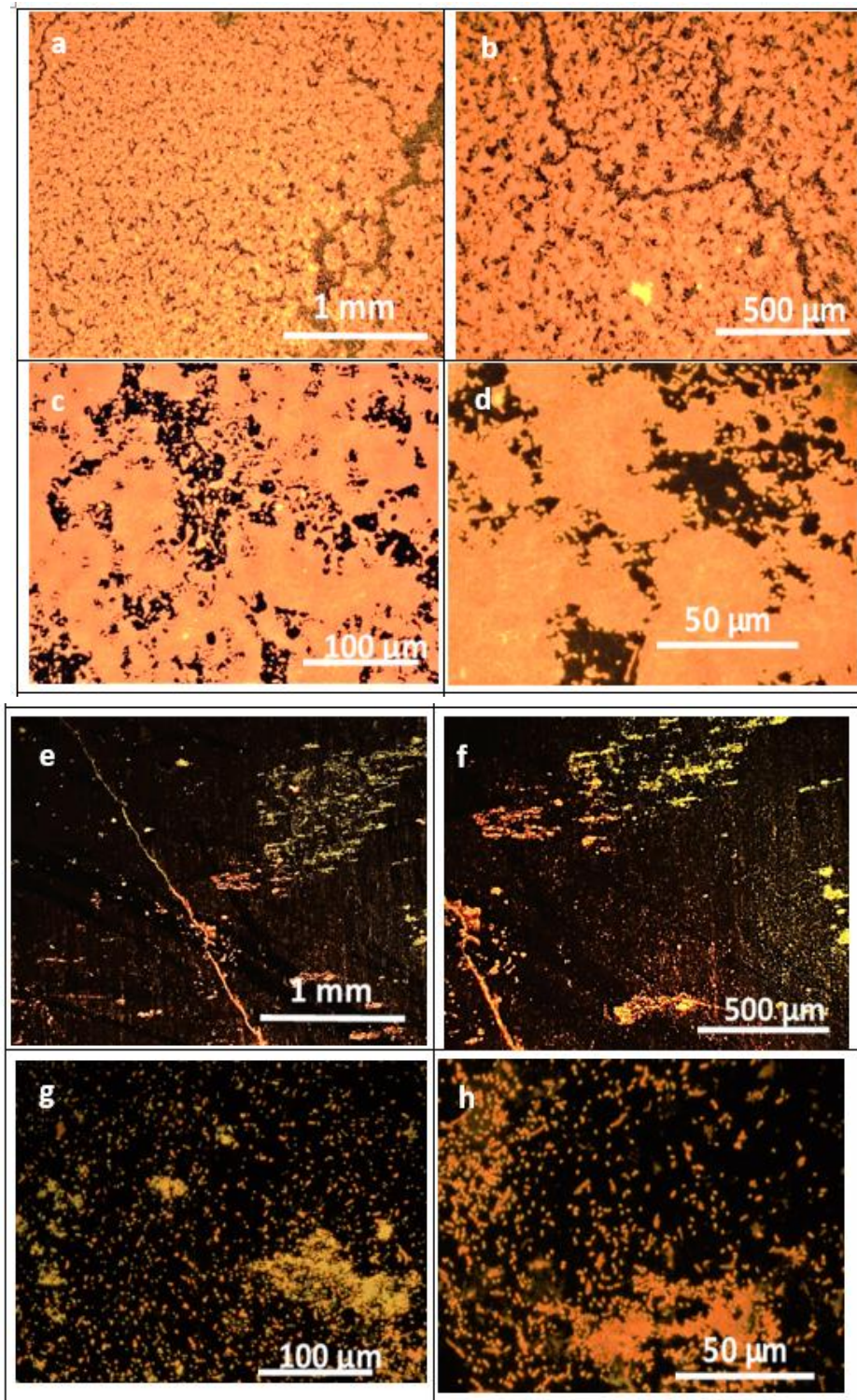


Figures 7.4 (a, b, c, d) Tukey's grouping for the decimal reduction (DR20) and kinetic parameters taking into account the velocities of foam flow and surfactant solution flow in CIP.

7.5 Fluorescence Microscopy

Fluorescence microscopy after dyeing with orange acridine dye as described in materials and methods was performed on coupons after fouling directly (time 0 for both biofilm grown positions); after cleaning with foam (only case of 6 cm.s⁻¹, vertical grown biofilm is presented) and cleaning with standard CIP like conditions (vertically grown biofilms). After cleaning, the

times observed with fluorescence microscopy were : 35 seconds, 3 and 20 minutes. Figures 7.5 and 7.6 present the obtained microscopic images at the different mentioned magnifications.



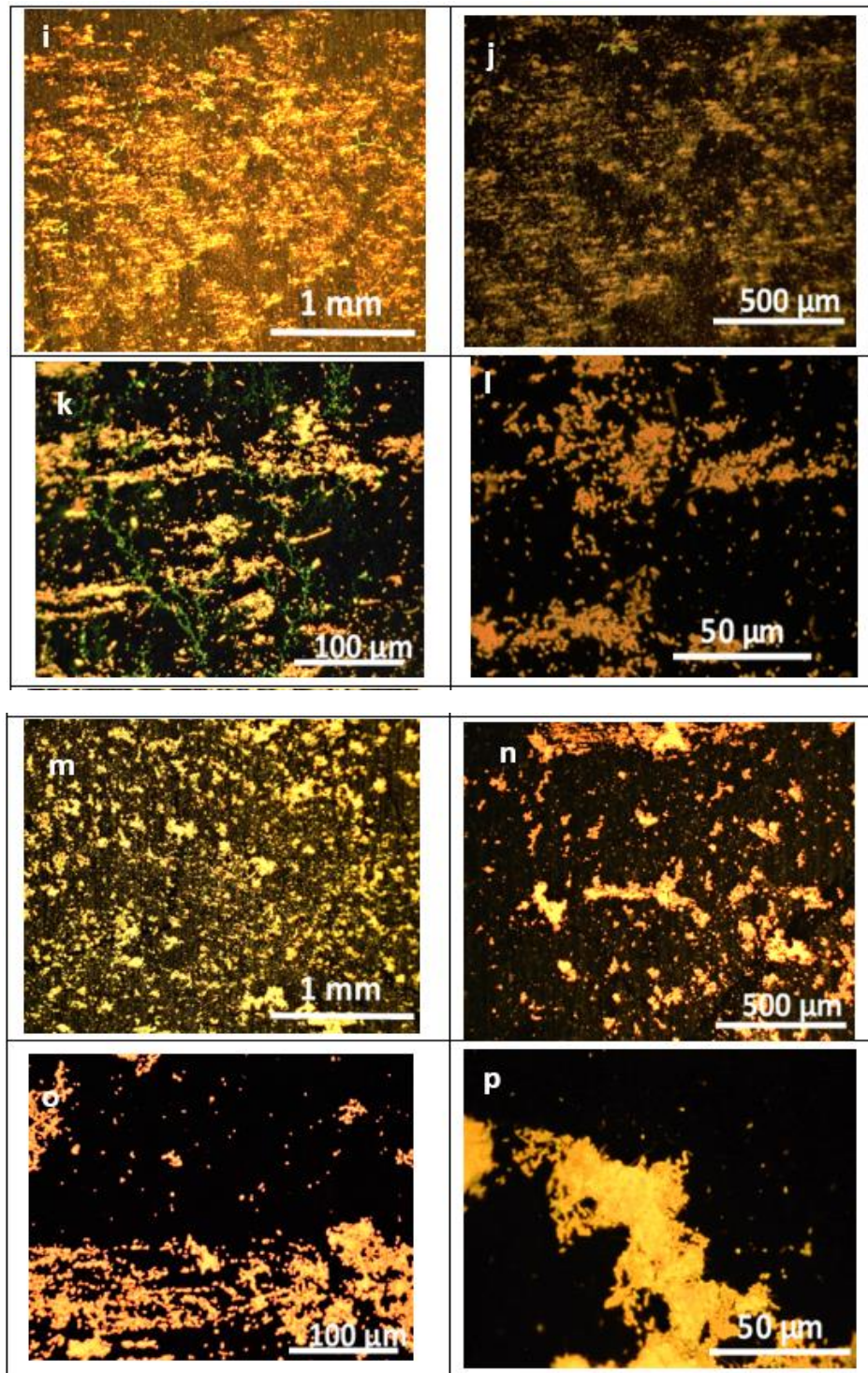
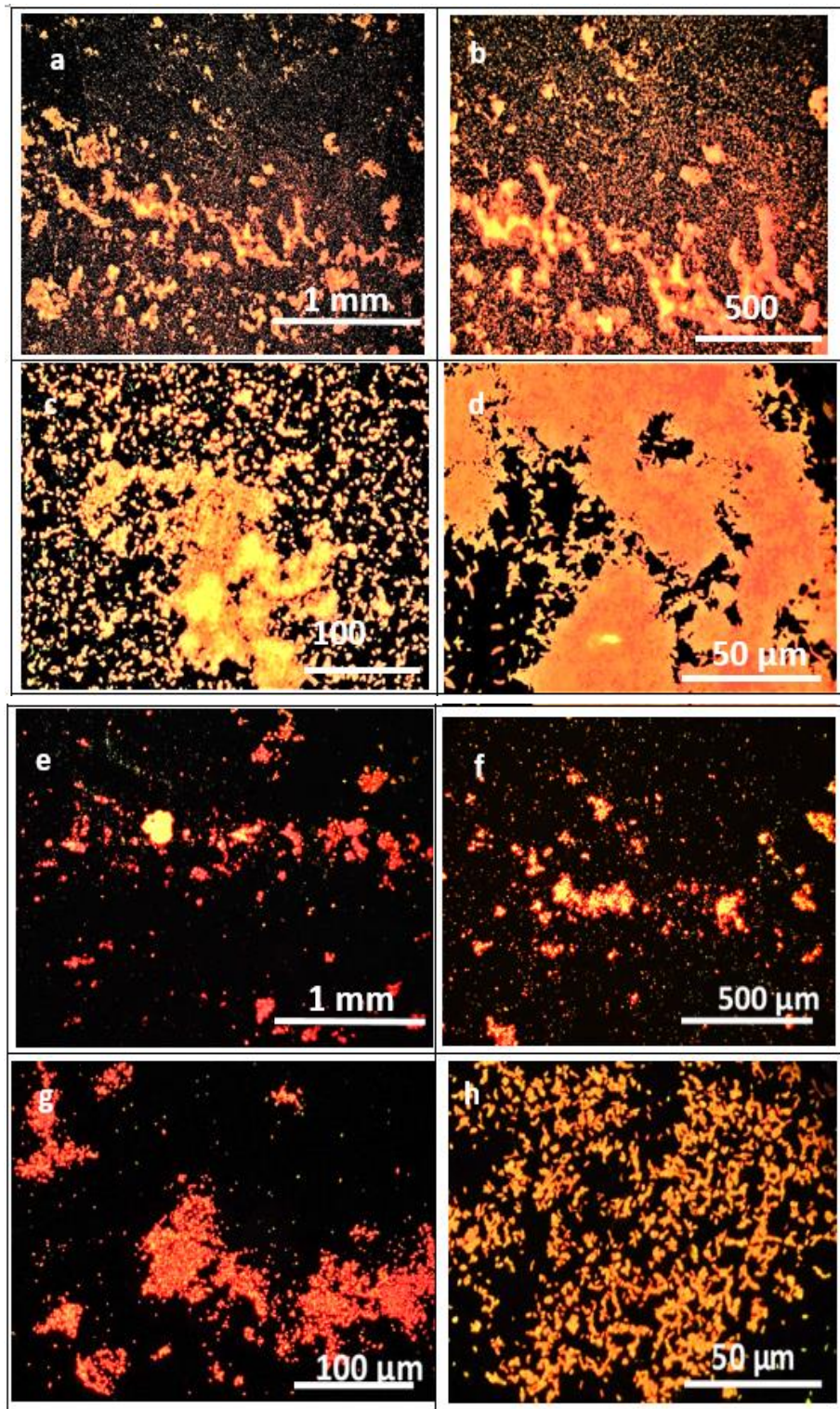


Figure 7.5 *P. fluorescens pf1* 24 hrs. biofilm before cleaning: time 0 (a, b, c, d). After cleaning with foam flow (6cm s⁻¹, vertical fouling): time 35 seconds (e, f, g, h), time 3 minutes (i, j, k, l), time 20 minutes (m, n, o, p). Dead cells after dyeing were observed in green color.



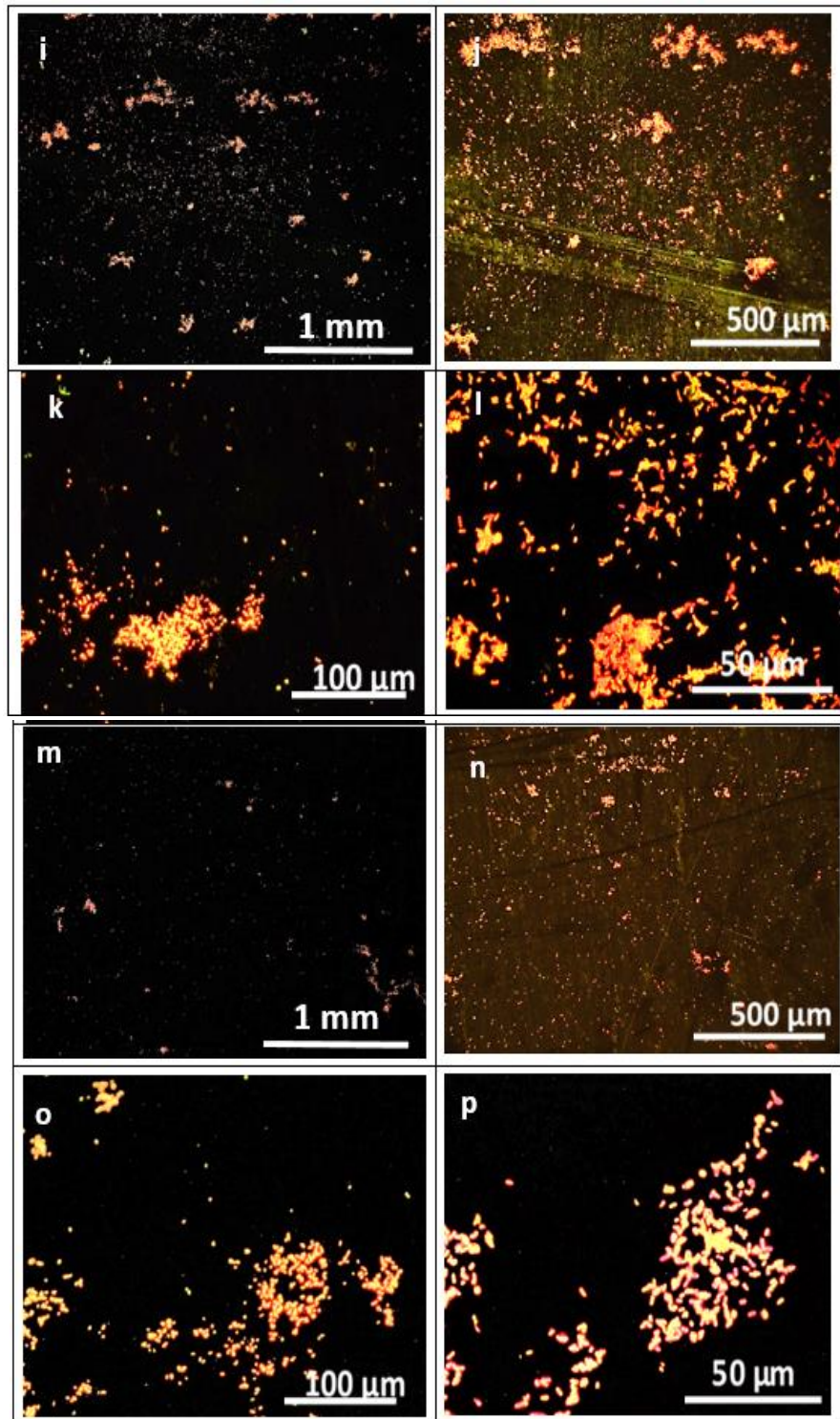


Figure 7.6 *P. fluorescens pfl* 24 hrs. biofilm, before cleaning: time 0 (a, b ,c ,d). After cleaning with CIP (120 cm.s⁻¹, vertical fouling): time 35 seconds (e, f, g, h), time 3 minutes (i, j, k, l), time 20 minutes (m, n, o, p).

Microscopic images showed that before cleaning (time 0) of *P. fluorescens pfl* biofilm, it was clear that there is a network of *pfl* cells which were either embedded in the extra cellular matrix (ECM) forming clusters or can be found around the clusters as sole cells (7.5 c, 7.6 c). Horizontally grown biofilms shown an apparently thicker structure potentially containing higher amount of exopolymers (not quantify) with a wide coverage of the surface.

After cleaning vertically grown biofilms, less number of clusters were observed. The remaining clusters decreased in size (7.5 o) after 20 minutes of cleaning. Sometimes only sole cells were observed without clusters (7.6 o) at some positions on the coupons. Shorter cleaning (35 seconds, 3 minutes) times showed either more or same amount of remaining clusters or sole cells compared to cleaning for 20 minutes.

Whether cleaning *pfl* biofilms with Cleaning in Place like conditions or with foam cleaning, both cleaning techniques showed the same impact on the organization of biofilms showing less-smaller cell clusters or sole cells. No complete cleaning was observed which was also validated by enumeration.

7.6 Discussion and Conclusion

Results obtained in this part, showed that the behavior of foam flow differs between detachment of *Pseudomonas fluorescens pfl* 24 hrs. biofilms formed upon fouling vertically or horizontally on 316L stainless steel coupons inserted in test ducts. Upon using foam flow, the decimal reduction (DR20) after 20 minutes of cleaning was higher (between 0.5 to 1 log) in the case of 2D50% (4cm.s^{-1}) and 3D50% (6cm.s^{-1}) for the vertically fouled biofilms compared to the horizontal ones. As for 1D50%, (2 cm s^{-1}) the decimal reduction was almost the same (1 log) between vertically and horizontally fouled biofilms. In our case, N0 on coupons after horizontal fouling was higher by an average of 0.6 log compared to N0 after vertical fouling, which means more cells were attached which form a denser biofilm. When increasing the foam flow velocity in the case of horizontal biofilms, no increase in the detachment was observed for a 20 minutes cleaning duration, indicating an higher resistance of the biofilm to higher shearing whatever the role of the capillary forces. According to Wilson et al (Wilson et al., 2017) bacteria adapt the physical structures and material properties of the matrix based on changes in microbial populations and environmental conditions such as shear stresses, nutrient availability, and competing organisms as a survival measure. As a bonus to these adaptations, biofilms demonstrate increased hardness against harsh chemical conditions, starvation, and antimicrobial agents. It can be thought the

coordination between bacterial cells along with extra cellular matrix can form a protective barrier to any invading physical or a chemical action, hence protecting the biofilm. In our case the conditions of horizontal fouling were different compared to vertical one which leads to the formation of a biofilm with a different attachment on the substrate and a different composition (number of cells, ECM density ...).

Surface contamination by *Pseudomonas fluorescens* biofilms was studied recently using pilot scale washing tanks with standard design features encountered in the fresh-cut vegetable processing industry (Cunault et al., 2019). Consequences on the biofilms' resistance to the shear stress and to enzymatic cleaning were analyzed. It was found that biofilm structures depended on the location in the tanks, which could range from discontinuous monolayer to large thick clusters. Biofilms grown in zones subjected to shear were significantly more resistant to mechanical stress but no difference were found comparing quasi-static vertical and horizontal areas. In (Cunault et al., 2019), quasi-static meant slow flow movement in the washing tanks which could be sufficient to allow biofilms quite the same resistance to further shear while cleaning. However, the resistance to enzyme cleaning was found significantly different comparing vertical and horizontal biofilms: horizontal biofilms being more resistant. Based on these results, probably the mechanical action of the foam flow did not affect preferentially one biofilm position but the SDS as a detergent appeared more effective on vertically grown biofilms. Depending on the values of the capillary numbers obtained in our case for the three foam flow velocities, the values falls in the capillary numbers range proposed by Bretherton law ($3.10^{-4} < Ca < 2.8.10^{-3}$), which also suggests the possibility of assuming our foam flow in the test duct as a one bubble flow in a capillary tube having same diameter as the bubble. In that case, we built the understanding of the interaction of foam with the *pf1* biofilm based on this assumption. According to (Kondjoyan et al., 2009b), who studied the detachment of latex microspheres ($2\mu\text{m}$ in size) by the passage of one bubble in a capillary , results obtained from the bell shaped curve showed the detachment of hydrophilic particles (amine-modified polystyrene beads) reached its maximum when the velocity of the bubble in the 0.15mm diameter micro-tube was about 3.5 cm.s^{-1} . On the other hand, for hydrophobic particles (carboxylate-modified polystyrene beads), the bell shaped curve showed that the maximum detachment obtained was at almost 7 cm.s^{-1} .

Increasing the velocity more than the values of the two mentioned velocities, detachment for both types of beads starts to decrease. As for the vertical *pf1* biofilms formed in our case it is clear that

when there was variation of the foam velocity it affected detachment of cells. When velocity increased up to 6 cm.s^{-1} or decreased to 2 cm.s^{-1} detachment decreases by a 0.5 and 1 log respectively compared to a 2 logs reduction at 4 cm.s^{-1} suggesting a close detachment behavior to the amine-modified polystyrene beads studied by (Kondjoyan et al., 2009). As for bubble size, it can be realized that as foam flow velocity increases while fixing the foam quality at 50%, bubbles radius decreases (see part 1). As for the thin liquid film thickness calculated in this part taking into account one bubble passage in capillary tube, the values obtained showed that the thickness did not widely vary between the three velocities, where the range was 2-3 μm . By assuming that the three flow regimes have the same film thickness, according to Tisné et al (Tisné, Aloui, et Doublier 2003) bubbles can impose different amplitudes of shear stress. Large bubble at low flow velocities can impose a higher amplitude of local shear stress (amplitude peaks are synchronized at the edges of the bubbles while passing) compared to small bubble sizes. On the other hand, the fluctuation of the local wall shear stress due to the velocity of the bubbles vary, where larger velocities will cause more fluctuation in the wall shear stresses. As for *pf1* biofilm studied in this part, an average foam flow velocity of 4 cm.s^{-1} , and an average bubble radius of 187 μm showed the highest detachment *pf1* cells. As for spores in part 1, the velocity 2 cm.s^{-1} (quality 50%) showed the highest detachment where also 4 cm.s^{-1} had almost the same log 10 reduction as 2 cm.s^{-1} . The shape of the vertically grown biofilms with isolated cells and separated clusters was probably more prone to detachment at 4 cm.s^{-1} than the horizontally grown biofilms presenting a thick unique covering of the surface. As already mentioned, for a mechanism showing an efficient detachment compared to CIP, while taking bubble sizes and the thin film adjacent to the top wall into account, the amplitude of the local shear stress and its fluctuation must be further studied.

Horizontal *pf1* biofilms in our case were not affected with low or even higher velocities of foam flow. As discussed above growing biofilms in horizontal position showed more resistance towards cleaning (Cunault et al., 2019). In this work, despite their specific surface features, welds placed in right angle corners surprisingly were cleanable when vertical but not when horizontal lead to state the importance of the position and of the design of the system to be cleaned. .. Variations in biofilm mechanical properties thus depend on changes in the local biofilm physical properties which, in turn, depend on both the growth processes and the effect of external forces that change the biofilm porosity (Paul et al., 2012), and its structural response towards the environment. Foam flow appeared here to be quite a good alternative for cleaning. To tackle a large variety of biofilm

structure and composition, probably formulated foam systems should be envisaged leading to both mechanical and chemical actions.

7.7 References

Blel, W., Legentilhomme, P., Bénézech, T., & Fayolle, F. (2013). Cleanability study of a Scraped Surface Heat Exchanger. *Food and Bioprocess Processing*, 91(2), 95–102. <https://doi.org/10.1016/j.fbp.2012.10.002>

Cunault, C., Faille, C., Bouvier, L., Fste, H., Augustin, W., Scholl, S., Debreyne, P., & Benezech, T. (2015). A novel set-up and a CFD approach to study the biofilm dynamics as a function of local flow conditions encountered in fresh-cut food processing equipments. *Food and Bioprocess Processing*, 93, 217–223. <https://doi.org/10.1016/j.fbp.2014.07.005>

Cunault, C., Faille, C., Calabozo-Delgado, A., & Benezech, T. (2019). Structure and resistance to mechanical stress and enzymatic cleaning of *Pseudomonas fluorescens* biofilms formed in fresh-cut ready to eat washing tanks. *Journal of Food Engineering*, 262, 154–161. <https://doi.org/10.1016/j.jfoodeng.2019.06.006>

Faille, C., Bénézech, T., Blel, W., Ronse, A., Ronse, G., Clarisse, M., & Slomianny, C. (2013). Role of mechanical vs. Chemical action in the removal of adherent *Bacillus* spores during CIP procedures. *Food Microbiology*, 33(2), 149–157. <https://doi.org/10.1016/j.fm.2012.09.010>

Gibbs, S. G., Meckes, M. C., Green, C. F., & Scarpino, P. V. (2004). Evaluation of the ability of chlorine to inactivate selected organisms from the biofilm of a drinking water distribution system simulator following a long-term wastewater cross-connection. *Journal of Environmental Engineering and Science*, 3(2), 97–105. <https://doi.org/10.1139/s03-061>

Kirtley, S. A., & McGuire, J. (1989). On Differences in Surface Constitution of Dairy Product Contact Materials1. *Journal of Dairy Science*, 72(7), 1748–1753. [https://doi.org/10.3168/jds.S0022-0302\(89\)79291-2](https://doi.org/10.3168/jds.S0022-0302(89)79291-2)

Kondjoyan, A., Dessaigne, S., Herry, J.-M., & Bellon-Fontaine, M.-N. (2009a). Capillary force required to detach micron-sized particles from solid surfaces—Validation with bubbles circulating in water and 2µm-diameter latex spheres. *Colloids and Surfaces B: Biointerfaces*, 73(2), 276–283. <https://doi.org/10.1016/j.colsurfb.2009.05.022>

Kondjoyan, A., Dessaigne, S., Herry, J.-M., & Bellon-Fontaine, M.-N. (2009b). Capillary force required to detach micron-sized particles from solid surfaces—Validation with bubbles circulating

in water and 2µm-diameter latex spheres. *Colloids and Surfaces B: Biointerfaces*, 73(2), 276–283. <https://doi.org/10.1016/j.colsurfb.2009.05.022>

Kusumaningrum, H. D., Riboldi, G., Hazeleger, W. C., & Beumer, R. R. (2003). Survival of foodborne pathogens on stainless steel surfaces and cross-contamination to foods. *International Journal of Food Microbiology*, 85(3), 227–236. [https://doi.org/10.1016/s0168-1605\(02\)00540-8](https://doi.org/10.1016/s0168-1605(02)00540-8)

Liu, X., Tang, B., Gu, Q., & Yu, X. (2014). Elimination of the formation of biofilm in industrial pipes using enzyme cleaning technique. *MethodsX*, 1, 130–136. <https://doi.org/10.1016/j.mex.2014.08.008>

Maloy, S., & Hughes, K. (2013). *Brenner's Encyclopedia of Genetics* | ScienceDirect. <https://www.sciencedirect.com/referencework/9780080961569/brenners-encyclopedia-of-genetics>

Marouani-Gadri, N., Firmesse, O., Chassaing, D., Sandris-Nielsen, D., Arneborg, N., & Carpentier, B. (2010). Potential of Escherichia coli O157:H7 to persist and form viable but non-culturable cells on a food-contact surface subjected to cycles of soiling and chemical treatment. *International Journal of Food Microbiology*, 144(1), 96–103. <https://doi.org/10.1016/j.ijfoodmicro.2010.09.002>

O'Toole, G. A., & Kolter, R. (1998). Initiation of biofilm formation in *Pseudomonas fluorescens* WCS365 proceeds via multiple, convergent signalling pathways: A genetic analysis. *Molecular Microbiology*, 28(3), 449–461. <https://doi.org/10.1046/j.1365-2958.1998.00797.x>

Paul, E., Ochoa, J. C., Pechaud, Y., Liu, Y., & Liné, A. (2012). Effect of shear stress and growth conditions on detachment and physical properties of biofilms. *Water Research*, 46(17), 5499–5508. <https://doi.org/10.1016/j.watres.2012.07.029>

Reij, M. W., Den Aantrekker, E. D., & ILSI Europe Risk Analysis in Microbiology Task Force. (2004). Recontamination as a source of pathogens in processed foods. *International Journal of Food Microbiology*, 91(1), 1–11. [https://doi.org/10.1016/S0168-1605\(03\)00295-2](https://doi.org/10.1016/S0168-1605(03)00295-2)

Scharff, R. L. (2012). Economic burden from health losses due to foodborne illness in the United States. *Journal of Food Protection*, 75(1), 123–131. <https://doi.org/10.4315/0362-028X.JFP-11-058>

Srey, S., Jahid, I. K., & Ha, S.-D. (2013). Biofilm formation in food industries: A food safety concern. *Food Control*, 31(2), 572–585. <https://doi.org/10.1016/j.foodcont.2012.12.001>

Tisn?, P., Aloui, F., & Doubriez, L. (2003). Analysis of wall shear stress in wet foam flows using the electrochemical method. *International Journal of Multiphase Flow*, 29(5), 841–854. [https://doi.org/10.1016/S0301-9322\(03\)00038-7](https://doi.org/10.1016/S0301-9322(03)00038-7)

Wilson, C., Lukowicz, R., Merchant, S., Valquier-Flynn, H., Caballero, J., Sandoval, J., Okuom, M., Huber, C., Brooks, T. D., Wilson, E., Clement, B., Wentworth, C. D., & Holmes, A. E. (2017). Quantitative and Qualitative Assessment Methods for Biofilm Growth: A Mini-review. *Research & Reviews. Journal of Engineering and Technology*, 6(4). <https://www.ncbi.nlm.nih.gov/pmc/articles/PMC6133255/>

Conclusion and Perspectives

Conclusion and Perspectives

Conclusion and Perspectives

The contamination of food products due to the presence of adherent bacteria in closed processing lines is a major concern in the food industry since many years, mainly due to their resistance to hygiene procedures (Andersson et al., 1995; Faille et al., 2001). Haeghebaert et al., (2001) have suggested that equipment contamination would have been responsible for around 40% of foodborne diseases caused by bacteria in France between 1996 and 1998. Such an issue is still of concern when looking at recent literature (Chen et al., 2020; Truchado et al., 2020).

The efficient cleaning is vital for hygiene of closed processing systems where the common practical way of cleaning is by using cleaning In place (CIP) procedures which is a method to clean the inner surface of equipment without disconnecting them (Friis and Jensen, 2005). A CIP procedure typically involves a warm water rinse, washing with alkaline and/or acidic solution, and a clear rinse with warm water to flush out residual cleaning agents (Dev et al., 2014). Efficient CIP processes will result not only in reduced downtime and costs for cleaning but also reduced environmental impact (in the disposal of spent chemicals) (Gillham et al., 1999). Previous works have shown that bacteria may remain on equipment surfaces after standard CIP procedures (Lelièvre et al., 2002, Elevers et al., 1999). Insufficient cleaning typically results in reduced efficiency, contamination in final products and energy loss (Avila-Sierra et al., 2019). Traditional methods of improving CIP efficiency include increasing the overall cleaning fluid velocity, the concentration and temperature of the cleaning chemical and longer running time, giving rise to increased costs and downtime, reduce production efficiency, and additional burden to the environment due to the extra chemical consumption.

Pioneering methodologies to enhance cleaning and reducing fouling have evolved, including modification of surfaces, pulsed flow, ozonised water rinse, electrolyzed oxidizing rinse water, and ultrasonic cleaning (Augustin et al., 2010). Nevertheless, all these methods require additional devices, wealth investment, and energy involvements (Fan et al., 2018). When comparing to the aforementioned solutions, the adjustment of the properties of the cleaning liquid solution for example may enhance the effectiveness of the cleaning method. As stated in the literature, cleaning operations in food industries require water, chemicals and energy inducing significant environmental influence ; however, Almost little knowledge is known on the potencies produced by flowing foam in cleaning operations working with much less energy and water, producing

considerably less waste water. Primary works have shown that flowing foams can produce higher wall shear stresses than single phase flow as in CIP.

In this study we investigated the effect of flowing foam in pipes and compared its efficiency with standard CIP like conditions on the detachment of spores and biofilms. For that goal, we decided to have different approaches so that we studied the efficiency of foam flow under different conditions. To reach this goal an original set-up was built to allow us to prepare the foam (air/liquid mixture) and obtain flow conditions to be characterized based on the choice of the surfactant, how wet could be the foam and velocities that could be double or triple while maintaining the foam structure. The first approach was working with different foam flow regimes (1D, 2D, 3D while increasing the velocity from 2 to 6 cm s⁻¹) having different foam qualities (amount of air: 50%, 60%, 70%) on different species of microorganisms where fouling was performed either by using spores of *B. amyloliquefaciens* 98/7 or *B. cereus* 98/4 that shows a difference by their hydrophobic/hydrophilic character amongst other differences related to their surface structure (exosporium and appendages for *B. cereus* and a outermost glycoprotein layer for *B. amyloliquefaciens*). As for *P. fluorescens pfl* it was used as a good biofilm former (24 hrs. biofilm) widely encountered in the food industry. All of these bacteria considered as spoilage microorganisms are not pathogenic but could be good representatives of some pathogenic ones. In case of biofilms, potential hosting of pathogenic bacteria is now well known as it the case for *Pseudomonas* species with i.e. *Listeria monocytogenes*. In this work fouling was performed either vertically or horizontally inducing biofilms with different structures. Results from foam cleaning were compared with CIP like conditions results (the same mean mechanical action, and the same concentration of surfactant).

The second approach was subjecting foam flow to different singularities (sudden expansion gradual reduction – bends) while working with one foam flow regime (1D 50%) and one species (*B. amyloliquefaiciens* 98/7 spores) to highlight any changes in the foam flow cleaning efficiency. The third approach was working also with one species (*B. amyloliquefaciens* 98/7) considered as a good “microbial tool” producing foam from the use of different surfactants (SDS, Capstone® FS 30, Ammonyx® LO) that differs by their chemical properties (nonionic, anionic and zwitterion) thus producing different foams having different physical properties in terms of bubbles size , number and repartition, and flow pattern.

Three different foam qualities in terms of air/liquid flow rates were chosen to clean stainless steel surfaces soiled by spores of two *Bacillus* species. Three different flow regimes were observed from a plug flow to a 3D flow regime bubbles velocities being related to their location in the flow. The increase of the velocity induced an increase of the mean wall shear stress as expected but also different bubble size arrangement at the top wall with the elimination of the largest bubbles at higher flow rates. With stainless steel coupons soiled by *B. amyloliquefaciens* 98/7 spores, a good global cleaning efficiency was observed with wetter foam (qualities of 50% and 60%) under the lowest flow rates, being comparable in terms of efficiency to the CIP conditions tested. The removal kinetics were modelled according to previous work on biofilm removal under CIP conditions. Amazingly the same removal shape was observed here than previously observed on biofilms with a strong decrease in the surface contamination in less than 1 min followed by a second phase less efficient with a quite low kinetics constant rate. For all foam qualities at the lowest flow rates, the constant rate of the first part of the removal kinetics were significantly higher. The efficiency of this first phase seemed to govern the whole cleaning efficiency. Comparing to previous related works on foam flow characterization, it was possible to highlight the potential role on the cleaning efficiency of the Wall Shear Stress variations (qualitatively) in parallel to the liquid film thickness variation at the wall with the bubbles' passage. In addition, according to previous work, the possible capillary forces exerted under the lowest flow rates and considering the hydrophilic nature of the *B. amyloliquefaciens* 98/7 spores would explain at least partly the surprising efficiency in the spores' removal by foam. The capillary number as defined by E. Rapp (E.Rapp, 2017) as the ratio of viscous forces to the surface tension were calculated. The capillary number is also the ratio of the viscous forces to the capillary forces (Fulcher et al., 1985). Thus when the capillary number is high the capillary forces are low. According to the literature, the detachment curve of micro size particles showed a bell shape as a function of velocity and capillary forces. The velocity of 2 cm s⁻¹ appeared to be a well-chosen value and explaining the high detachment of the highly hydrophilic spores of *B. amyloliquefaciens* 98/7. Hence, the difficulty in eliminating the hydrophobic *Bacillus* spores under the same assuming optimum foam flow conditions could be explained in the same way, the chosen mean velocity of the foam being thus too low.

Concerning the detachment of the *P. fluorescens* pf1 biofilm formed by vertical fouling. Results showed that the log10 reduction at a foam flow velocity of 2 cm.s^{-1} (1D50%), was almost 1 log (after 20 minutes of cleaning) which is different from the result of *B. amyloliquefaciens* 98/7. In the case of biofilm detachment almost 2 log 10 reduction was observed at a velocity of 4 cm.s^{-1} (2D50%) whereas the increase in the velocity up to 6 cm.s^{-1} (3D50%) showed lower detachment (1.5 log) after 20 minutes of cleaning. The capillary numbers for the three flow regimes (1D 50% , 2D 50% , 3D 50%) fall in the Bretherton range suggesting the one bubble –microtube assumption. Again our results were comparable with that of previous work which showed the detachment of hydrophilic micro beads was maximum at a bubble velocity of 3.5 cm.s^{-1} . The detachment of pf1 biofilm was optimum at a foam flow of 4 cm.s^{-1} (2D 50%), biofilms being vertically grown and presenting some clusters and numerous isolated cells (vegetative cells being hydrophilic as commonly acknowledged).

As for singularities, results of detachment were obtained from ducts placed after sudden expansion/ gradual reduction singularity or bends. For the case of the sudden expansion/gradual reduction, the singularity was placed either after the foam generation source or after 1 m pipe used as establishment pipe (connected to foam generation source) where foam flow for 1m before it passes through the singularity. Results showed that the log10 reduction in the test duct after 20 minutes of cleaning is the same whether the sudden expansion/ gradual reduction singularity is placed directly after the foam generation source or after the establishment pipe (1m), where the log reduction in both cases was almost 1 log reduction. The log10 reduction after singularities was lower by 1 log compared to a 2 log reduction obtained from the test duct placed after a 1 m establishment pipe only. As for bend singularities, whether after 1 or 2 90° bends, the detachment was the same representing almost a 1 log 10 reduction. In the case of singularities, we studied the bubbles structure at the top wall after the passage foam through the singularity. In our case, it was clear that when foam passes through a singularity, whether sudden expansion /gradual reduction or bends, bubbles shape at the top wall of the test duct were more polygonal compared the their shape after passing a 1 m establishment only. The change in the bubbles shape can be a result of more drainage of the liquid in foam upon facing a structural change in the flow passage (expansion, bending ..).

When performing tests with foam produced from other surfactants such as Capstone® FS 30 (fluorosurfactant) and Ammonyx® LO for the detachment of *B. amyloliquefaciens* 98/7 spores,

the log₁₀ reduction after 20 minutes of cleaning (1D 50%) was lower compared to SDS foam which showed the highest log₁₀ reduction (~2 logs).

As for Ammonyx® LO the detachment was about 1 log while Capstone® FS 30 was about 0.5 log. For all surfactants the flow regime was 1D 50%. Taking into account the different viscosities of the surfactants (velocity was the same), capillary number was calculated for each surfactant. The highest was for Capstone FS 30 which shows a lower value of the capillary force thus a lower impact on the spore's detachment, while for SDS it had the lowest capillary number showing the highest value of the capillary force among the surfactants. Not only we studied the capillary force effect, we went further to study the bubbles pattern and shape at the top wall. Images of bubbles showed three different patterns which can be clearly visible by the naked eye. Capstone® FS 30 showed giant bubbles with a large diameter compared to bubbles in SDS foam which showed moderate to small diameter sized bubbles, and Ammonyx® LO which showed moderate to small/tiny bubbles. According to what we have mentioned, large sized bubbles will decrease the fluctuations of the local shear stress magnitude due to the fact a large part of the bubble is in contact with the wall (local shear stress tends to be zero at the middle of the bubble), however, the amplitude of the shear stress is higher when compared with smaller bubbles. In Ammonyx® LO, tiny bubbles were frequently observed suggesting a very low amplitude of local wall shear stress. SDS showed a moderate to large bubble sizes, suggesting a better impact of the fluctuations and the amplitude of the local wall shear stress on the detachment of *B. amyloliquefaciens* 98/7 spores. As a final point in this study, foam cleaning (double phase fluid) has shown that it can be as effective as Cleaning in Place like conditions (one phase fluid) concerning detachment of *B. amyloliquefaciens* 98/7 spores and *P. fluorescens* pfl biofilm after a 1m straight pipe.

Even though foam flow showed its detachment efficiency changes when the surfactant is changed or when foam flow is subjected to singularities, however, different steps can be taken into account to improve the foam flow ability for more detachment. Improving effective foam in terms of cleaning efficiency can be on the chemical level, which can be using a formulated cocktail of surfactants comprising foaming, stabilizers, dispersants. Also the addition of disinfectants would play a major role in increasing the log₁₀ reduction. In addition, other chemical properties can be modified such as pH through the use of acidic or basic compounds (NaOH, KOH).

From the above results, different parameters can be considered which play a role in the foam detachment efficiency. The parameters are film thickness, capillary force, amplitude and the fluctuations of the local shear stress imposed by the bubbles. Of course other parameters may intervene such as chemical action but it was not covered in the scope of this study. The coordination of the mentioned parameters can have impact on the detachment of microorganisms ranging from a very low (in the case of capstone FS 30) up to very high (in the case of 2cm.s^{-1} hydrophilic spores). As for moderate detachment it was realized in the cases of singularities and Ammonyx LO.

It is important to note that the results does not take into account other factors such as the attachment forces of the microorganism on the surface which can be sometimes an obstacle to overcome. Even though the control of the parameters did not show a good detachment in some cases, however it opens the door towards controlling foam flow under different conditions for a better detachment. Foam flow can be promising for cleaning in closed systems where its cleaning impact was competitive with the results from CIP like conditions while consuming much less resources. On the other hand, different steps are still necessary to go from low TRL (Technology Readiness Level) as in this work which is still at the TRL 3 – experimental proof of concept and TRL 4 level – technology validated in lab (still ongoing work to be done). The project to be implemented in food industries, needs to pass additional TRL steps that will lift the project to be in practice. The TLR steps to be finished still according to the EU ranking are:

- TRL 5 - Technology validated in relevant environment (industrially relevant environment in the case of key enabling technologies).
- TRL 6 – Technology demonstrated in relevant environment (industrially relevant environment in the case of key enabling technologies)
- TRL 7 – System prototype demonstration in operational environment
- TRL 8 – System complete and qualified
- TRL 9 – Actual system proven in operational environment (competitive manufacturing in the case of key enabling technologies)

After TRL 4, our next step for the project concerning the TRL steps, has to pass the component and/or breadboard validation in relevant environment, and that would be in TRL 5 level, where the basic technological components are integrated with reasonably realistic supporting elements so it can be tested in a simulated environment.

After passing through the different TRL steps, employing foam cleaning technology in food industries for closed systems such as pipes can be beneficial on the level of water consumption (high consumption of water in Dairy industries), which stands as a burden for food industries with their traditional Cleaning in Place procedures. For instance in dairy industries the consumption of water by CIP can reach up to 28% according to the Dairy Australia 2006 (Australian national body for the dairy industry). Not only the amount of water used, also in some food industries water recycling is an essential step. This concept is at the basis of the development of in-site water recycling strategies. This implies the practice of specific chemical or physical interventions aiming to modify water properties before re-entering in the production cycle.

Even though water recycling generates the possibility to locally clean wash water and diverge it from municipal wastewater, decreasing the social costs for water treatment and the overall water footprint of the produce, however it is cost effective (Manzocco et al., 2015) and can be also obstacle to overcome in many food industries. Foam, this complex non-Newtonian double phase fluid can be of a wide interest in cleaning procedures where unlike other fluids, foam structure can be controlled and optimized accordingly. Of course in our case using foam does not exclude the fact that there are chemicals that need to be treated before foam is disposed to the environment. An alternative to surfactants with toxic chemicals is the use of green surfactants that can be environmental friendly. Green surfactants are defined as biobased amphiphilic molecules obtained from nature or synthesized from renewable raw materials (Rebello et al., 2014). Green surfactants could be used in this project that takes into account decreasing the toxicity impact on the environment.

Apart from foam flow usage in food industries at a large scale, other applications can be related to hospital devices. The endoscope which is a lighted optical instrument that is used to get a deep look inside the body can be contaminated after its usage. Complex endoscope design features may allow organic debris and microorganisms to accumulate, making manual cleaning essential. For instance in GI endoscopes there is a pre cleaning step which involves wiping of the tube by a cloth soaked with a special enzymatic detergent, then aspiration of the enzymatic solution, in addition to further complementary steps. On the other hand, some companies are using new technology based on foam. For instance, CANTEL, a medical operation company uses INTERCEPT™ encapsulated foam in the pre-cleaning step, where foam is disposed on the endoscope externally and internally, in order to extend the time between the pre-cleaning and the cleaning step up to 72

hrs. The foam will flow inside the endoscope to detach microorganisms, and biofilms and preserve the endoscope from further microbial and biofilm growth.

Finally, our next step for this flow foam project will be improving foam flow efficiency based on the structural level, taking into account bubbles size, velocity of the foam flow, and controlling thin film thickness at the walls. A complementary step would be the chemical advancement in the formulation of foam through the use of different compounds that can destabilize the adhesive forces between the microorganisms and the surface and will facilitate detachment. This improvement will be employed at large scale for food industries. Not only food industries, our collaboration with ANIOS laboratories which is interested for cleaning small scaled devices such as endoscopes would be based on this foam flow technology that will preserve the hygiene of these devices for longer times before manual cleaning.

Regarding the experimental conditions taken into account in foam cleaning and cleaning in place like conditions, it is important to perform a comparison between resources consumption (water, gas, fuel, electric energy) between the two cleaning techniques. Also comparing the Life Cycle Analysis (LCA) of both techniques will be one of our next goals in this project.

References

- Andersson, A., Ronner, U., & Granum, P. E. (1995). What problems does the food industry have with the spore-forming pathogens *Bacillus cereus* and *Clostridium perfringens*? *International Journal of Food Microbiology*, 28(2), 145-155. [https://doi.org/10.1016/0168-1605\(95\)000534](https://doi.org/10.1016/0168-1605(95)000534)
- Augustin, W., Fuchs, T., Föste, H., Schöler, M., Majschak, J.-P., Scholl, S., 2010. Pulsed flow for enhanced cleaning in food processing. *Food and Bioproducts Processing*, Special Issue on Fouling and cleaning in food processing 2010 88, 384–391. <https://doi.org/10.1016/j.fbp.2010.08.007>
- Avila-Sierra, A., Zhang, Z.J., Fryer, P.J., 2019. Effect of surface characteristics on cleaning performance for CIP system in food processing. *Energy Procedia*, Proceedings of the 2nd International Conference on Sustainable Energy and Resource Use in Food Chains including Workshop on Energy Recovery Conversion and Management; ICSEF 2018, 17 – 19 October 2018, Paphos, Cyprus 161, 115–122. <https://doi.org/10.1016/j.egypro.2019.02.067>
- Boxler, C., Augustin, W., Scholl, S., 2013. Cleaning of whey protein and milk salts soiled on DLC coated surfaces at high-temperature. *Journal of Food Engineering* 114, 29–38. <https://doi.org/10.1016/j.jfoodeng.2012.07.023>

- Chen, S.H., Fegan, N., Kocharunchitt, C., Bowman, J.P., Duffy, L.L., 2020. Impact of Poultry Processing Operating Parameters on Bacterial Transmission and Persistence on Chicken Carcasses and Their Shelf Life. *Appl. Environ. Microbiol.* 86, e00594-20. <https://doi.org/10.1128/AEM.00594-20>
- Christian, G.K., Fryer, P.J., 2006. The Effect of Pulsing Cleaning Chemicals on the Cleaning of Whey Protein Deposits. *Food and Bioproducts Processing, Fouling, Cleaning and Disinfection in Food Processing* 84, 320–328. <https://doi.org/10.1205/fbp06039>
- Dev, S.R.S., Demirci, A., Graves, R.E., Puri, V.M., 2014. Optimization and modeling of an electrolyzed oxidizing water based Clean-In-Place technique for farm milking systems using a pilot-scale milking system. *Journal of Food Engineering* 135, 1–10. <https://doi.org/10.1016/j.jfoodeng.2014.02.019>
- E.Rapp, B., 2017. *Microfluidics: Modelling, Mechanics and Mathematics*. Elsevier. <https://doi.org/10.1016/C2012-0-02230-2>
- Faille, C., Fontaine, F., & Bénézech, T. (2001). Potential occurrence of adhering living *Bacillus* spores in milk product processing lines. *Journal of Applied Microbiology*, 90(6), 892-900. <https://doi.org/10.1046/j.1365-2672.2001.01321.x>
- Fan, M., Phinney, D.M., Heldman, D.R., 2018. The impact of clean-in-place parameters on rinse water effectiveness and efficiency. *Journal of Food Engineering* 222, 276–283. <https://doi.org/10.1016/j.jfoodeng.2017.11.029>
- Friis, A., Jensen, B.B.B., 2005. 11 - Improving the hygienic design of closed equipment, in: Lelieveld, H.L.M., Mostert, M.A., Holah, J. (Eds.), *Handbook of Hygiene Control in the Food Industry*, Woodhead Publishing Series in Food Science, Technology and Nutrition. Woodhead Publishing, pp. 191–211. <https://doi.org/10.1533/9781845690533.2.191>
- Fulcher, R.A.J., Ertekin, T., Stahl, C.D., 1985. Effect of Capillary Number and Its Constituents on Two-Phase Relative Permeability Curves. *Journal of Petroleum Technology* 37, 249–260. <https://doi.org/10.2118/12170-PA>
- Gillham, C.R., Fryer, P.J., Hasting, A.P.M., Wilson, D.I., 2000. Enhanced cleaning of whey protein soils using pulsed flows. *Journal of Food Engineering* 46, 199–209. [https://doi.org/10.1016/S0260-8774\(00\)00083-2](https://doi.org/10.1016/S0260-8774(00)00083-2)

- Gillham, C.R., Fryer, P.J., Hasting, A.P.M., Wilson, D.I., 1999. Cleaning-in-Place of Whey Protein Fouling Deposits: Mechanisms Controlling Cleaning. *Food and Bioproducts Processing* 77, 127–136. <https://doi.org/10.1205/096030899532420>
- Guzel-Seydim, Z.B., Wyffels, J.T., Greene, A.K., Bodine, A.B., 2000. Removal of Dairy Soil from Heated Stainless Steel Surfaces: Use of Ozonated Water as a Prerinse1. *Journal of Dairy Science* 83, 1887–1891. [https://doi.org/10.3168/jds.S0022-0302\(00\)75061-2](https://doi.org/10.3168/jds.S0022-0302(00)75061-2)
- Haeghebaert, S., Le Querrec, F., Vaillant, V., Delarocque Astagneau, E., Bouvet, P., 2001. Les toxi-infections alimentaires collectives en France en 1998. *Bulletin Epidémiologique Hebdomadaire* 15, 1–12.
- Lelièvre, C., Legentilhomme, P., Gaucher, C., Legrand, J., Faille, C., Bénézech, T., 2002. Cleaning in Place: effect of local wall shear stress variation on bacterial removal from stainless steel equipment. *Chemical Engineering Science* 57, 1287–1297. [https://doi.org/10.1016/S0009-2509\(02\)00019-2](https://doi.org/10.1016/S0009-2509(02)00019-2)
- Manzocco, L., Ignat, A., Anese, M., Bot, F., Calligaris, S., Valoppi, F., Nicoli, M.C., 2015. Efficient management of the water resource in the fresh-cut industry: Current status and perspectives. *Trends in Food Science & Technology, Novel strategies meeting the needs of the fresh-cut vegetable sector. The STAYFRESH project* 46, 286–294. <https://doi.org/10.1016/j.tifs.2015.09.003>
- Muthukumaran, S., Yang, K., Seuren, A., Kentish, S., Ashokkumar, M., Stevens, G.W., Grieser, F., 2004. The use of ultrasonic cleaning for ultrafiltration membranes in the dairy industry. *Separation and Purification Technology, Selected Papers from the 9th APPChE Conference, September 2002, Christchurch, New Zealand* 39, 99–107. <https://doi.org/10.1016/j.seppur.2003.12.013>
- Rebello, S., Asok, A., Mundayoor, S., & Shanavas, J. (2014). Surfactants : Toxicity, remediation and green surfactants. *Environmental Chemistry Letters*, 12, 275-287. <https://doi.org/10.1007/s10311-014-0466-2>
- Rosmaninho, R., Santos, O., Nylander, T., Paulsson, M., Beuf, M., Benezech, T., Yiantsios, S., Andritsos, N., Karabelas, A., Rizzo, G., Müller-Steinhagen, H., Melo, L.F., 2007. Modified stainless steel surfaces targeted to reduce fouling – Evaluation of fouling by milk components. *Journal of Food Engineering* 80, 1176–1187. <https://doi.org/10.1016/j.jfoodeng.2006.09.008>

Truchado, P., Gil, M.I., Larrosa, M., Allende, A., 2020. Detection and Quantification Methods for Viable but Non-culturable (VBNC) Cells in Process Wash Water of Fresh-Cut Produce: Industrial Validation. *Front. Microbiol.* 11, 673. <https://doi.org/10.3389/fmicb.2020.00673>

Scientific Production

1- Articles

- A.Al Saabi, C. Faille, H. Dallagi, C. Lemy, L. Wauquier, F. Aloui, et T. Bénézech . Flowing Foam for the Removal of *B. subtilis* and *B. cereus* Spores From Stainless Steel Surfaces, Fouling and Cleaning in Food Processing, April 2018, Lund, Sweden, <https://www.ceb.cam.ac.uk/system/files/documents/FCFP2018ListofAbstractsinorderofprogramme.pdf>
- Al Saabi, A., Dallagi, H., Aloui, F., Faille, C., Rauwel, G., Wauquier, L., Bouvier, L., & Bénézech, T. (2020). Removal of *Bacillus* spores from stainless steel pipes by flow foam : Effect of the foam quality and velocity. *Journal of Food Engineering*, 289, 110273. <https://doi.org/10.1016/j.jfoodeng.2020.110273>

2-Communications orales nationales et internationales (presentations)

- A.Al Saabi, C. Faille, H. Dallagi, C. Lemy, L. Wauquier, F. Aloui, et T. Bénézech . Flowing Foam for the Removal of *B. subtilis* and *B. cereus* Spores From Stainless Steel Surfaces, Fouling and Cleaning in Food Processing, April, 2018, Lund, Sweden.
- A.Al Saabi, H. Dallagi, C. Faille, F. Aloui et T. Bénézech. Cleaning in Place by flowing foams: a sustainable way to remove biofilms from pipes. UGéPE 2018, Université de Lille, France.
- A.Al Saabi, H. Dallagi, C. Faille, P. Debreyne, F. Aloui et T. Bénézech. Flowing foam for the removal of bio-contamination from food processing equipment surfaces, Journée des Doctorants JDD2018, Université de lille, France.
- A.Al Saabi, H. Dallagi, C. Faille, F. Aloui et T. Bénézech. Cleaning in Place by flowing foams: a sustainable way to remove *Bacillus* spores from stainless steel surface. Journée des doctorants JDD2019. Janvier 11, 2019 | Université de Lille, France.

3- Communications par affiche nationales et internationales (posters)

- Al Saabi, C. Faille, H. Dallagi, T. Setiao, L. Bruguier, A. Funffrock, F. Aloui, T. Bénézech. Cleaning in Place by flowing foams: a sustainable way to remove soiled *Bacillus* spores from stainless steel surface, Congrès Nationale de la Société Française de Microbiologie, 1-3 Octobre, 2018, Paris , France
- A.Al Saabi, C. Faille, H. Dallagi, Julien Demeester, L. Wauquier, F. Aloui, T. Bénézech. Cleaning in Place by flowing foams: a sustainable way to remove soiled *Bacillus* spores from stainless steel surface, Journée Mardi des chercheurs, Mars 05, 2019 | Université de Mons, Belgique
- A.Al Saabi, C. Faille, H. Dallagi, L. Wauquier, F. Aloui, et T. Bénézech. Cleaning in Place by flowing foams: a sustainable way to remove biofilms from stainless steel pipes. 6ème Edition Wallonie/Nord de France de la Journée des Jeunes Chercheurs : Vers la conception de procédés éco-innovants UGéPE JJC2019, Novembre 06, 2019 | Université de Mons, Belgique.
- A.Al Saabi, C. Faille, H. Dallagi, J. Demeester, L. Wauquier, F. Aloui, T. Bénézech, Cleaning in Place by flowing foams: a sustainable way to remove soiled *Bacillus* spores from stainless steel surface, Février 27, 2019 | Université de Lille, France.

International Conference: Fouling and Cleaning in food processing, 17 – 20 April 2018, Lund Sweden (Conference article).

FLOWING FOAM FOR THE REMOVAL OF *B. SUBTILIS* AND *B. CEREUS* SPORES FROM STAINLESS STEEL SURFACES

Ahmad Al Saabi^{1*}, Féthi Aloui², Christine Faille¹, Laurent Wauquier¹, Christelle Lemy¹, Heni Dallagi², Thierry Bénézech¹

¹*UMR UMET, INRA, CNRS, Univ. Lille 1, 59650, Villeneuve d'Ascq, France*

²*LAMIH UMR CNRS 8201, University of Valenciennes (UVHC) Department of Mechanics, Campus Le Mont Houy 59313 Valenciennes Cedex 9 – France*

Abstract

Bacillus spores in food processing environments are known to induce food cross-contamination and possible consumer health concerns. Spores are also known to attach firmly to any kind of solid surfaces. Cleaning efficiency is of prime importance for food industries to ensure both the quality and safety of the products [1]; however, with present standard cleaning in place (CIP) operations, high level of energy and potable water are being enormously consumed and this can be a main concern for many governments. Flowing foam cleaning may highly reduce water and energy consumption. Preliminary works have shown that flowing foam can produce the same wall shear stress conditions than a single phase flow but under a flow rate divided by a factor of 40. In this work pilot plant CIP and foam cleaning setup were used. Removal kinetics were obtained by cleaning stainless steel AISI 316 L coupons inserted in stainless steel pipes after soiling by *B. cereus*, and *B. subtilis* spores at a surface load of 10^5 cfu.cm⁻², strains being chosen for their differing surface properties of their spores. Using CIP conditions (sodium dodecyl sulfate (SDS) 0.15%ww, 20°C and a mean wall shear stress of 5 Pa) up to 1 log₁₀ spores of *B. subtilis* were removed compared to only 0.25 log₁₀ for *B. cereus* after 20 min cleaning. Flowing foam (same SDS conditions and 50% air/liquid) generated a thin liquid film at the coupon surfaces under identical mean wall shear stress, inducing an increase in the cleaning efficiency by a factor of 20 for *B. subtilis* and a factor of 7.5 for *B. cereus*.

1. Introduction

In agro-food industrial environments, surfaces have been reported to be contaminated by a range of microorganisms, including pathogenic and spoilage bacteria (Srey et al., 2013). Once introduced, many bacteria are able to persist on the contaminated surfaces or even to grow if environmental conditions are suitable. The aerobic spore-forming bacteria *Bacillus* greatly impact on quality, food safety, and the economy due to their spoilage-causing capabilities and to a lesser extent, disease-causing potential and are well known to attach to any kind of surfaces and therefore food equipment surfaces (Faille et al., 2018).

Over the recent years, apart from numerous studies of surface disinfections, deep interest has been shown in both the mechanisms of (i) surface contamination, including the probable roles of materials and environmental conditions and of (ii) surface cleaning, the machinery design impacting the mechanical action of the detergent stream under standard cleaning in place (CIP) conditions (Faille et al., 2017). Cleaning is one of the most critical stages in quality control of food processing operations (Kulkarni et al., 1975). Failure to appropriately clean processing lines and equipment not only increases the cost due to the decreased heat transfer coefficient, but also jeopardized plant operations with microbial contamination (Gillham et al., 1999; J FRYER et al., 2006; Kulkarni et al., 1975; Mattila et al., 1990). Cleaning in Place (CIP) is a widely-used method of automated cleaning in food industries, while decreasing labor and time for cleaning; on the other hand, CIP systems require significant capacities of water, detergent, and energy. In addition, in-place cleaning generates large quantities of waste water, with additional economic burden for the industry, and environmental burden for the general public (Lyndgaard et al., 2014). The basic understanding of the fouling and cleaning processes in dairy plants has increased extensively over the past two decade (Fryer and Robbins, 2005; Wilson, 2005; Xin et al., 2002).

Pioneering methodologies to enhance cleaning and reducing fouling have evolved, including modification of surfaces, pulsed flow, ozonised water rinse, electrolyzed oxidizing rinse water, and ultrasonic cleaning (Augustin et al., 2010; Boxler et al., 2013; Christian and Fryer, 2006; Dev et al., 2014; Gillham et al., 2000; Guzel-Seydim et al., 2000; Muthukumaran et al., 2004;

Rosmaninho et al., 2007). Nevertheless, all these methods require additional devices, wealth investment, and energy involvements (Fan et al., 2018). When compared to the aforementioned solutions, the adjustment of the properties of the cleaning liquid solution for example may enhance the effectiveness of the cleaning method. As stated in the literature, cleaning operations in food industries require water, chemicals and energy inducing significant environmental influence ; however, Almost little knowledge is known on the potencies produced by flowing foam in cleaning operations working with much less energy and water, producing considerably less waste water. Primary works have shown that flowing foams can produce up to 1000 times higher wall shear stresses than single phase flow. Whereas stationary dry foams have been a major subject of fundamental studies and empiric or semi-empiric models have been developed for foams with void fractions over 85% with few practical applications. Aqueous foams are complex fluids consisting of concentrated dispersions of gas bubbles in a soapy liquid. Depending on the amount of water they contain, they are either dry or wet. They have original mechanical properties which rely on their low density and high surface area combined with their ability to elastic response to low stresses and to flow like a viscous liquid with large distortions. The characterization of the foam and of the liquid film formed on the inside walls of pipes is of paramount interest in the understanding of phenomena at the interfaces. Indeed, foam flows are governed by the properties of a thin near wall region, which induces a sliding effect. The most important parameter in controlling the flow of foam would therefore be the thickness of this sliding layer (a few micrometers to a few tenth of micrometers). Foams mainly composed of gases have complex rheological properties which can be compared to those of a solid, but also to those of a liquid(Aloui and Madani, 2008). In this case, the wall shear stress (tangential constraint) is a key parameter in the flows of these foams. This constraint, which plays an important role in the characterization of the rheological properties of the foam, depends mostly on the size of the bubbles and mainly on the volume fraction of the liquid(Chovet, 2015; Chovet et al., 2014).

In this study, the efficiency of the thin liquid film generated by flowing foam in detaching *B. subtilis* and *B. cereus* spores will be studied inside a square pipe geometry. The objective of this investigation is to compare the effect of flowing foam and corresponding CIP conditions.

2. Materials and methods

2.1. Detergent used in standard Cleaning in Place (CIP) and Foam cleaning

Sodium Dodecyl Sulfate or SDS ($\text{CH}_3(\text{CH}_2)_{11}\text{SO}_4\text{Na}$), an anionic surfactant was used at a concentration of 0.15 % ww.

2.2. Coupons and test pipes

Stainless steel AISI 314 L coupons of $6.75 \cdot 10^{-4} \text{ m}^2$ (0.045×0.015) of 1mm width were designed to be inserted to cover one internal face of the square stainless steel pipes (Figure 1).

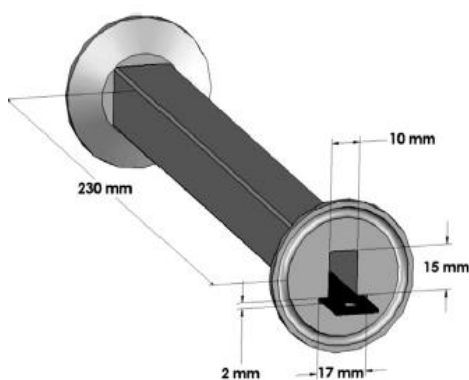


Figure 1. Test pipes (Cunault et al., 2015)

Before each experiment whether in standard CIP or with foam, coupons and test pipes were cleaned by rubbing using RBS cleaning solution (5%ww). They were scrubbed using rubber hand gloves to remove any attached particles on their surface. After a final rinsing step with softened water, the coupons were hanged on a metallic stand inside a beaker. Coupons and test pipes were sterilized in a Pasteur oven during a cycle of 2 hrs at a maximum temperature reached~ 185°C during the sterilisation cycle. Additional lab instruments needed for the experiments were also sterilised.

2.3 Surface soiling with *Bacillus* spores

The cleaning experiments; whether using CIP or foam cleaning, were done to see their effect in detaching the spores of two *Bacillus* strains: *Bacillus subtilis* 98/7 and *Bacillus cereus* 98/4. About 250 ml of spores' suspension at 10^7 cfu.ml⁻¹ (*B. subtilis*) or 10^5 cfu.ml⁻¹ (*B. cereus*) were prepared to soil the coupons which were maintained vertically for 4 hours in the suspensions. Around 10^5 cfu.cm⁻² of spores attached on coupons' surfaces. Coupons were then slid inside the stainless steel square test pipes and subjected either to CIP or foam cleaning.

2.4 Cleaning in place

A square pipe containing the soiled coupons was installed in the pilot rig previously described in (Le Gentil et al., 2010). An entry pipe of 1.5 m length was inserted upstream the test section ($L/D_h = 25$) to generate a fully developed flow in the test tubes. The cleaning solution was circulated at 650 L h⁻¹ to allow a mean wall shear stress of 5 Pa obtained experimentally from power loss measurements using differential pressure sensors (Shlumberger, type 8D). The temperature of the cleaning solution was maintained at 25°C by cooling while circulating in a tubular heat exchanger (spiraflow, Tetra Pak Processing, Sweden). Kinetics were carried out with the following cleaning times: 15s, 35s, 1, 3, 5, 10 and 20 min. Each time corresponded to cleaning of the three fouled coupons enclosed in one square pipe.

2.5 Foam cleaning in place

The foam rig prototype shown below (Figure 2) consisted in a mother tank (100 L) that contained the SDS solution (0.15% ww). This tank supplied a feeding tank (50 L) placed at 3m high from the level of three foam generators. The role of the feeding tank was to supply a constant flow of SDS solution to the foam generators connected to an air flow circuit. As air and SDS solution mix inside the foam generator, foam produced flowed through a 1 m Poly(methyl methacrylate) (PMMA) square pipe for foam visualisation and steady state flow conditions according to Chovet (2015). After the PMMA transparent pipe, the test pipe with the fouled coupons was connected. The foam leaved the circuit to a collecting tank, then to the sewer. Kinetics' times were those chosen for CIP. The foam generated liquid films at the wall (Figure 3) according to Chovet (2015). Coupons were placed at the top of the pipe to be cleaned under thin liquid film conditions (between 1 and 3 μ m).

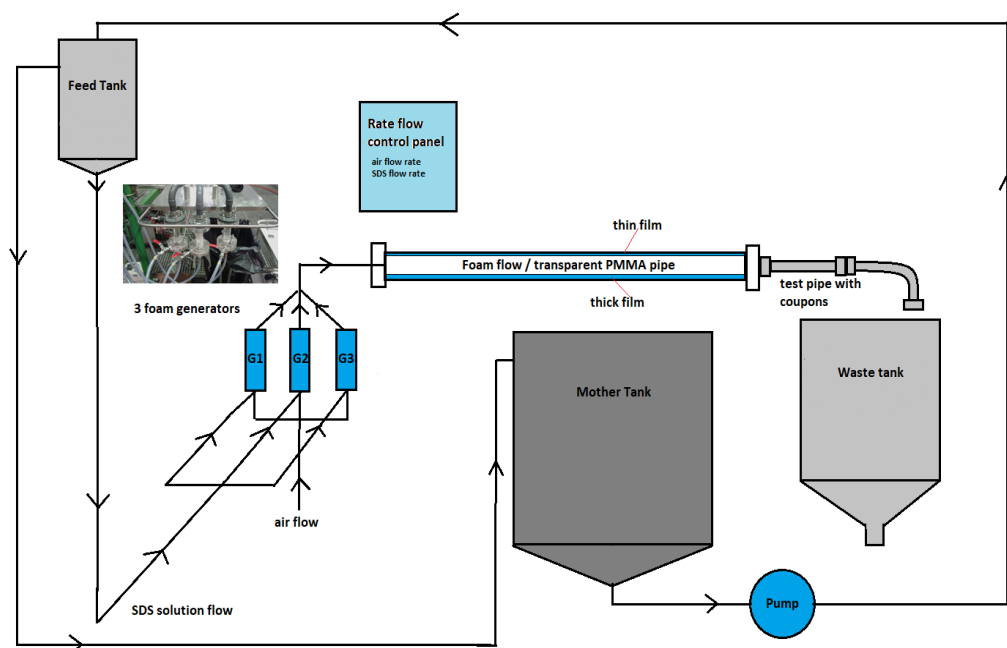


Figure 2. Foam cleaning in place prototype

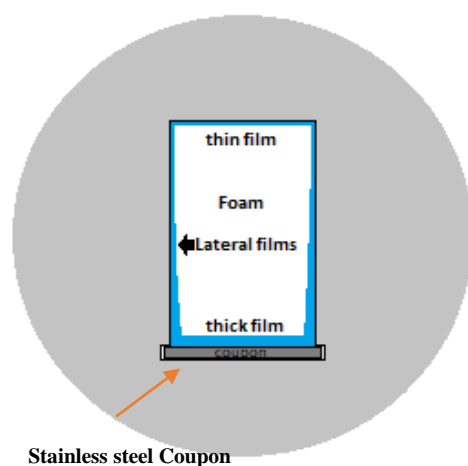


Figure 3. Scheme showing the transverse cross section of the stainless steel pipes with films surrounding the flowing foam (white color) inside the tested pipe (schema not to scale).

2.6 Coupons surface contamination assessment before and after cleaning

After cleaning, the face not in contact with the cleaning fluid were disinfected using swabs moistened with oxygal (ICL France-ANTI-GERM, 0.1% ww). Coupons were then immersed

quickly in purified water for few seconds before being placed in a glass tube containing 10 ml peptone water (1/1000) without indole and tween 80 (2 %ww) and subjected to a sonication step for 2.5 min in an ultrasonic bath (Branson 2510, 40 kHz). Detached spores were plated on nutrient agar and counted after 24 h incubation at 30°C.

Trials were performed in triplicate.

2.7 Kinetics modeling

Inspection of the kinetic profiles suggested that a two-phase model (equation 1) could be used to fit the data as previously proposed in Bénézech and Faille (2018).

$$\frac{N}{N_0} = f \exp(-k_{\max 1} t) + (1 - f) \exp(-k_{\max 2} t) \quad [1]$$

Where N_0 is the initial bacteria count, f is the poorly adherent fraction of the population (less resistant to detachment), $(1-f)$ is the more adherent fraction, and $k_{\max 1}$ and $k_{\max 2}$ [s⁻¹] are the specific detachment rates of the two sub-populations.

2.8 Statistical analysis

Data were analyzed by general linear model procedures using SAS V8.0 software (SAS Institute, Gary, NC, USA). Variance analysis was performed to determine which parameters affected the biofilm detachment (f , $k_{\max 1}$, and $k_{\max 2}$). Analysis were performed to investigate the influence of the detachment conditions (Foam vs CIP) and the strain used (*B. cereus* vs *B. subtilis*). These analyses were followed by multiple comparison procedures using Tukey's test (Alpha level = 0.05).

3. Results and discussion

A direct comparison between spores' kinetics removal by CIP and foam cleaning (thin liquid film condition) was carried out. Both conditions resulted in the same mean wall shear stress of 5 Pa, with identical temperature and SDS concentration.

Kinetics are shown in Figure 5. Whatever the cleaning conditions (CIP vs foam) *B. subtilis* spores were less resistant to detachment (up to 2.5 log) than *B. cereus* spores (less than 1 log). Foam cleaning

appeared to be more efficient than CIP. Indeed less remaining contamination in 20 min cleaning was observed with foam.

Except for *B. cereus* spores removed by CIP, detachment curves appeared clearly in two distinct phases.

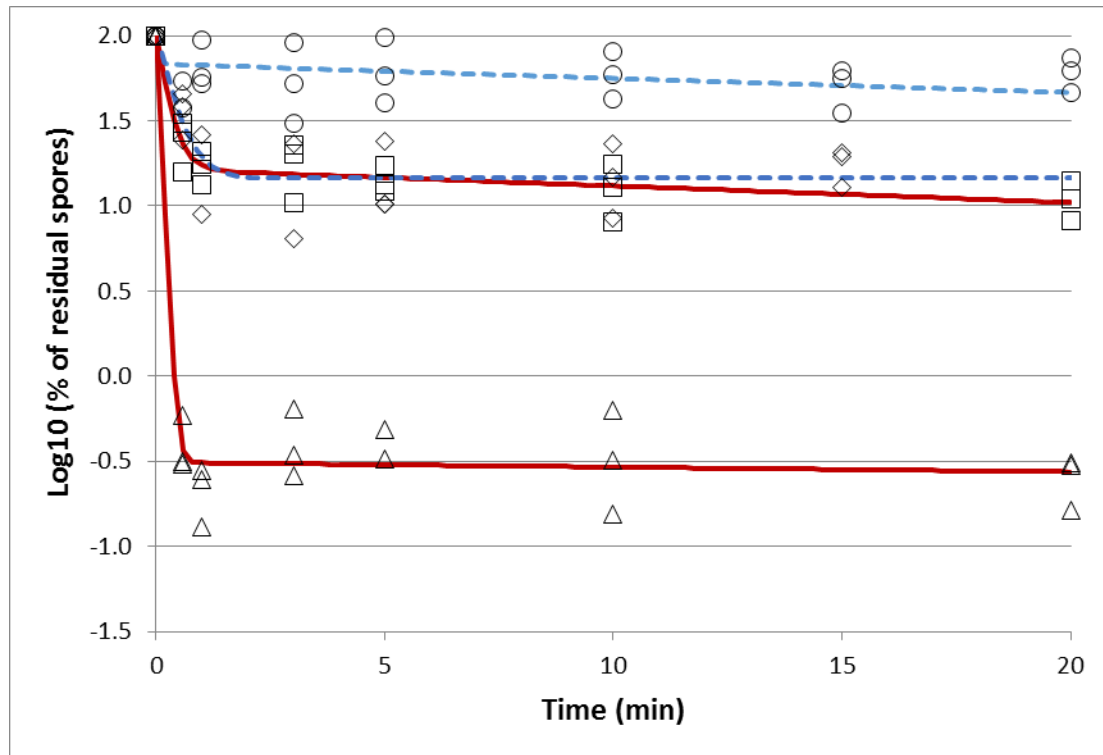


Figure 5. Log (% residual spores) as a function of the cleaning time for (i) *B. subtilis* with solid red line and squares (CIP) vs triangles (Foam), (ii) *B. cereus* with blue dotted lines and circles (CIP) vs diamonds (Foam)

The first phase lasted for less than 3 min with most of the total spore detachment. The removal detachment phenomenon during the second phase was very slow. Hence, both phases appeared to be exponential and therefore were accurately described by the biphasic model, with R^2 over 0.91.

The role of the liquid film vs CIP on the kinetics parameters were investigated. For *B. subtilis* a significant effect was observed on f when comparing foam vs CIP, f mean values being respectively of 0.99 and 0.86. More interesting, a significant effect ($Pr < 0.0001$) on the first constant rate k_{max1}

was observed comparing CIP (mean $k_{max1}=2.87$) and foam (mean $k_{max1}=12.8$). For *B. cereus*, a mean value of 4.3 for k_{max1} for foam significantly differ from the constant rate of 0.03 under CIP conditions.

No significant effect were observed on k_{max2} whatever the conditions tested, k_{max2} ranging from 0 up to 0.03.

According to Faille et al., (2013) spore resistance to CIP (NaOH 0.5%, 60°C at a mean wall shear stress of 4 Pa) varied greatly among strains and notably with a percentage of residual spores of around 1% for *B. subtilis* 98/7 and over 20% for *B. cereus* 98/4. In the CIP conditions tested here (SDS, 20°C and a mean wall shear stress of 5 Pa) the percentage of residual spores was up to 1% for *B. subtilis* 98/7 and up to 22% for *B. cereus* 98/4 which did not differ greatly from the previous works.

As shown previously Faille et al., (2013), *B. subtilis* 98/7 spores, were found to be damaged by NaOH. One could suggest to have a similar effect of the SDS responsible for the higher detachment rate of *B. subtilis* spores. This hypothesis has to be investigated in future works.

The first phase kinetics was proven more efficient under foam cleaning conditions. According to Chovet (2015) bubble passage along the film induced local variations in the film thickness and likely wall shear stress fluctuations. Such fluctuations would impact positively the removal rate. Hence, Blel et al.,(2007) have already highlighted the significant role of the wall shear stress fluctuation working on the cleaning efficiency of specific pipe features widely encountered in food processing lines arrangements.

4. Conclusions

Cleaning with flowing foam appeared to be significantly more efficient than CIP in detaching *Bacillus* spores. It was hypothesised that the flow dynamics within the thin liquid film was deeply affected by the bubble phase of the foam. Further investigations will be carried out to study how the liquid film thickness and its dynamics along with the foam characteristics would impact the removal phenomenon. Hence, in actual equipment such liquid films induced by the foam would probably greatly vary depending on the foam velocity and quality and therefore impact the cleanability.

5. Acknowledgements

This work was financed by the region Hauts-de-France and the European Funds for Regional Development. This work was a part of Ahmad Al Saabi's PhD thesis financially supported by the European Funds for Regional Development, INRA and ANIOS. The authors were thankful to Lauryne Thiebaut, Clémence Thébaud, Christelle Lemy, Anne-Sophie Wroblack, and Heni Dallagi for valuable help.

6. References

- Aloui, F., and Madani, S. (2008) Experimental investigation of a wet foam flow through a horizontal sudden expansion. *Exp. Therm. Fluid Sci.* 32, 905–926.
- Augustin, W., Fuchs, T., Föste, H., Schöler, M., Majschak, J.-P., and Scholl, S. (2010) Pulsed flow for enhanced cleaning in food processing. *Food Bioprod. Process.* 88, 384–391.
- Bénézech, T., and Faille, C. (2018) Two-phase kinetics of biofilm removal during CIP. Respective roles of mechanical and chemical effects on the detachment of single cells vs cell clusters from a *Pseudomonas fluorescens* biofilm. *J. Food Eng.* 219, 121–128.
- Blel, W., Bénézech, T., Legentilhomme, P., Legrand, J., and Le Gentil-Lelièvre, C. (2007) Effect of flow arrangement on the removal of *Bacillus* spores from stainless steel equipment surfaces during a Cleaning In Place procedure. *Chem. Eng. Sci.* 62, 3798–3808.
- Boxler, C., Augustin, W., and Scholl, S. (2013) Cleaning of whey protein and milk salts soiled on DLC coated surfaces at high-temperature. *J. Food Eng.* 114, 29–38.
- Chovet, R. (2015) Experimental and numerical characterization of the rheological behavior of a complex fluid: application to a wet foam flow through a horizontal straight duct with and without flow disruption devices (FDD). Université de Valenciennes et du Hainaut-Cambresis.
- Chovet, R., Aloui, F., and Keirsbulck, L. (2014) Gas-Liquid Foam Through Straight Ducts and Singularities: CFD Simulations and Experiments.
- Christian, G.K., and Fryer, P.J. (2006) The Effect of Pulsing Cleaning Chemicals on the Cleaning of Whey Protein Deposits. *Food Bioprod. Process.* 84, 320–328.
- Cunault, C., Faille, C., Bouvier, L., Föste, H., Augustin, W., Scholl, S., Debreyne, P., and Benezech, T. (2015) A novel set-up and a CFD approach to study the biofilm dynamics as a function of local flow conditions encountered in fresh-cut food processing equipments. *Food Bioprod. Process.* 93, 217–223.

- Dev, S.R.S., Demirci, A., Graves, R.E., and Puri, V.M. (2014) Optimization and modeling of an electrolyzed oxidizing water based Clean-In-Place technique for farm milking systems using a pilot-scale milking system. *J. Food Eng.* 135, 1–10.
- Faille, C., Bénézech, T., Blel, W., Ronse, A., Ronse, G., Clarisse, M., and Slomianny, C. (2013). Role of mechanical vs. chemical action in the removal of adherent *Bacillus* spores during CIP procedures. *Food Microbiol.* 33, 149–157.
- Faille, C., Cunault, C., Dubois, T., and Bénézech, T. (2017) Hygienic design of food processing lines to mitigate the risk of bacterial food contamination with respect to environmental concerns. *Innov. Food Sci. Emerg. Technol.*
- Fan, M., Phinney, D.M., and Heldman, D.R. (2018) The impact of clean-in-place parameters on rinse water effectiveness and efficiency. *J. Food Eng.* 222, 276–283.
- Fryer, P.J., and Robbins, P.T. (2005) Heat transfer in food processing: ensuring product quality and safety. *Appl. Therm. Eng.* 25, 2499–2510.
- Gillham, C.R., Fryer, P.J., Hasting, A.P.M., and Wilson, D.I. (1999) Cleaning-in-Place of Whey Protein Fouling Deposits: Mechanisms Controlling Cleaning. *Food Bioprod. Process.* 77, 127–136.
- Gillham, C.R., Fryer, P.J., Hasting, A.P.M., and Wilson, D.I. (2000) Enhanced cleaning of whey protein soils using pulsed flows. *J. Food Eng.* 46, 199–209.
- Guzel-Seydim, Z.B., Wyffels, J.T., Greene, A.K., and Bodine, A.B. (2000) Removal of Dairy Soil from Heated Stainless Steel Surfaces: Use of Ozonated Water as a Prerinse¹. *J. Dairy Sci.* 83, 1887–1891.
- J fryer, P., K christian, G., and Liu, W. (2006) How hygiene happens: Physics and chemistry of cleaning.
- Kulkarni, S.M., Maxcy, R.B., and Arnold, R.G. (1975) Evaluation of Soil Deposition and Removal Processes: An Interpretive Review¹. *J. Dairy Sci.* 58, 1922–1936.
- Le Gentil, C., Sylla, Y., and Faille, C. (2010) Bacterial re-contamination of surfaces of food processing lines during cleaning in place procedures. *J. Food Eng.* 96, 37–42.
- Lyndgaard, C.B., Rasmussen, M.A., Engelsen, S.B., Thaysen, D., and van den Berg, F. (2014) Moving from recipe-driven to measurement-based cleaning procedures: Monitoring the Cleaning-In-Place process of whey filtration units by ultraviolet spectroscopy and chemometrics. *J. Food Eng.* 126, 82–88.

- Mattila, T., Manninen, M., and Kyläsiurola, A.L. (1990) Effect of cleaning-in-place disinfectants on wild bacterial strains isolated from a milking line. *J. Dairy Res.* *57*, 33–39.
- Muthukumaran, S., Yang, K., Seuren, A., Kentish, S., Ashokkumar, M., Stevens, G.W., and Grieser, F. (2004) The use of ultrasonic cleaning for ultrafiltration membranes in the dairy industry. *Sep. Purif. Technol.* *39*, 99–107.
- Rosmaninho, R., Santos, O., Nylander, T., Paulsson, M., Beuf, M., Benezech, T., Yiantsios, S., Andritsos, N., Karabelas, A., Rizzo, G., et al., (2007) Modified stainless steel surfaces targeted to reduce fouling – Evaluation of fouling by milk components. *J. Food Eng.* *80*, 1176–1187.
- Srey, S., Jahid, I.K., and Ha, S.-D. (2013) Biofilm formation in food industries: A food safety concern. *Food Control* *31*, 572–585.
- Wilson, I. (2005) Challenges in Cleaning: Recent Developments and Future Prospects.
- Xin, H., Chen, X.D., and Özkan, N. (2002) Cleaning Rate in the Uniform Cleaning Stage for Whey Protein Gel Deposits. *Food Bioprod. Process.* *80*, 240–246.

ABSTRACT**Thesis Abstract****Reduction of potable water consumption by using flowing foam for cleaning equipment and surfaces**

Contaminants such as spores/biofilms are problematic in many food industry sectors. Indeed even after hygiene procedures, biofilms/spores could be found on every surface that is in direct contact or not with food (Bénézech & Faille, 2018). Risks associated with microorganisms can be controlled either by limiting the number of adherent cells or by facilitating the removal of adherent bacteria. Even though Cleaning in Place (CIP) is widely used and it is a common cleaning practice in food industries; however, it remains at some level a high- water consumption procedure. In addition, some studies, presented some bacterial species that still survived even after CIP and maybe a probable source of product contamination.

On the other hand, a double phase fluid such as foam can impose the same wall shear stress with less water being consumed. Foam with its properties such as shearing can be a key parameter for a mechanical cleaning of closed systems such as pipes with a lower consumption of water.

In this study we investigated the effect of flowing foam in pipes and compared its efficiency with standard CIP like conditions on the detachment of spores and biofilms. The first approach was working with different foam flow regimes (1D, 2D, 3D while increasing the velocity from 2 to 6 cm s⁻¹) having different foam qualities (amount of air: 50%, 60%, 70%) on different species of microorganisms where fouling was performed either by using spores of *B. amyloliquefaciens* 98/7 or *B. cereus* 98/4 that shows a difference by their hydrophobic/hydrophilic character. As for *P. fluorescens pfl* it was used as a good biofilm former (24 hrs. biofilm) widely encountered in the food industry. Fouling was performed either vertically or horizontally inducing biofilms with different structures. Results from foam cleaning were compared with CIP like conditions results (the same mean mechanical action, and the same concentration of surfactant).

The second approach was subjecting foam flow to different singularities (sudden expansion gradual reduction – bends) while working with one foam flow regime (1D 50%) and one species (*B. amyloliquefaciens* 98/7 spores) to highlight any changes in the foam flow cleaning efficiency. The third approach was working also with one species (*B. amyloliquefaciens* 98/7) considered as a good “microbial tool” producing foam from the use of different surfactants (SDS, Capstone® FS 30, Ammonyx® LO) that differs by their chemical properties (nonionic, anionic and zwitterion) thus producing different foams having different physical properties in terms of bubbles size , number and repartition, and flow pattern.

Comparing to previous related works on foam flow characterization, it was possible to highlight the potential role on the cleaning efficiency of the Wall Shear Stress variations in parallel to the liquid film thickness variation at the wall with the bubbles' passage. In addition, according to previous work, the possible capillary forces exerted under the lowest flow rates and considering the hydrophilic/hydrophobic nature of the spores, in addition to biofilm structure would explain at least partly the surprising efficiency in the spores' removal by foam.

Key words: foam flow, biofilm, spores, fouling, stainless steel

RESUMÉ

Resumé de Thèse

Réduction de la quantité d'eau potable utilisée pour nettoyer conduites et équipements par des mousses en écoulement

Les contaminants tels que les spores / biofilms sont problématiques dans nombreux secteurs de l'industrie alimentaire. En effet, même après les procédures d'hygiène, ces biofilm/spores pouvaient être retrouvés sur toutes les surfaces en contact direct ou non direct avec les aliments (Bénézech & Faille, 2018). Les risques associés aux biofilms peuvent être contrôlés soit en limitant le nombre des cellules adhérentes, soit en facilitant l'élimination des bactéries adhérentes. Le nettoyage en place (CIP) est une pratique de nettoyage courante et est largement utilisée dans les industries alimentaires ; cependant, il reste à un certain niveau une procédure de forte consommation d'eau. De plus, certaines études ont présenté quelques espèces bactériennes qui ont survécu même après le CIP et peuvent-être une source probable de contamination du produit.

D'un autre côté, un fluide biphasique tel que la mousse peut exercer la même contrainte de cisaillement en paroi générée par un fluide monophasique, avec moins d'eau consommée. La mousse avec ses propriétés telles que le cisaillement peut être un paramètre clé pour un nettoyage mécanique des systèmes fermés tels que les tuyaux à faible consommation d'eau.

Dans cette étude, nous avons étudié l'effet de l'écoulement de mousse dans les tuyaux et comparé son efficacité avec des conditions du type CIP standard sur le détachement des spores et des biofilms. La première approche consistait à travailler avec différents régimes d'écoulement de mousse (1D, 2D, 3D tout en augmentant la vitesse de 2 à 6 cm.s⁻¹) ayant différentes qualités de mousse (quantité d'air: 50%, 60%, 70%) sur différentes espèces de micro-organismes où l'encrassement a été effectué soit en utilisant des spores de *B. amyloliquefaciens* 98/7 ou *B. cereus* 98/4 qui montrent une différence par leur caractère hydrophobe / hydrophile. Quant à *P. fluorescens pfl*, il a été utilisé comme un bon formateur de biofilm (biofilm de 24 heures) largement utilisé dans l'industrie alimentaire. L'encrassement a été réalisé à la position verticale ou à l'horizontale induisant des biofilms avec différentes structures. Les résultats du nettoyage de la mousse ont été comparés aux résultats des conditions de type CIP (la même action mécanique moyenne et la même concentration de tensioactif).

La deuxième approche consistait à soumettre le flux de mousse à différentes singularités (réduction progressive de l'expansion soudaine - coudes) tout en travaillant avec un régime d'écoulement de mousse (1D 50%) et une espèce (*B. amyloliquefaiciens* 98/7 spores) pour mettre en évidence tout changement dans le flux de mousse sur l'efficacité de nettoyage.

La troisième approche portait sur le travail avec une espèce (*B. amyloliquefaciens* 98/7) considérée comme un bon « outil microbien », en produisant la mousse à partir des différents surfactants (SDS, Capstone® FS 30, Ammonyx® LO). Ces derniers diffèrent par leurs propriétés chimiques (non ionique, anionique et zwitterion) et donc permettant de produire des mousses avec des propriétés physiques différentes en termes de taille, de nombre et de répartition des bulles, et de profil d'écoulement.

Les précédents travaux sur la caractérisation de mousse en écoulement ont synchronisé l'évolution de la contrainte de cisaillement en parois et l'évolution de l'épaisseur du film liquide avec le passage des bulles. Selon ces travaux antérieurs, la vibration des bulles, l'évolution de la contrariante et l'épaisseur, les forces capillaires exercées avec les débits les plus faibles, la nature

hydrophile / hydrophobe des spores et la structure du biofilm pourraient expliquer au moins en partie l'efficacité surprenante de l'élimination des spores par la mousse.

Mots clés : mousse, biofilm, spore, encrassement, acier inoxydable